

SYNTHESIS, CHARACTERIZATION AND FUNCTIONALIZATION OF ANTI-
BISARENE SCAFFOLDS

by

Joseph Livingston Franklin

A thesis submitted to the faculty of
The University of North Carolina at Charlotte
in partial fulfillment of the requirements
for the degree of Master of Science in
Chemistry

Charlotte

2017

Approved by:

Markus Etzkorn

Craig Ogle

Jerry Troutman

Eric Heberlig

ABSTRACT

JOSEPH LIVINGSTON FRANKLIN. Synthesis, Characterization and Functionalization of *Anti*-Bisarene Scaffolds (Under the direction of MARKUS ETZKORN)

Since the advent of rational organic synthesis, practitioners in the field have been refining their craft to target compounds of immense complexity. Synthetic methodologies discovered through these pursuits have provided a fertile ground to expand our understanding of conceptually important ideas (e.g., bonding, aromaticity, solid-state interactions, reaction mechanisms). While intellectually stimulating, the focus of this field has been shifting toward the targeted synthesis of compounds with desirable properties. Our project aligns with this shift and has produced novel molecules of fundamental importance and a foundation toward functional organic materials.

Organic chemists continue to uncover synthetic methodology that is perceptively simple to apply to ‘classical’ structures, but many compounds of interest are exceedingly difficult to obtain or have remained elusive. Thus, the preparation of various 2-indanone derivatives provided interesting challenges with surprising outcomes. A small library of aryl-substituted 2-indanones was obtained where individualized synthetic routes were necessary according to the electronic requirements of each system. Through meticulous optimization, reproducible routes were realized to produce multigram quantities of these precursors for the generation and dimerization of their respective isoindenone derivatives.

Through this project, we have developed reliable protocols to a series of isoindenone and selected isoindene dimers, both novel scaffolds which may be utilized to study their fleeting-intermediate monomers and construct functional organic materials. The novelty of this scaffold is derived from the offset arene units, demonstrated to direct

arene-arene interactions in the solid state – a necessary property for organic semiconductors. The introduction of electron-donating or withdrawing arene substituents provides electronic contrast between these structures while selected derivatives may be amenable to *N*-heterocyclic rectilinear arene extension.

TABLE OF CONTENTS

LIST OF TABLES	vii
LIST OF FIGURES	ix
LIST OF ABBREVIATIONS	xiv
CHAPTER 1: INTRODUCTION	1
1.1 Isoindenones	1
1.1.1 Isoindenone Generation	3
1.1.2 Stabilized Isoindenones	5
1.1.3 Alternate Approach to Isoindenone Dimers	7
1.1.4 ‘Simple’ Isoindenones and Their Respective Dimers	8
1.2 Azaacenes and Their Role in Organic Electronics	11
1.2.1 (Hetero)arene Functionalization Approaches Toward Functional Organic Materials	13
1.2.2 Azaacene Synthetic Approaches	15
1.2.2.1 Aryl Substitution Methods	16
INTERLUDE: Aromaticity of Azaacenes	17
1.2.2.2 Quinone Condensation Approach	18
1.2.2.3 The Palladium Way to <i>N</i> -Heteroacenes	19
1.2.2.3.1 “Domino” Double <i>N</i> -Arylations	21
CHAPTER 2: RESEARCH GOALS	23
CHAPTER 3: RESULTS AND DISCUSSION	26
3.1 Syntheses, Characterization, and Structures of Selected 2-Indanone Derivatives	26

3.1.1 Synthesis of 5,6-Difluoro-2-indanone	26
3.1.2 Synthesis of 5,6-Dichloro-2-indanone	29
3.1.3 Synthesis of 5,6-Dimethoxy-2-indanone	32
3.1.4 Toward 5,6-Dibromo-2-indanone	37
3.2 Novel Arene-Substituted Isoindenone dimers	39
3.2.1 Fluorinated Isoindenone Dimers	39
3.2.1.1 <i>Ortho</i> -Difluoro-Isoindenone Dimer Synthesis	41
3.2.1.2 Additional Fluorinated Isoindenones	44
3.2.2 Isoindenone Dimers Incorporating Electron-Donating Arene Substituents	47
3.2.2.2 Methoxy-Substituted Isoindenone Dimer Synthesis	47
3.2.2.3 Additional Isoindenone Derivatives Incorporating Electron-Donating Aryl Substituents	50
3.2.3 Spectroscopic Data of Isoindenone Dimers	51
3.3 Synthetic Transformations and Characterization of Isoindenone Dimer Derivatives	51
3.3.1 Toward the Formal <i>Ortho</i> -Difluoro-Isoindene Dimer	53
3.3.2 Methoxy-Substituted Isoindene Dimer Synthesis	59
3.3.2.1 X-ray Structures and Spectroscopic Data	62
3.4 Extended <i>Anti</i> -Bisheteroarene Scaffolds	65
3.4.1 Toward Extended <i>Anti</i> -Bisheteroarene Scaffolds	69
3.4.1.1 Indane-Derived Quinone Approach	71
3.4.1.2 The Palladium Way to Azaacenes	79
3.4.1.3 Diamino-Indane Condensation Approaches Toward <i>Anti</i> -Bisheteroarenes	87

CHAPTER 4: SUMMARY AND OUTLOOK	95
CHAPTER 5: EXPERIMENTAL	99
5.1 Instruments and Materials	99
5.2 Procedures and Experimental Data	102
5.2.1 Disubstituted 2-Indanones	102
5.2.2 Isoindenone Generation and Dimerization	120
5.2.3 Toward Azaacenes	141
5.3 X-ray Crystallographic Reports	153
REFERENCES	156

LIST OF TABLES

TABLE 1.	Summary of fluorinated isoindenone generation attempts.	46
TABLE 2.	HOMO-LUMO energies calculated for selected azaacenes using Spartan '16 : B3LYP/6-31G*.	69

LIST OF FIGURES

FIGURE 1:	Selected resonance structures of isoindenone.	1
FIGURE 2:	Literature-known isoindenone dimers (2-6 , all substituents are omitted for clarity) and selected isoindenones from which they are derived (7-10).	2
FIGURE 3:	Selected strategies for the generation of isoindenone and derivatives thereof.	3
FIGURE 4:	1,3-substituted cyclopentaphenanthren-2-one (16).	4
FIGURE 5:	Isoindenone derivatives reported by the Jones group	6
FIGURE 6:	One additional resonance form available to MeO-substituted isoindenones.	6
FIGURE 7:	<i>N</i> -phenylmaleimide trapped isoindenone derivatives.	6
FIGURE 8:	The product obtained after exposure of isoindenone 22 to air.	7
FIGURE 9:	The reported synthesis of the formal tetrachloro-isoindenone dimer 34 through a Diels-Alder approach.	8
FIGURE 10:	Biradical system speculated by Jones to be an intermediate of isoindenone dimer formation and dissociation.	9
FIGURE 11:	Isoindenone-derived non-classical dication 38 and related structures alongside a table of the primary substitution patterns targeted in our group.	11
FIGURE 12:	General azaacene structure.	12
FIGURE 13:	Functionalization strategies for tetracene leading to a variety of π -stacked arrangements.	14
FIGURE 14:	Examples of ethynyl-substituted tetraacenes.	15
FIGURE 15:	General synthetic strategies toward azaacenes.	17
FIGURE 16:	Azaacenes (43) and their reduced <i>N,N'</i> -dihydro (52) species.	17
FIGURE 17:	Calculated heats of hydrogenation (B3LYP/6-311+G**) for the reduction of azaacene 53 .	18

FIGURE 18:	Dialkylbiaryl phosphane ligand system (56).	19
FIGURE 19:	Proposed catalytic cycle for palladium-catalyzed amination.	20
FIGURE 20:	Targeted polycyclic frameworks and compounds from which they are derived alongside a table of the primary thesis-relevant substituents.	23
FIGURE 21:	Selected literature-reported 2-indanones.	26
FIGURE 22:	The sequence utilized to produce 5,6-difluoro-2-indanone (11c) alongside a table of substitution patterns relevant to this chapter.	27
FIGURE 23:	Optimized synthesis of 5,6-dichloro-2-indanone (11f).	29
FIGURE 24:	Two 1-indanone products obtained through various conditions from propionic acid 68f .	31
FIGURE 25:	Crystal structure and unit cell of 5,6-dimethoxy-1-indanone (69h).	33
FIGURE 26:	Formal indene dimer (17) obtained through the dehydration of indanol 70h .	34
FIGURE 27:	Reported preparation of 5,6-dimethoxy-2-indanone (11h).	34
FIGURE 28:	The optimized synthesis of 5,6-dimethoxy-2-indanone (11h) following the general methodology reported by J.B. Taylor et al.	35
FIGURE 29:	Crystal packing of 5,6-dimethoxy-2-indanone (11h).	37
FIGURE 30:	Efforts completed toward the synthesis of 5,6-dibromo-2-indanone (11g).	38
FIGURE 31:	General scheme for isoindenone generation and dimerization including a table with substituent patterns that either delivered dimer 2 (green), did not (red), or were inconclusive (yellow).	39
FIGURE 32:	Attempted synthetic routes toward the formal tetrafluoro-isoindeneone dimer 2b .	40
FIGURE 33:	Synthetic route utilized for isoindenone generation and dimerization from substituted 2-indanones (11).	41

FIGURE 34:	A typical crude product obtained following <i>ortho</i> -difluoro-isoindenone dimerization.	42
FIGURE 35:	Unit cell of <i>ortho</i> -difluoro-isoindenone dimer 2c and the parent isoindenone dimer 2a .	43
FIGURE 36:	(a) Partial crystal system of <i>ortho</i> -difluoro-isoindenone dimer 2c showing face to face π -stacking interactions and (b) all short contacts (orange).	44
FIGURE 37:	Crude spectrum of <i>ortho</i> -dimethoxy-isoindenone dimer 2h following aqueous workup.	48
FIGURE 38:	An atypical ^1H NMR (500 MHz, CDCl_3) recorded following <i>ortho</i> -difluoro-isoindenone (1c) generation.	50
FIGURE 39:	Spectroscopic comparison between isoindenone dimers. All NMR data was recorded in CDCl_3 and UV-Vis Data was recorded in ACN.	51
FIGURE 40:	Isoindene dimers (57) targeted through carbonyl reduction of their corresponding isoindenone dimers 2 .	52
FIGURE 41:	Attempted syntheses of the formal isoindene dimer 57a .	53
FIGURE 42:	Synthetic sequence previously utilized for the production of the parent isoindene dimer (57a).	54
FIGURE 43:	Generalized Barton-McCombie radical reduction pathway.	57
FIGURE 44:	Barton-McCombie methodology applied toward isoindene dimer 57c .	58
FIGURE 45:	Possible over-reduced products.	60
FIGURE 46:	Unit cells for the crystal structures of <i>ortho</i> -methoxy isoindenone dimer 57h (a) and parent isoindenone dimer 57a (b) where some portions are shown as a space-filling model for clarity.	63
FIGURE 47:	Crystal structure of <i>ortho</i> -methoxy isoindene dimer 57h showing all twenty short contacts (orange).	63
FIGURE 48:	NMR characterization of parent isoindene dimer 14a and <i>ortho</i> -dimethoxy-substituted isoindenone dimer 14e .	64

FIGURE 49:	Tunable azaacene targets.	65
FIGURE 50:	Isoindenone and isoindene dimers.	66
FIGURE 51:	Crystal structures of the parent and <i>ortho</i> -difluoro-isoindenone dimers (2a/2c) where molecules experiencing face-to-face arene interactions are displayed as space-filled models.	66
FIGURE 52:	Crystal structure of parent isoindene dimer 57a highlighting the T-shaped arene interaction with space-filled models.	67
FIGURE 53:	Selected synthetic avenues to polycyclic azaacene scaffolds of type 58 or 59 .	70
FIGURE 54:	Potential approach toward azaacenes (58/59) through functionalization of methoxy groups.	71
FIGURE 55:	Previously reported oxidations of methoxy units on structurally related triptycene scaffolds.	72
FIGURE 56:	¹ H NMR (500 MHz, CDCl ₃) spectrum of crude product from reaction of isoindene dimer 57h with 0.25 M HNO ₃ .	73
FIGURE 57:	Previously reported oxidations of methoxy units on pentiptycene scaffolds.	74
FIGURE 58:	¹ H NMR spectrum (500 MHz, ACN-D ₃) recorded of crude product obtained after CAN treatment of isoindene dimer 57e .	75
FIGURE 59:	Derivation of methoxy groups to potentially oxidizable catechols.	76
FIGURE 60:	¹ H NMR spectrum recorded of product obtained after isoindene dimer 57h was treated with neat BBr ₃ in CD ₂ Cl ₂ , subjected to aqueous workup and triturated with chloroform (500 MHz, acetone-D ₆ , 256 scans).	77
FIGURE 61:	¹ H NMR spectrum recorded of product obtained after isoindenone dimer 3e was refluxed in benzene for an hour and subjected to aqueous workup (500 MHz, methanol-D ₃).	78
FIGURE 62:	Alternative demethylation route through derivation of 11h to bis-imine 127 .	79
FIGURE 63:	Proposed catalytic cycle for palladium-catalyzed amination.	80

FIGURE 64:	Optimized conditions reported by J. Laha et al. for double <i>N</i> -arylations where a series of substituted <i>ortho</i> -dihalides and <i>ortho</i> -phenylene diamines were cross-coupled (20 examples).	81
FIGURE 65:	¹ H NMR (300 MHz, CDCl ₃) recorded of the crude product obtained through an attempt to synthesize the <i>ortho</i> -dichloro-isoindenone dimer 2f .	82
FIGURE 66:	Potential synthesis of azacene 58 via dimerization of an <i>N</i> -heterocyclic isoindenone (130).	83
FIGURE 67:	Potential Buchwald-Hartwig coupling toward the <i>N</i> -heterocyclic 2-indanone derivative 111 .	84
FIGURE 68:	¹ H NMR (500 MHz, CDCl ₃) recorded following a Buchwald-Hartwig coupling reaction of dichloro ketal 131 with phenylene diamine (50).	86
FIGURE 69:	Potential route to azaacene 2-indanone derivative 44 .	87
FIGURE 70:	5,6- diamino-2-indanone (31g) target.	89
FIGURE 71:	Attempts toward 5,6-diamino-2-indanone (111).	90
FIGURE 72:	Optimized synthetic pathway to 5,6-dimethoxy-2-indanone (11) and attempted application to dinitro-substituted arenes.	90
FIGURE 73:	Products obtained from NBS bromination of dinitro xylene 146 .	91
FIGURE 74:	Synthesis of 2-nitrobenzyl cyanide (156) and side products obtained through alternate reaction pathways.	92
FIGURE 75:	Potential pathway toward cyclopenta[<i>b</i>]quinoxaline-2-one (159).	93
FIGURE 76:	Targeted polycyclic frameworks and compounds from which they are derived alongside a table of the primary thesis-relevant substituents.	95
FIGURE 77:	Envisioned synthesis of azaacene 58 through 2-indanone derivative 111 .	97
FIGURE 78:	Synthetic scheme to an alternative isoindenone derived azaacene (164).	98

FIGURE 79:	¹ H-NMR spectrum of (2 <i>E</i>)-2-(2,3-dihydro-5,6-difluoro-1 <i>H</i> -inden-1-ylidene)-2,3-dihydro-5,6-difluoro-1 <i>H</i> -inden-1-one (165) (300 MHz, CDCl ₃).	105
FIGURE 80:	¹ H-NMR spectrum of 5,6-difluoro-2-indanone (11c) (500 MHz, CDCl ₃).	112
FIGURE 81:	¹⁹ F-NMR spectrum of 5,6-difluoro-2-indanone (11c) (300 MHz, CDCl ₃).	113
FIGURE 82:	¹ H-NMR spectrum of 5,6-dichloro-2-indanone (11f) (500 MHz, CDCl ₃).	114
FIGURE 83:	¹³ C-NMR spectrum of 5,6-dichloro-2-indanone (11f) (500 MHz, CDCl ₃).	114
FIGURE 84:	¹ H-NMR spectrum of 1',3'-dihydro-spiro[5,6-dichloro-1,3-dioxolane-2,2'-[2 <i>H</i>]indene] (167) (500 MHz, CDCl ₃).	116
FIGURE 85:	¹ H-NMR spectrum of 2-(<i>tert</i> -butyldimethylsiloxy)-5,6-difluoro-indene (89c) (500 MHz, CDCl ₃).	121
FIGURE 86:	¹⁹ F-NMR spectrum of 2-(<i>tert</i> -butyldimethylsiloxy)-5,6-difluoro-indene (89c) (500 MHz, CDCl ₃).	121
FIGURE 87:	¹ H-NMR spectrum of 2-(<i>tert</i> -butyldimethylsiloxy)-5,6-dichloro-indene (89f) (500 MHz, CDCl ₃).	122
FIGURE 88:	¹ H-NMR spectrum of 2-(<i>tert</i> -butyldimethylsiloxy)-5,6-dimethoxy-indene (89h) (500 MHz, CDCl ₃).	123
FIGURE 89:	¹³ C-NMR spectrum of 2-(<i>tert</i> -butyldimethylsiloxy)-5,6-dimethoxy-indene (89h) (500 MHz, CDCl ₃).	124
FIGURE 90:	¹ H-NMR spectrum of 3-bromo-2-(<i>tert</i> -butyldimethylsiloxy)-5,6-difluoro-indene (90c) (500 MHz, CDCl ₃).	125
FIGURE 91:	¹ H-NMR spectrum of 3-bromo-2-(<i>tert</i> -butyldimethylsiloxy)-5,6-dichloro-indene (90f) (300 MHz, CDCl ₃).	126
FIGURE 92:	¹ H-NMR spectrum of 3-bromo-2-(<i>tert</i> -butyldimethylsiloxy)-5,6-dimethoxy-indene (90h) (500 MHz, CDCl ₃).	127
FIGURE 93:	¹ H-NMR spectrum of <i>anti</i> -3,4;7,8-bis[3,4-difluorobenzo]-tricyclo[4.2.1.1 ^{2,5}]deca-9,10-dione (2c) (500 MHz, Acetone-D ₆).	129

FIGURE 94:	^{19}F -NMR spectrum of <i>anti</i> -3,4;7,8-bis[3,4-difluorobenzo]-tricyclo[4.2.1.1 ^{2,5}]deca-9,10-dione (2c) (500 MHz, CDCl_3).	129
FIGURE 95:	UV-VIS spectrum of <i>anti</i> -3,4;7,8-bis[3,4-difluorobenzo]-tricyclo[4.2.1.1 ^{2,5}]deca-9,10-dione (2c) recorded in ACN.	130
FIGURE 96:	^1H -NMR spectrum of <i>anti</i> -3,4;7,8-bis[3,4-dimethoxybenzo]-tricyclo[4.2.1.1 ^{2,5}]deca-9,10-dione (2h) (300 MHz, CDCl_3).	131
FIGURE 97:	^{13}C -NMR spectrum of <i>anti</i> -3,4;7,8-bis[3,4-dimethoxybenzo]-tricyclo[4.2.1.1 ^{2,5}]deca-9,10-dione (2h) (300 MHz, CDCl_3).	131
FIGURE 98:	UV-VIS spectrum of <i>anti</i> -3,4;7,8-bis[3,4-dimethoxybenzo]-tricyclo[4.2.1.1 ^{2,5}]deca-9,10-dione (2h) recorded in ACN.	132
FIGURE 99:	^1H -NMR spectrum of <i>anti</i> -3,4;7,8-bis[3,4-dimethoxybenzo]-tricyclo[4.2.1.1 ^{2,5}]deca-9,10-diol (97h) (300 MHz, CDCl_3).	134
FIGURE 100:	^{13}C -NMR spectrum of <i>anti</i> -3,4;7,8-bis[3,4-dimethoxybenzo]-tricyclo[4.2.1.1 ^{2,5}]deca-9,10-diol (97h) (300 MHz, CDCl_3).	134
FIGURE 101:	^1H -NMR spectrum of <i>anti</i> -3,4;7,8-bis[3,4-difluorobenzo]-tricyclo[4.2.1.1 ^{2,5}]deca-9,10-dichloro (41c) (300 MHz, CDCl_3).	136
FIGURE 102:	^{19}F -NMR spectrum of <i>anti</i> -3,4;7,8-bis[3,4-difluorobenzo]-tricyclo[4.2.1.1 ^{2,5}]deca-9,10-dichloro (41c) (300 MHz, CDCl_3).	136
FIGURE 103:	^1H -NMR spectrum of <i>anti</i> -3,4;7,8-bis[3,4-dimethoxybenzo]-tricyclo[4.2.1.1 ^{2,5}]deca-9,10-dichloro (41h) (300 MHz, CDCl_3).	138
FIGURE 104:	^1H -NMR spectrum of <i>anti</i> -3,4;7,8-bis[3,4-dimethoxybenzo]-tricyclo[4.2.1.1 ^{2,5}]decane (57h) (300 MHz, CDCl_3).	139
FIGURE 105:	UV-VIS spectrum of <i>anti</i> -3,4;7,8-bis[3,4-dimethoxybenzo]-tricyclo[4.2.1.1 ^{2,5}]decane (57h) recorded in ACN.	139
FIGURE 106:	^1H -NMR spectrum of 2,3-dimethyl-6-quinoxalinepropenoic ethyl ester (166) (300 MHz, CDCl_3).	143
FIGURE 107:	^{13}C -NMR spectrum of 2,3-dimethyl-6-quinoxalinepropenoic ethyl ester (166) (300 MHz, CDCl_3).	143
FIGURE 108:	^1H -NMR spectrum of 2,3-dimethyl-6-quinoxalinepropanoic ethyl ester (169) (300 MHz, CDCl_3).	145

FIGURE 109:	¹ H-NMR spectrum of 2,3-dimethyl-6-quinoxalinepropanoic methyl ester (170) (300 MHz, CDCl ₃).	146
FIGURE 110:	¹ H-NMR spectrum of 2,3-dimethyl-6-quinoxalinepropanoic acid (135) (500 MHz, CDCl ₃).	147
FIGURE 111:	¹³ C-NMR spectrum of 2,3-dimethyl-6-quinoxalinepropanoic acid (135) (300 MHz, CDCl ₃).	147
FIGURE 112:	¹ H-NMR spectrum of 1,2-bis(bromomethyl)-4-nitrobenzene (147) (300 MHz, CDCl ₃).	149
FIGURE 113:	¹³ C-NMR spectrum of 1,2-bis(bromomethyl)-4-nitrobenzene (147) (300 MHz, CDCl ₃).	150
FIGURE 114:	¹ H-NMR spectrum of 1-(dibromomethyl)-2-(bromomethyl)-4,5-dinitrobenzene (151) (500 MHz, CDCl ₃).	151
FIGURE 115:	¹³ C-NMR spectrum of 1-(dibromomethyl)-2-(bromomethyl)-4,5-dinitrobenzene (151) (500 MHz, CDCl ₃).	152
FIGURE 116:	Crystal structure of 5,6-dimethoxy-1-indanone (69h).	153
FIGURE 117:	Crystal structure of 5,6-dimethoxy-2-indanone (11h).	154
FIGURE 118:	Crystal structure of <i>anti</i> -3,4;7,8-bis[3,4-difluorobenzo]-tricyclo[4.2.1.1 ^{2,5}]deca-9,10-dione (2c).	155
FIGURE 119:	Crystal structure of <i>anti</i> -3,4;7,8-bis[3,4-dimethoxybenzo]-tricyclo[4.2.1.1 ^{2,5}]decane (57h).	156

LIST OF ABBREVIATIONS

Å	Angstrom
ACN	Acetonitrile
B3LYP	Becke, three-parameter, Lee-Yang-Parr basis set
CAN	Cerium ammonium nitrate
DCM	Dichloromethane
DFT	Density functional theory
DMSO	Dimethyl sulfoxide
HOMO	Highest occupied molecular orbital
IR	Infrared spectroscopy
LAH	Lithium aluminum hydride
LUMO	Lowest unoccupied molecular orbital
NMR	Nuclear magnetic resonance
PTSA	<i>Para</i> -toluene sulphonic acid
THF	Tetrahydrofuran
UV/Vis	Ultraviolet/Visible spectroscopy

CHAPTER 1: INTRODUCTION

1.1 Isoindenones

Isoindenones are of particular interest to theoreticians and synthetic chemists as highly reactive derivatives of both *ortho*-quinodimethane (**1**, bold) and cyclopentadienone (**1**, blue). Analyzing the resonance structures depicted in **Figure 1**, the high reactivity of this system is evident as plausible resonance structures exist to provide nonionic, ionic, and radical character. The cross-conjugated 10 π -electron system **1** and derivatives thereof have been utilized as fleeting intermediates that can be trapped under a variety of conditions or dimerize in unique fashion.¹⁻⁴ Thus, **1** represents an interesting system to study its reactivity and application as a synthetic intermediate toward novel polycyclic scaffolds.

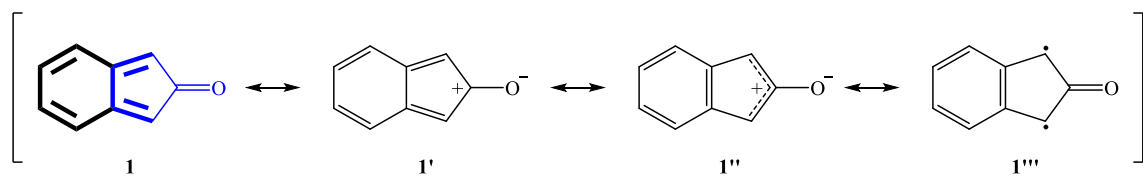


Figure 1. Selected resonance structures of isoindenone.

In the absence of alkene or alkyne scavengers, isoindenone and derivatives thereof dimerize along various modes (**2-6**) that reflect their steric demands and electronic properties.¹⁻³ Many of the reported dimers are poorly characterized due to limited solubility (e.g., compound **2** lacks any analytical details).^{1, 5} Subsequent chemical transformations are usually limited to photochemical or thermal isomerization reactions.²⁻⁹

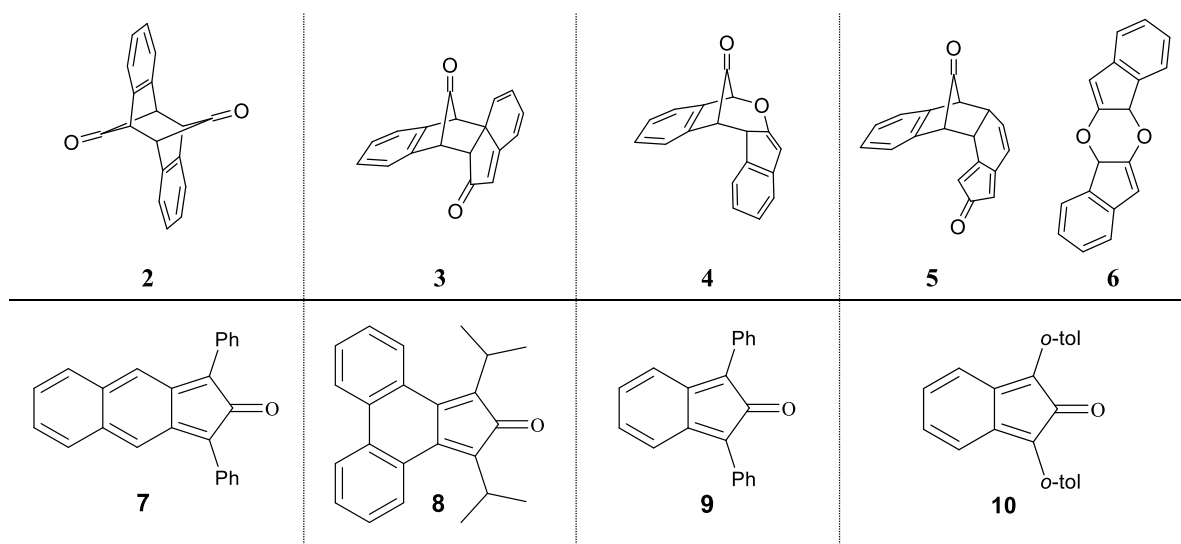


Figure 2. Literature-known isoindenone dimers (**2-6**, all substituents are omitted for clarity) and selected isoindenones from which they are derived (**7-10**).

While dimers of type **3**, **4** and **5** can be reasoned through their respective [4+2], [6+4] and [4+2] π cycloaddition mechanisms, compounds of type **2** and **6** are formal orbital symmetry forbidden [4+4] and [6+6] π dimers, respectively. The radical character of isoindenone resonance structure **1'''** and ionic 2π character of **1''** seemingly allow for plausible mechanisms to structures of type **2** or **6** but no experimental evidence has yet been obtained for contributions from either structure to the resonance hybrid. A recent theoretical study provides evidence that the structure of isoindenone is most similar to **1** through nucleus independent chemical shift (NCIS) calculations that predict a weakly antiaromatic six-membered ring and strongly antiaromatic five-membered ring.¹⁰ In addition, the generation of isoindenone derivatives in the presence of various dienophiles has provided no evidence of either resonance structure. If biradical resonance form **1'''** contributed significantly to the resonance hybrid, formal [4+2] π cycloaddition reactions should proceed in a nonstereoselective manner but trapping experiments with *cis*- or *trans*-

alkenes produced defined products through suprafacial orbital interactions according to Woodward-Hoffman rules.⁴

1.1.1 Isoindenone Generation

Several avenues have been reported with varying success for the generation of isoindenone derivatives (**Figure 3**).^{1, 3, 8, 11} These pathways are restricted by the availability of the required precursor or by the precursor's substituent pattern (e.g., **14** $R' = \text{Ph}$ vs. $R' = \text{H}$: in the latter case, the base will deprotonate the more acidic halo-methylene position).

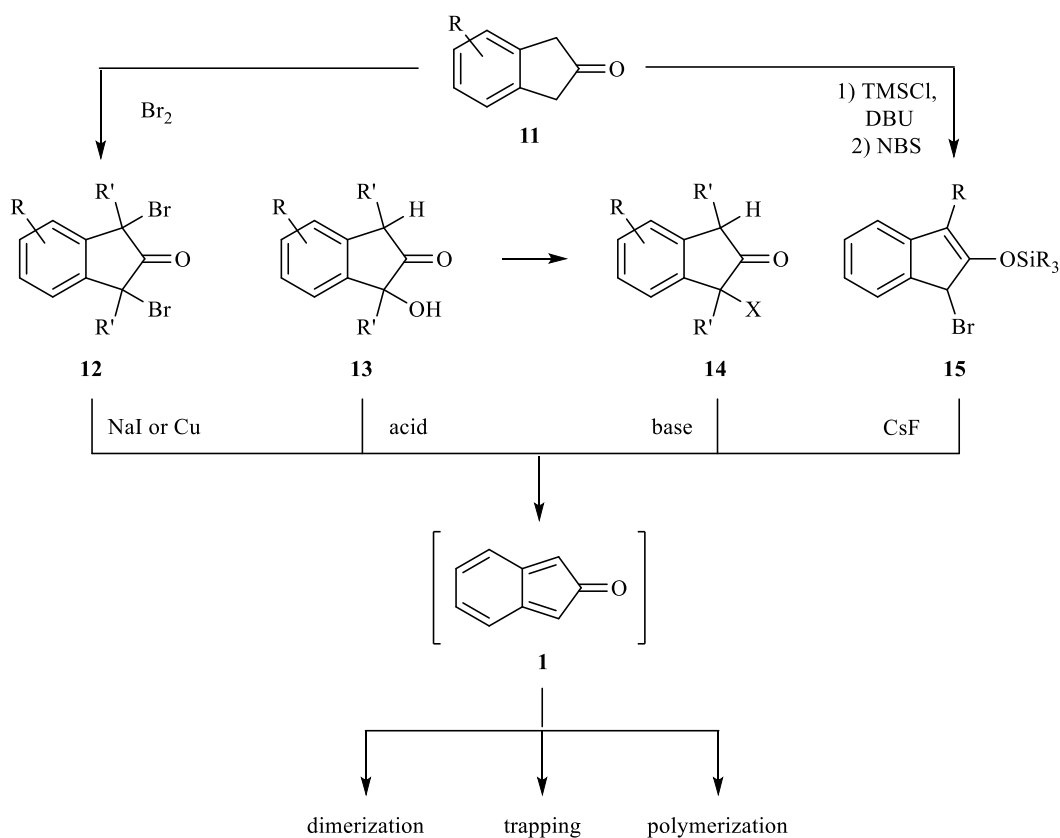


Figure 3. Selected strategies for the generation of isoindenone and derivatives thereof.

One of the earliest strategies for isoindenone generation utilized the reduction of a 1,3-dibromo adduct (**12**, $R' = H$) with iodide, sodium amalgam or copper powder.^{4, 8} This method was inefficient for the generation of the parent isoindenone (**1**)—only 8% yield of the cyclopentadiene adduct was obtained when refluxed with copper powder in benzene—¹² but was successfully applied to a variety of derivatives.^{4, 11} All three conditions were effectively applied to 1,3-dibromo-1,3-diphenyl-2-indanone (**12**, $R = H$, $R' = Ph$, $X = Br$) to afford the [4+4] π *anti*-dibenzo dimer of type **2** in good yield.⁸

Although the dehydration of alcohol **13** is an attractive approach for the generation of isoindenone derivatives, this methodology has been restricted to 1,3-diaryl-cyclopentaphenanthren-2-ones (**16**). These α -alcohols (**13**) are readily accessible through the condensation of quinones and substituted ketones but only through dehydroxychlorination to derivatives of **14** could an elimination be applied to other

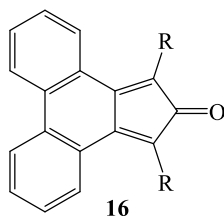


Figure 4. 1,3-substituted cyclopentaphenanthren-2-one (**16**).

systems. Dehydroxyhalogenation has been widely applicable toward isoindenone derivatives when the 1- and 3-positions are occupied by a carbon containing group. Treatment of these precursors with alcoholic KOH has been reported to afford dimers of type **2** or **3** in up to quantitative yield.^{3, 7}

Jones pioneered a more elegant route for the generation of isoindenone (**1**) that is generally more tolerable of additional functional groups. Starting from 2-indanone or select derivatives (**11**), bromo-silyl enol ethers (**15**) were prepared via a two-step procedure as the direct precursors to isoindenones (**1**). The isoindenone generation step takes advantage of the strong silicon-fluorine bond to cleave the enol-ether bond and

introduce two additional π -electrons while extruding bromide in concerted fashion.

Isoindenones generated through this method have been trapped with alkenes stereoselectively in up to 66% yield or, in the case of unsubstituted **1**, has been claimed to dimerize to the *anti*-dibenzo polycycle **2**.¹ Since the initial disclosure of this approach, no further utilization of this sequence has been reported.

1.1.2 Stabilized Isoindenones

Previous investigations, in particular by three groups (Jones [Leeds]⁸, Fuchs [Tel Aviv],³ Hoffmann [Darmstadt]¹¹), focused on designing persistent isoindenone derivatives through the introduction of substituents for electronic stabilization or steric protection. Select approaches are described below.

The first isoindenone derivatives were reported in 1932 as isolable diaryl-substituted cyclopentanophenanthrene-2-ones (**16**). Upon the introduction of one non-aromatic group in an α -position, polymers or other homocycloaddition products were obtained. Lacking steric protection about the α -carbons, two derivatives with small R groups (**16**, R = Me, Et) were reported to dimerize to their corresponding [4+2] π dimers of type **3** that could be thermally rearranged to its formal [4+4] π dimer of type **2**. Upon an increase of the steric demand at the reactive centers, the diisopropyl derivative (**16**, R = *i*Pr) was stable in solution and isolable as a green solid.⁵

Following a similar arene addition approach, the Jones' group investigated isoindenone stability on benzanulated systems (**17**, **18**). Although this approach did not yield any persistent species, the further sterically hindered tetraphenyl substituted derivative **18** delivered the new [6+6] π dimer of type **6**. Similar to 1,3-

diphenylisoindenone (**19**), the naphthyl system **17** formed only the type **2** dimer in the absence of a trap.⁴

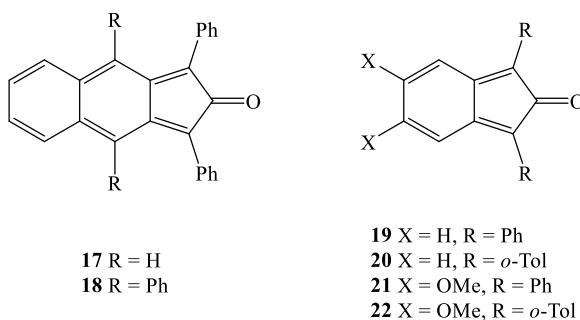


Figure 5. Isoindenone derivatives reported by the Jones group

In a different approach toward electronically stabilized isoindenone derivatives, methoxy-substituted systems were investigated due to the additional 'push-pull' resonance (**Figure 6**). Although the methoxy-substituted 1,3-diphenyl isoindenone (**21**) dimerized to the same type **4** [4+4] π dimer as its parent system (**19**), increased stability of **21** was evidenced through reaction kinetics. When either dimer was stirred with *N*-phenylmaleimide, trapped products were obtained much faster for the methoxy-substituted system. A 92% yield of methoxy-substituted adduct **24** was obtained after four hours at 20 °C while less than 40% of the type **4** dimer of the parent system **19** was consumed after eighteen hours.²

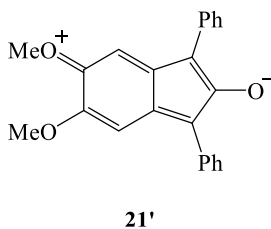


Figure 6. One additional resonance form available to MeO-substituted isoindenones.

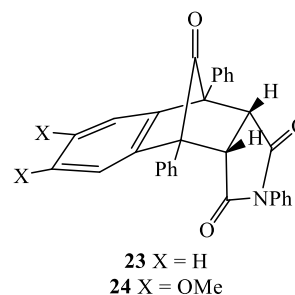


Figure 7. *N*-phenylmaleimide trapped isoindenone derivatives.

In a novel approach, Jones and co-workers introduced more sterically demanding *o*-tolyl α,α' -substituents that hindered isoindenone conjugation due to the nonplanarity of these groups.² Unlike the type **2** and **3** dimers formed from 1,3-diphenyl substituted **19**, 1,3-di-*o*-tolyl substituted isoindenone **20** forms the [6+6] π dimer of type **6** and a different [4+2] π dimer of type **5**. When alkoxy stabilization was combined with this approach to produce 5,6-dimethoxy-1,3-di-*o*-tolyl-isoindenone (**22**), none of these dimers formed! Under inert conditions, the deep green color associated with **22** was observed in solution and found to be indefinitely stable. Upon exposure to oxygen, the color rapidly disappears and the diketone **25** is formed after the loss of carbon monoxide. Isoindenone **22** could not be isolated but was characterized by UV-Vis spectroscopy ($\lambda_{\text{max}} = 708 \text{ nm}$) and further supported through a [4+2] π cycloaddition reaction with *N*-phenylmaleimide.²

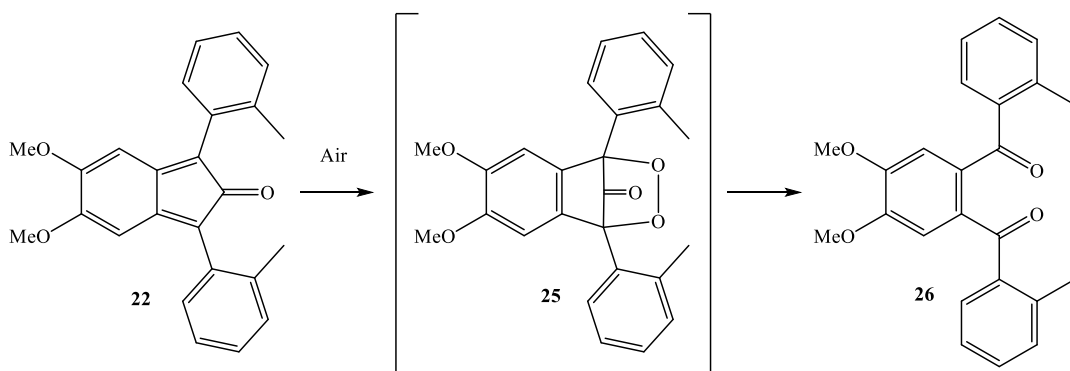


Figure 8. The product obtained after exposure of isoindenone **22** to air.

1.1.3 Alternative Approach to Isoindenone Dimers

Rather than through the dimerization of isoindenone derivatives, scaffolds of type **2** were previously targeted in our group through the benzannulation of dienedione **30**.¹³

To circumvent the rapid thermal isomerization of **30** to **29**, hydroxyketone **31** was prepared as an alternative substrate for Diels-Alder cycloaddition. Utilizing tetrachlorothiophene dioxide (**32**) as the diene for this reaction, the formal isoindenone dimer **35** was prepared through an eight-step procedure. Only trace quantities of poorly soluble **35** could be obtained through this route and alternative pathways were deemed necessary for investigation into aryl-substituted isoindenone dimers of type **2**.¹³

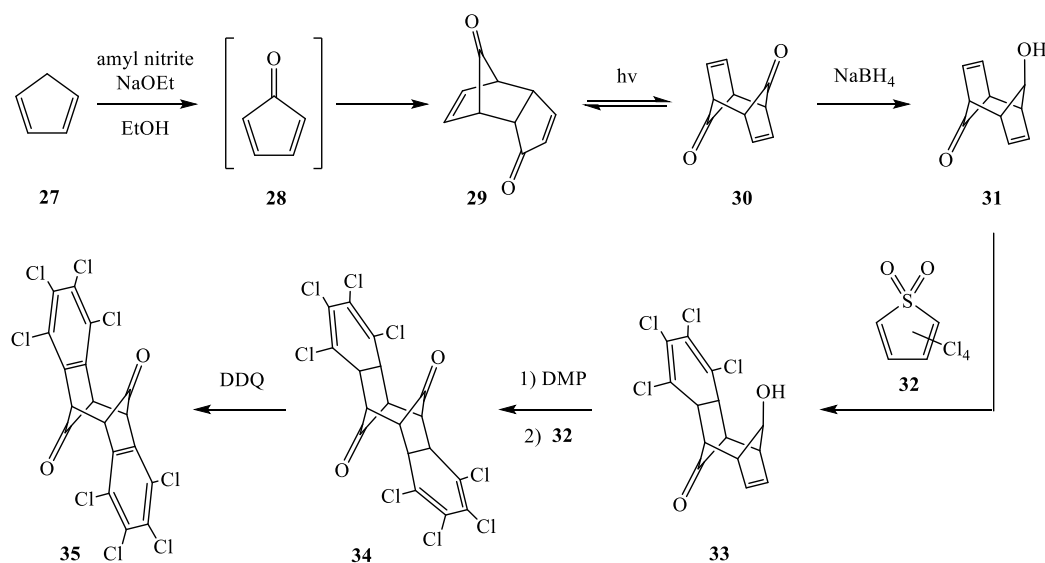


Figure 9. The reported synthesis of the formal tetrachloro-isoindenone dimer **34** through a Diels-Alder approach.¹³

1.1.4 ‘Simple’ Isoindenones and Their Respective Dimers

Recently, the focus of the Etzkorn group has shifted toward arene-substituted derivatives of isoindenone **1** and their respective [4+4] π dimers of type **2**. These ‘simple’ isoindenones, lacking conjugative stabilization or steric protection in the α, α' -positions, as well as heterocyclic derivatives, are prominently absent in the experimental literature. Recent interest has been brought to these fleeting intermediates through a theoretical

study of fluorine's effects on the aromaticity of **1** alongside select *N*-heterocyclic derivatives.¹⁰

Isoindenone dimers of type **2** are intriguing substrates for thermally or photochemically initiated isomerization reactions to further understand the electronic structure of their monomers. If the dimers fragment through either method, capturing the intermediates with radical traps or dieneophiles may assist in the elucidation of reaction pathways. It has been demonstrated that 1,3-diphenyl isoindenone dimers of type **2** can be dissociated thermally into their monomers and trapped with dieneophiles,² but intermediates in this fragmentation are of greater interest. Jones states that the biradical intermediate **36** is likely involved in isoindenone dimer formation and dissociation,^{1,2} but no attempts to directly trap this intermediate with a radical scavenger have been reported. Preliminary results from our lab indicate that reaction occurs when a solution of the parent isoindenone dimer **2** and bromine in ACN is irradiated with UV light, but the structure of the products could not be elucidated.

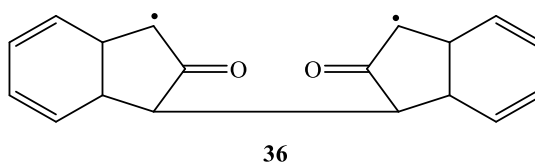
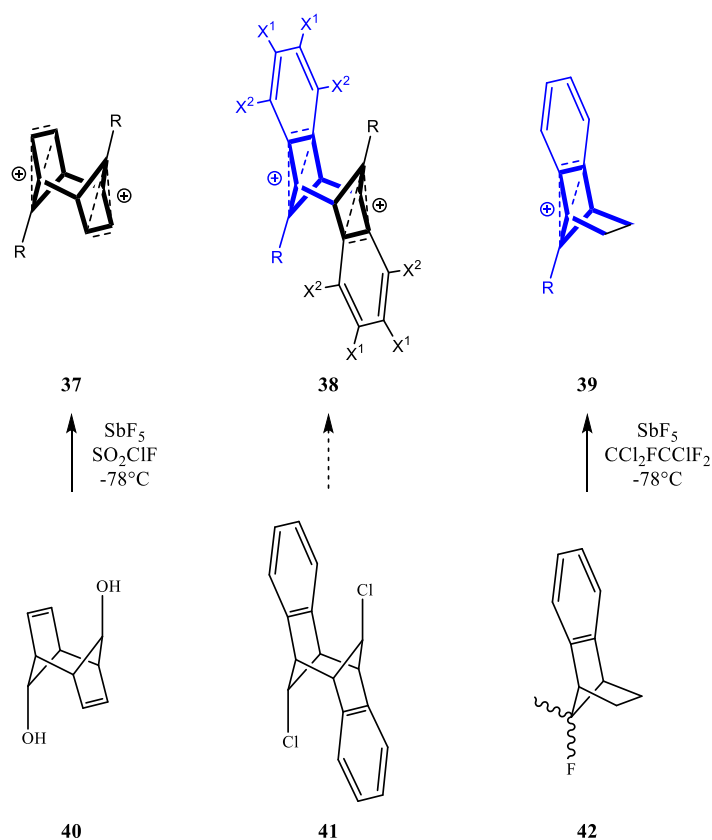


Figure 10. Biradical system speculated by Jones to be an intermediate of isoindenone dimer formation and dissociation^{1,2} (substituents omitted for clarity).

Isoindenone dimers of type **2** also provide an interesting architecture on which to study non-classical cations. The ‘unusual’ electron delocalization in non-classical carbocations, though no longer a controversial question, is still drawing significant attention. Primarily, their solid-state structures are of interest as only a limited number of

experimentally determined crystal structures are known of these sensitive compounds.¹⁴⁻

¹⁶ Thus, dication **38** represents a hybrid architecture of the known benzonorbornenyl cation **39**¹⁴ and the tricyclic, sandwiched bishomo-aromatic species **37**.¹⁷ Conjugation within arenes hinders their π -electron donating capabilities for through-space cation stabilization and led to the requirement of R-substitution to obtain single crystals of the benzonorbornenyl cation (**38**, R = CH₃).¹⁴ With enhanced π -electron donating capabilities from its olefin precursor (**40**), the sandwiched bishomo-aromatic dication **36** did not require this substitution to be characterized in solution.¹⁷ Electron-donating arene substituents may increase π -electron donation for this purpose and are of interest when probing the requirement of R-substitution on the structural hybrid of these two known systems: isoindenone-derived **38**. Preliminary evidence for dication **38** was obtained from MS data where the base peak corresponded to its m/z ratio following fragmentation from its dichloride precursor (**41**). While SPARTAN calculations show almost no substituent effects on the structures of the derived dications, only experimental characterization (e.g., NMR, X-ray structure determination) will confirm or refute these expectations.



	a	b	c	d	e	f	g	h	i	j	k	l	m
X ¹	H	F	F	H	Cl	Cl	Br	OCH ₃	H	H	H	NH ₂	NO ₂
X ²	H	F	H	F	Cl	H	H	H	OCH ₃	CH ₃	Ph	H	H

Figure 11. Isoindenone-derived non-classical cation **38** and related structures alongside a table of the primary substitution patterns targeted in our group.

1.2 Azaacenes and Their Role in Organic Electronics

Acenes have recently been established as an important class of organic semiconductors for applications in field-effect transistors,¹⁸ photovoltaic devices,¹⁹ light-emitting diodes²⁰ and sensors.²¹ In order to further tune their application-relevant properties, modification through the introduction of functionalized groups or fused arene

units has become an area of intensive investigation for both theoreticians and synthetic chemists.²²⁻²⁶

Similar to the doping method widely employed in the silicon industry, many groups have investigated the use of heteroatoms (B, P, O, S, N) to replace CH groups in the backbone of acenes.^{23, 27, 28} While the physical process of "doping" is markedly different between these two, they both aim to tune aspects of these systems. The properties of these 'doped' acenes are strongly dependent on the type and number of heteroatoms, as well as their positions and orbital hybridizations.²⁶ Although the present investigation provides the groundwork for the exploration of a variety of heteroacenes, this thesis project focuses on *N*-heterocyclic rectilinear arranged arenes.

Acenes are generally utilized as hole transporters due to the facile delocalization of positive charges through extended π -systems. Their effectiveness as electron transporters is hampered by the reduced species' acute sensitivity to water and oxygen, along with easily accessible trap states;²⁹ however, various functionalization approaches have produced moderately appealing n-type semiconducting acenes.³⁰ The introduction of nitrogen atoms has recently become a point of interest for this purpose due to the improved resistance toward oxidation while significantly increasing the arene's electron

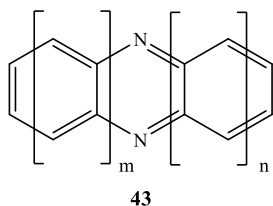


Figure 12. General azaacene structure.

affinity.³¹ When nitrogen atoms are symmetrically placed across the acene backbone (i.e. as in structures of type **43**) the HOMO-LUMO gaps are similar to those of their hydrocarbon derivatives³² while diverse synthetic avenues exist to tune application-relevant properties (e.g.,

charge carrier mobility, intermolecular coupling, solid-state packing motifs).²² Thus,

azaacenes have been gaining significant attention within the synthetic community as they retain a close structural relationship to their hydrocarbon analogs while displaying different property profiles.²²

1.2.1 (Hetero)arene Functionalization Approaches Toward Functional Organic Materials

The diverse synthetic pathways to azaacenes have allowed the exploration of vast functionalization approaches. The incorporation of arene substituents has been explored primarily to alter electron affinities, solid state packing motifs, kinetic stabilities and solubilities within this class of compounds.²² These strategies are not exclusive to azaacenes and are generally drawn from structurally related acenes.³³

Significant literature precedence exists for the utilization of aryl substituents to direct solid-state packing of extended acenes. For example, tetracene crystalizes in a herring bone motif with predominant edge-to-face interactions, common to all unfunctionalized acenes, but the addition of a small substituent is sufficient to disrupt this order. Further functionalization was required to induce long-range π -stacking order of tetracene derivatives and could be accomplished through the addition of a second substituent in various positions. Adding substituents symmetrically across the acene backbone is a common approach to produce slipped stack (**Figure 13-A/D**) or columnar arrangements (**Figure 13-B**). Other symmetrical substitutions similar to **Figure 13-C** have also been utilized to direct stacking through steric or electronic means.³³

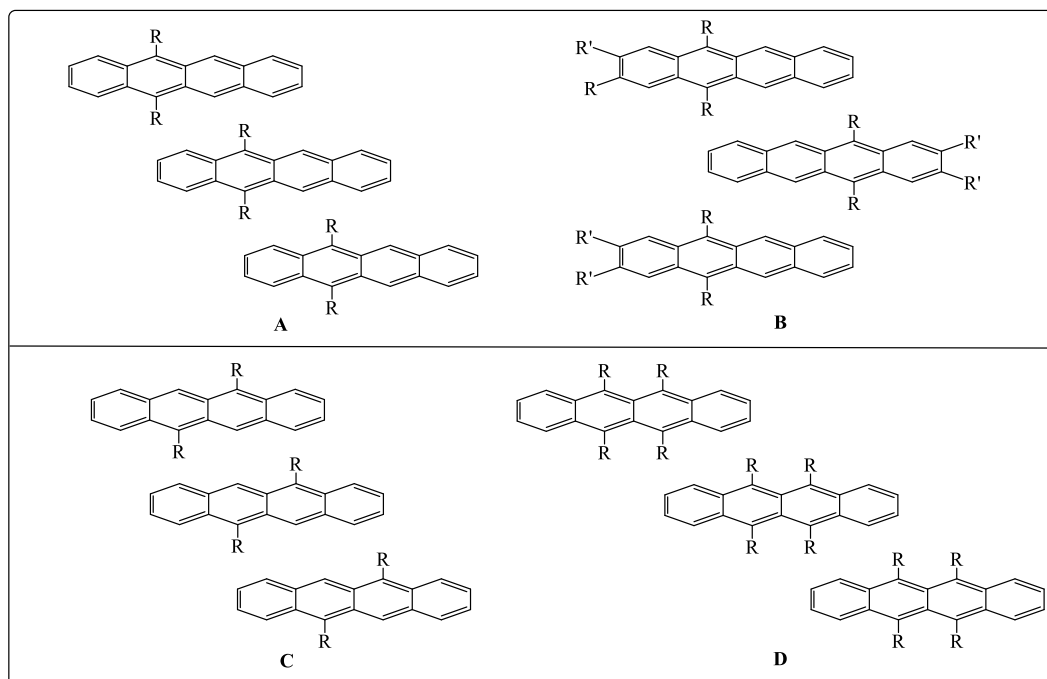


Figure 13. Functionalization strategies for tetracene leading to a variety of π -stacked arrangements.³³

A diverse array of functional groups has been utilized for these approaches. Simple substituents such as methyl groups may be sufficient to direct stacking but multi-purpose functions are typically desired. Electron-withdrawing substituents have gained significant attention for this purpose (e.g., fluorine, trifluoromethyl) as their local dipoles can drive solid state packing while increasing the electron affinity of the molecule.³⁴ The nitrogen atoms within azaacenes are similarly multifunctional as their lone pairs can be used analogously to an R-substituent (**Figure 13**) due to their local dipoles and frequently engender edge-to-edge arene interactions with electron-deficient aryl hydrogens.³⁵

The decreasing singlet-triplet gap for higher (hetero)acene homologs presents a significant challenge to the preparative chemist and has stimulated innovative approaches to ever larger, kinetically protected acenes. Rectilinear arranged arene systems are

attractive for their decreased HOMO-LUMO gaps but homocycloaddition reactions (polymerization) often render these compounds useless for application purposes.³⁶ In order to prepare acenes longer than pentacene that are stable under ambient conditions, bulky protecting groups must be used to kinetically prevent dimerization and facilitate

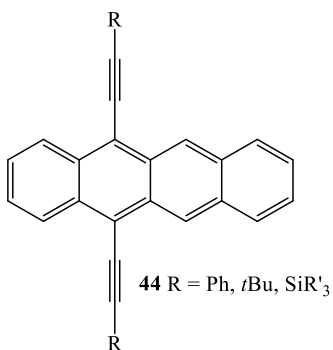


Figure 14. Examples of ethynyl-substituted tetraacenes.

solubility. Substituted alkynes, such as **44**, have been widely utilized for this purpose as they effect only marginal changes to the electronic properties of the acene. Fine tuning of the alkyne substituents are necessary as excessive bulk hinders face-to-face interactions although the insulation of a fluorescent chromophore is desirable for OLED emitters.³³

1.2.2 Azaacene Synthetic Approaches

Robust synthetic methodology is critical in developing a class of organic compounds for use in materials science. Although many computationally studied azaacenes predict appealing properties, the synthetic routes available for their preparation have been limited until recently. No generally applicable synthesis of azaacenes has been realized though significant experimentation since the first fully aromatic *N*-heterocyclic polycycle, quinoxaline (**43**, $m+n = 1$), was prepared in 1884.³⁷ Aryl-extended azaacenes had been previously known since the late 19th century but were only reported in their *N,N'*-dihydro reduced state. While many molecules of interest for organic semiconductor applications have been synthesized, the fine tuning of these compounds requires widely

applicable methodologies to better correlate functionalization motifs with experimental properties.²²

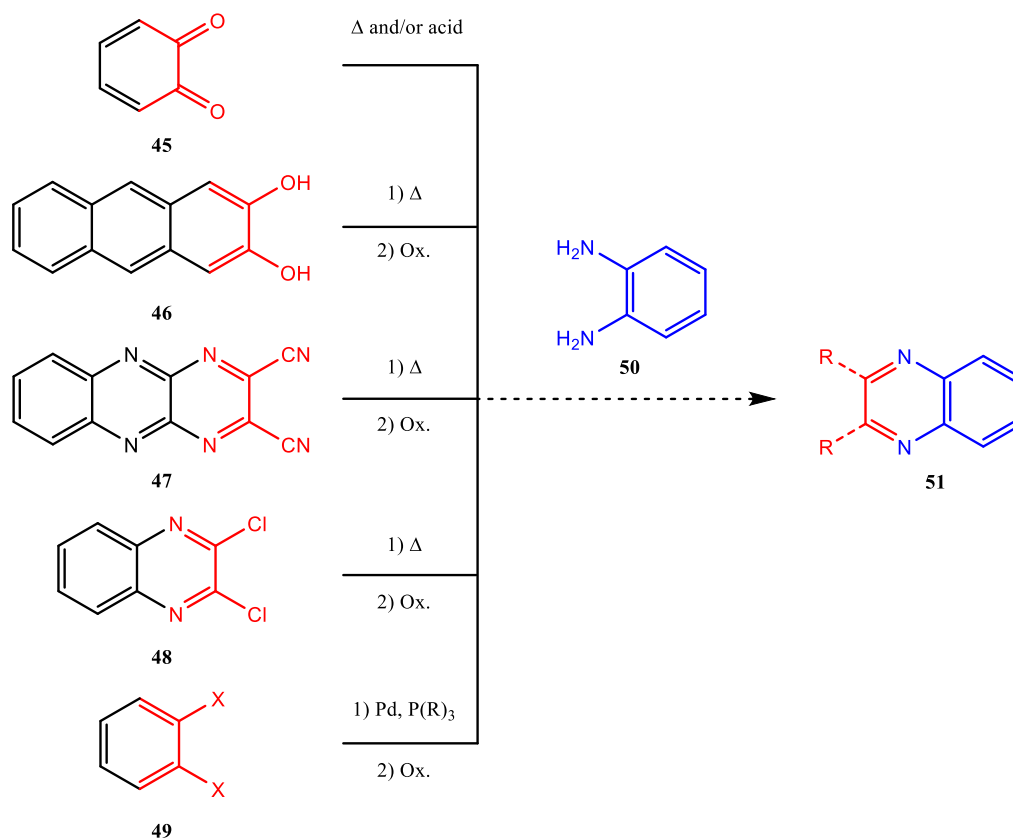


Figure 15. General synthetic strategies toward azaacenes.

1.2.2.1 Aryl Substitution Methods

In the earliest azaacene syntheses, “fire and sword” methods were used to melt dihydroxyarenes such as **46** or dichloroquinoxaline **48** with *ortho*-phenylenediamine (**50**). These reactions often provided good to excellent yields but did not translate well to substituted compounds. A variant of this condensation employs the nucleophilic reaction of diamine **50** in the presence of sodium amide with fully fluorinated acenes. These

methods, along with the palladium-catalyzed approach discussed later in this section, afford formally antiaromatic N,N' -dihydro acenes that must be oxidized, typically with manganese dioxide or chloranil, to afford the corresponding azaacene.³⁸

Interlude: Aromaticity of Azaacenes

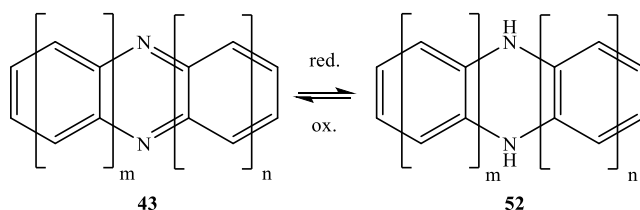


Figure 16. Azaacenes (**43**) and their reduced N,N' -dihydro (**52**) species.

In addition to their appeal for materials science applications, azaacenes represent an interesting case to probe the concept of aromaticity. Many synthetic routes to electron deficient $[4n + 2]$ π -electron compounds of type **1** rely on the oxidation of formally antiaromatic, electron rich $4n$ π -electron N,N' -dihydro precursors (**52**). When five or more rings are linearly connected, an oxidant must be employed to form the azaacene of type **43** while oxidation is spontaneous upon exposure to air for smaller systems. The reasoning for this phenomenon was revealed through nucleus-independent chemical shift and thermochemical calculations which demonstrated that the classifications of molecules of type **43** or **52** is more complex than aromatic or antiaromatic, respectively.^{22, 23}

In small molecules of type **52** where $m+n$ is less than four, aromaticity is reduced when compared to their oxidized counterparts of type **43**; however, these systems are not antiaromatic. When more rings are introduced, the total energy differences between the two becomes less pronounced. Clar's sextet rule reveals

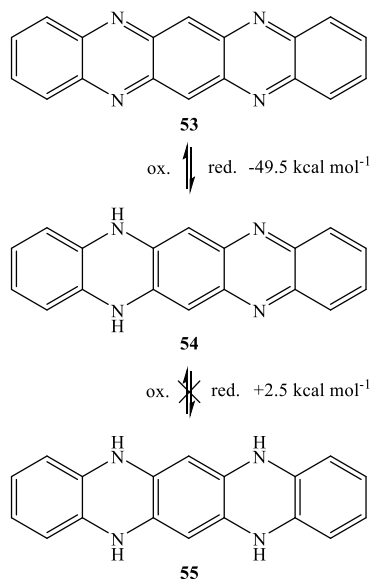


Figure 17. Calculated heats of hydrogenation (B3LYP/6-311+G**) for the reduction of azaacene **53**.²²

that the breakup of a large aromatic system into its smaller components is thermodynamically favorable and is particularly evident in the strongly exothermic hydrogenation of **53** to **54** ($-49.5 \text{ kcal mol}^{-1}$ calculated). As the azaacene is extended, this exothermicity only becomes greater; however, a second direct reduction is not yet known and calculated to be slightly thermodynamically unfavorable ($+2.5 \text{ kcal/mol}$, **54** to **55**).²²

1.2.2.2 Quinone Condensation Approach

The most broadly applicable route to azaacenes has been the condensation of *ortho*-quinones and *ortho*-phenylenediamines. This strategy toward extended azaacenes was pioneered by Mastalerz and co-workers to assemble aromatic systems consisting of up to eleven fused six-membered rings.³⁹ *Ortho*-quinones are more reactive than dihydroxy compounds and are often less stable and harder to synthesize. Many *ortho*-quinones, such as *ortho*-benzoquinone (**45**), are not stable enough to be isolated and must

be generated in situ from their corresponding catechol or alkoxy precursors. These oxidation conditions tolerate a limited number of functional groups and narrows the scope of this approach. Quinones are often readily condensed with phenylene diamines in the presence of a Brønsted acid catalyst in a thermodynamically favorable process with water as the only byproduct. Many of these reactions can occur without a catalyst or neat due to the highly polar nature of the reacting groups and generally low thermodynamic activation barriers to overcome.³⁸

1.2.2.3 The Palladium Way to *N*-Heteroacenes

The amination methods developed independently by Buchwald⁴⁰ and Hartwig⁴¹ have become an important class of reactions to form sp^2 C-N bonds by cross-coupling amines with aryl halides. Central to this methodology is the monodentate phosphane precatalyst based on the dialkylbiaryl phosphane backbone **56**. Although palladium-catalyzed C-N cross-coupling reactions were reported as early as 1983,⁴² the mechanism of this reaction is still a subject of intensive study with significant attention brought to the phosphane ligand (**Figure 18**).^{40, 43}

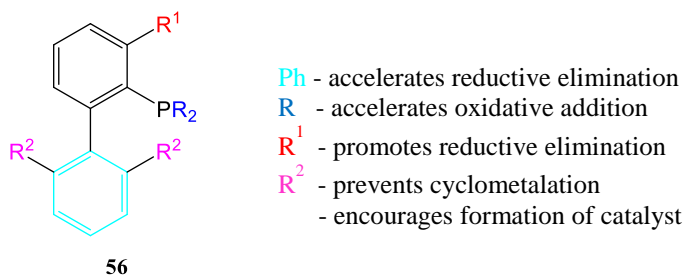


Figure 18. Dialkylbiaryl phosphane ligand system (**56**).

When dialkylbiaryl phosphanes (**56**) are utilized, the catalytically active species is believed to be the monoligated $[L_1Pd^0]$ complex which exists in equilibrium with the thermodynamically favored $[L_2Pd^0]$ species. Many “generations” of the dialkylbiaryl phosphane ligands have been developed to vary the steric bulk and electron-donating abilities of these precatalysts to encourage the formation of this active species. Other variations serve to promote reductive elimination, prevent cyclometalation and retard oxidation (**Figure 18**).⁴⁰ At the time of this publication, Sigma-Aldrich lists forty different catalysts based on this backbone.

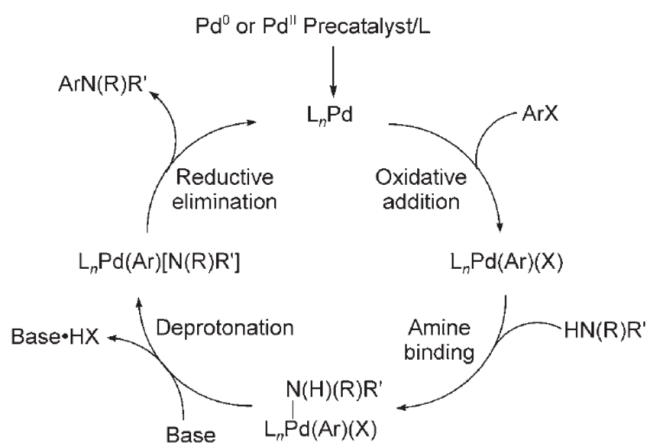


Figure 19. Proposed catalytic cycle for palladium-catalyzed amination.⁴⁰

Although aryl bromides typically undergo oxidative addition with transition metals more readily than aryl chlorides, the bulky $[L_1Pd^0]$ complex is often inaccessible to the sterically encumbered aryl bromide bond. With dialkylbiaryl phosphane-ligated Pd^0 , oxidative addition generally occurs most readily with electron-deficient aryl chlorides and has been demonstrated to allow reaction with unactivated aryl chlorides.⁴⁰

Amine binding follows in the catalytic cycle (**Figure 19**) but the order in which deprotonation and coordination occur is unclear.⁴³ The subsequent reductive elimination is facilitated by the steric bulk of the lower aryl ring and substitution on the phosphorus atom which closes the catalytic cycle.⁴⁰

1.2.2.3.1 “Domino” Double *N*-Arylations

The synthesis of five-membered rings, particularly of the indole type, has found broad applicability of this methodology while the use of palladium catalysis to form six-membered *N*-heterocycles is much less explored. Buchwald-Hartwig methodology has only recently been applied to intermolecular double *N*-arylations.⁴⁴ Significant specificity for these two-fold coupling reactions exists in the selection of palladium source, phosphane ligand, aryl halide and base to the extent where trends have not been adequately established for these variables. When this methodology is applied to unactivated aryl halides, catalyst screening and meticulous optimization are typically required for this coupling reaction to be valuable as an intermediate transformation. Strong bases can be utilized to promote this reaction but this approach often leads to catalyst decomposition.³⁸

Interestingly, no mechanistic insights have been published on how this double *N*-arylation may differ from the single process. While a handful of groups have explored how different catalysts can affect a particular double *N*-arylation reaction,^{38, 45} only one report exists covering the applicability of a particular catalyst to a variety of substrates.⁴⁶ The Laha group describes the reaction as a “domino” process, implying the first *N*-arylation causes the next,⁴⁶ although examples exist elsewhere where exclusively mono-

coupled products could be obtained or both two-fold and mono-coupled products were isolated.³⁸ The regeneration of the catalytically active, thermodynamically disfavored, $[L_1Pd^0]$ complex in close proximity to the adjacent uncoupled aryl halide could lead to an increased rate for the 2nd coupling reaction; however, no evidence exists to support this theory.

CHAPTER 2: RESEARCH GOALS

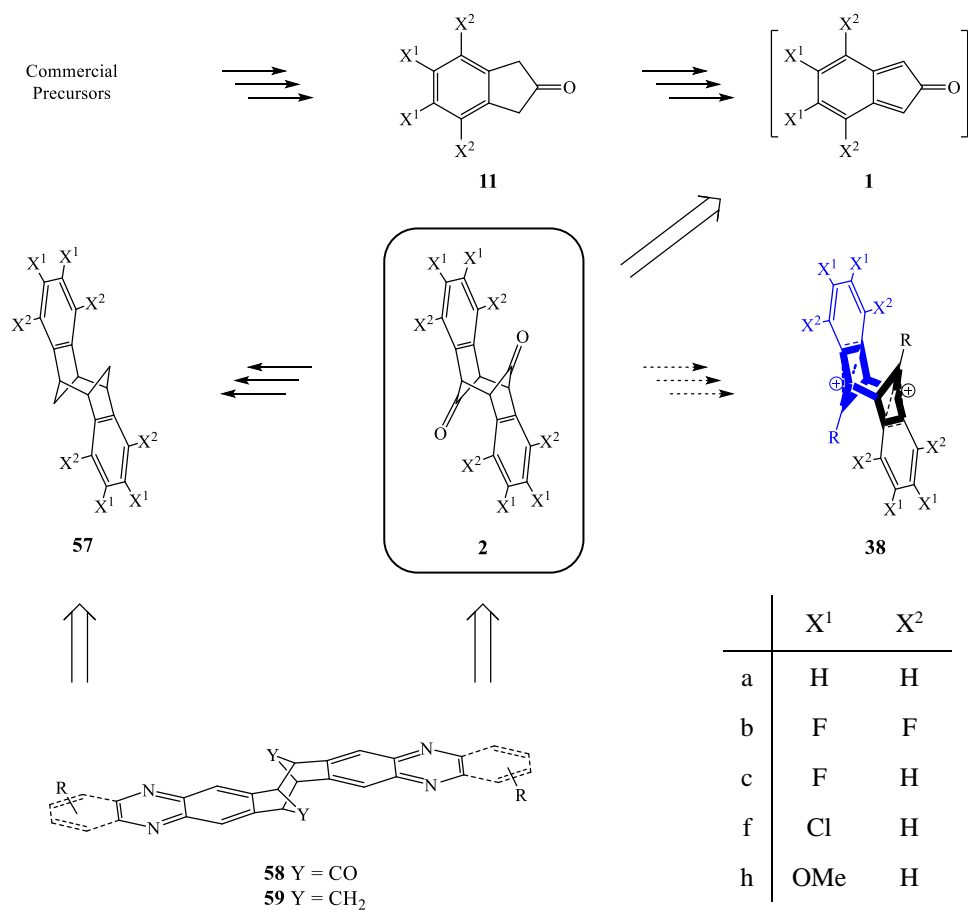


Figure 20. Targeted polycyclic frameworks and compounds from which they are derived alongside a table of the primary thesis-relevant substituents.

While the focus of this work is of preparative nature, unusual polycyclic scaffolds were targeted herein to investigate relatively ‘simple’ isoindenones (**1**) and the reactivity of their respective arene-functionalized dimers (**2**) (**Figure 20**). *N*-Heterocyclic derivatives of these frameworks (**58**, **59**) with judiciously placed functional groups are expected to display unique properties in their solid state that may lead to n-type semiconducting materials. In particular, four specific research goals were formulated:

I) A small library of 2-indanone derivatives (**11**) were targeted as the fundamental precursors to all polycyclic scaffolds targeted in this project. The specific aim of this goal was to optimize synthetic routes toward *ortho*-difluoro- and *ortho*-dimethoxy-2-indanone derivatives (**11c** and **11h**, respectively). These substitution patterns will serve to provide electronic contrast for further experimentation and may be amenable to further arene functionalization.

II) Based on the inability to obtain the tetrafluoro-isoindenone dimer **2b** through the three-step transformation demonstrated on the parent system **2a**, isoindenones with a spectrum of electronic structures (**1c/1h**) were targeted to ascertain structure-reactivity relationships between these fleeting intermediates. An investigation into the reactivity of isoindenone dimer derivatives (**2**) toward formal isoindene dimer derivatives (**57**) was also a primary focus of this project to study their solid-state structures in addition to preparing precursors for the generation of non-classical carbocations (**38**).

III) Utilizing methoxy-substituted *anti*-bisarene scaffolds (**2h** and **57h**), a series of *N*-heterocyclic polycycles (**58** and **59**) were targeted for the rational design of compounds with potential materials science applications. The implementation of various aryl substituents was envisioned to assist in tuning target properties of these novel azaacenes (e.g., HOMO-LUMO gap, charge carrier mobility). The judicious placement and selection of functions has been demonstrated to strengthen intermolecular coupling or insulate fluorescent chromophores, leading to functional devices from various azaacenes.²⁴

IV) A series of non-classical cations (**38**), representing a hybrid architecture of the known tricyclic, sandwiched bishomo-aromatic species **38** (bold, R = H)¹⁷ and the

benzonorbornenyl cation **38** (blue, $R = \text{CH}_3$),¹⁴ were targeted to determine their solid-state structures and spectroscopic properties in collaboration with Dr. M. Gerken (University of Lethbridge). While SPARTAN calculations show almost no substituent effects on the structures of the derived dication, only experimental characterization will confirm or refute these expectations.

CHAPTER 3: RESULTS AND DISCUSSION

3.1 Syntheses, Characterization, and Structures of Selected 2-Indanone Derivatives

Numerous 2-indanone derivatives have been reported in the literature as precursors to functional organic materials or medically relevant compounds (**Figure 21**).⁴⁷⁻⁵² Consequently, various routes to these building blocks have been described with some of these synthetic protocols following unique synthetic avenues to adapt to unusual substituent patterns. Access to the thesis-relevant *ortho*-dimethoxy- and *ortho*-dihalo-2-indanones (**11**) on the multi-gram scale are discussed below.

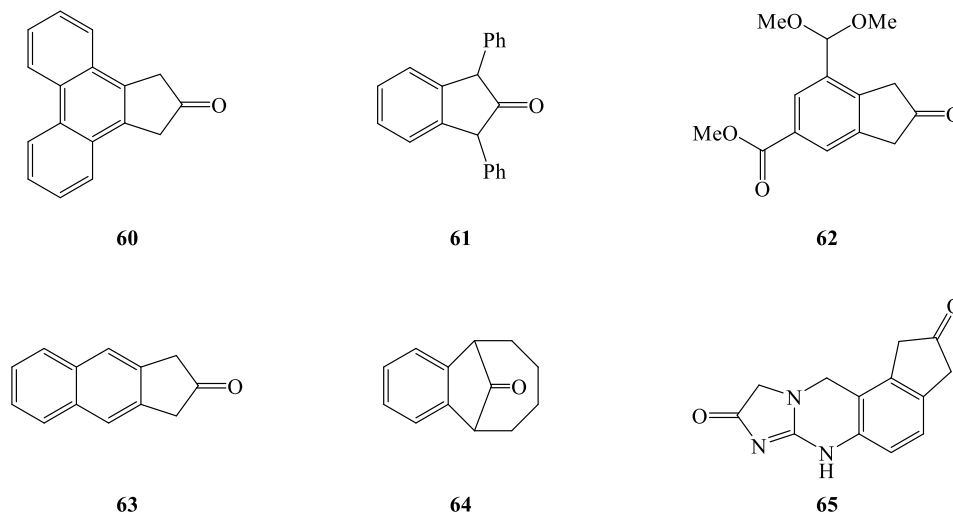


Figure 21. Selected literature-reported 2-indanones.⁴⁷⁻⁵²

3.1.1 Synthesis of 5,6-Difluoro-2-indanone

5,6-Difluoro-2-indanone (**11c**) has been previously utilized as a synthetic intermediate for the preparation of liquid crystals⁵³ or biologically active compounds such as spiro-oxazolone derivatives.⁵⁴ The reported preparations of **11c** follow different

synthetic routes with some steps relying on specialized reagents. In our efforts to obtain compound **11c** along these procedures, we encountered several challenges in the early stage of the project and ultimately followed the sequence depicted in **Figure 22**.

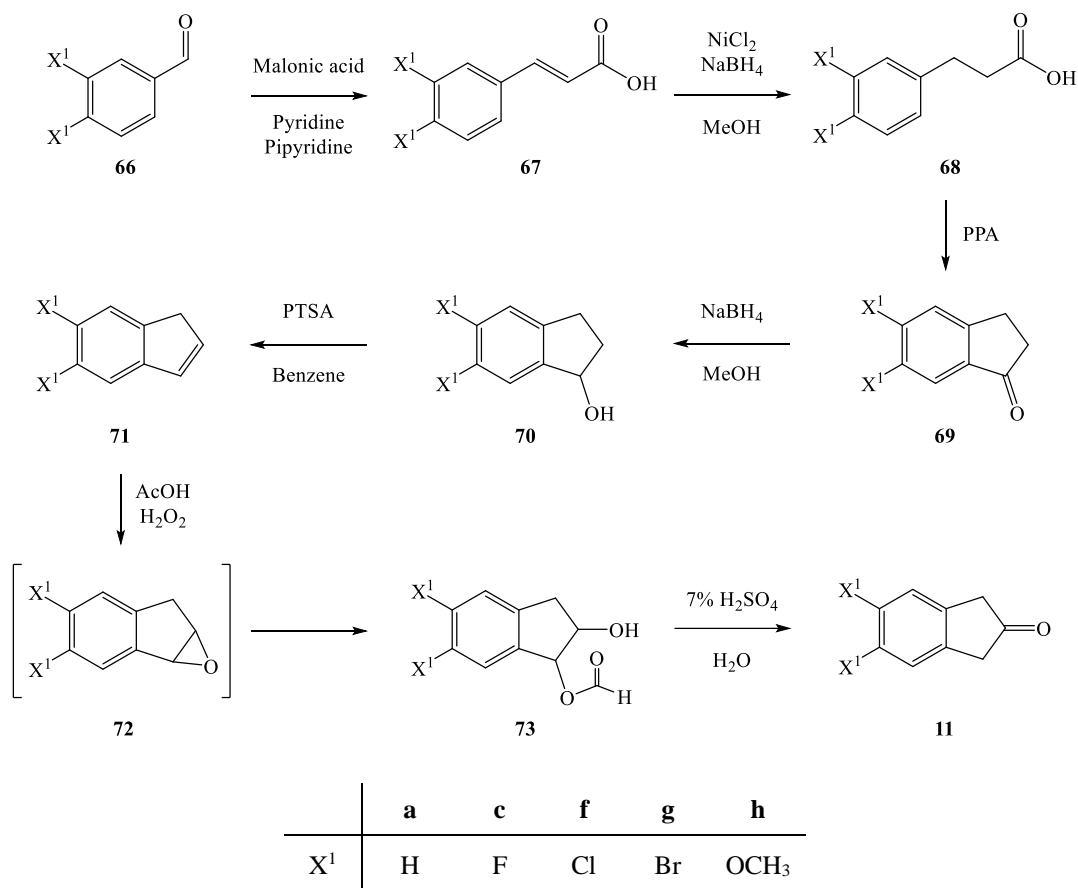


Figure 22. The sequence utilized to produce 5,6-difluoro-2-indanone (**11c**) alongside a table of substitution patterns relevant to this chapter.

Thus, commercially available 3,4-difluorobenzaldehyde (**66c**) was subjected to a Knoevenagel condensation with malonic acid under standard conditions⁵⁵ to afford the corresponding cinnamic acid **67c** quantitatively. Reduction of the conjugated olefinic bond was accomplished by reacting **67c** with in situ generated nickel boride to afford

propionic acid **68c** in 70% yield. Subsequent cyclization to 1-indanone **69c** was mediated by PPA along strict reaction protocols, as high temperature or extended reaction times produced an undesired aldol dimer in varying yields; however, the desired 1-indanone (**69c**) could be easily purified by trituration with ether and final sublimation.

The following ketone transposition had been explored on a variety of 1-indanone derivatives and was frequently accomplished through the acid catalyzed opening of an epoxide intermediate.^{56, 57} The corresponding fluorinated epoxide **72c** was anticipated to be readily accessible from 1-indanone **69c** through the short sequence of carbonyl reduction, elimination, and epoxidation. While the first two reactions proceeded smoothly, the isolation and characterization of the required epoxide (**72c**) proved equivocal at the time.

When MCPBA was utilized as the epoxidizing reagent, partial conversion was evident by ¹H NMR during the first twenty minutes. After this time, the product slowly decomposed through cationic mechanisms to unidentified products while significant quantities of indene **71c** remained. The instability of epoxide **72c** led us to seek an alternative procedure that did not require its isolation. A reaction vetted by Organic Synthesis for the production of the parent 2-indanone **11a** from indene (**71a**) was employed to epoxidize **71c** using in situ generated peroxyformic acid.⁵⁶ Epoxide **72c** was subsequently ring opened by excess formic acid to afford **73c** and transformed to 2-indanone **11c** within a modified steam distillation apparatus. Rather than using a traditional setup where steam is introduced from an external source, it was simpler and equally effective to condense the product onto a condenser loop following hydrolysis and dehydration of **73c** in refluxing 7% aqueous sulfuric acid. This method provided 2-

indanone **11c** in 45% yield over two steps and was scalable to 1 gram, although larger batches occasionally contained the respective 1-indanone (**69c**).

3.1.2 5,6-Dichloro-2-indanone

The moderate similarities between aryl fluorides and chlorides lead us to apply the above synthetic sequence toward 5,6-dichloro-2-indanone (**11f**). Following optimization, **11f** was obtained but the final steps suffered from poor yields and reproducibility. Thus, an alternative synthetic pathway was realized following the same general methodology (*Figure 23*).

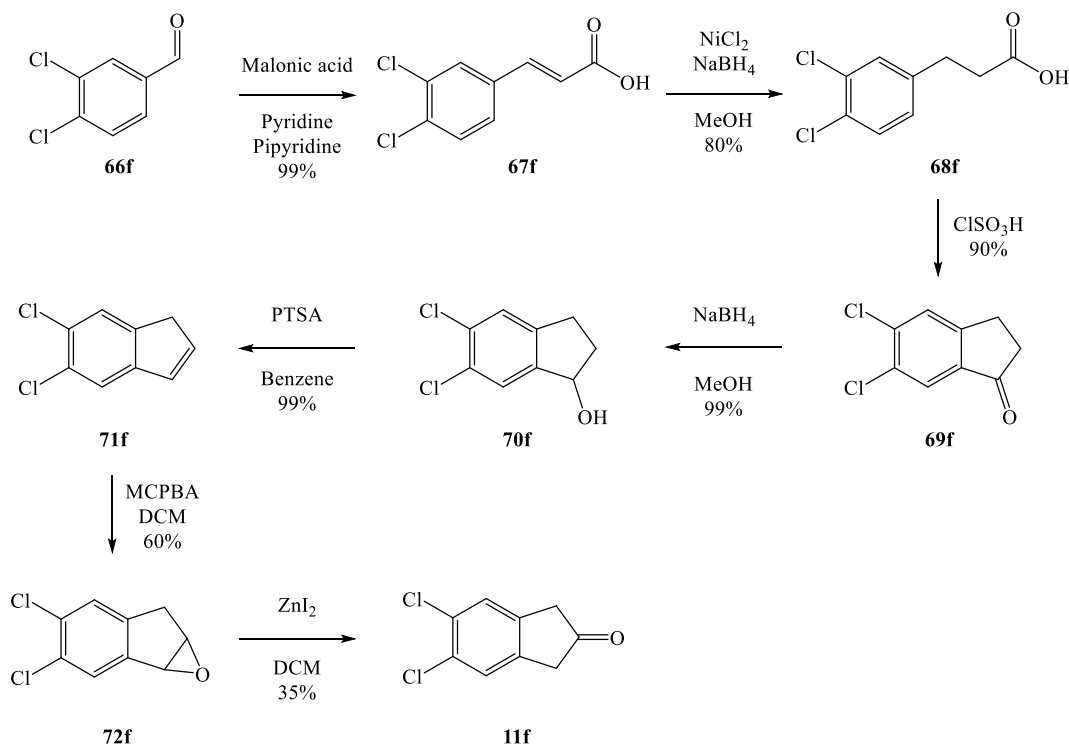


Figure 23. Optimized synthesis of 5,6-dichloro-2-indanone (**11f**).

Optimization was first necessary in the reduction of the poorly soluble cinnamic acid derivative **67f** to the propionic acid **68f**. Following standard protocol, the product was obtained in 65% yield but heating to 60 °C overnight could afford the propionic acid derivative **68f** in 80% yield.

To our surprise, PPA mediated cyclization of 3,4-dichloropropionic acid (**68f**) at 80 °C produced a 1:1 mixture of 6,7-dichloro- and 5,6-dichloro-1-indanone (**69[6,7-Cl]** and **69f**, respectively) (**Figure 24**). Cyclization *ortho* to the 3-fluoro substituent in propionic acid **68c** was not possible due to the strong σ -withdrawing nature of this group but this effect is less pronounced for chlorinated derivative **68f** and led to nonselective cyclizations. Small amounts of aldol condensation products also contributed to the 75% mass balance for the reaction.⁵⁸ The 1-indanones could be isolated from the mixture by sublimation with the same relative ratio between the regioisomers.

A Friedel-Crafts type cyclization was subsequently attempted after conversion to the acyl chloride derivative of **68f** utilizing AlCl₃ in refluxing DCM. Similarly, the reaction produced both 1-indanone regioisomers but the desired product was favored (**Figure 24**). Separation of the products was attempted by column chromatography but only minor enrichment of the desired product was possible after repeated chromatography. Procedures analogous to the fluorinated system were utilized for reduction and dehydration to the corresponding indene regioisomers with retention of their relative abundances near quantitative yield. The two-step procedure optimized for fluorinated 2-indanones was applied to the indenenes and afforded a mixture of chlorinated 2-indanones (**11[6,7-Cl]** and **11f**) with relative abundances similar to the starting material

in 10% isolated yield. At least a gram of 5,6-dichloro-2-indanone (**11f**) was required for further experimentation and the cyclization step was revisited to enhance selectivity.

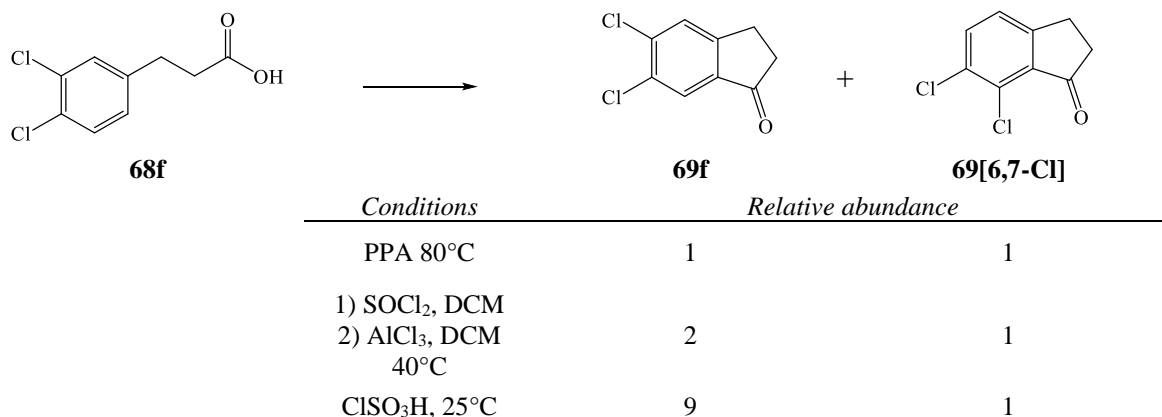


Figure 24. Two 1-indanone products obtained through various conditions from propionic acid **68f**.

Noticing that the lower temperature utilized for the Friedel-Crafts type cyclization favored the desired isomer, kinetic, rather than thermodynamic, control was explored. Thus, chlorosulfonic acid was employed for this cyclization and produced a 9:1 mixture of the 1-indanone products, favoring the desired isomer **69f**.⁵⁹ Trituration with ether was utilized to isolate 5,6-dichloro-1-indanone (**69f**) in 70% yield. Analogously to the 1-indanone mixture previously reacted, this clean material was subjected to the four step ketone transposition⁵⁶ optimized for the fluorinated system and provided a 10% yield of 2-indanone **11f** over the final two steps. In a second attempt, the formate ester intermediate (**73f**) clumped significantly upon refluxing in 7% aqueous sulfuric acid and provided only traces of the product. The clumped material was determined to contain the intermediate **73f** along with significant quantities of unidentified side products and only traces of 2-indanone **11f**. Additional concentrated sulfuric acid was added but the clumps

could not be dispersed and no additional product could be isolated. Reproducibility of the final two steps became an issue as a subsequent attempt, employing the same 1.1 g batch size utilized for the successful reaction, provided no product with identical clumping. The reaction was attempted once more and the intermediate formate ester **73f** was found to contain a significant amount of unrecognizable side products by ^1H NMR and the final step was not attempted.

Although fluorinated epoxide **72c** could not be isolated through MCPBA mediated reaction, successful epoxidations of indenenes possessing electron-withdrawing aryl substituents still made a ketone transposition through this route an attractive option. The same conditions applied to fluorinated indene **72c** were translated to chlorinated **72f** and provided epoxide **72f** in 60% yield. For subsequent rearrangement to the target 2-indanone, zinc iodide was utilized as the Lewis acid catalyst⁵⁷ to afford **11f** with quantitative mass balance. A GC-MS recorded of the crude product appeared to exclusively contain the 2-indanone **11f** but the ^1H NMR contained many aromatic signals with small integration which could not be assigned. Column chromatography was subsequently employed to furnish 2-indanone **11f** in 35% yield. A methanol wash of the column recovered the remaining mass but contained unidentified rearranged products due to interaction of the acidic α -hydrogens with silica gel.

3.1.3 5,6-Dimethoxy-2-indanone

5,6-Dimethoxy-2-indanone (**11h**) was previously reported in the literature as a synthetic intermediate for pharmaceuticals and was accessible through an eight-step sequence starting from phthalide **20**.⁶⁰ In the interest of utilizing familiar reaction

conditions and probing the applicability of the sequence depicted in **Figure 22**, the procedures optimized for the syntheses of electron-deficient 2-indanones **11c** and **11f** were applied to 3,4-dimethoxy-benzaldehyde (**66h**). Without significant deviation from the optimized protocols, 5,6-dimethoxy-1-indanone (**69h**) was obtained in 40% yield over three steps.

Compound **69h** crystallizes in the monoclinic system with the space group $P2_1/c$ and exhibits typical bond lengths and angles. The carbon scaffold of 1-indanone **69h** was not planar in the solid state as the 6-methoxy group deviated by 10.1° . T-shaped arene interactions were present as the proton on carbon 5 is oriented toward the high electron

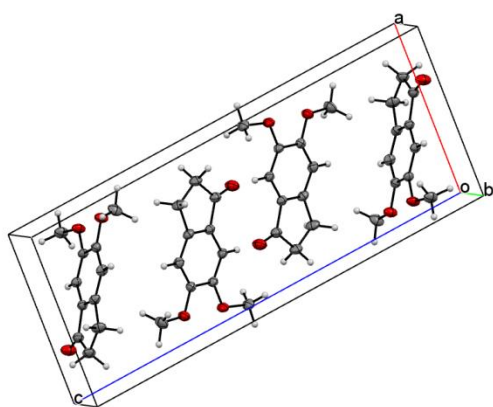


Figure 25. Crystal structure and unit cell of 5,6-dimethoxy-1-indanone (**69h**).

density over the aromatic ring while the planes of these two arenes are offset by 65.9° . The molecule pairs that lie over the faces of one another are inverted to offset the strong molecular dipole. Steric effects

elongated the 6-7 arene bond to 1.424 Å while ring strain contracted the 3'-7' arene bond to 1.362 Å. Conjugative effects contracted the 1-9 σ bond to 1.468 Å and stretched the carbonyl bond to 1.214 Å.

While the reduction to the 5,6-dimethoxy-1-indanol (**70h**) proceeded in 95% yield, the envisioned sequence to 2-indanone **11h** failed in the dehydration step. The cation intermediate **74** was more stable than any indanol derived cations previously generated for this project due to the increased resonance structure provided by the 5-

methoxy group (**74'**). This cation reacted with an indene molecule to afford dimer **75** as previously reported (*Figure 26*).⁶¹

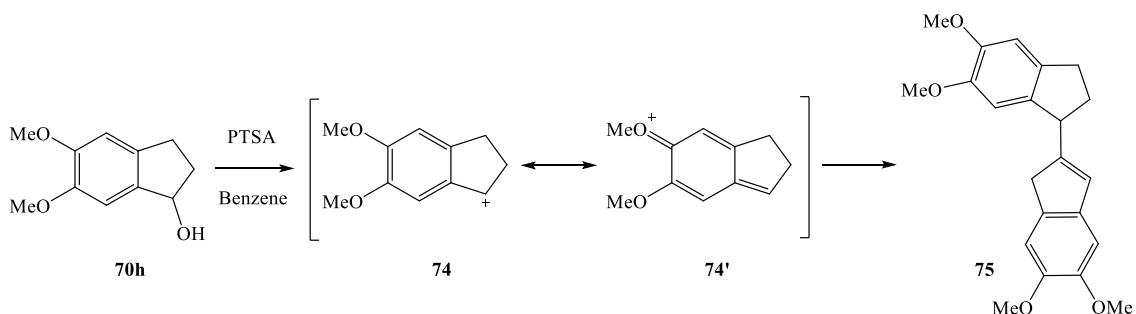


Figure 26. Formal indene dimer (**17**) obtained through the dehydration of indanol **70h**.

As we had already optimized reactions toward 5,6-dimethoxy-1-indanone (**69h**) on a multigram scale, we sought to scale up a reported four-step procedure that obtained milligram quantities of 2-indanone **11h** by preparatory TLC (*Figure 27*).⁶² In our hands, no conversion occurred in the final step of oxalic acid-catalyzed dehydration of diol **77**. In an isolated incident, the hydrolysis after borane-mediated reduction of dicarbonyl **76** produced 2-indanone **11g**, rather than diol **77**, in nearly quantitative yield. The striking result was never reproduced where variations of the acid concentration, reaction time, and temperature only produced product mixtures.

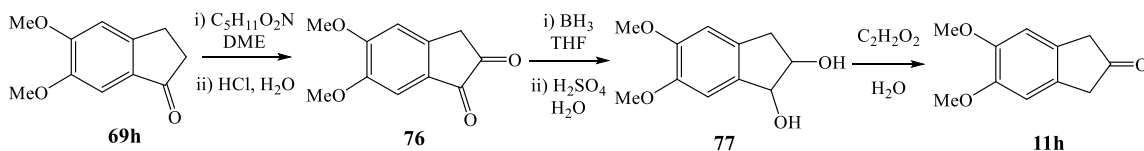


Figure 27. Reported preparation of 5,6-dimethoxy-2-indaone (**11h**).⁶²

The PTSA catalyzed dehydration in benzene was the only reproducible procedure found to afford 2-indanone **11h** from diol **77**. A 10% isolated yield was obtained after silica chromatography while decomposition was observed on neutral alumina.

Due to the quickly diminishing mass balance from this sequence, the general approach published by J.B. Taylor et al.⁶⁰ was modified to decreased the number of steps and avoid hazardous reagents (**Figure 28**). Rather than starting from phthalide **78** as published,⁶⁰ veritrol (**79**) was utilized to afford bisbromomethyl derivative **80** in a single step.⁶³ To avoid gaseous HCl,⁶⁰ solvolysis of the dinitrile derivative **81** was completed with SOCl₂ in methanol to afford diester **82** in 70% yield.⁶⁴ Conserving the hallmark step of the published sequence, an analogous Diekmann condensation was utilized to produce the 2-keto methyl ester **83** in 32% yield.⁶⁰ This step allowed for the extraction of all non-ionic intermediates following anionic cyclization and eliminated the need for purification prior to this step.

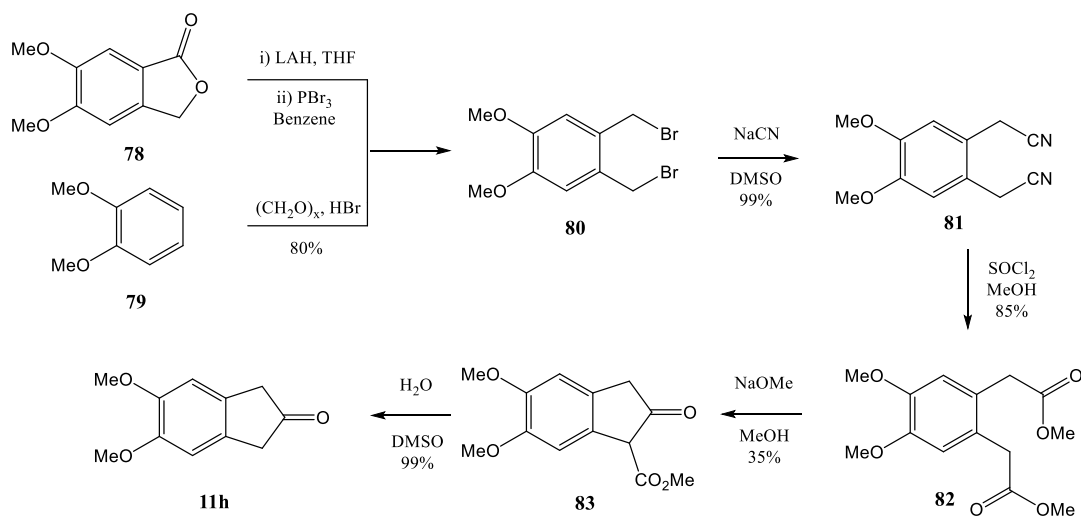


Figure 28. The optimized synthesis of 5,6-dimethoxy-2-indanone (**11h**) following the general methodology reported by J.B. Taylor et al.⁶⁰

Following the published single-pot hydrolysis and decarboxylation of β -keto ester **83** in 20% aqueous sulfuric acid,⁶⁰ 2-indanone **11h** could be obtained in adequate purity in 40% yield as a beige crystalline solid. Batch-to-batch variations became particularly evident during attempts scale the reaction up to 500 mg as significant clumping of the organic material occurred in the aqueous solution. The addition of inert boiling chips or vigorous mechanical stirring were utilized in an attempt to disperse the clumps to no avail.

A column chromatography using benzene as the eluent was performed as described⁶⁰ using nearly pure 2-indanone **11h**, but significant retention was evidenced over a short pad of fluorisil. The crude mass could be recovered via a methanol wash but slight decomposition was evident. Attempts at chromatography on alumina afforded a similar 30% recovery with significant decomposition occurring.

After optimization failed with the published reagents, the use of an alternative acid was explored. 20% aqueous HCl was initially selected but no changes were evident. Thus, it was deemed necessary for the reaction to occur in solution to circumvent this clumping. Although β -keto ester **83** was soluble in dichloromethane, trifluoroacetic acid⁶⁵ effected no reaction while the use of PTSA in benzene produced a complex product mixture. Conditions from a patent were later explored that had produced a 1-phenyl-2-indanone derivative from its β -keto ester in milligram quantities.⁶⁶ Without the need of a strong acid as typically described, simply heating a solution of β -keto ester **83** in a 9:1 mixture of DMSO:water accomplished this transformation and produced analytically pure 2-indanone **11h** in quantitative yield, albeit containing residual DMSO. This reaction was easily scaled up to over 6 grams.

Compound **11h** crystallizes in orthorhombic system with the space group *Pnma* and exhibits typical bond lengths and angles. Unlike 1-indanone **69h**, all carbon and oxygen atoms were planar. Molecules stacked parallel over one another were oriented in opposing directions and slipped from one another so both protons on the 1 carbons were 2.599 Å from the center of either arene unit. The low electron density around in the plane of the molecule allows for a further stabilizing interaction of the 4-proton with the

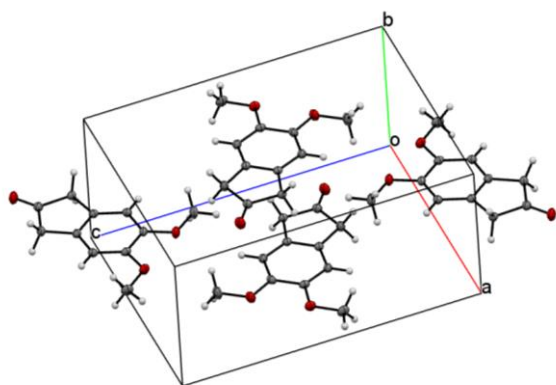


Figure 29. Crystal packing of 5,6-dimethoxy-2-indanone (**11h**).

oxygen in the 5-methoxy group of an adjacent molecule angled 64.1° from each other within the same plane.

Similar to 1-indanone **69h**, the 5-6 carbon bond is elongated due to steric repulsion of the methoxy groups (1.422 Å). This strained bond along, with strain from the 5-membered ring, compressed the 3'-8' arene bond (1.386 Å).

3.1.4 Toward 5,6-Dibromo-2-indanone

The synthesis of 5,6-dibromo-2-indanone (**11g**) was previously reported⁶⁷ using methodology that differed significantly from our general approach. Rather than starting with a substituted benzaldehyde, the aryl bromines were introduced onto the aromatic ring of the indane scaffold by means of electrophilic aromatic substitution.

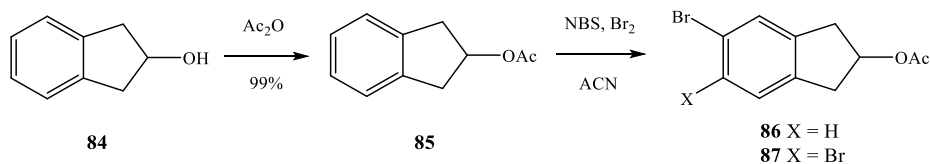


Figure 30. Efforts completed toward the synthesis of 5,6-dibromo-2-indanone (**11g**).

When the bromination procedure was attempted in our hands, the first electrophilic aromatic substitution proceeded rapidly to monobromo **86** but only traces of the dibrominated product **87** were observed. After stirring the reaction for a month with a large excess of NBS and Br_2 , only 20% conversion to dibromo **87** was observed. FeBr_3 was added as a catalyst to an otherwise identical reaction completed in tandem, but no improvements were made. After repeated chromatography, the product could only be enriched to a 1:1 mixture of monobromo **86** to dibromo **87**. These conditions only deviated from those reported in the use of acetonitrile from a dry solvent system rather than freshly distilled from P_2O_5 . Any water present in the reaction would hinder the generation of reactive the bromonium species and hydrolyze NBS.

Through this project, diverse synthetic approaches toward 2-indanones were explored while meticulously optimized sequences provided gram quantities of these precursors for isoindenone generation and dimerization. The various substituents effected unique reactivities in pursuit of their 2-indanone derivatives according to their electronic requirements. This individual nature was expected to translate to their corresponding isoindenone derivatives while select substituents were envisioned to be amenable to *N*-heterocyclic arene extension.

3.2 Novel Arene-Substituted Isoindenone Dimers

Our group's recent focus has been centered on the generation and dimerization of a small library of relatively 'simple' isoindenones to correlate substituent effects with their dimerization behavior – an important factor for further synthetic applications of these fleeting intermediates. The isoindenone dimer **2** represents the central unit of our synthetic platform and, in the context of this thesis, derivatives bearing *ortho*-difluoro or -dimethoxy groups were investigated to provide electronic contrast and functional groups amenable to further synthetic transformations.

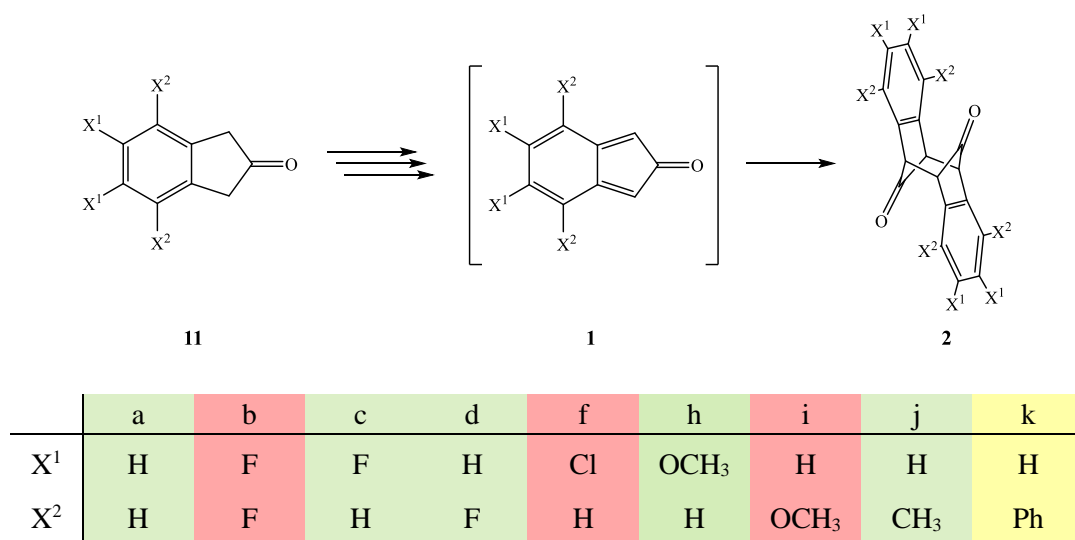


Figure 31. General scheme for isoindenone generation and dimerization including a table with substituent patterns that either delivered dimer **2** (green), did not (red), or were inconclusive (yellow).

3.2.1 Fluorinated Isoindenone Dimers

The formal dimer of tetrafluoroisoindenone (**2b**) has so far been an elusive target for the Etzkorn group that has been approached through various methodologies (**Figure 32**).¹³ Most notably, an elegant route utilized by Jones¹ for isoindenone generation and

dimerization was optimized and applied towards our target by Alexander B. Smith of our group. Through an analogous, synthetically challenging, three-step procedure starting from tetrafluoro-2-indanone **11b** (**Figure 33**), only poorly characterized, presumably polymeric, material could be obtained. Jones' report provided no analytical details of isoindenone dimer **2a** and the sequence was reproduced to fully characterize the product and serve as a control. Thus, we began investigating this unsuccessful translation to identify whether the degree of fluorination or substitution at a particular position was responsible for the change in reactivity. Against our intuition, we were able to generate both *ortho*-difluoro and *para*-difluoro-isoindenone intermediates and obtained the two dimers **2c/2d** in 40-50% yield. The present thesis work describes the preparation of *ortho*-difluoro *anti*-dibenzo derivative **2c**, its spectroscopic characterization and its crystal structure.

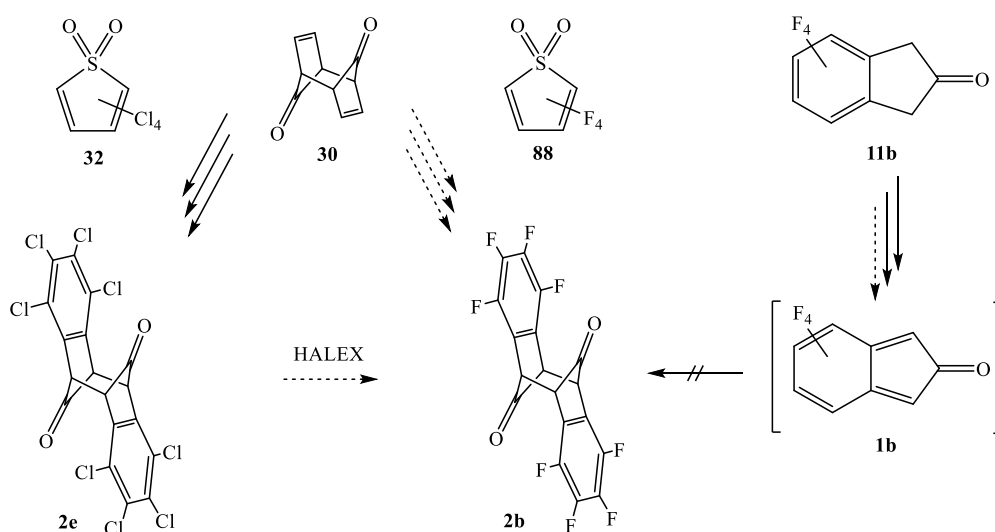


Figure 32. Attempted synthetic routes toward the formal tetrafluoro-isoindeneone dimer **2b**.

3.2.1.1 *Ortho*-Difluoro-Isoindenone Dimer Synthesis

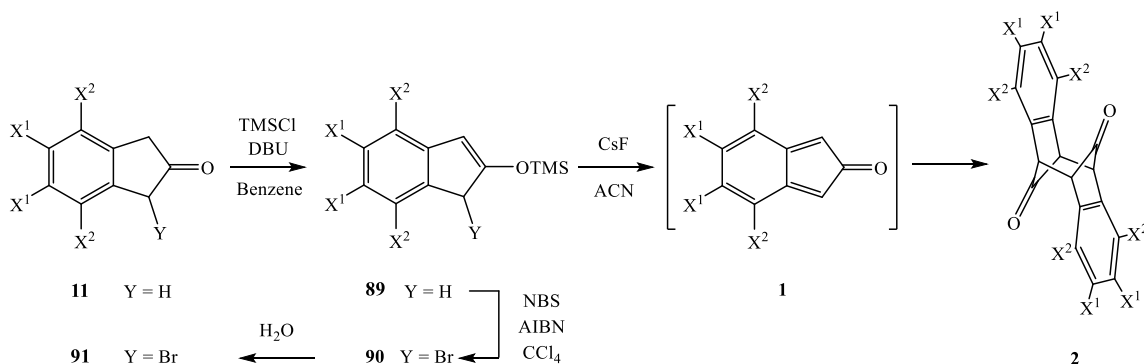


Figure 33. Synthetic route utilized for isoindenone generation and dimerization from substituted 2-indanones (**11**).

To probe the effect of partial fluorination on isoindenone generation and dimerization, 5,6-difluoro-2-indanone (**11c**) was subjected to an analogous procedure utilized for the preparation of the parent isoindenone dimer **2a**.¹ Thus, silyl enol ether **89c** was synthesized along an optimized protocol utilizing DBU, rather than LDA as described, to generate the enolate intermediate so low temperature could be avoided. NBS radical bromination proceeded rapidly to afford bromo-silyl enol ether **90c** in less than ten minutes rather than the two hours reported for the synthesis of parent **90a**. Fluorinated **90c** proved to be hydrolytically labile as some 5,6-difluoro-1-bromo-2-indanone (**91c**) was occasionally present after aqueous workup. This side product displayed an easily recognizable pair of doublets in the ¹H NMR from the magnetically inequivalent methylene protons. Alternatively, 1-bromo-2-indanone derivative **91c** could arise from small amounts of 2-indanone **11c** left over from the previous step; however, hydrolysis of bromo-silyl enol ether **90c** was demonstrated in solution as an NMR sample slowly converted to 2-indanone **11c**.

Generation of 5,6-difluoro-isoindenone (**1c**) and subsequent dimerization were accomplished analogously to the parent system **2a**. Slow addition of bromo-silyl enol ether **90c** to a refluxing suspension of cesium fluoride in acetonitrile was required to minimize polymerization of the reactive intermediate. The mass balance following an aqueous workup was typically near quantitative over three steps but multiple, presumably polymeric, side products remained in minute quantities. Purification of **2c** was accomplished by dissolving the mixture in acetone and precipitating the desired product through the addition of pentane. Typically, three repetitions were required to afford the clean *ortho*-difluoro-isoindenone dimer **2c** in 50% yield. The high C_{2h} symmetry of dimer **2c** led to facile NMR data interpretation as only two sets of magnetically equivalent protons, five sets of carbons, and one set of fluorines were present. The aromatic protons and fluorine signals appeared as pseudo-triplets due to strong $^3J_{\text{HF}}$ and $^4J_{\text{HF}}$ coupling interactions.

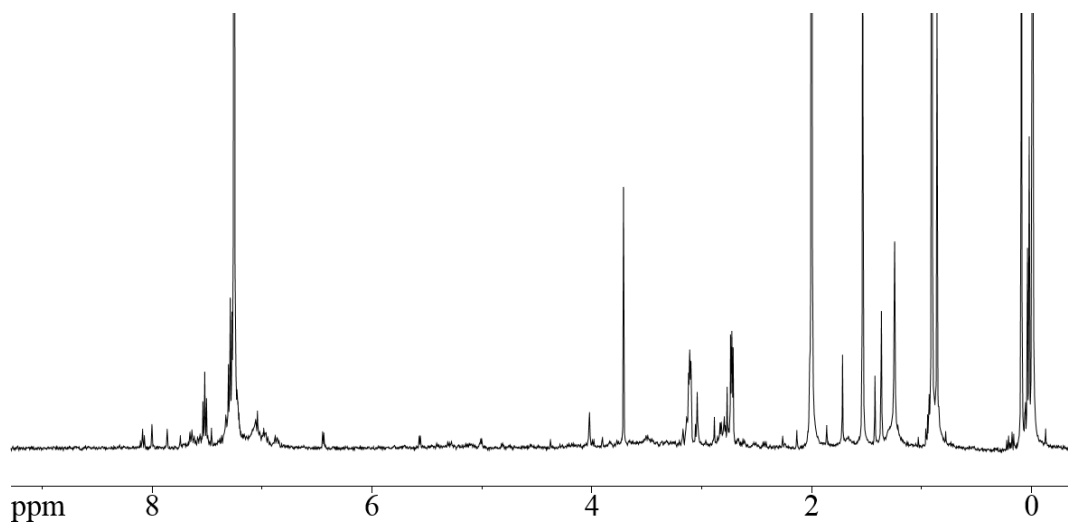


Figure 34. A typical crude product obtained following *ortho*-difluoro-isoindenone generation and dimerization.

Occasionally present in large batches, broad peaks were observed over 6.5-8.5 and 2.5-4 ppm in the ^1H NMR (500 MHz, CDCl_3), presumably corresponding to polymeric material, that could not be removed via crystallization. This impurity is further discussed in Chapter 3.2.2.2 as similar broad peaks were present following the preparation of all other isoindenone dimer derivatives. While isoindenone dimer **2c** could be readily characterized by ^1H and ^{19}F NMR, its poor solubility prevented adequate characterization by ^{13}C NMR. Further confirmation of the product was obtained by DI-MS and X-ray diffraction of a single crystal.

Ortho-difluoro-isoindenone dimer **2c** crystallized in a monoclinic system with the space group $P2_1/c$. The molecular structure exhibited typical bond lengths and angles other than the two new bonds formed between formal isoindenone molecules (1.588 Å). Unlike the parent isoindene dimer **2c** (*Figure 35*), the π -faces exhibited significant

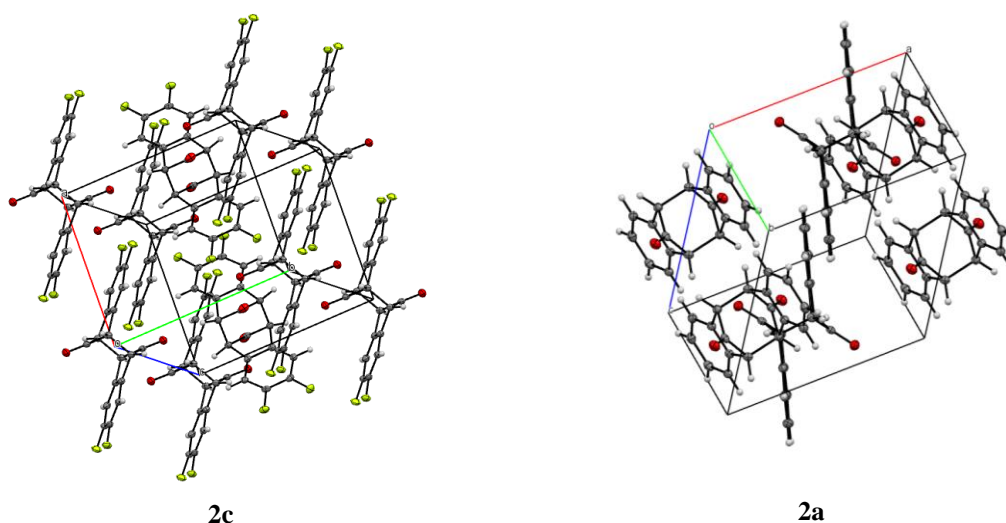


Figure 35. Unit cell of *ortho*-difluoro-isoindenone dimer **2c** and the parent isoindenone dimer **2a**.

interaction with one another in the solid state through four short carbon-carbon contacts per molecule (*Figure 36*). These interactions lead to a chain-like substructure within the

crystal where molecules were oriented parallel to one another and slipped by 8.312 Å along the long axis and 0.994 Å over the short axis of the molecule. In addition to the π - π stacking, this orientation was also driven by strong dipole-dipole interactions between the electronegative fluorines oriented over either carbonyl carbon (**Figure 36a**).

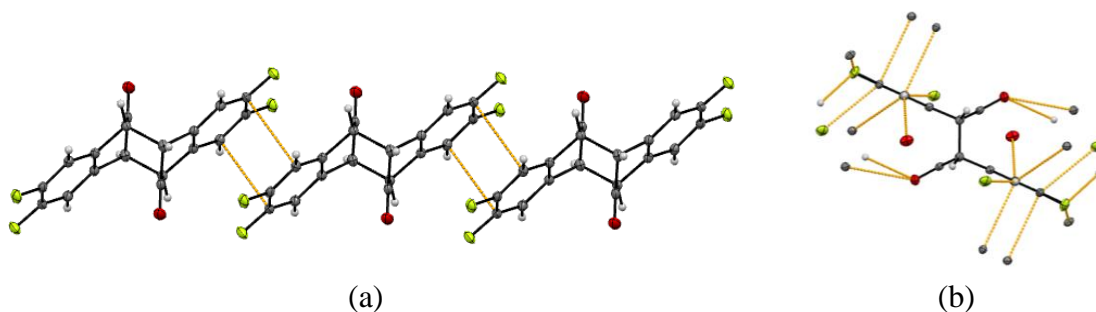


Figure 36. (a) Partial crystal system of *ortho*-difluoro-isoindenone dimer **2c** showing face to face π -stacking interactions and (b) all short contacts (orange).

The crystal system was more complex than this chain as each molecule had short contacts to twelve others. On the arene face opposite of that exhibiting face-to-face interactions, additional π -stacking was evident through a T-shaped interaction of a $7\text{-H}^{\delta+}$ separated by 3.250 Å from the arene centroid. The low electron density within the arene plane also led to a $7\text{-H}^{\delta+}\cdots\text{O}^{\delta-}\cdots 7\text{-C}^{\delta+}$ short contact. Between the same pair of molecules, a $6\text{-F}^{\delta-}\cdots 5\text{-C}^{\delta+}$ short contact is also present. Through interaction with a separate molecule, a $6'\text{-F}^{\delta-}\cdots 4\text{-H}^{\delta+}$ close contact also aids to stabilize the crystal system. All interactions are symmetrical to produce a total of twenty short contacts per molecule.

3.2.1.2 Additional Fluorinated Isoindenones

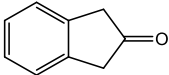
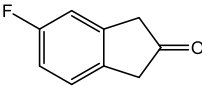
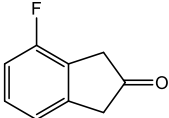
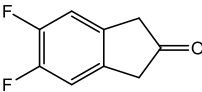
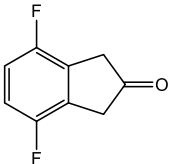
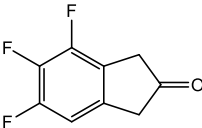
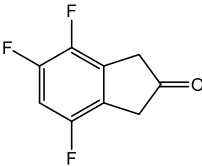
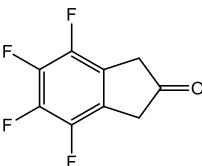
The successful production of *ortho*-difluoro-isoindenone dimer **2c** without significant deviation from the parent system **2a** did not provide significant insight into the

previous failure to obtain the tetrafluoro-isoindenone dimer **2b** along this route. Thus, our group has explored the generation and dimerization of other fluorinated isoindenones.

4,7-Difluoro-2-indanone (**11c**), 4-fluoro-2-indanone (**11[4-F]**) and 5-fluoro-2-indanone (**11[5-F]**) were subjected to the typical three-step protocol to furnish their expected *anti*-benzo scaffolds (**2**). Selective dimerization of the unsymmetrical monofluoro systems would have provided information concerning the electronic effects of fluorine at either position, but two products were obtained. The two products from each monofluoro dimerization were synthesized in almost equal amounts, reflecting the high reactivity of the short-lived isoindenones.

When the same three-step sequence was applied to 4,5,6-trifluoro-2-indanone (**11[4,5,6-F]**) and 4,5,7-trifluoro-2-indanone (**11[4,5,6-F]**), no distinguishable products were obtained. Only slight humps over the aromatic were observed in the ¹H NMR for either system. Unfortunately, no concrete trends could be drawn from these eight fluorinated systems other than the inability to obtain defined products from isoindenones possessing three or more fluorine atoms.

Table 1. Summary of fluorinated isoindenone generation attempts.

2-Indanone derivative		Result of attempted isoindenone generation
1		3a (60% yield)
1[5-F]		two different <i>anti</i> -dibenzo dimers of type 3 (40% yield)
1[4-F]		two different <i>anti</i> -dibenzo dimers of type 3 (20% yield)
1c		3b (50% yield)
1d		3d (50% yield)
1[4,5,6-F]		polymer formation
1[4,5,7-F]		polymer formation
1b		polymer formation

3.2.2. Isoindenone Dimers Incorporating Electron-Donating Arene Substituents

Considering the individual reactivities of fluorinated isoindenone derivatives along the Jones route,¹ species with other steric and electronic requirements shifted into our focus. Furthermore, selected derivatives could become amenable to further synthetic transformation of the arene units. While nucleophilic aromatic substitution is possible on fluorinated arenes, these reactions are often difficult to control and minimally tolerant of other functional groups. In the context of this thesis, it was of interest to introduce functional groups amenable to rectilinear *N*-heterocyclic arene extension onto the aromatic rings of this scaffold (Chapter 3.3). Methoxy-substituted scaffolds were targeted not only for their reactivity as alcohol or carbonyl equivalents, but also to further explore the applicability of Jones' synthetic strategy for isoindenone generation.

3.2.2.2 Methoxy-Substituted Isoindenone Dimer Synthesis

5,6-Dimethoxy-2-indanone **11h** was subjected to the optimized three-step isoindenone generation protocol and delivered the targeted [4+4] π dimer **2h**. Optimization of this sequence was required in the silylation as 2-indanone **11h** was poorly soluble in benzene. Utilizing 1.1 equivalents of DBU and TBDMSCl, the reaction was particularly sluggish and could not be driven to completion unless an additional 0.3 equivalents of both reagents were added. Owing to the stabilizing effect of the 5-methoxy group, the activation barrier for NBS bromination was lowered and the radical reaction producing bromo-silyl enol ether **89h** could be completed at room temperature in less than ten minutes. Subsequent isoindenone generation furnished dimer **2h** and some unidentified side products with a quantitative mass balance over three steps. Initial

purification of the amply soluble dimer was accomplished by precipitating the product with *n*-pentane from acetone thrice to afford **2h** in 45% yield, although some, presumably polymeric, side products remained.

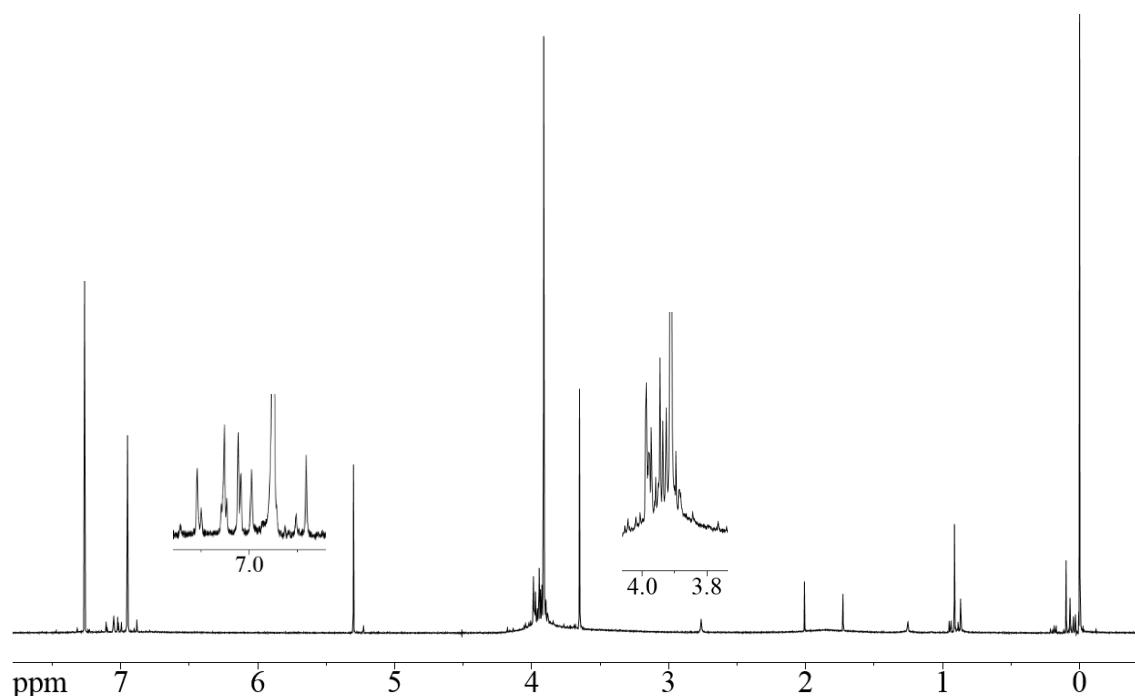


Figure 37. Crude spectrum of *ortho*-methoxy isoindenone dimer **2h** following aqueous workup. (Note: DCM contaminate identified at 5.30 ppm)

Analytically pure isoindenone dimer **2h** could be isolated from the mixture by column chromatography in only 10% isolated yield as undesired streaking was observed. Washing the column with methanol recovered the crude mass that contained significant amounts of the desired product. Crystals of purified **2h** were grown from the chromatographed material in both 1,2-dichloroethane and chloroform, but both sets quickly weathered upon exposure to air. These crystals were likely solvent inclusion complexes with limited stability which lead to rapid solvent evaporation and crystal degradation upon removal from a solvent-saturated environment.

The polymeric material was particularly pronounced when the sequence to methoxy-substituted dimer **2h** was scaled up to gram quantities. The ^1H NMR (500 MHz, CDCl_3) showed broad signals with low intensity over the 3.2-4.3 and 6.5-7.5 ppm regions, corresponding to aromatic and aliphatic protons. These ‘humps’ resembled signals one might expect for exchangeable protons but their ^1H NMR signal structure was unaltered in spectra recorded at various temperatures between -60 and 50 $^\circ\text{C}$.

Although the composition of this side product could not be determined, evidence exists for a similar polymeric material following isoindenone generation for all other derivatives studied. In select cases, this material was obtained exclusively (**Table 1**). Methoxy substituents generally provided the most visible broad ^1H NMR peak, due to their six protons per isoindenone subunit, while aromatic signals were occasionally masked by the baseline. A similar, less intense, broad aromatic signal was present from the attempted synthesis of tetrafluoro-isoindenone dimer **2c** in the ^1H NMR from 2-4 ppm while two overlapping broad signals were distinguishable in the ^{19}F NMR. Broad ^1H NMR signals were also evident in the aromatic region from the synthesis of the *ortho*-difluoro dimer **2c** with minimal indication elsewhere in the spectra. In an isolated case, *ortho*-difluoro-isoindenone **1c** delivered a significant fraction of the polymer where broad signals over the aliphatic region were also observed (**Figure 38**). Broad ^{19}F signals were not distinguishable following isoindenone generation but could have been masked by the baseline. Organic polymers typically have an abundance of sharp signals but the high reactivity of isoindenones through plausible radical, ionic and cycloaddition pathways was thought to produce a broad distribution of products.

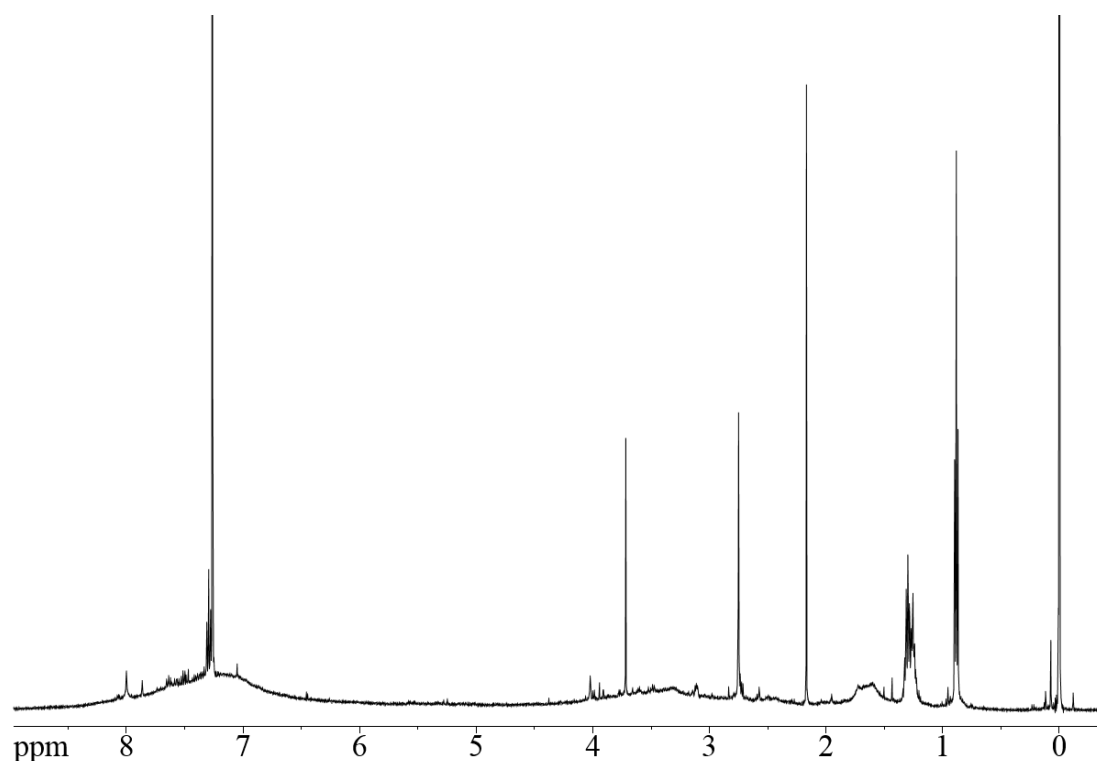


Figure 38. An atypical ¹H NMR (500 MHz, CDCl₃) recorded following *ortho*-difluoro-isoindenone (**1c**) generation.

3.2.2.3 Additional Isoindenone Derivatives Possessing Electron-Donating Aryl Substituents

The generation and dimerization of *ortho*-dimethoxy-isoindenone **2e** did not deviate significantly from other systems in ways that provided insight into its electronic structure. Other derivatives were subsequently explored by Victoria L. Hamilton, Kyle Moran and Markus Etzkorn to provide electronic and steric variations.

Para-dimethoxy-isoindenone dimer **2i** was targeted concurrently in our group but ultimately failed to produce the expected product. Evidence was obtained for an isoindenone dimer through direct-insertion mass spectrometry but its structure could not be elucidated. The additional steric bulk of the methoxy groups in close proximity to the reactive carbon was proposed to explain this result, thus other *para*-substituted systems

were investigated. Substantiating this hypothesis, the smaller *para*-dimethyl isoindenone dimer **2j** was successfully synthesized from its 2-indanone derivative (**11j**) while inconclusive results were obtained from the dimerization of the further sterically demanding *para*-diphenyl-isoindenone **1k**. ^1H NMR appears to indicate dimer formation in the latter case and this derivative is currently under investigation.

3.2.3 Spectroscopic Data of Isoindenone Dimers

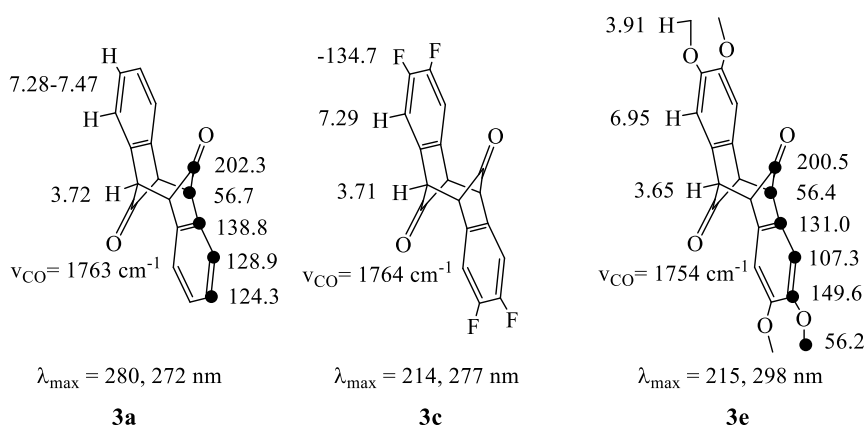


Figure 39. Spectroscopic comparison between isoindenone dimers. All NMR data was recorded in CDCl_3 and reported in ppm from a TMS standard. UV-Vis Data was recorded in ACN.

3.3 Synthetic Transformations and Characterization of Isoindenone Dimer Derivatives

The reduction of substituted isoindenone dimers **2a**, **2c** and **2h** to novel formal isoindene dimers **57a**, **57c** and **57h**, respectively, was subsequently explored to obtain trends in their solid-state packing motifs, spectroscopic properties and in their photochemical and thermal stabilities. Further functionalization of these scaffolds toward azaacenes of interest for materials science applications was envisioned and carbonyl reduction was desirable so subsequent transformations could be focused on the arene

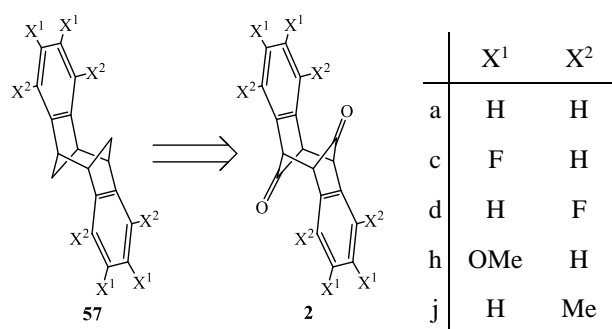


Figure 40. Isoindene dimers (**57**) targeted through carbonyl reduction of their corresponding isoindenone dimers **2**.

units without concerning additional functional groups (Chapter 3.3). This reduction also decreases the steric demands about the center of the scaffold and was predicted to allow arene-arene interactions in the solid state – a property desirable for functional organic semiconductors. Isoindene dimers possessing arene substituents of inverse electronic demands (i.e., electron-withdrawing fluorines or electron-donating methoxy groups) were targeted to introduce local dipoles and study their effects on solid-state packing. Furthermore, the photochemical and thermal stabilities of these novel scaffolds may provide important data about cycloreversion reactions to their isoindene monomers while either set of substituents may direct a particular mode of fragmentation (e.g., methoxy substituents at the proper position may stabilize radicals through resonance).

While at least three groups attempted to synthesize the parent isoindene dimer **57a** – either involving the generation of isoindene **1a** as a fleeting intermediate or by photochemical reaction – Alexander B. Smith of our group prepared the unusual polycycle for the first time. The formal isoindene dimer **57a** was previously targeted through photochemical extrusion of C₂O₂ from compound **92**, but the fleeting intermediate **93** forms a different dimer (**94**) via an $[8\pi+8\pi+2\sigma]$ reaction. Photochemical reaction of styrene derivative **95** was also sought for the synthesis of the formal isoindene dimer **57a** but only polycycle **96** was obtained.

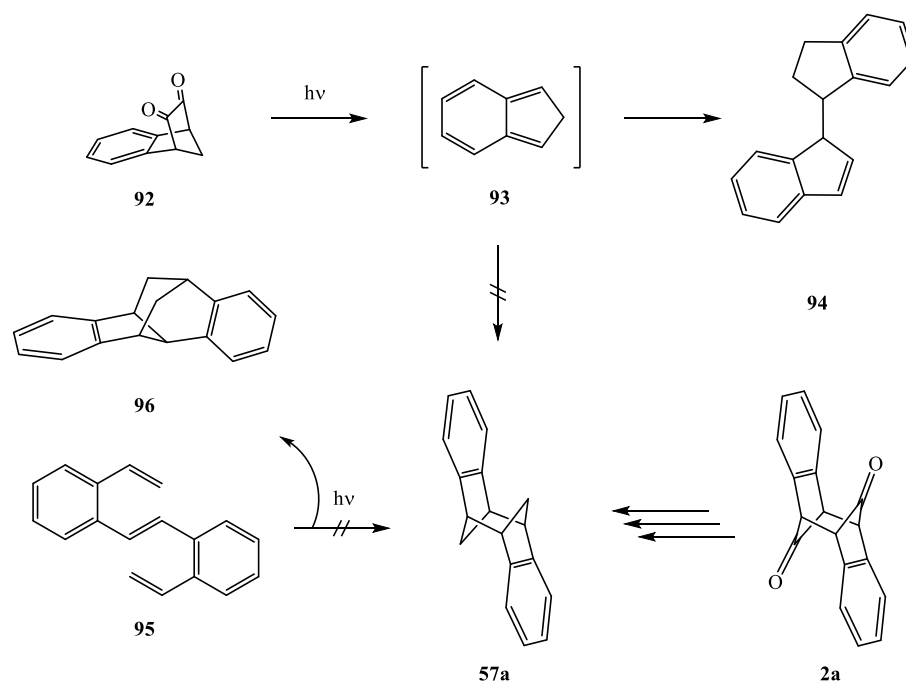


Figure 41. Attempted syntheses of the formal isoindene dimer **57a**.

The seemingly trivial double carbonyl reduction on parent isoindenone dimer **2a** could only be solved through a short reaction sequence (**Figure 42**) that posed several preparative challenges and provided some surprising outcomes. Intermediates along this pathway also served as precursors for the generation of non-classical carbocations. While our group has prepared, isolated and characterized two additional isoindene dimer derivatives (**57c**, **57j**), there remain challenges in the preparation of fluorinated derivatives.

3.3.1 Toward the Formal *Ortho*-Difluoro-Isoindene Dimer

The formal fluorinated isoindene dimer **57c** was subsequently targeted as an electron-deficient arene system primarily to investigate its photochemical and thermal

stabilities in addition to its solid-state structure. Considering the mostly ‘individual’ isoindenone dimer chemistry, we sought to probe the applicability of the three-step route utilized to produce the parent system, **57a** (*Figure 42*).

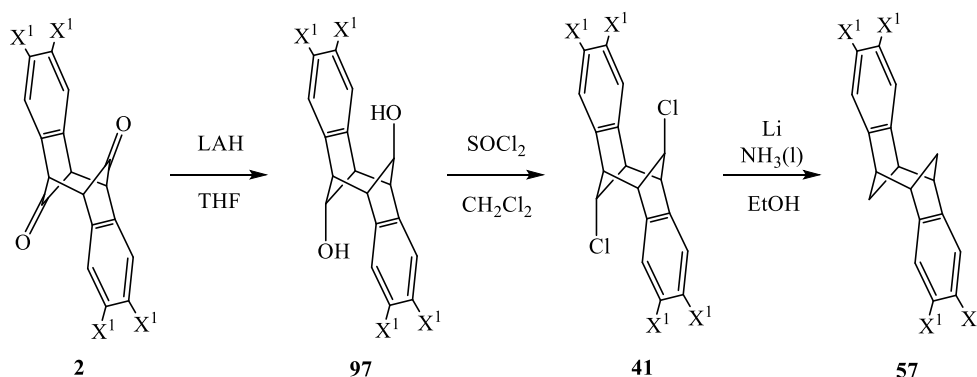


Figure 42. Synthetic sequence previously utilized for the production of the parent isoindene dimer (**57a**).

Although direct carbonyl reduction reactions are widely known, none of the standard protocols were successful in producing the parent isoindenone dimer **57a**. Nevertheless, Clemmensen reduction conditions⁶⁸ were applied to fluorinated **2c** but effected no reaction. The limited solubility in the aqueous environment likely contributed to this failure and a modified Clemmensen reduction⁶⁹ was attempted. The substrate was again poorly soluble in ether saturated with HCl and produced the same result. A Wolff-Kishner reduction⁷⁰ was subsequently attempted but failed in the condensation of the sterically hindered carbonyl units with anhydrous hydrazine.

Returning to the synthetic strategy utilized to synthesize the parent isoindene dimer **57a**, a stereoselective carbonyl reduction of tetrafluorinated **2c** was accomplished by LAH to afford the C_{2h} symmetrical diol **97c** in 95% yield. While we could not obtain single crystals of diol **97c**, stereoselectivity of the reaction was proven by NMR. Single

signals at 3.18 and 63.0 ppm (300 MHz, CDCl₃), corresponding to the bridgehead protons and carbons, respectively, were evident in these spectra while these atoms within stereoisomers would experience significantly different shielding due to interactions with the nearby arene. The α -alcohol protons were evident as an apparent pentet at 3.88 ppm due to higher order coupling with all four bridgehead protons.

A stereoselective S_Ni chlorination, confirmed following the same rational as the alcohol, was utilized to produce the dichlorinated derivative **41c** in quantitative yield. Initial reactions were stirred for sixteen hours and utilized twenty molar equivalents, as noted for the parent system, in small quantities where mini-workups would be detrimental to the yield of this twelfth synthetic step. This excess led to many unidentified side products with indication of other chlorinated stereoisomers. It was later discovered that dilute conditions and 2.2 molar equivalents of SOCl₂ could afford the target compound in two hours, containing only minor side products carried over from the synthesis of isoindenone dimer **2c**.

The Birch-type reduction⁷¹ previously utilized for the synthesis of the parent isoindene dimer **57a** was subsequently applied to the reduction of the carbon-chlorine bond in fluorinated scaffold **41c**. Although similar radical conditions have been utilized for the reduction of arene-fluorine bonds, lithium has been utilized to exclusively reduce the aromatic ring of a polyfluorinated naphthalene derivative.⁷² With the reduction susceptibility of an aliphatic carbon-chlorine bond being greater than that of aromatic or arene-fluorine reduction, this single-electron transfer reaction was predicted to proceed smoothly under substoichiometric lithium addition. Upon implementation of these conditions, analysis of the products was particularly difficult as the peaks overlapping the

entire 1-3 ppm range comprised the vast majority of the peak area within the ^1H NMR spectrum (300 MHz, CDCl_3), presumably from reduction of the polymeric material and multiple carbon-carbon bonds in dichloride **41c**. Significant quantities of the starting material were present and no new signals were observed by ^{19}F NMR. Ultimately, complete halogen reduction to small quantities of the parent isoindene dimer **57a** was confirmed by GC-MS and ^1H NMR, providing us with a new route to this compound, albeit quite costly.

Significant literature precedence exists for carbonyl reduction through single or multistep reactions but the limited accessibility of fluorinated isoindenone dimer **2c** confined our options. Both ionic and radical reduction conditions were subsequently sought to circumvent the observed carbon-fluorine bond reduction. Isoindenone dimer **2c**, diol **97c** or dichloride **41c** each provided plausible precursors to **57c** through various synthetic transformations.

Although a single-electron transfer reaction had failed to deliver **57c**, alternative radical pathways exist to deliver aliphatic functionalities. Although alcoholic functionalities are compatible with radical reducing agents as the direct homolytic scission of the C-O bond is not a thermodynamically favored process, Barton-McCombie methodology has been reported to reduce sterically encumbered alcohol functionalities.⁷³
⁷⁴ This process utilizes derivatization to xanthates, thiobenzoates or thiocarbonyl imidazolides and tributyltin hydride as the reducing agent to accomplish this reaction. The initial step of this reduction mechanism requires a tributyltin radical to attack the thiocarbonyl sulfur atom and produces the resonance stabilized radical intermediate **100**. Homolytic carbon-oxygen bond cleavage follows to afford an alkyl radical (**102**) and the

thioester derivative **101**. The alkyl radical subsequently abstracts a hydrogen radical from tributyltin hydride to afford the reduced product (**103**) while consuming the reagent stoichiometrically to restart the radical chain reaction (**Figure 43**).⁷⁵

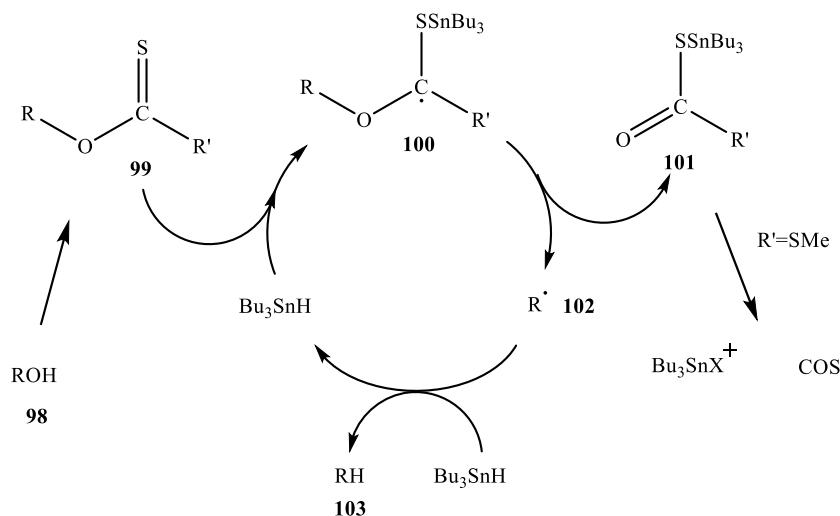


Figure 43. Generalized Barton-McCombie radical reduction pathway.⁷⁵

Utilizing diol **97c**, proof of a thiono-ester or -amide intermediate (**106**) could not be conclusively obtained. Condensations with thiocarbonyldiimidazole (**104**) or *O*-phenyl chlorothiocarbonate (**105**) using DMAP, BuLi or without the use of a base^{73, 74, 76} led to minimal conversion to multiple products as evidenced by ¹H NMR although their identification proved to be equivocal at the time. ¹H NMR spectral identification of the xanthogenates (**106**) were predicted to be difficult as both the product and the thiono ester (**105**) or amide (**104**) possessed phenyl or imidazolyl protons, respectively, that overlapped with each other and the substrate. Minor evidence existed for these intermediates in new minor aliphatic triplets in the ¹H NMR, possibly corresponding to the bridgehead protons experiencing complex coupling with the two α-thioester hydrogens. Only one signal in

this region was expected but between two and four triplets were observed along with other multiplets, possibly corresponding to a mono-condensed product. Conversely, only the ^{19}F NMR pseudo-triplet signal of the starting material was observed. Further characterization of the mixture was attempted by DI-MS and ESI-MS, but only diol **97c** was observed and provided no evidence for a mono- or di-condensed product. It is of note that a significant amount of dark material was still present in sample cups utilized for DI-MS after heating to 400 °C and the expected product could have charred prior to vaporization. Nevertheless, radical reduction conditions^{73, 74, 76} were applied to all crude intermediates to afford highly convoluted ^1H NMR spectra and no evident change by ^{19}F NMR. Spectrometric characterization was attempted analogously to the previous reaction, in addition to GC-MS, and produced no evidence for the targeted fluorinated isoindene dimer **57c**.

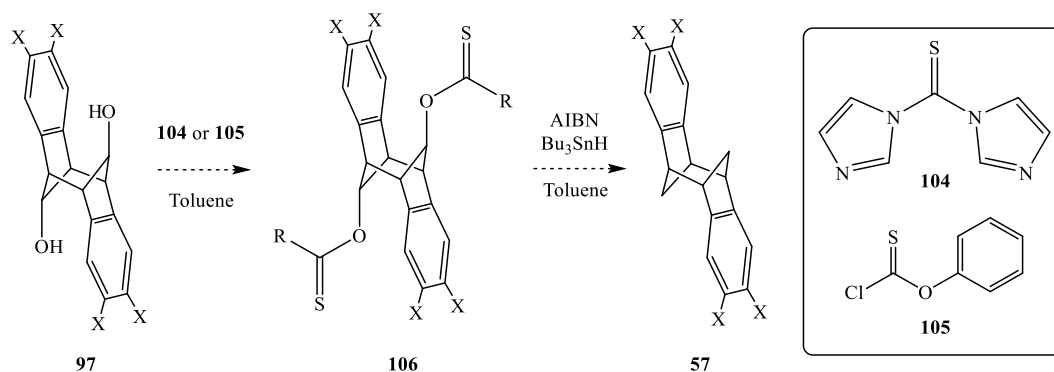


Figure 44. Barton-McCombie methodology applied toward isoindene dimer **57c**.

The time and relative costs associated with exploring this reduction through other methodologies barred further attempts toward the fluorinated isoindene dimer **57c**.

Around this time, *ortho*-dimethoxy-substituted isoindenone dimer **2h** became available in

gram quantities and alternative reduction pathways were explored on this easily accessible and more synthetically valuable scaffold.

3.3.2 Methoxy-Substituted Isoindene Dimer Synthesis

To gain further insight into the stability of formal isoindene dimers and to provide a polycyclic scaffold incorporating a single class of functions, reduction of the carbonyl units within methoxy-substituted isoindenone dimer **2h** to methylene groups was accomplished. This seemingly trivial complete reduction to the formal isoindene dimer **57h** was attempted along various methodologies, but only accomplished through the three-step sequence previously utilized for the parent isoindene dimer **57a** on the milligram scale. The inability of this sequence to produce fluorinated isoindene dimer **57c** did not impede our efforts as the methoxy groups are not susceptible to the same carbon-halide reduction in the final step.

LAH reduction of the methoxy-substituted isoindenone dimer **2h** afforded a 95% yield of diol **97h** stereoselectively within short time, owing to the ample solubility of the starting material. The presumably polymeric material carried over from the synthesis of **2h** could not be removed via crystallization but other minor unidentified side products were purified. Chlorination was accomplished along a protocol optimized for the synthesis of fluorinated **41c** to afford methoxy-substituted **41h** quantitatively.

Methoxy-substituted isoindene dimer **57e** was obtained following the optimized Birch-type reduction procedure utilized for the parent compound **57a** with no evidence for reduction of the aromatic ring. This over-reduction was a limiting factor for the parent system (**57a**) as analogues of **107** or **108** were evident prior to complete consumption of

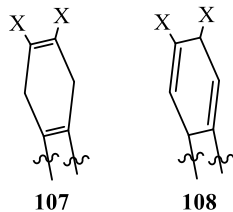


Figure 45. Possible over-reduced products.

the dichloride precursor (**41a**). Reduction of the aromatic rings within methoxy-substituted **57h** was only observed once in small quantities as their electron affinities are reduced in comparison to parent **57a**.

Poor phase separation made the aqueous workup difficult after the evaporation of ammonia, but the mass balance was typically near quantitative. In the region from 1-3 ppm in the ^1H NMR (300 MHz, CDCl_3), broad signals that could not be conclusively assigned were always present, possibly originating from reduction of the polymeric impurities. Minor side products possessing aromatic protons were observed in the crude material, but they could not be isolated by chromatography.

Similar to its isoindenone dimer precursor **2h**, column chromatography of the crude Birch-reduction product was not as straightforward as the TLC suggested due to significant streaking. Dichloride **41h** was easily removed from batches intentionally stopped prior to complete conversion, but excessive quantities of solvent were required to elute the analytically pure target in only 5% isolated yield. A methanol wash of the column recovered the crude mass and was found to contain significant quantities of the desired product. This fraction could be resubjected to chromatography to furnish a decreased amount of isoindene dimer **57h**. The rigidity of the product along with strong arene-arene intermolecular interactions were hypothesized to explain the significant retention. Through attempts to obtain single crystals of the purified material, its lack of solubility in ether was realized and exploited for purification. In lieu of chromatography for batches where no dichloride **41h** remained, isoindene dimer **57h** could be obtained

through repeated trituration of the crude product in 10% yield, albeit still containing a minor amount of the polymeric material. An additional 5-10% could be obtained from the mother liquor with an increased amount of polymer.

In an effort to obtain larger quantities of isoindene dimer **57h**, alternative syntheses were explored. Although some of the reaction conditions had been previously applied to the parent or fluorinated isoindenone dimer derivatives, the enhanced solubility of methoxy-substituted scaffolds was predicted to assist in the reactive species accessing the sterically encumbered carbonyl units. This property, along with gram quantities of **2h** becoming available, made this scaffold attractive to explore alternative pathways to isoindene dimer derivatives.

Direct carbonyl reductions were first formulated to reduce the number of steps in the lengthy synthesis; however, both standard⁶⁸ and modified Clemmensen reductions⁶⁹ demonstrated no conversion. Wolff-Kishner reduction conditions⁷⁰ were not useful as the hydrazone intermediate was elusive due to steric hindrance. Moving one step further into the successful sequence, Barton-McCombie type reductions were attempted on diol **97h** analogously to the fluorinated system.^{73, 74, 76} Again, no conclusive evidence could be obtained for xanthogenate intermediates (**106h**) or the known, targeted product (**57h**).

Alternative reductions of dichloride **41h** were subsequently explored that had not been attempted on fluorinated derivative **41c**. A less synthetically demanding alkali metal reduction using sodium in *tert*-butanol at room temperature was first attempted,⁷⁷ but no trace of the desired product was observed. Minor conversion was observed through new ¹H NMR signals in the aliphatic region, but these products likely originated from reduction of the polymeric material carried over from isoindenone dimerization. An

attempt was also made to prepare a Grignard reagent using magnesium in THF for subsequent acid-base proton exchange with similar results to the previous attempt.⁷⁸ Reduction of a carbon-bromine bond would be ideal for this type of reaction but attempts to synthesize a dibrominated derivative of **41a** were minimally successful on the parent system and not attempted on a methoxy-substituted scaffold.

An electrophilic reaction was thus sought as the dications formed after the loss of two chlorine atoms were calculated to be particularly stable. π -donation from the aromatic ring was envisioned to aid in stabilizing an ionic transition state using a Lewis acid to remove the chlorine atoms of **41h**; however, a complex product mixture was obtained using borane in nitromethane for hydride-chloride exchange⁷⁹ with little indication of the starting material and no evidence of the desired product.

In a final effort, nucleophilic hydride substitution conditions were applied in an attempt to displace the chlorine atoms in **41h** using LAH⁸⁰ or Superhydride,⁸¹ but no conversion was observed in both cases. The transition state for this S_N2 reaction would orient the chlorine atoms toward the aromatic ring with little room to elongate the carbon-chlorine bond and likely explains the ineffectiveness of these reactions.

3.3.2.1 X-ray Structures and Spectroscopic Data

Ortho-dimethoxy-substituted isoindenone dimer **57h** crystallizes in the monoclinic system with space group *P2₁/c*. The molecular structure exhibited typical bond lengths and angles other than the bonds between the formal isoindene monomers (1.579 Å). Unlike the parent isoindene dimer **57a** that crystallizes in a herring bone motif and exhibits T-shaped π -stacking interactions, arene-arene interactions were not present.

Rather, **57h** was primarily stabilized by $5\text{-O}^{\delta-}\cdots 4\text{-H}^{\delta+}$ and $7\text{-C}^{\delta-}\cdots 3\text{-H}^{\delta+}$ short contacts. Other short contacts were made to the methoxy groups while the interactions were symmetrical over the molecule to provide twenty short contacts per molecule.

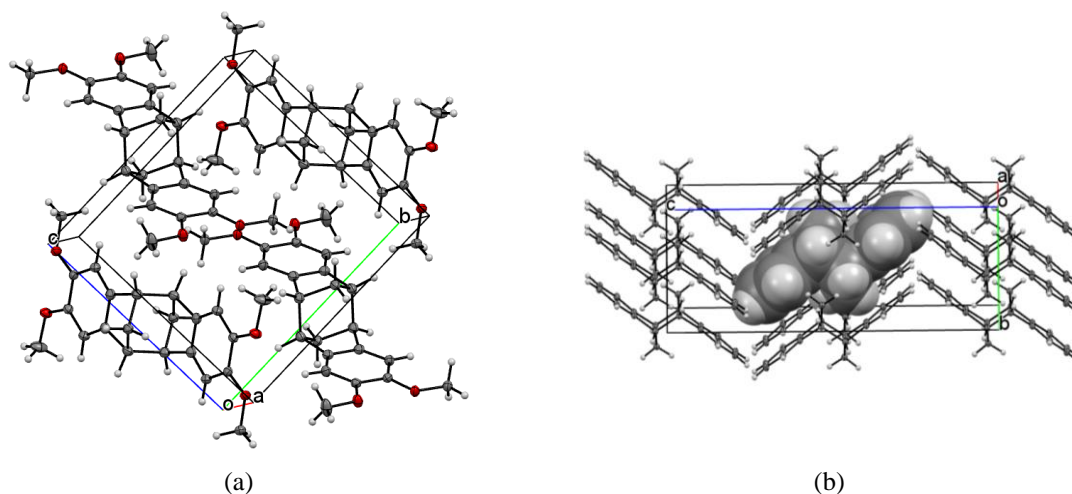


Figure 46. Unit cells for the crystal structures of *ortho*-methoxy isoindenone dimer **57h** (a) and parent isoindenone dimer **57a** (b) where some portions are shown as a space-filling model for clarity.

The 1-1' and 3-3' carbon bonds, corresponding to the bonds between two formal isoindene molecules, are the longest in the molecule. This bond length in methoxy-

substituted **57h** was slightly decreased when

compared to the same bonds in parent **57a** (1.579 Å and 1.583 Å, respectively). The electron-donating

characteristics of the methoxy groups were predicted

to engender a stabilizing interaction between the

monomers and decrease the bonding order but the

crystal structure provides evidence for this difference arising from steric considerations.

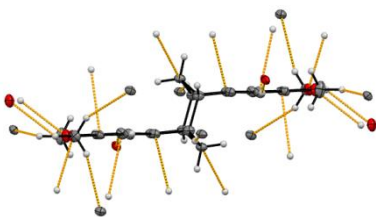


Figure 47. Crystal structure of *ortho*-methoxy isoindene dimer **57h** showing all twenty short contacts (orange).

The adjacent methoxy groups, oriented in opposing directions within the arene plane, led to elongation of the 5-6 arene bonds to 1.412 Å when compared to the 1.391 Å bond lengths in parent **57a**. This interaction introduces ring strain into the arene unit and compresses the 3'-7' and 3''-7'' arene bonds by 0.007 Å when compared to the 1.411 Å distance in parent **14a**. The ring strain in the five-membered rings is subsequently lowered due to this compression so that the $\angle C_{\text{arene}}CH$ and $\angle C_1C_1C_{\text{methylene}}$ are increased by 0.24° and 0.49° , respectively, when compared to parent **57a**. A crystal structure of the elusive fluorinated isoindene dimer **57b** would have been useful to further establish trends in the structural characteristics of this novel isoindene scaffold.

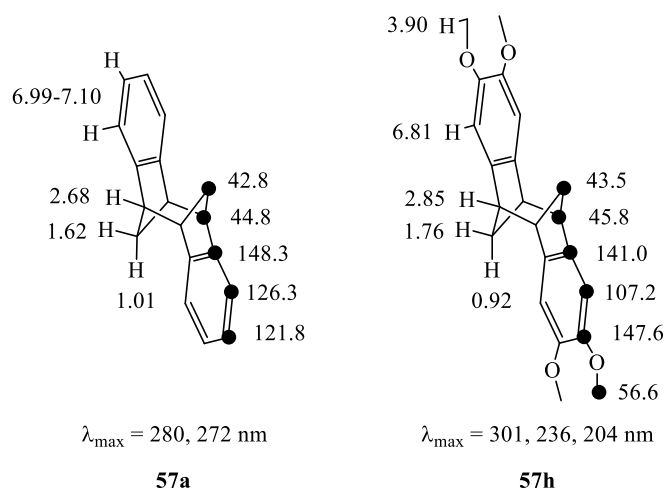


Figure 48. Spectroscopic comparison between isoindene dimers. NMR data for **14a** was recorded in C_6D_6 while **14e** was studied in $CDCl_3$. Chemical shifts are reported in ppm from a TMS standard. The UV-Vis Data was recorded in ACN.

3.4 Extended *Anti*-Bisheteroarene Scaffolds

Azaacenes, a diverse class of π -stackable aromatic compounds, have not only the potential to overcome some shortcomings of their hydrocarbon analogs, but also offer readily tunable scaffolds through flexible synthetic approaches (Chapter 1.2.2). Many pathways have been developed for the synthesis of azaacenes and their exploration comprises the thrust of the latter work completed for this thesis project.

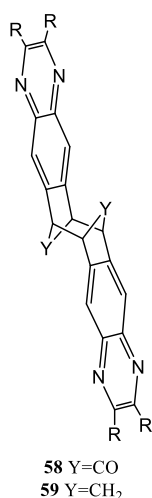


Figure 49.
Tunable
azaacene targets.

Recent attention has been brought to azaacenes for use as electron-transporting materials in their solid state.²² These compounds are targeted for either of two mutually exclusive properties: efficient charge transport, governed by molecular nearest-neighbor electronic coupling, or fluorescence where aggregation-precluding appendages are necessary to prevent quenching.³³ Structurally novel azaacenes of type **58** or **59** were targeted herein primarily to maximize intermolecular coupling through unique solid-state packing motifs in addition to realizing their fluorescent properties through the introduction of bulky substituents.

Through previous efforts in the Etzkorn lab, crystal structures of the parent isoindenone (**2a**) and isoindene dimers (**57a**), central to scaffolds of type **1** and **2**, respectively, have been obtained alongside select derivatives (i.e., **2c**, **2j**, **57h**). Although solid state packing patterns are difficult to predict,³⁵ these structures help identify the predominant forces stabilizing the central subunit to aid in the rational design of *N*-heterocyclic scaffolds.

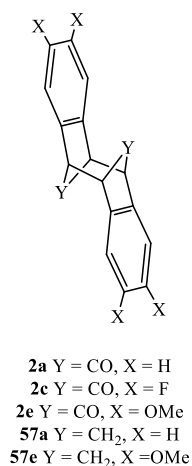


Figure 50.
Isoindenone and
isoindene
dimers.

The value of fluorination to direct stacking was substantiated when comparing the crystal structures of the parent isoindenone dimer **2a** to its tetrafluorinated analog **2c**. In the case of **2a**, the local dipoles of the carbonyl units lack a strong electronegative force to pair with and are stabilized through a short contact with an electron-poor arene hydrogen located perpendicular to the long axis of the molecule. Interactions between the arene π -clouds are evident through a T-shaped packing motif between the unhindered arene face and terminal arene hydrogens on an adjacent molecule (**Figure 51**). The introduction of terminal *ortho*-difluoro substituents in **2c**

was demonstrated to direct stacking through a dipole-dipole interaction with the carbonyl units. The strongest form of intermolecular coupling arises between π -clouds of aromatic subunits adopting a face-to-face interaction³³ and the aforementioned dipoles direct significant overlap and short contacts between atoms within these faces in the solid state

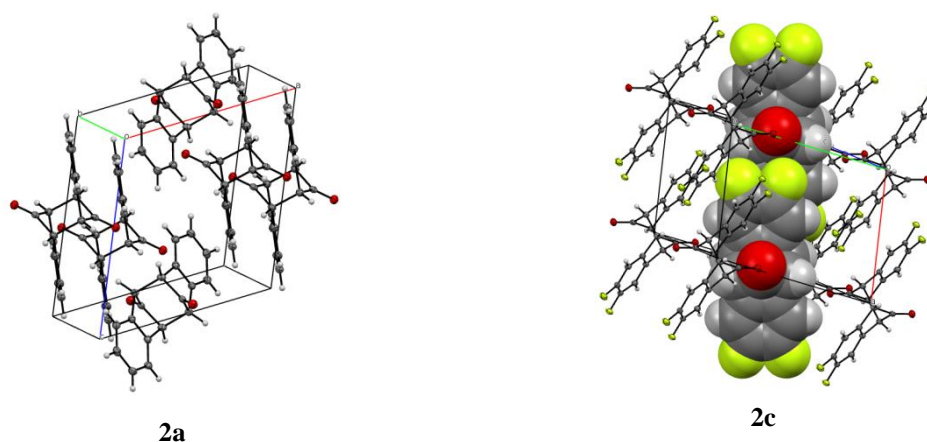


Figure 51. Crystal structures of the parent and *ortho*-difluoro-isoindenone dimers (**2a/2c**) where molecules experiencing face-to-face arene interactions are displayed as space-filled models.

(**Figure 51**)! When the aromatic rings are linearly extended – leading to smaller HOMO-LUMO gaps necessary for organic field effect transistors²⁶ – the carbonyl carbon-fluorine interaction is still possible and is envisioned to be a primary functionalization approach toward compounds useful in materials science.

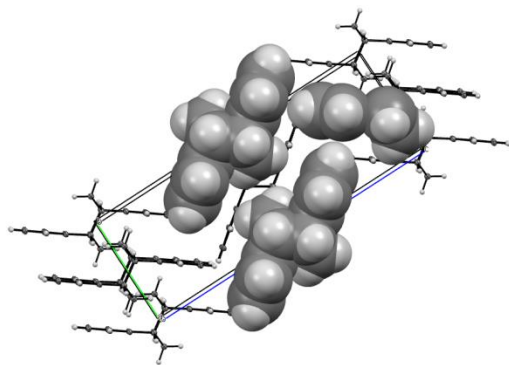


Figure 52. Crystal structure of parent isoindene dimer **57a** highlighting the T-shaped arene interaction with space-filled models.

Lacking the strong local dipoles from the carbonyl units, the crystal structure of the parent isoindene dimer **57a** exhibits a herringbone motif common to all unfunctionalized acenes.³³ π -stacking is present through T-shaped interactions where the two terminal hydrogens are oriented over the aromatic

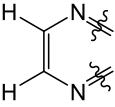
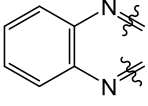
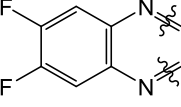
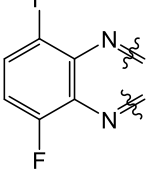
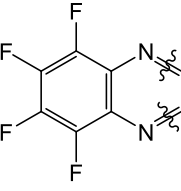
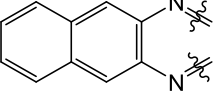
ring while no face-to-face interactions are present. However, planes of the arene faces lie parallel to one another but are separated by adjacent molecules interjecting their protons perpendicular to the long axis of the molecule. When an *N*-heterocycle is incorporated onto an isoindene dimer scaffold (**59**), T-shaped interactions, similar those exhibited by parent isoindene dimer **57a**, are predicted to be less favorable while edge-to-edge interactions between electron-deficient arene hydrogens and nitrogen atoms should be a driving force. The packing motif of isoindene dimer **57a** leaves little area of the π -face unstabilized while only the terminal arene units in azaacene scaffolds of type **59** would pair through this geometry. When compared to the dicarbonyl functionalized azaacene **58**, face-to-face interactions would be less sterically hindered by methylene units in extended scaffolds of type **59** and are predicted to have a greater role in stabilizing their

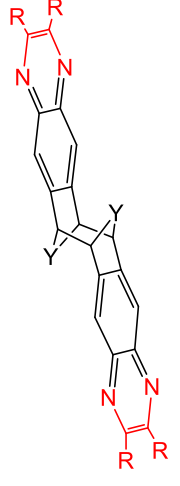
large arene faces. A variety of functionalization approaches are envisioned to direct face-to-face stacking and strengthen intermolecular coupling to produce compounds useful as n-type semiconductors (Chapter 1.2).

HOMO and LUMO energies for selected azaacenes of type **58** and **59** were calculated to establish general trends within this class of molecules. The HOMO-LUMO gap represents the bandgap of an organic semiconductor and can also be utilized to calculate the fluorescence wavelength. Upon $\pi \rightarrow \pi^*$ singlet excitation or the introduction of a charge to the system, molecular relaxation will occur and alters the energy of this gap.⁸² The values presented in **Table 2** serve to demonstrate general trends but more sophisticated computational methods are necessary to precisely design materials for application.

The HOMO-LUMO gaps between the *N*-heterocyclic formal isoindenone (**58**) and isoindene (**59**) dimers were similar but the presence of the nonbonding electrons in the carbonyl units of **1** are predicted to effect a slight blue-shift when compared to **2**. Drastic changes are present when the extent of conjugation is increased and the energy of the HOMO-LUMO gap of an azaacene with four fused aromatic rings approaches that of visible light. This energy gap is comparable to that of tetracene (2.67 eV, B3LYP/6-311G*) and this trend continues for the smaller analogues.⁸³ Thus, communication between the aromatic rings is hampered by the bridging aliphatic groups in derivatives of **58** or **59** and gap energies are closer to that of their isolated aromatic rings in hydrocarbon⁸³ and azaacene^{23, 32} derivatives. As expected, fluorination did not significantly affect the HOMO-LUMO gaps but may increase their electron affinities.³⁴

Table 2. HOMO-LUMO energies calculated for selected azaacenes using Spartan '16 : B3LYP/6-31G*.

<i>N</i> -heterocycle	Calculated Energies (eV)	
	58	59
	$\Delta E_{\text{(HOMO/LUMO)}}$	$\Delta E_{\text{(HOMO/LUMO)}}$
	4.33	4.47
	3.44	3.56
	3.46	3.60
	3.24	3.36
	3.26	3.38
	2.61	2.70



58 Y=CO

59 Y=CH₂

3.4.1 Toward Extended *Anti*-Bisheteroarene Scaffolds

With adequate control of isoindenone generation and dimerization to form the central carbon scaffold of general azaacenes **58** and **59**, incorporation of the heterocyclic component was envisioned to be the terminal synthetic step so that a variety of substituents could be introduced to readily tune various properties of the system (e.g. solid-state packing motif, electron mobility, spectroscopic properties). This goal was

formulated to avoid potential reactivity of the heterocyclic components or its substituents in earlier synthetic transformations. A second de novo strategy would explore the concept of *N*-heterocyclic isoindenone generation and dimerization. Three main approaches were envisioned for the synthesis of extended *anti*-bisheteroarene scaffolds: 1) condensation of indane-derived quinones with diamines, 2) Buchwald-Hartwig cross-coupling reactions and 3) condensation of diamino-substituted indane derivatives with quinones.

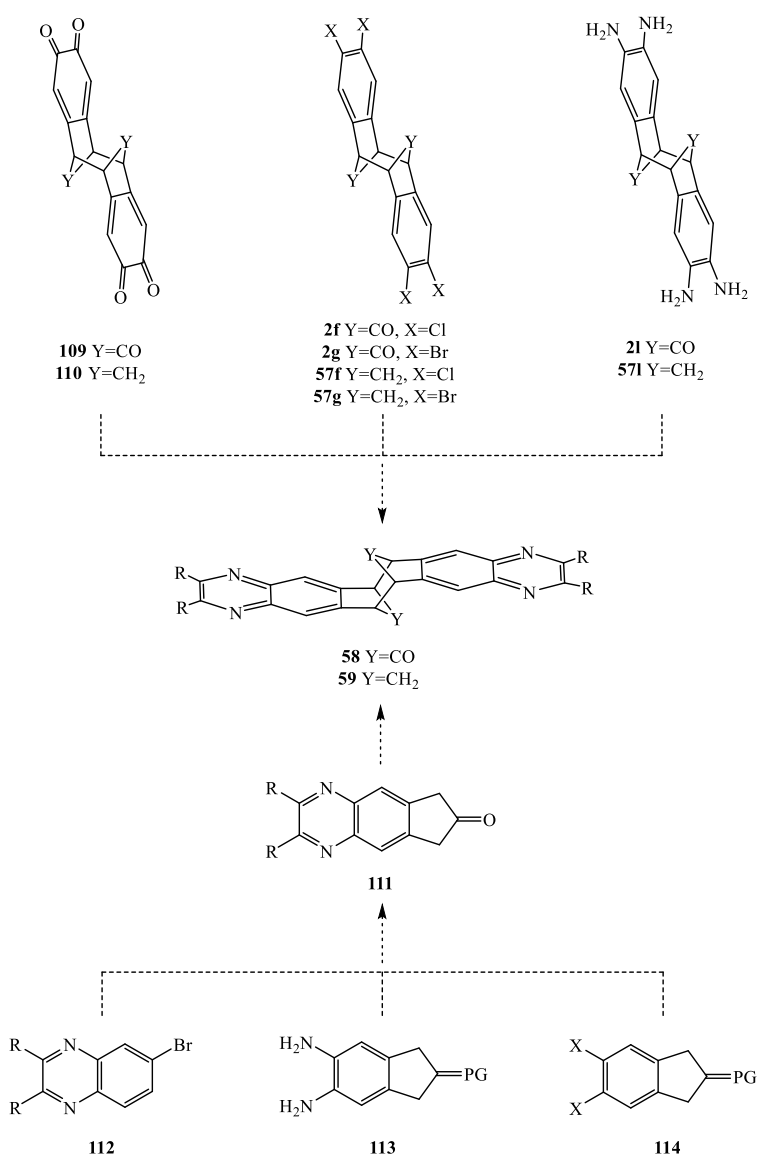


Figure 53. Selected synthetic avenues to polycyclic azaacene scaffolds of type **58** or **59**.

3.4.1.1 Indane-Derived Quinone Approach

The condensation of *ortho*-quinones with *ortho*-phenylene diamines has been a widely applicable approach to synthesize a variety of symmetrically substituted azaacenes.^{22, 38, 84, 85} *Ortho*-methoxy arenes were envisioned to provide a redox-active group for access to azaacenes through condensation with quinones **109** or **110**. Great solubility and stability of these quinones were not expected but literature precedence exists for the synthesis and reactivity of similar rigid poly-quinone scaffolds.^{84, 85}

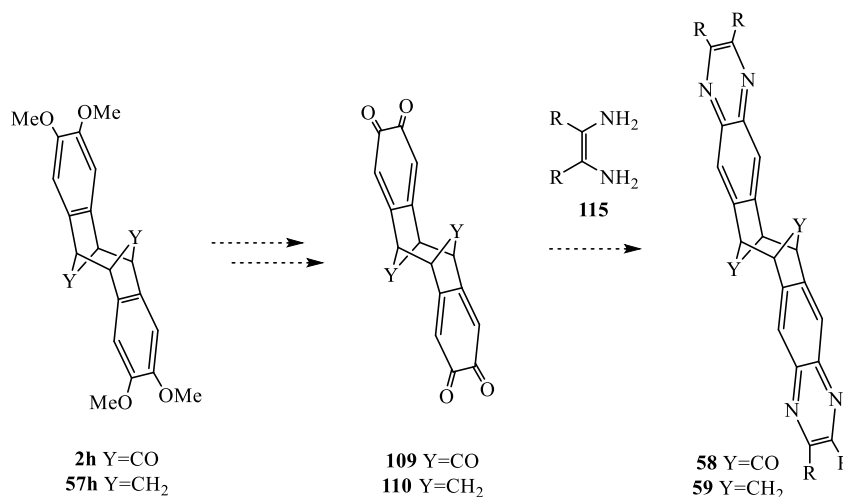


Figure 54. Potential approach toward azaacenes (**58/59**) through functionalization of methoxy groups.

The oxidation of multiple sets of *ortho*-methoxy groups is often difficult to control, but sufficient precedence has been set for this type of reaction. Many oxidation attempts to quinones **109** or **110** were based on the reactivity of structurally related triptycene scaffolds. The triptycene scaffold possesses similarities to methoxy-substituted isoindenone and isoindene dimers **2h** and **57h**, respectively, in their geometry, rigidity and presence of aliphatic bridgehead protons.

Chen et al. reported that one set of methoxy groups on triptycene **117** could be selectively oxidized using 1.1 equivalents of 0.25 M nitric acid in a 1:1 mixture of DCM and AcOH in five minutes at room temperature. Concomitant oxidation to **120** was also possible with an increase in the concentration of nitric acid to 1.25 M and an extension of the reaction time to thirty minutes (**Figure 55**).⁸⁵ When the latter conditions were applied to isoindenone dimer **2h**, black tarry matter immediately precipitated with minimal indication for the expected product by ¹H NMR. The product should have been readily identified in ¹H NMR as the signals from equivalent olefinic protons should be well resolved from those corresponding to the starting material. More than ten new signals were resolved between 6-8 ppm while the proton signals in the range of 3.5-4.2 ppm comprised the vast majority of the peak area within the spectrum (300 MHz, CDCl₃). Some spikes were observed in the range between 3.5 and 4.2 ppm, but a large hump characterized this region in the area of typical bridgehead resonances.

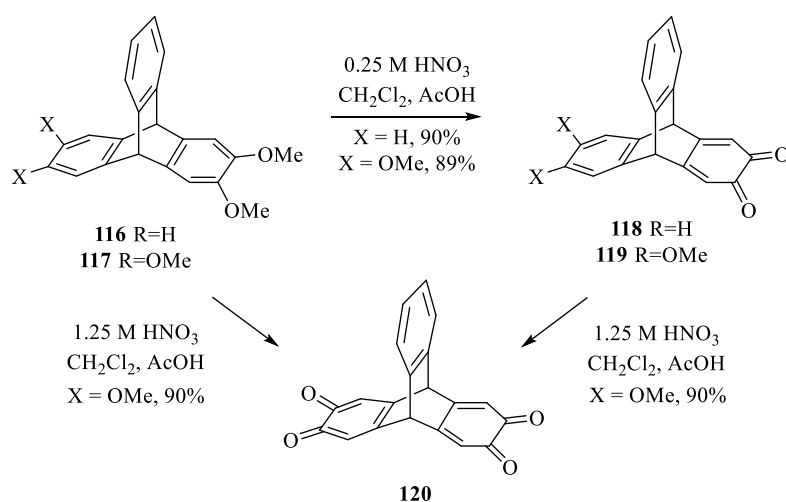


Figure 55. Previously reported oxidations of methoxy units on structurally related triptycene scaffolds.⁸⁵

Efforts to improve the poor selectivity of this transformation were made, but cooling the reaction mixture to 0 °C and reducing the nitric acid concentration to 0.25 M did not alter reaction outcomes (**Figure 56**). It is worth noting that these experiments were only performed on material containing the presumed polymer contaminant. Identical reaction conditions were applied to methoxy-substituted isoindene dimer **57h** with a similar inconclusive result.

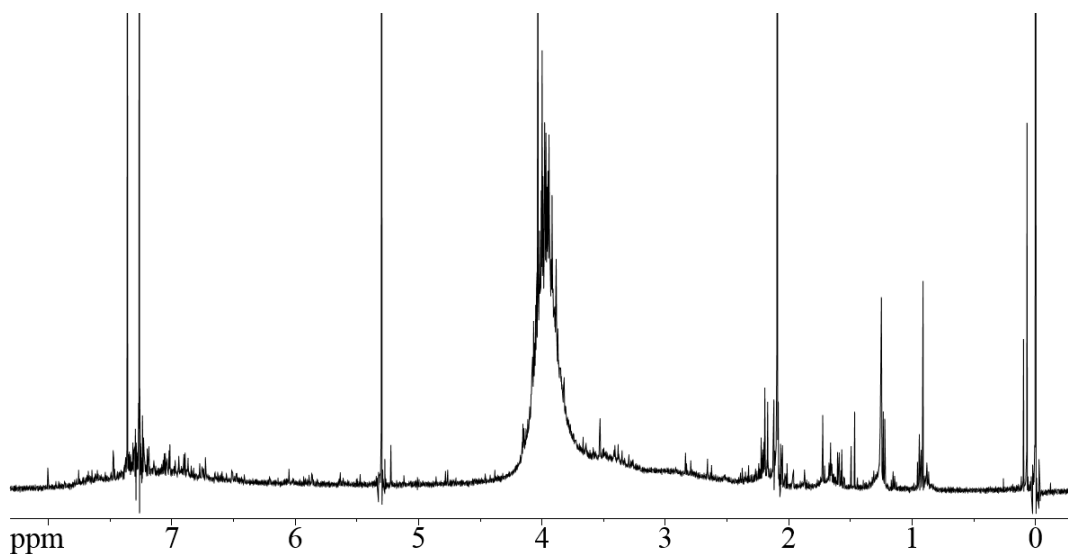


Figure 56. ^1H NMR (500 MHz, CDCl_3) spectrum of crude product from reaction of isoindene dimer **57h** with 0.25 M HNO_3 . (Note: DCM observed at 5.3 ppm)

The use of the milder, and usually more selective, oxidant, cerium ammonium nitrate (CAN), was subsequently explored. This reagent was previously utilized for the oxidation of *ortho*-dimethoxy-substituted pentiptycenes (**19** and **21**) in which chemically equivalent *ortho*-dimethoxy groups could be selectively oxidized at room temperature. For these substrates, the concentration of CAN could be varied to obtain the desired extent of oxidation in yields ranging from 35-94% (**Figure 57**).⁸⁴ Upon application of

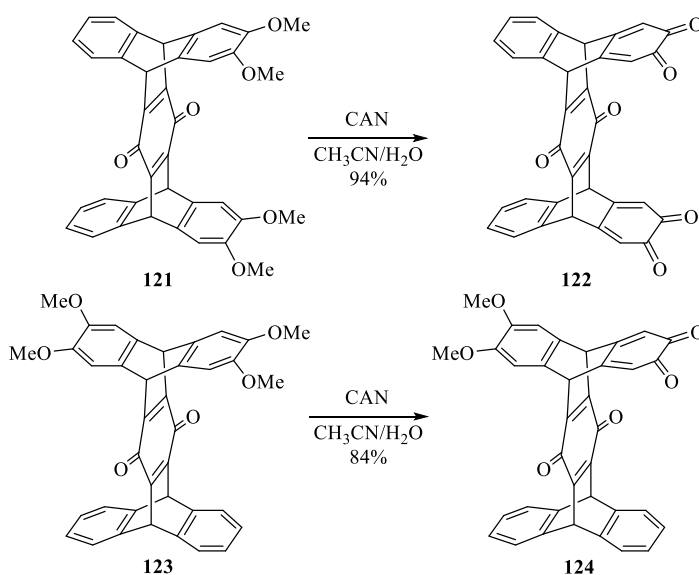


Figure 57. Previously reported oxidations of methoxy units on pentiptycene scaffolds.⁸⁴

these conditions to methoxy-substituted isoindenone and isoindene dimers, **2h** and **57h**, respectively, it was evident that the rate of reaction was significantly slower but no evidence for the targeted quinones could be obtained. When isoindenone dimer **2h** was treated with CAN, new minor signals were present in the aromatic region of the ¹H NMR, while significant quantities of **2h** had not reacted after 24 hours. A large hump was present over the methoxy region (300 MHz, CDCl₃, 3.8-4.2 ppm) in the crude product that comprised a majority of the peak area within the spectrum. When isoindene dimer **57h** was subjected to the same conditions, ¹H NMR revealed a major product with an unusual spectroscopic signal pattern. Three equally spaced, slightly broad aromatic signals with equal integration were present in addition to a similarly broad aliphatic signal with half of the total peak area of the three signals. A second set of three signals overlapped with the three aromatic signals and were shifted 0.03 ppm upfield (*Figure*

58). A GC-MS of this product did not contain any major signals and the elucidation of this product was not possible.

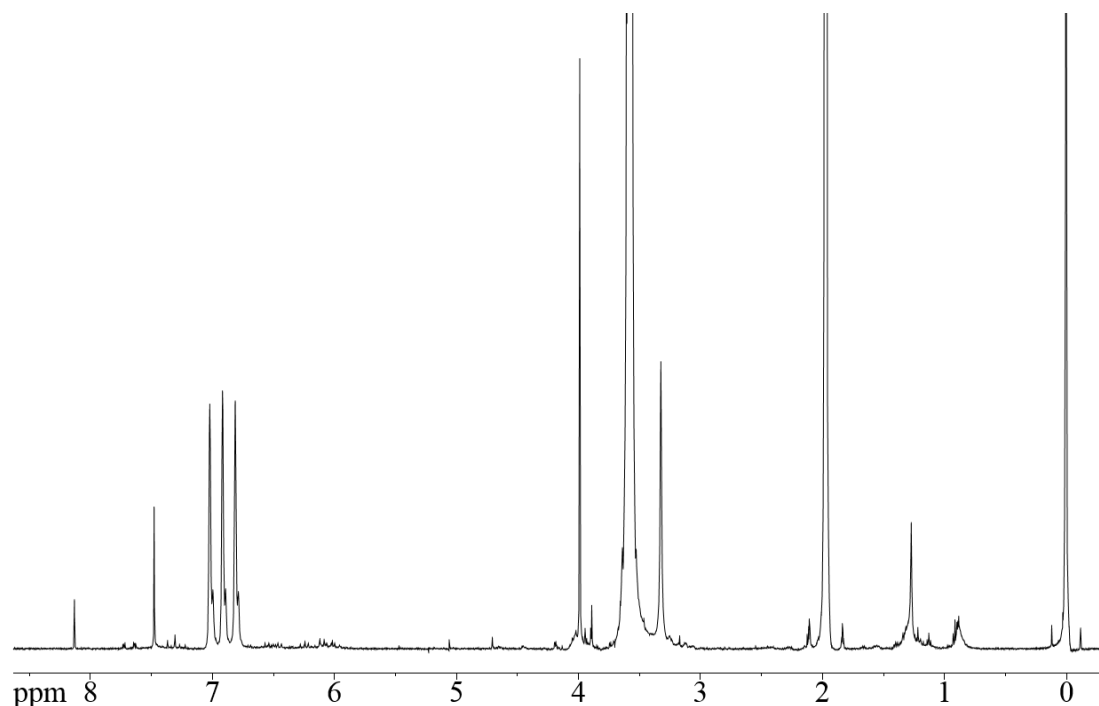


Figure 58. NMR spectrum (500 MHz, ACN-D₃) recorded of crude product obtained after CAN treatment of isoindene dimer **57e**.

Attempts towards quinones **5** and **6** were not stopped after these direct oxidations failed and cleavage of the methoxy groups to provide alcohol functionalities was subsequently attempted. Catechols require less forcing conditions for oxidation as the lack of carbon-oxygen bond cleavages often leads to a more selective reaction.⁸⁶

Due to the limited availability of *ortho*-dimethoxy isoindene dimer **57h**, a demethylation experiment was attempted at the NMR scale; thus a drop of neat BBr₃ was added to a solution of **57h** in CD₂Cl₂ at 0 °C.⁸⁷ A ¹H NMR recorded five minutes after BBr₃ addition showed complete consumption of the starting material along with traces of

the presumed tetrol **126**. Upon aqueous workup, a ^1H NMR recorded of a suspension of the crude product in CDCl_3 showed nearly the same mixture. The solid material was isolated and contained a significant fraction of what appeared to be tetrol **126** within a light blue solution in acetone- D_6 (**Figure 60**). Most indicative of the product was a single new triplet signal at 3.74 ppm, removed by 0.15 ppm downfield from its precursor, corresponding to a new bridgehead proton. The aromatic region was convoluted with many signals of small integration but contained a strong signal indicative of the product. The methylene protons were also resolved with their expected signal structure. The lack of signals corresponding to methoxy groups further hinted at tetrol **14**. Unfortunately, this sample was too dilute for ^{13}C NMR and only showed insignificant peaks after signal averaging overnight. The product could not be confirmed by GC-MS, DI-MS or ESI.

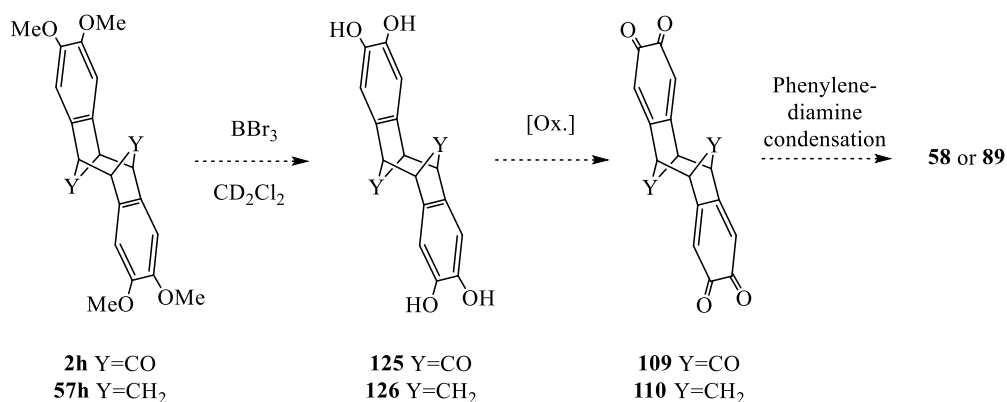


Figure 59. Derivation of methoxy groups to potentially oxidizable catechols.

The reaction was repeated twice using four molar equivalents of 0.25 M BBr_3 in DCM^{88} with similar results. Again, only minor indication of tetrol **126** could be obtained by ^1H NMR after triturating the resulting solid with chloroform but the tentatively

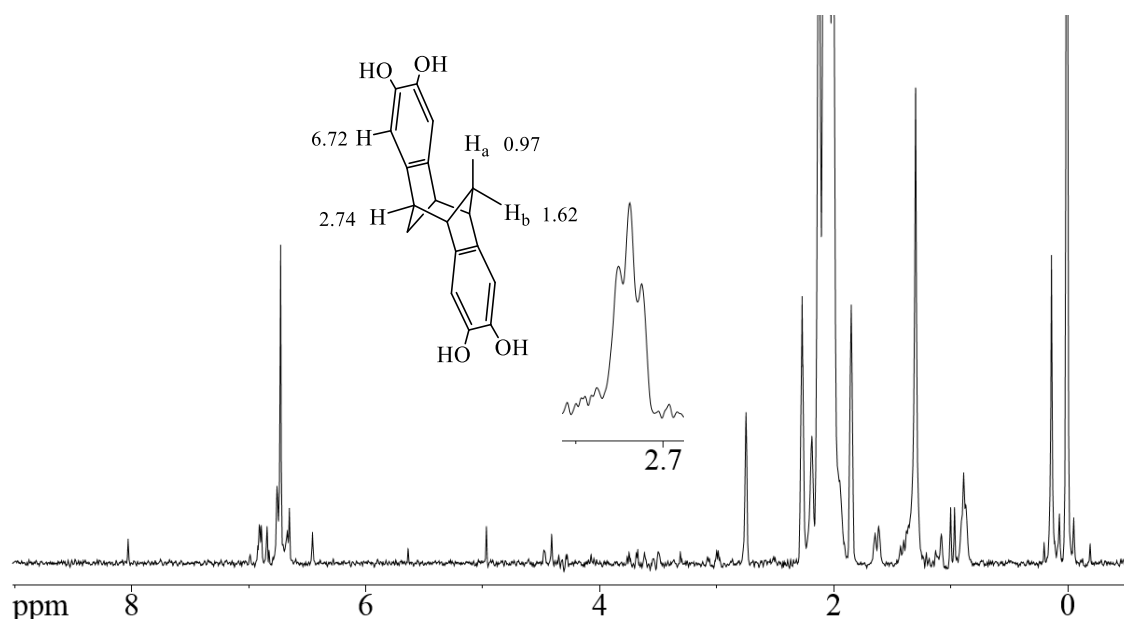


Figure 60. ^1H NMR spectrum recorded of product obtained after isoindene dimer **57h** was treated with neat BBr_3 in CD_2Cl_2 , subjected to aqueous workup and triturated with chloroform (500 MHz, acetone- D_6 , 256 scans).

assigned signals, that were resolved from other side products, were consistent between all three batches. It is estimated that less than 1 mg of **126** could have been produced after consuming 100 mg of the precious, analytically pure **57h** and it was evident that this route was not feasible to scale up.

After exhausting options to obtain the tetrol **126**, substrates available en route to this compound were subjected to similar conditions. Attempts to synthesize the tetrol derivative of isoindeneone dimer **57h** with BBr_3 under a variety of conditions did not show any indication of the product and only black tarry matter was obtained.

Aluminum trichloride in benzene was also employed in the demethylation of isoindenone dimer **2h** in a 5 mg scale experiment.⁸⁹ After refluxing one hour, a black tarry matter precipitated revealing a product with odd signal structure in the ^1H NMR

(**Figure 61**). Similar to the product obtained after CAN oxidation of isoindene dimer **57h** (**Figure 58**), three broad signals with equal integration were present in the aromatic region in addition to an aliphatic signal with half of the total peak area of the three peaks. This type of broadening could be explained by the coordination to a paramagnetic metal center, such as that found in AlCl_3 , but the equal integration of the three aromatic signals was inexplicable. A GC-MS was recorded of this sample but no signals distinguishable from the noise were observed. A ^{13}C NMR was also recorded of this sample but only minor aliphatic signals were observed after signal averaging for two days.

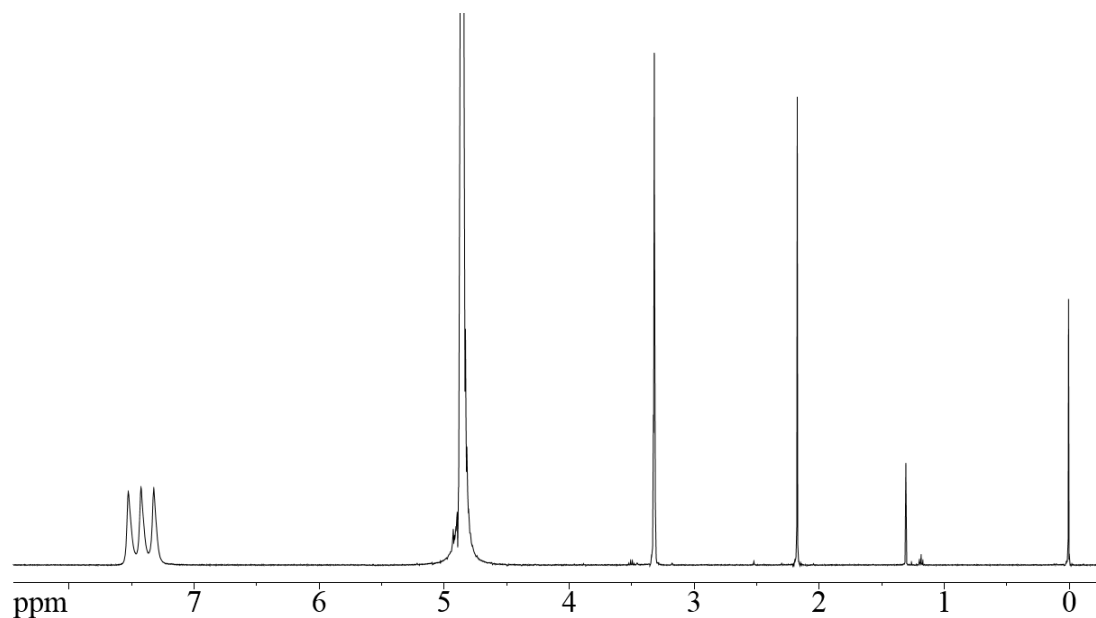


Figure 61. NMR spectrum recorded of product obtained after isoindenone dimer **3e** was refluxed in benzene for an hour and subjected to aqueous workup (500 MHz, methanol- D_3).

The demethylation of two, rather than four, methoxy groups within 5,6-dimethoxy-2-indanone (**11h**) was envisioned to be an easier transformation to control, but a reaction with BBr_3 at $-80\text{ }^\circ\text{C}$ produced a multitude of products as indicated by ^1H NMR.

To provide a different electron donating group and alter the interaction of BBr_3 with the substrate, the ketone group of **11h** was transformed into the bis-imine **127**.⁹⁰ Utilizing four equivalents of 0.25 M BBr_3 in DCM ⁸⁸ for the demethylation of **127**, a complex product mixture was obtained as a black tarry matter. When the quantity of BBr_3 was reduced to one third molar equivalents per methoxy group, the minimum necessary for stoichiometric conversion, only minor indication of the product was obtained by ^1H NMR in a mixture of other products, including 2-indanone **11h** obtained via hydrolysis.

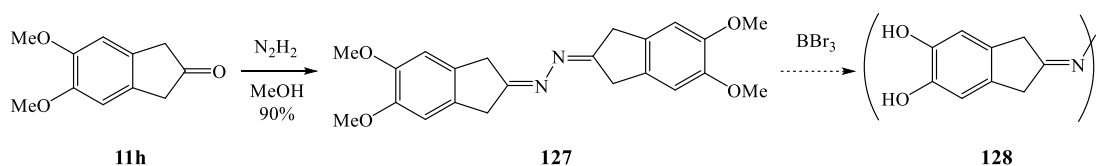


Figure 62. Alternative demethylation route through derivation of **11h** to bis-imine **127**.

3.4.1.3 The Palladium Way to Azaacenes

A recently published report analyzing the scope of palladium catalyzed double *N*-arylations⁴⁶ sparked our interest in utilizing Buchwald-Hartwig methodology^{30, 38, 40} for construction of the azaacene subunit in the formal isoindenone or isoindene dimers **58** or **59**, respectively. This publication was not the first to explore double *N*-arylations but the Laha group produced the first study examining the applicability of a single set of reaction conditions to a variety of substrates.⁴⁶ Following the same trend established for single *N*-arylation products, Laha et al. demonstrated that electron-poor *ortho*-dihalides generally couple most readily with electron-rich *ortho*-phenylene diamine derivatives although exceptions were identified. These properties are reasoned in the C-X bond's increased

susceptibility to oxidative addition and enhanced basicity for amine binding to the sterically hindered L_nPdArX complex in the catalytic cycle (**Figure 63**).⁴⁰

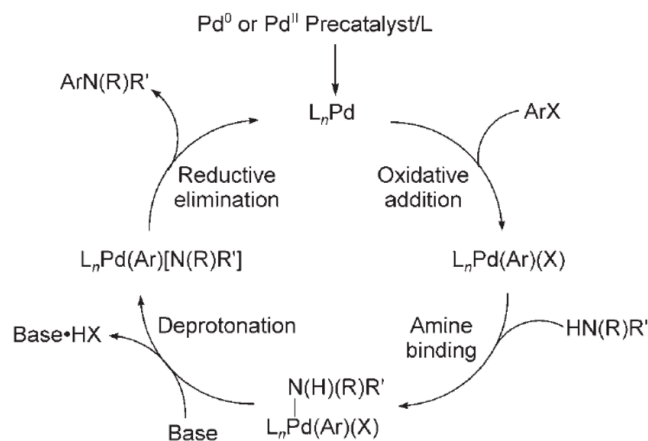


Figure 63. Proposed catalytic cycle for palladium-catalyzed amination.⁴⁰

After optimizing the Pd source, ligand, base, and solvent for the condensation of phenylenediamine (**50** $R'=H$) and 1,2-dibromobenzene (**49** $R=H$, $X=Br$) to produce phenazine (**51** $R=R'=H$) in 89% yield, the Laha group applied these conditions to twenty combinations of phenylenediamines and dihalo-arenes bearing electron-donating or -withdrawing substituents. Their study demonstrated decreased efficacy when coupling 1,2-dibromobenzene or 1,2-dichlorobenzene with an *ortho*-phenylene diamine derivative (**50**) bearing a strongly electron withdrawing substituent (e.g. 5-trifluoromethyl) but minor enhancement when a mildly electron withdrawing group (e.g. 5-methyl ester) was present. Additional deviations from general trends were noted without a plausible explanation, demonstrating the high substrate specificities for double *N*-arylation conditions as previously described by other groups.^{40, 45}

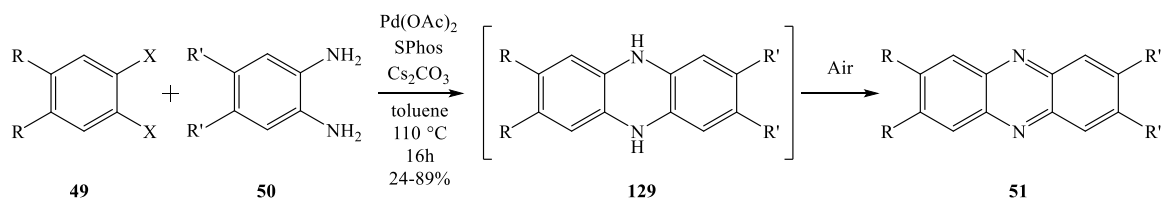


Figure 64. Optimized conditions reported by J. Laha et al. for double *N*-arylations where a series of substituted *ortho*-dihalides and *ortho*-phenylene diamines were cross-coupled (20 examples).⁴⁶

Harnessing the general applicability of the optimized conditions, we sought to apply this methodology towards the synthesis of azaacenes **58** and **59**. Before translating these conditions to synthetically valuable materials, the reported condensation of 1,2-dichlorobenzene with 1,2-phenylenediamine to afford phenazine (**51** $\text{R} = \text{R}' = \text{H}$) was reproduced to serve as a control.

Standing by a central dogma of this project, the formation of the heterocyclic component as late as possible in the synthetic sequence toward scaffolds of type **1** or **2**, dihalo-isoindenone dimers **2f** and **2g** were the sought synthetic intermediates for this goal. As presented in Chapter 3.1.4, a literature reported synthesis of 5,6-dibromo-2-indanone (**11g**) could not be reproduced or optimized to furnish the desired quantities. Our focus subsequently shifted to *ortho*-dichloro-isoindeneone dimer **2f**. Its 2-indanone precursor **11f** was synthesized along two separate pathways and obtained in an optimized 10% yield over seven steps (Chapter 3.1.3).

Products from both pathways were subjected to isoindenone generation and dimerization utilizing procedures optimized for the synthesis of the *ortho*-difluoro-isoindenone dimer **2c**. Much to our surprise, no indication for the product **2f** could be obtained, although its direct precursor, bromo-silyl enol ether **90f**, was synthesized in

high purity with no unidentified side products. Similar to the trifluoro systems that failed to produce their expected dimer (Chapter 3.2.1.1), upon crystallization from acetone by the addition of pentane, the product contained only broad ^1H NMR signals and comprised a majority of the crude mass. A mass balance of 10% was obtained from the mother liquor that exhibited less intense broad ^1H NMR signals and a multitude of products. This result was puzzling as electronic differences between the difluoro- and dichloro-isoindenones **1c** and **1f**, respectively, do not differ extensively.

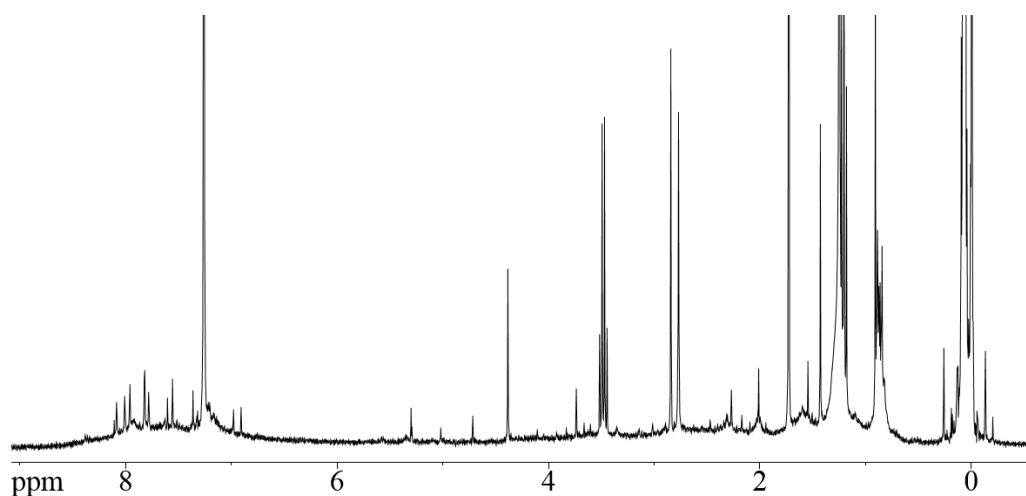


Figure 65. ^1H NMR (300 MHz, CDCl_3) recorded of the crude product obtained through an attempt to synthesize the *ortho*-dichloro-isoindenone dimer **2f**.

The failure to utilize isoindenone or isoindene dimer substituents toward azaacene functionalization led us to target the heterocycles through a different approach: the dimerization of *N*-heterocyclic isoindenone derivatives (**34**). The additional conjugation of this 16 π -electron system could allow alternative modes of dimerization and is of interest to study its electronic structure.

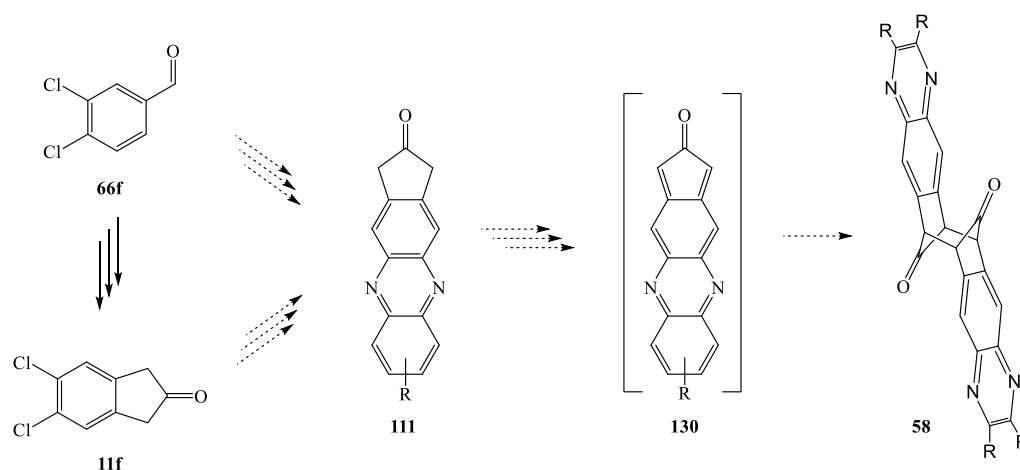


Figure 66. Potential synthesis of azacene **58** via dimerization of an *N*-heterocyclic isoindenone (**130**).

Thus, 5,6-dichloro-2-indanone (**11f**) was chosen as an ideal substrate for Buchwald-Hartwig coupling. 1,2-Phenylenediamine (**50**) was selected as the ideal amine due to its success in control experiments and for ease of data interpretation with its easily distinguishable AA'BB' aromatic splitting pattern in the ^1H NMR. Following Laha's protocol,⁴⁶ no evidence for the product could be obtained through ^1H NMR or GC-MS, although 2-indanone **11f** had been completely consumed. This result was only moderately surprising as enolizable protons on **11f** could lead to a variety of products from aldol condensation or imine formation. Neither of these reaction pathways could be confirmed as the ^1H NMR spectrum of the crude material indicated that a significant quantity of *o*-phenylenediamine had not reacted and all other major aromatic signals could be attributed to the phosphane catalyst. The reaction workup required filtering over celite and washing with both ethyl acetate and acetone and any coupled products were likely insoluble in these solvents.

To eliminate the presumed reactivity of the carbonyl unit within 5,6-dichloro-2-indanone (**11f**), this functional group was protected in the form of its ketal (**131**) in quantitative yield. Following a coupling reaction, deprotection would have been necessary by acidic hydrolysis to afford 2-indanone derivative **111**. Hydrolysis of the azaacene is also possible, but this reaction typically requires a strong acid and extended heating while ketal hydrolysis is kinetically much faster and occurs under less forcing conditions.

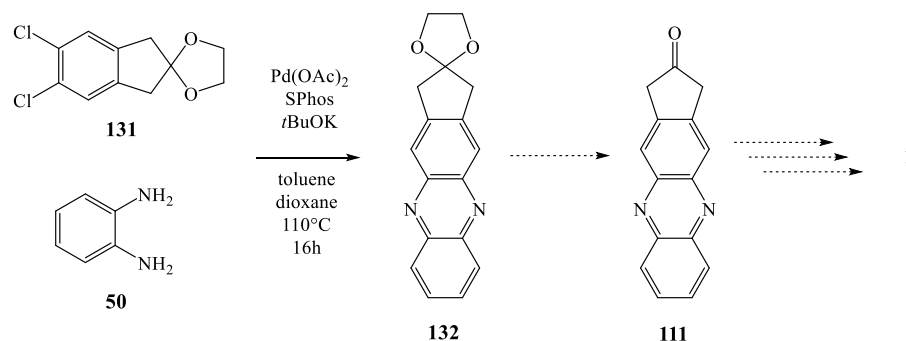


Figure 67. Potential Buchwald-Hartwig coupling toward the *N*-heterocyclic 2-indanone derivative **111**.

The first coupling attempt between ketal **131** and diamine **50** followed Laha's optimized protocol⁴⁶ and did not produce the expected product. Undesired reactivity was indicated by a multitude of ¹H NMR (300 MHz, CDCl₃) signals from 7.0-7.2 ppm that could not be assigned to a particular product. The 80% mass balance indicated that significant product had not been lost due to insolubility as in the previous reaction and that this set of conditions was not optimal for the synthesis of **132**.

The necessitation of reaction optimization, demonstrated for many reported double *N*-arylations, was subsequently realized as the nature of the aryl chlorides and

amine groups were not significantly different from previous reports.^{38, 46} Little could be done to optimize the oxidative addition of the chloride to the L_nPd^0 complex and the problem in the catalytic cycle was thought to occur in the amine coordination step. It was hypothesized that deprotonation of the amine can precede or follow coordination and it can be reasoned that the latter would be more suited to reduce the activation energy needed to reach a bulky transition state,⁴³ particularly evident in the attempted reaction. Thus, KOtBu was selected as a stronger base for subsequent attempts in combination with a small amount of dioxane, a cosolvent frequently reported for this type of reaction.^{40, 46}

Following a reaction with these two modifications, indication for azaacene **132** was obtained although unequivocal identification was not realized. Product formation was indicated by the 1H NMR where signals with the expected AA'BB' coupling pattern were observed at 7.8 and 8.2 ppm (*Figure 68*), near those of phenazine. The other pair of aromatic protons were also visible at 8.0 ppm. Multiple singlets were present with fitting integration for the two pairs of methylene protons in the expected product, while none of the ketal **131** remained. A GC-MS provided evidence for the phenazine-derived ketal **132** with the base peak corresponding to the expected mass. Other than signals with 205 and 206 m/z of near equal intensity, 75% and 70%, respectively, all major fragments could be assigned.

A significant fallacy in the identification of **131** was the inability of the reaction to be reproduced to provide quantities necessary for full characterization. No evidence for product formation could be obtained through two subsequent attempts utilizing the same

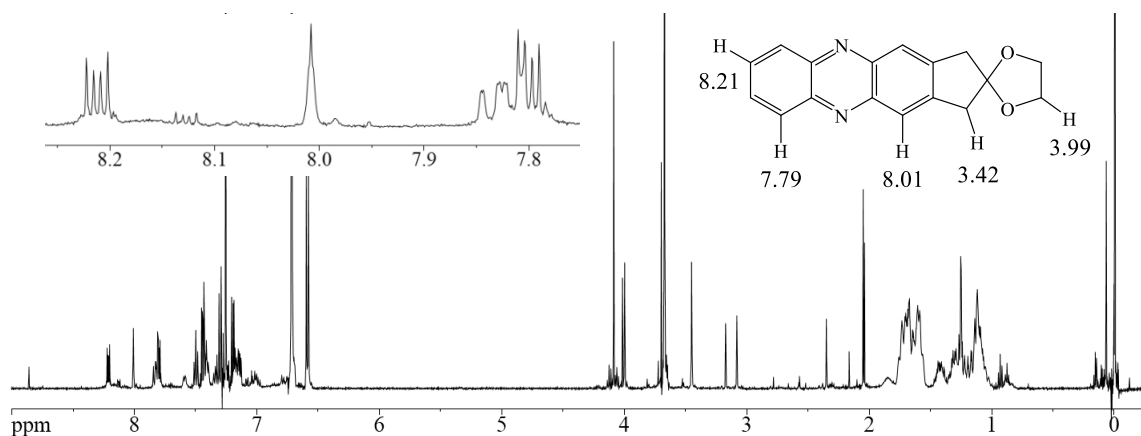


Figure 68. ¹H NMR (500 MHz, CDCl₃) recorded following a Buchwald-Hartwig coupling reaction of dichloro ketal **131** with phenylene diamine (**50**).

reaction conditions. In a final attempt, Xphos was utilized as the phosphane catalyst⁴⁰ with otherwise identical conditions to no avail.

We next envisioned to apply Buchwald-Hartwig methodology to dichlorinated substrates obtained en route to 2-indanone **11f** and selected the acetal derivative of 3,4-dichlorobenzaldehyde **66f**. Utilizing either the optimized conditions reported by Laha, those applied to ketal **131** or adapted conditions where sodium methoxide was utilized as base with a dioxane cosolvent,⁴⁶ the reactants could be reisolated with only trace impurities. To ensure strict inert atmosphere, Laha's optimized conditions were utilized after a solution of the acetal derivative of **66f** in toluene was subjected to two freeze-pump-thaw cycles with no change in reactivity.

Laha's reports of successful coupling reactions with substrates bearing methylenedioxy or ester functionalities made these results particularly difficult to reason as ketal and carbonyl units within our substrates possess similar properties, respectively.⁴⁶ Reagent impurities could be excluded as no single source of a chemical

was common to each reaction. Through the palladium-catalyzed coupling reactions attempted herein, the high specificity of reaction conditions to coupling partners was robustly demonstrated.

3.4.1.3 Diamino-Indane Condensation Approaches Toward *Anti*-Bisheteroarenes

Although we were unable to utilize *ortho*-methoxy groups in 2-indanone derived substrates as redox-active functionalities, the quinone condensation approach remained attractive towards azaacenes through an inversion of this methodology: synthesizing diamino-indane derivatives for condensation with functionalized *ortho*-quinones.

After struggling to synthesize the heterocyclic component for a compound useful toward *anti*-bisheteroarene scaffolds **59** or **59** thus far, this functionality was envisioned to be incorporated into the first stages of a synthetic pathway that utilized familiar polycycle construction. The experience gained through this project with the construction of five-membered rings fused to an arene and subsequent transformation to its 2-indanone derivative was envisioned to aid in this targeted synthesis.

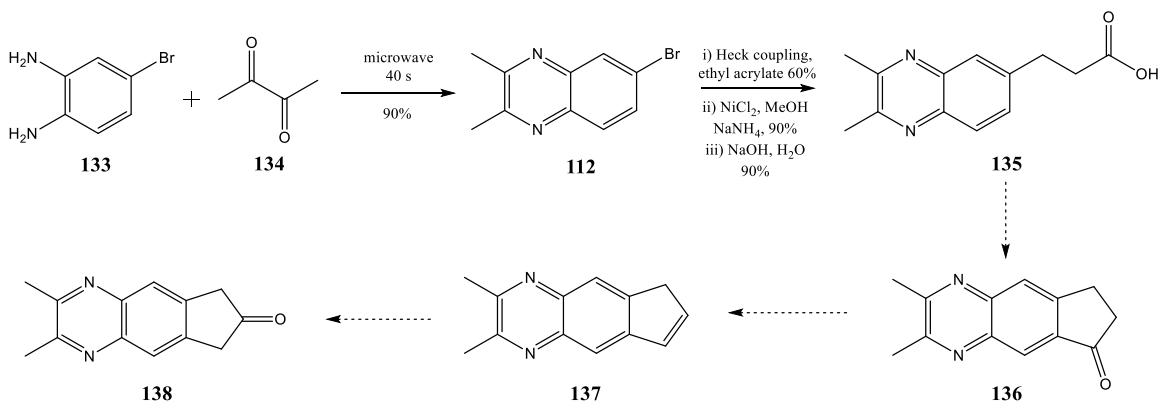


Figure 69. Potential route to azaacene 2-indanone derivative **44**.

Following a literature protocol, diamine **133** was successfully condensed with diketone **134** in a neat microwave-assisted reaction to afford the first confirmed azaacene substrate of this project, 4-bromo-2,3-dimethylquinoxaline (**112**).⁹¹ Subsequent Heck coupling⁹² produced the cinnamic ester derivative which was easily reduced to its corresponding propionic ester derivative and subjected to saponification to afford propionic acid derivative **135** in a 50% yield over three steps. The subsequent cyclization was predicted to be challenging as the *N*-heterocyclic component is deactivating toward electrophilic aromatic substitution and becomes more electron withdrawing following coordination to a Lewis acid. In fact, electrophilic acylations are unknown to quinoxaline derivatives without the presence of an activating methoxy group *ortho* to the position of substitution.⁹³

The use of neat chlorosulphonic acid was first selected as the most practical forcing reaction for electrophilic cyclization to 1-indanone derivative **136**. Conditions optimized for the synthesis of 5,6-dichloro-1-indanone (**69f**) were applied to the propionic acid derivative **135** but no reaction was observed. Protonation of one or both nitrogen atoms in **135** was likely with the large excess of chlorosulphonic acid and prevented the acylation. Reaction of **135** with neat aluminum trichloride produced a complex product mixture that was not explored further. Conversion of **135** to its acid chloride derivative was subsequently attempted and produced a black insoluble solid which could not be characterized. Nevertheless, cyclizations using AlBr₃ in dibromomethane⁹⁴ or AlCl₃ in either benzene⁹⁵ or DCM⁹⁶ were attempted without providing evidence for the formation of **136**.

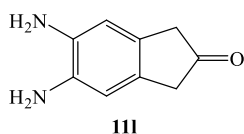


Figure 70. 5,6-diamino-2-indanone (**31g**) target.

5,6-diamino-2-indanone (**111**) was subsequently targeted for condensation with substituted quinones. Heck coupling of dinitro derivative **141** with ethyl acrylate proceeded in an exceedingly poor yield of 15%, while coupling with acrylic acid only produced trace quantities of the corresponding cinnamic acid derivative. Reduction of the conjugated olefin within the cinnamic ester **47** was attempted utilizing in situ generated nickel boride, but the nitro-group was reduced concomitantly to afford the diamino propionic ester **142** in 10-30% yield. Contamination with nickel salts was evident in the ^1H NMR through signal broadening and ester **142** could only be identified by GC-MS. This phenomenon had been observed previously and had no effect on subsequent reactions of other derivatives; however, the subsequent saponification of ester **142** produced a complex product mixture. An alternative reduction of cinnamic ester **141** using hydrazine was employed to preserve the substitution pattern.⁹⁷ Through the use of eight molar excess hydrazine and subsequent resubjection with twelve molar excess over a total of 38 hours, 80% conversion to the dinitro-propionic ester **143** was observed with a 65% mass balance for the reaction. Hydrogenation over a Pd catalyst is the only other reaction frequently employed for this type of olefin reduction but this method would also reduce the nitro group.⁹⁸ Due to the quickly diminishing yield for this pathway requiring significant quantities of $\text{Pd}(\text{OAc})_2$, this sequence was abandoned for alternative methodology.

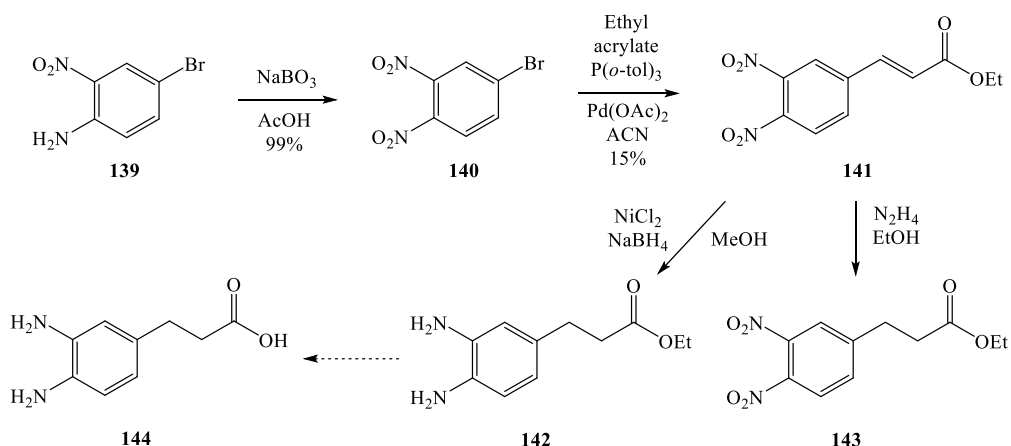


Figure 71. Attempts toward 5,6-diamino-2-indanone (**11l**).

The difficulties experienced in the synthesis of the five-membered ring through electrophilic reactions lead us to explore its formation through a familiar Dieckmann condensation, previously utilized for the production 5,6-dimethoxy-2-indanone (**31e**).⁶⁰ *Ortho*-dinitro functionalities were predicted to have a negligible effect on the cyclization as the acidity of the benzylic hydrogen should not be a limiting factor.

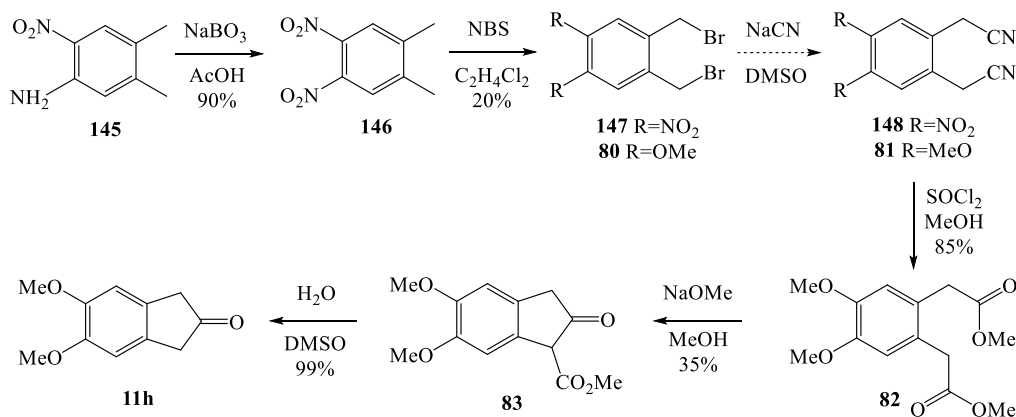


Figure 72. Optimized synthetic pathway to 5,6-dimethoxy-2-indanone (**11**) and attempted application to dinitro-substituted arenes.

As seen in **Figure 72**, these pathways were envisioned to converge following the synthesis of their bis-bromomethyl derivatives **141** and **80**. NBS bromination of 4,5-dimethyl-1,2-dinitrobenzene (**146**) was surprisingly minimally selective as geminal dibromo (**150**) and tribromo products (**151**) were obtained alongside the desired product.

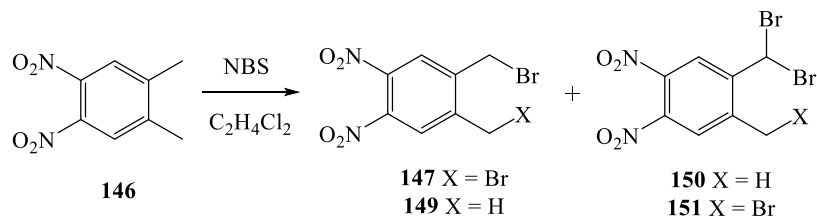


Figure 73. Products obtained from NBS bromination of dinitroxylylene **146**.

Bisbromomethyl **147** could be enriched by chromatography and recrystallized to analytical purity in a maximum of 20% yield. Dinitrile synthesis was envisioned to proceed analogously to the methoxy-substituted derivative but this substitution using sodium cyanide in DMSO⁶⁰ provided only traces of the presumed dinitrile derivative **148** along with a multitude of other products with a 60% mass balance.

Similar conditions had been applied to electronically related 2-bromomethyl-nitrobenzene (**152**) and produced none of the expected nitrile **153**. Rather 2,3-bis(2-nitrophenyl)propanenitrile (**155**) was produced along with 2,2'-dinitrostilbene (**154**) through intermediate carbanions or carbenes.⁹⁹ Through the addition of a small amount of sulfuric acid to tame the basicity of cyanide, 2-nitrobenzyl cyanide **153** could be obtained in 90% yield.¹⁰⁰ When these conditions were applied to nitro-substituted **147**, incomplete conversion was observed and a complex product mixture with no indication for dinitrile **148**.

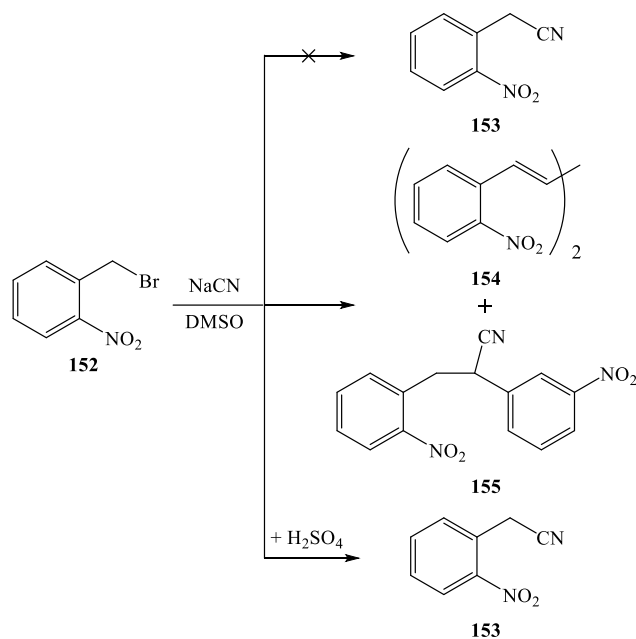


Figure 74. Synthesis of 2-nitrobenzyl-cyanide (**156**) and side products obtained through alternate reaction pathways.

When the solvent was changed to an ethanol/water mixture,¹⁰¹ ¹H NMR signals initially assigned to dinitrile **148** at 8.05 and 4.80 ppm were observed in trace quantities (300 MHz, CDCl₃). Unfortunately, the reaction occurred with a significant loss of material as a 25% mass balance was obtained containing side products similar to those from the substitution reaction in DMSO.

While not an initial goal of this project, cyclopenta[*b*]quinoxaline-2-one (**159**) was targeted through the Diekmann condensation approach.⁶⁰ Due to the symmetrical placement of the nitrogen atoms, isoindenone and isoindene dimers thereof were predicted to have electronic structures and HOMO-LUMO gaps similar to the initial targets **58** and **59**.²²

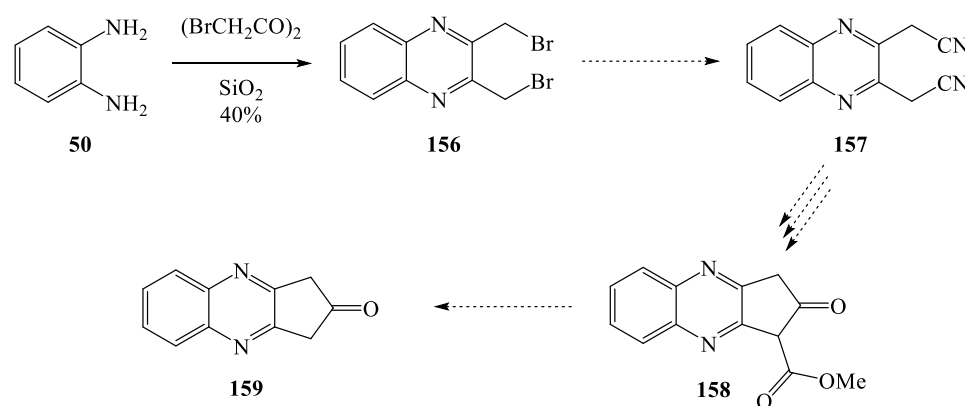


Figure 75. Potential pathway toward cyclopenta[*b*]quinoxaline-2-one (**159**).

The highly lachrymatory bisbromomethyl derivative **156** was obtained from a solid-phase condensation reaction and was envisioned to be the convergence point along the synthesis of 5,6-dimethoxy-2-indanone (**11h**) (*Figure 72*). Substitution of **156** using sodium cyanide in DMSO produced a complex product mixture exhibiting minimal conversion and a 15% mass balance that was not investigated further. When the solvent was changed to an ethanol/water mixture,¹⁰¹ the reaction selectivity was enhanced but the mass balance remained near 15%. A mini-workup from this reaction removed after one hour revealed that all starting material had been consumed to afford a symmetric and an asymmetric product as evidenced by the ^1H NMR aromatic splitting patterns. Only insignificant ^1H NMR signals corresponding to benzylic bromomethyl hydrogens were observed, eliminating the possibility of a single substitution. The crude material obtained after the reaction had stirred for an additional thirty minutes contained additional side products with the symmetrical product, displaying AA'BB' splitting, as the primary product. The mini-workup was most likely from a non-homogenous sample as two ^1H NMR signals corresponding to benzylic bromomethyl protons were observed in the final

product. No signals corresponding to the methylene units in the targeted product dinitrile **157** could be consistently assigned between the two spectra from the reaction.

Three otherwise identical substitution reactions were attempted on a smaller scale and worked up after fifteen, thirty and forty-five minutes in an attempt to monitor conversion. All three afforded similar mass balances near 15% that contained a significant fraction of the bisbromomethylated substrate (**156**). Interestingly, none of the ^1H NMR aromatic signals assigned to the symmetrical product from in the first reaction were present in these three reactions. Conversion to one symmetrical product and one asymmetric product occurred over this time period but the product obtained after forty-five minutes still contained nearly half of the starting material. The asymmetric product exhibited a splitting pattern that differed from those noted in first batch with a similar chemical shift. These signals present near half of the concentration of the symmetrical product in the three reactions started at the same time. The symmetrical product was most likely dinitrile **157** as the aromatic ^1H NMR signal integrations consistently fit that of the methylene signal at 4.23 ppm (300 MHz, CDCl_3). GC-MS could not confirm the presence of any postulated products.

Due to the time constraints of the surprisingly short two year Master's program, good faith efforts culminated with this attempt. Alternative pathways exist toward our target azaacenes and are currently under investigation in our lab. This project explored diverse approaches toward *N*-heterocyclic isoindenone dimer **58** and revealed the non-trivial nature of synthesizing rectilinear arranged azaacenes.

CHAPTER 4: SUMMARY AND OUTLOOK

Through this targeted synthetic project, novel isoindenones were investigated as building blocks for polycyclic scaffolds with relevance for materials science and academic investigations.

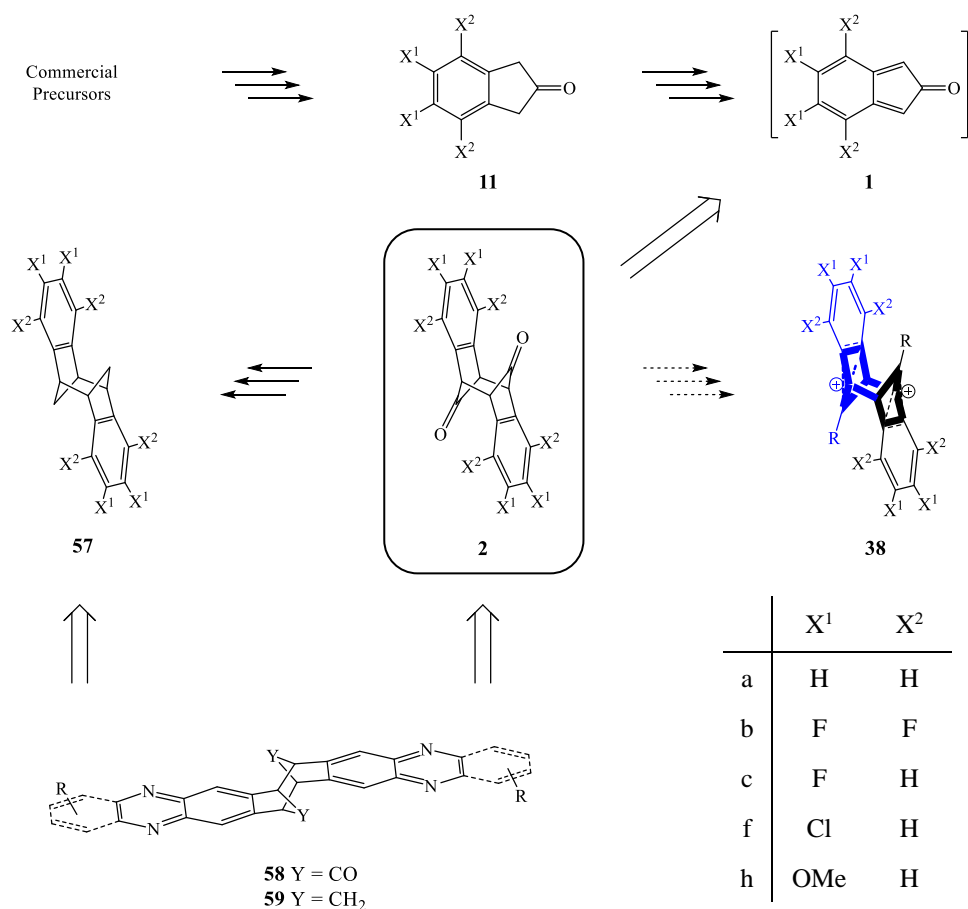


Figure 76. Targeted polycyclic frameworks and compounds from which they are derived alongside a table of the primary thesis-relevant substituents.

Aryl-substituted 2-indanones (**11**) were synthesized as precursors to all novel polycyclic frameworks targeted within this project. Thus, their synthetic routes were optimized to produce multigram quantities along individual pathways.

Isoindenone generation and dimerization was studied using synthetic protocols developed by Jones and optimized in our group. As we were previously unable to obtain the octafluoro-isindenone dimer **2b** through this route, fluorinated and methoxy-substituted isoindenones **1c/1h** were investigated to provide electronic contrast. Much to our surprise, each system successfully afforded isoindenone dimers analogous to the parent system. Isoindenones possessing various functional groups were explored concurrently in our group and provided little insight into the failure to obtain the octafluoro system **2b**. Preliminary data on the parent system indicates that these scaffolds may undergo cycloreversion reactions as reported for some 1,3-disubstituted systems.² Thus, it would be of interest to trap intermediates of these transformations and probe substituent effects on the various reaction pathways.

Formal isoindene dimers **57c** and **57h** were targeted to study their spectroscopic properties and for consideration of further functionalization. Fluorinated **57c** remained elusive through our efforts but methoxy-substituted **57e** was synthesized and subjected to further transformations. Precursors for non-classical carbocations (**38**) were prepared as synthetic intermediates in the pursuit of formal isoindene dimers (**57**) and preliminary data has provided evidence for their formation. The spectroscopic properties and solid-state structures of these dications will be studied in collaboration with Dr. Michael Gerken (University of Lethbridge, Canada).

Azaacenes of type **58** and **59** were targeted in this project, but their syntheses eluded our efforts. Methoxy groups were envisioned to provide access to *ortho*-quinones for condensation reactions but were unable to obtain any indication of isoindene or isoindenone derived quinones. Buchwald-Hartwig aminations have recently become

attractive for the synthesis of azaacenes but we were unsuccessful in applying this methodology toward **58** and **59**.

In an alternative approach toward scaffolds of type **58** and **59**, azaacene 2-indanone derivatives (**111**) were targeted for subsequent isoindenone generation and dimerization. The reactivity of isoindene **111** will be interesting to follow as we have realized that Jones' three-step sequence has certain limitations. While efforts toward 2-indanone **111** produced a variety of azaacenes, ring closure to the indane derivative was elusive.

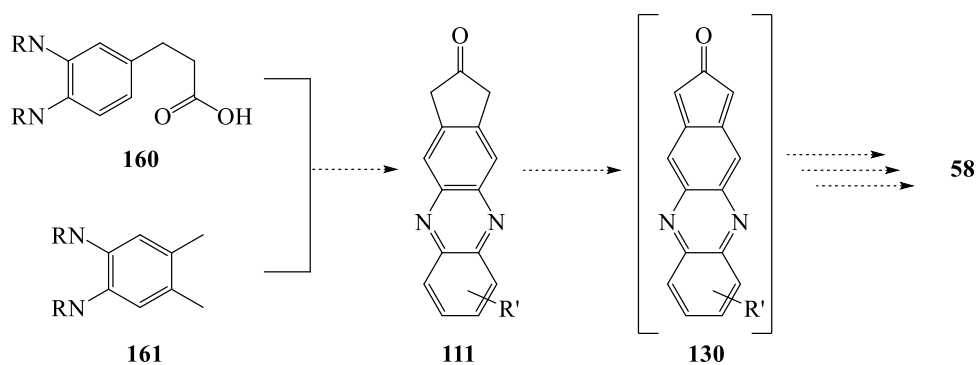


Figure 77. Envisioned synthesis of azaacene **58** through 2-indanone derivative **111**.

Alternative routes to azaacene 2-indanone derivatives exist and currently being explored within our group. Although not original targets for this project, the synthesis of 2-indanone derivative **159**, with the nitrogens moved in tandem by one arene unit, remains attractive through the condensation of pentane-1,2-dione (**162**) with substituted *o*-phenylene diamines (**50**). This approach avoids the troublesome five-membered ring formation while azaacene formation is incorporated early in the synthetic sequence. The

transformation of this indane derivative **163** to 2-indanone **159** will not be trivial, but the Etzkorn lab has acquired adequate control of this transformation on other derivatives.

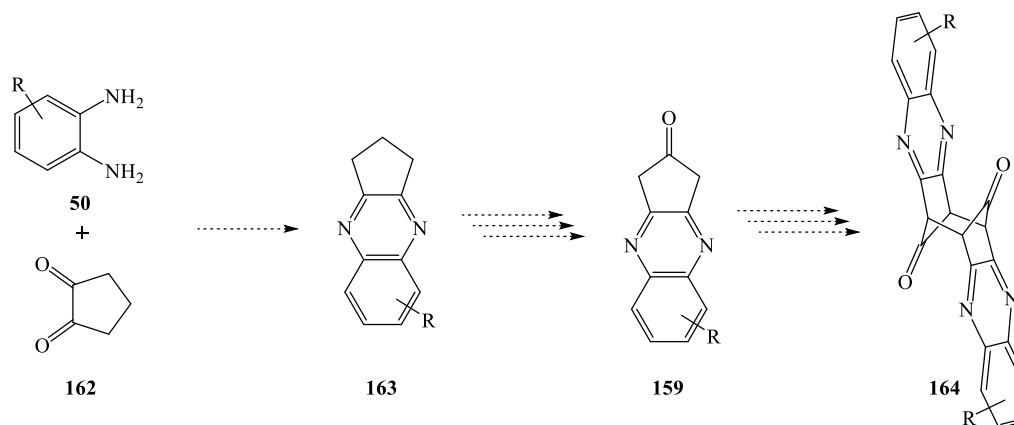


Figure 78. Synthetic scheme to an alternative isoindenone derived azaacene (**164**).

This project produced novel architectures and multiple solid-state structures that have provided us with guidelines toward the rational design of azaacenes of type **58** and **59**. When these architectures are synthesized, functionalization approaches will need to be carefully considered to direct solid-state packing and kinetically hinder dimerization so functional devices can be made.

Through this project, we have synthesized novel polycyclic scaffolds and have not failed in the synthesis of azaacenes **58** and **59**, rather, we have discovered many unsuccessful routes. The efforts described herein have provided guidelines for future exploration of these scaffolds in terms of their stabilities, use in organic electronics and feasibility as precursors for the generation of non-classical carbocations.

CHAPTER 5: EXPERIMENTAL

5.1 Instruments and Materials

Nuclear Magnetic Resonance

^1H NMR 300 MHz JOEL ECX-300

500 MHz Joel As500

^{13}C NMR 300 MHz JOEL ECX-300

500 MHz Joel As500

^{19}F NMR 300 MHz JOEL ECX-300

500 MHz Joel As500

All spectra were recorded at 298 K unless otherwise specified. Delta NMR software v. 4.3.5 was used for data analysis. Chemical shifts are reported in ppm, assigning tetramethylsilane (Acros Organics, NMR grade, 99.9% purity), [$\delta(\text{TMS}) = 0.00$ ppm] as ^1H and ^{13}C reference and trichlorofluoromethane [$\delta(\text{CFCl}_3) = 0.00$ ppm] as ^{19}F reference. Signal assignments were made based on homo- and heteronuclear 2D NMR experiments and on comparison with analogous compounds when applicable. Chemical shifts denoted with * were not conclusively assigned. The signal structure is indicated with the usual abbreviations for singlet (s), doublet (d), etc., and multiplets are quoted over the entire signal range. If a multiplet has an apparent doublet or triplet structure it is quoted as d_{app} or t_{app} respectively.

UV/Vis Spectroscopy

Spectra were recorded on a Varian Cary 300 Bio UV/Vis spectrophotometer using Simple Reads Scan v. 1.00(6) software for data analysis.

Infrared Spectroscopy

AT-IR spectra were collected on a PerkinElmer SpectrumOne FT-IR Spectrometer with Spectrum software version 5.0.2.

Mass Spectroscopy

GC-MS measurements were taken using an Agilent Technologies 6850 Network GC System with Agilent MSD Chemstation and GC-MS Data Analysis Software.

ESI-MS were recorded on a PerSeptive Biosystems: Mariner Biospectrometry Workstation model using Mariner Instrument Control Panel v. 4.0.0.0 software and Data Explorer v. 4.0.0.1 software for data analysis.

Microwave Apparatus

Microwave experiments were carried out on a CEM Discover model 908005 microwave reactor with ChemDriver v. 3.6.0 software.

X-ray Crystallographic Analysis

X-ray diffraction data were collected using a Bruker SMART APEX II diffractometer equipped with an APEX II 4 K charge-coupled device (CCD) area detector (by use of the program APEX)²⁰⁷ and a sealed-tube X-ray source (graphite-monochromated Mo-K α radiation, $\lambda = 0.71073$ Å). A complete sphere of data was collected to better than 0.8 Å resolution. Processing was carried out by using the program SAINT,²⁰⁸ which applied Lorentz and polarization corrections to three-dimensionally integrated diffraction spots. The program, SADABS,²⁰⁹ was used for the scaling of diffraction data, the application of decay correction based on redundant reflections. All calculations were made using the SHELXTL Plus package²¹⁰ for structure determination, refinement and molecular graphics. Unit cell dimensions and crystal lattice are confirmed using the XPREP²¹⁰

program. Unit cells, distance and angle measurements were found using Mercury 2.2 software. A solution was obtained using direct methods. Successive difference Fourier syntheses revealed all atoms. The final refinement was obtained by introducing a weighting factor and anisotropic thermal parameters for all non-hydrogen atoms.

Chemicals and Materials

All chemicals were purchased commercially and used as received unless otherwise specified. For column chromatography, alumina (basic, neutral and acidic) was purchased from Aldrich and silica gel was purchased from Silicycle Chemical Division.

5.2 Procedures and Experimental Data

5.2.1 Disubstituted 2-Indanones

Cinnamic Acid Derivatives via Knoevenagel Condensation

To 150 mmol of the corresponding benzaldehyde and 28.1 g (270 mmol) malonic acid, 80 mL of pyridine and 6 mL piperidine were added and vigorously stirred at 100°C for 4 h. The yellow solution was stirred at 80°C overnight and subsequently poured into 400 mL ½ conc. HCl to precipitate the product. The solid was collected in a fine frit, washed with 200 mL water and extensively dried under high vacuum to obtain the corresponding cinnamic acid in quantitative yields as a beige to purple solid.

(2*E*)-3-(3,4-difluorophenyl)-2-propenoic acid (67c):

¹H-NMR (300 MHz, CDCl₃): δ = 7.60 (d, 1H, 4-H), 7.05-7.38 (m, 3H, 3-, 7-, 8-H), 6.27 (d, 1H, 2-H) ppm

¹⁹F-NMR (300 MHz, CDCl₃): δ = -133.7 (m, 1F), -136.8 (m, 1F) ppm

(2*E*)-3-(3,4-dichlorophenyl)-2-propenoic acid (67f):

¹H-NMR (300 MHz, DMSO-d₆): δ = 8.04 (d, 1H, 4-H), 7.75-7.65 (m, 2H, 1'-, 8-H), 7.58 (d, 1H, 7-H), 6.55 (d, 1H, 2-H) ppm

(2*E*)-3-(3,4-dimethoxyphenyl)-2-propenoic acid (67h):

¹H-NMR (300 MHz, CDCl₃): δ = 7.68 (d, 1H, 5-H), 7.20 (d, 1H, 6-H), 7.04 (s, 1H, 2-H), 6.86 (d, 1H, 1'-H), 6.29 (s, 1H, 1''-H), 3.88 (s, 6H, -OMe) ppm

Propionic Acid Derivatives via Nickel Boride Mediated Reduction

To a bright green solution containing 82.0 mmol of the corresponding cinnamic acid, 5.30 g (22.2 mmol) nickel chloride hexahydrate and 450 mL methanol, 370 mmol of sodium borohydride was added in small portions over 1 h at room temperature to afford a dark black suspension. After stirring for an additional 3 h, the suspension was filtered over ample celite in a coarse frit. Firm packing of the celite and a preliminary wash with methanol were necessary to prevent elution of inorganic salts. The solvent was subsequently removed in vacuo to afford a beige to black solid. This solid was taken up in 200 mL 5% aq. KOH (w/w) to afford a yellow to black suspension and extracted once with 50 mL DCM that was discarded. This step often suffered from poor phase separation that could be improved by the addition of brine. The solution was subsequently acidified to pH 4 using half conc. HCl and extracted using DCM (4 x 80 mL). The combined organic phases were dried over MgSO₄ and concentrated in vacuo to furnish the corresponding propionic acid.

3,4-difluoro-benzenepropanoic acid (68c):

Yield: 85%, purple to black solid

¹H-NMR (300 MHz, CDCl₃): δ = 6.86-7.12 (m, 3H, 4-, 7-, 8-H), 2.90 (t, 2H, 3-H), 2.66 (t, 2H, 2-H) ppm

¹⁹F-NMR (300 MHz, CDCl₃): δ = -137.8 (m, 1F), -141.2 (m, 1F) ppm

3,4-dichloro-benzenepropanoic acid (68f):

Modifications: Heating to 60 °C prior to NaBH₄ addition was required to obtain maximum yield. The substrate was not dissolved at this temperature.

Yield: 75-85%, beige to green solid

$^1\text{H-NMR}$ (300 MHz, CDCl_3): δ = 7.35 (dd, 1H, 4-H), 7.30 (dd, 1H, 7-H), 7.04 (dd, 1H, 8-H), 2.89 (t, 2H, 3-H), 2.65 (t, 2H, 2-H) ppm

3,4-dimethoxy-benzenepropanoic acid (68h):

Modifications: Heating to 40 °C prior to NaBH_4 addition was required to obtain maximum yield. The substrate was not dissolved at this temperature.

Yield: 60%, beige to purple solid

$^1\text{H-NMR}$ (300 MHz, CDCl_3): δ = 6.71-6.81 (m, 3H, 4-, 7-, 8-H), 3.86 (s, 6H, OMe-H), 2.91 (t, 3H, 3-H), 2.67 (t, 3H, 2-H) ppm

1-Indanone Derivatives via PPA Mediated Cyclization

To 30 mL of PPA heated to 85°C with uninterrupted stirring, 13.4 mmol of the pulverized, vacuum-dried propionic acid derivative was added and stirred for 4 h.

Swirling of the flask by hand was initially required to obtain a homogenous light yellow solution. This solution was subsequently poured into 100 mL water and stirred by hand to ensure dissolution. This yellow to purple solution was extracted with DCM (6 x 50 mL), dried over MgSO_4 and concentrated in vacuo to obtain the 1-indanone derivative.

Reactions heated higher than 85°C or stirred longer than 4 h produced the aldol dimer thereof. The pure 1-indanone derivative could be obtained from a mixture containing the aldol dimer by extracting the solid with ether as the dimer exhibited poor solubility. The product could also be sublimed in vacuo for additional purification.

5,6-difluoro-1-indanone (69c):

Note: 3.5 h required with adequate stirring

Yield: 90%, beige solid

^1H -NMR (300 MHz, CDCl_3): δ = 7.26 (t_{app}, 1H, 4-H), 7.51 (t_{app}, 1H, 7-H), 3.11 (t, 2H, 3-H), 2.72 (t, 2H, 2-H) ppm

^{19}F -NMR (300 MHz, CDCl_3): δ = -126.1 (m, 1F), -137.3 (m, 1F) ppm

(2*E*)-2-(2,3-dihydro-5,6-difluoro-1*H*-inden-1-ylidene)-2,3-dihydro-5,6-difluoro-1*H*-inden-1-one (165):

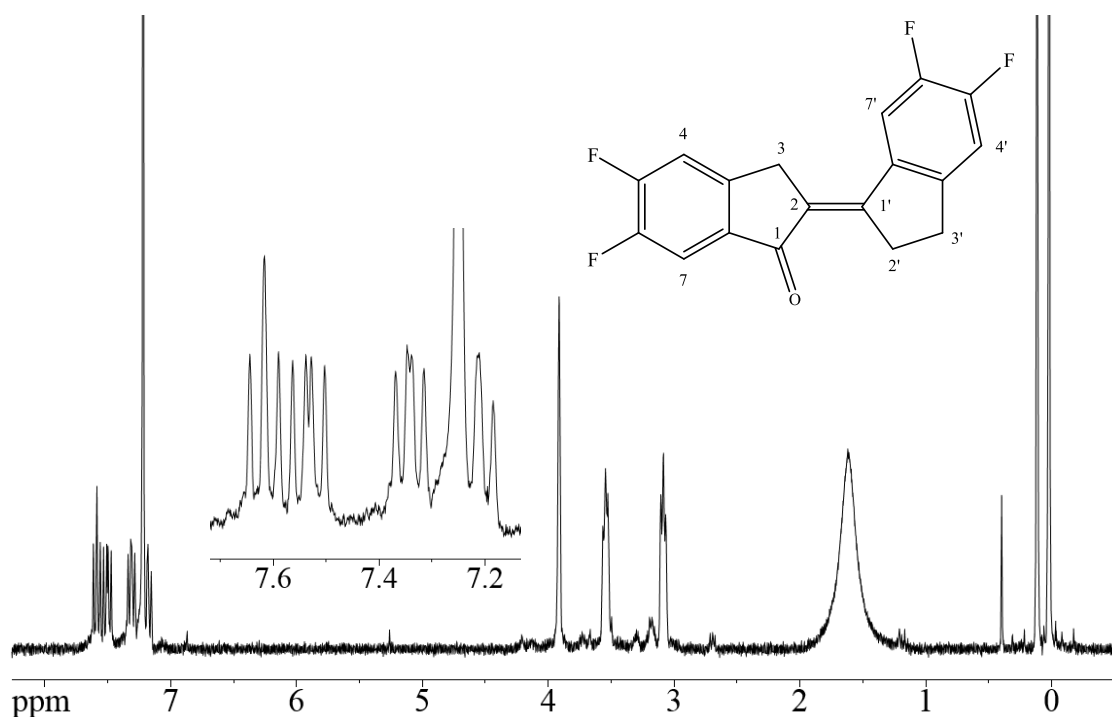


Figure 79. ^1H -NMR spectrum of (2*E*)-2-(2,3-dihydro-5,6-difluoro-1*H*-inden-1-ylidene)-2,3-dihydro-5,6-difluoro-1*H*-inden-1-one (**165**) (300 MHz, CDCl_3).

Note: The title compound was obtained as a poorly soluble solid in increasing quantities upon extended reaction time. This compound could be triturated to high purity with ether.

^1H -NMR (300 MHz, CDCl_3): δ = 7.56 (m, 1H, 7'-H), 7.47 (m, 1H, 7-H), 7.29 (m, 1H, 4-H), 7.12 (m, 1H, 4'-H), 3.89 (s, 1H, 3-H), 3.51 (t, 2H, 3'-H), 3.06 (t, 2H, 2'-H) ppm

^{19}F -NMR (300 MHz, CDCl_3): $\delta = -127.1$ (m, 1-F), -132.2 (m, 1-F), -137.2 (m, 1-F), -138.9 (m, 1-F) ppm

FT-IR (KBr): $\tilde{\nu} = 3062$ (w, Ar-H), 2926 (w, CH_2 -H), 1681 (s, C=O), 1594 (s), 1489 (s), 1449 (s), 1426 , 1325 (s), 1264 (s), 1214 (s), 1184 (s), 1132 , 1114 , 1084 , 1031 , 978 (w), 956 , 874 (s), 843 , 797 , 770 , 735 , 670 cm^{-1}

DI-MS: m/z (%) = 318.13 (14), 303.03 (7), 287.10 (5), 269.14 (14), 175.16 (11), 167.18 (47), 151.19 (100), 139.16 (19), 138.16 (38), 127.16 (22), 126.16 (21), 125.12 (41), 119.14 (36), 114.14 (22), 103.14 (22), 101.15 (22), 81.16 (24), 75.16 (47), 74.15 (20), 63.18 (41), 62.14 (25), 51.14 (53)

MP = $247\text{--}248$ $^{\circ}\text{C}$

5,6-dichloro-1-indanone (69f):

Yield: 40% in a mixture with **69[6,7-F]**, beige solid

^1H -NMR (500 MHz, CDCl_3): $\delta = 7.81$ (s, 1H, 7-H), 7.56 (s, 1H, 4-H), 3.10 (t, 2H, 2H, 2-H), 2.71 (t, 2H, 3-H) ppm

6,7-dichloro-1-indanone (69[6,7-F]):

Yield: 40% in a mixture with **69f**, beige solid

^1H -NMR (500 MHz, CDCl_3): $\delta = 7.61$ (d, 1H, 5-H), 7.30 (d, 1H, 4-H), 3.08 (t, 3H, 2-H), 2.77 (t, 3H, 3-H) ppm

5,6-dimethoxy-1-indanone (69h):

Yield: 95%, beige solid

^1H -NMR (300 MHz, CDCl_3): $\delta = 7.19$ (s, 1H, 7-H), 6.90 (s, 1H, 7-H), 3.98 (s, 3H, OMe-H), 3.93 (s, 3H, OMe-H), 3.06 (t, 3H, 3-H), 2.69 (t, 3H, 2-H) ppm

5,6-dichloro-1-indanone (69f):

To 5.08 g (24.4 mmol) 3,4-dichloro-benzenepropanoic acid, 16 mL ClSO_3H was added dropwise and stirred for 1 h. Subsequently, the brown solution was carefully poured into 100 mL ice water, extracted 4x60 ml DCM, dried over MgSO_4 and concentrated in vacuo to afford 4.05 g of the title compound as a light yellow solid (87% yield). (Characterized above)

1-Indanol Derivatives via NaBH_4 Mediated Reduction

To a solution of 11.9 mmol of the respective 1-indanone derivative in 60 mL 95% ethanol, sodium borohydride (230 mg, 6.08 mmol) was added portion-wise over 15 min. After stirring overnight, the light-yellow solution was carefully poured into 100 mL 1 M HCl and extracted with chloroform (3x50 mL). The combined organic phase was dried over MgSO_4 and concentrated in vacuo to afford the indanol derivative as a light-yellow oil.

5,6-difluoro-1-indanol (70c):

Yield: 95%

$^1\text{H-NMR}$ (300 MHz, CDCl_3): δ = 7.01 (m, 1H, 7-H), 7.17 (m, 1H, 4-H), 5.16 (t, 1H, 1-H), 2.99 (m, 1H, 3-H), 2.77 (m, 1H, 3-H), 2.51 (m, 1H, 2-H), 1.96 (m, 1H, 2-H) ppm

$^{19}\text{F-NMR}$ (300 MHz, CDCl_3): δ = -138.3 (m, 1F), -140.7 (m, 1F) ppm

5,6-dichloro-1-indanol (70f):

Yield: 95%

^1H -NMR (300 MHz, CDCl_3): δ = 7.47 (s, 1H, 4-H), 7.30 (s, 1H, 7-H), 5.18 (t, 1H, 1-H), 2.99 (m, 1H, 3-H), 2.78 (m, 1H, 3-H), 2.50 (m, 1H, 2-H), 1.98 (m, 1H, 2-H) ppm

6,7-dichloro-1-indanol (70h):

Note: This product not isolated and was produced from the reduction of 6,7-dichloro-1-indanone (**69[6,7-F]**) carried over from the cyclization reaction

^1H -NMR (300 MHz, CDCl_3): δ = 7.42 (m, 1H, 7-H), 7.23 (m, 1H, 4-H), 5.26 (t, 1H, 1-H), 3.05 (m, 1H, 3-H), 2.85 (m, 1H, 3-H), 2.50 (m, 1H, 2-H), 1.98 (m, 1H, 2-H) ppm

5,6-dimethoxy-1-indanol (70h):

Note: The product often contained multiple, presumably boronic ester derived, side products upon initial workup. After standing overnight, ^1H NMR indicated a nearly pure product.

Yield: 99%

^1H -NMR (500 MHz, CDCl_3): δ = 6.95 (s, 1H, 7-H), 6.75 (m, 1H, 5-H), 5.19 (t, 1H, 1-H), 3.89 (s, 3H, OMe-H), 3.86 (s, 3H, OMe-H), 2.99 (m, 1H, 3-H), 2.75 (m, 1H, 3-H), 2.48 (m, 1H, 2-H), 1.94 (m, 1H, 2-H) ppm

Indene Derivatives via PTSA Catalyzed Dehydration

A catalytic amount of PTSA was added to a solution of 8.83 mmol of the 1-indanol derivative in 50 mL benzene and refluxed at 110°C in a 100 ml RBF equipped with a well-insulated Dean-Stark trap for 4-6 h. The reaction progress was monitored by ^1H NMR. The resulting yellow solution was washed with a saturated solution of aqueous sodium bicarbonate, dried over MgSO_4 and concentrated at 40°C under vacuum not

below 100 mbar to avoid distilling the product. Indene derivatives were obtained as a colorless to light yellow oil in quantitative yields containing residual benzene.

5,6-difluoroindene (71c):

$^1\text{H-NMR}$ (300 MHz, CDCl_3): δ = 7.24 (t_{app} , 1H, 7-H), 7.16 (dd_{app} , 1H, 4-H), 6.79 (m, 1H, 1-H), 6.59 (m, 1H, 2-H), 3.36 (t, 2H, 3-H) ppm

$^{19}\text{F-NMR}$ (300 MHz, CDCl_3): δ = -142.0 (m, 1F), -143.7 (m, 1F) ppm

5,6-dichloroindene (71f):

$^1\text{H-NMR}$ (300 MHz, CDCl_3): δ = 7.52 (s, 1H, 7-H), 7.45 (s, 1H, 4-H), 6.79 (m, 1H, 1-H), 6.61 (m, 1H, 2-H), 3.38 (t, 2H, 3-H) ppm

1,2-epoxy-5,6-dichloro-indene (72f):

To a stirring solution of 100 mg (0.54 mmol) 5,6-dichloroindene in 2 ml DCM, 146 mg (0.59 mmol) PTSA (70% w/w) was added portionwise and stirred for 3 h. The resulting light yellow suspension was diluted with 20 ml DCM, washed once with sat. 10 ml aq. sodium sulfite then twice with 10 ml sat. aq. sodium bicarbonate. The organic phase was dried over MgSO_4 and concentrated in vacuo to afford the title compound as a pale yellow solid in 64% yield.

$^1\text{H-NMR}$ (300 MHz, CDCl_3): δ = 7.49 (s, 1H, 7-H), 7.18 (s, 1H, 4-H), 4.13 (m, 1H, 1-H), 4.08 (m, 1H, 2-H), 3.12 (m, 1H, 3-H), 2.98 (m, 1H, 3-H) ppm

5,6-dimethoxy-2-oxime-indan-1-one (166):

To a suspension of 10 mmol of 5,6-dimethoxy-1-indanone in 8 mL dimethoxy ethane, 2.7 mL of 37% aq. HCl was added and stirred for 5 min to afford a dark brown solution. 12 mmol of amyl nitrite were subsequently added dropwise and the mixture was stirred overnight. As the product precipitated, the suspension became lighter in color. The fine product was isolated as a brown solid by filtering through a filter paper covering a fine frit and washing with water. The filtrate could be refiltered to collect additional product. The title compound was obtained as yellow to brown solid in 70% yield after extended drying under high vacuum

¹H-NMR (300 MHz, CDCl₃): δ = 7.32 (s, 1H, 5-H), 6.92 (s, 1H, 4-H), 4.00 (s, 3H, OMe-H), 3.92 (s, 3H, OMe-H), 7.78 (s, 1H, 4-H) ppm

5,6-dimethoxy-indan-1,2-dione (76):

A brown suspension of 6.79 mmol of 2-oxime **166**, 3.1 mL 37% formaldehyde and 5.5 mL conc. HCl were stirred overnight to precipitate the product. The diketone was isolated analogously to the oxime to afford the title compound in 68% yield as a yellow to brown solid.

¹H-NMR (300 MHz, CDCl₃): δ = 7.34 (s, 1H, 5-H), 6.96 (s, 1H, 4-H), 4.05 (s, 3H, OMe-H), 3.96 (s, 3H, OMe-H), 3.53 (s, 2H, 3-H) ppm

5,6-dimethoxy-indan-1,2-diol (77):

To 1.0g (5.0 mmol) of the diketone **76** contained in a Schlenk flask degassed with argon and cooled to 0°C, 60 mL of dry THF (obtained from a sodium/benzophenone still)

was added to afford a light brown suspension. 0.70 mL (7.3 mmol) of a borane•dimethyl sulfide complex was added dropwise and the suspension was stirred for 3 days at room temperature. After 1 h, the mixture was a light burgundy red solution that darkened slightly over 3 days. 5 mL of water was subsequently added followed by 0.1 mL of 2 M aq. H₂SO₄ and stirred for 30 min. Phase separation was achieved via the addition of 15 mL brine and the aqueous phase was extracted with ether (4 x 10 mL), dried over MgSO₄ and concentrated in vacuo to afford the title compound in quantitative yield as a tacky brown solid.

¹H-NMR (300 MHz, CDCl₃): δ = 6.89 (s, 1H, 7*-H), 6.72 (s, 1H, 4*-H), 4.96 (m, 1H, 1-H), 4.36 (m, 1H, 2-H), 3.90 (s, 6H, OMe-H), 3.22 (dd, 1H, 3-H), 2.73 (dd, 1H, 3-H) ppm

2-Indanone Derivatives via Peroxyformic Acid

To a stirring solution of 18 mL formic acid and 3.0 mL of 30% aq. hydrogen peroxide heated to 35°C, 16.4 mmol of the respective indene derivative was added dropwise over 45 min and stirred for an additional 2 h at this temperature. After stirring the yellow solution at room temperature overnight, excess formic acid was distilled under an aspirator vacuum with heat not exceeding 60°C to afford an orange solid. Additional drying under high vacuum was occasionally necessary to obtain a solid. The formate ester intermediate could be stored at -10 °C overnight with no effect on the yield. 25mL of 7% aq. H₂SO₄ was subsequently added to the intermediate in a 50 ml RBF fitted with a spiraling cooled reflux condenser. The suspension was vigorously stirred and refluxed at 120°C to condense the product onto the cooling loop through a modified steam distillation until no further condensation was observed (8-30 h). When significant

amounts were visible in the condenser, the product was washed off into an Erlenmeyer flask with DCM followed by a wash with water (~every 2 h). 1-2 mL conc. H_2SO_4 were added to the modified steam distillation when no product had condensed after 4 h with no effect on the yield. The organic phase was separated, dried over MgSO_4 and concentrated in vacuo to afford the analytically pure 2-indanone derivative as a colorless to light yellow solid.

5,6-difluoro-2-indanone (11c**):**

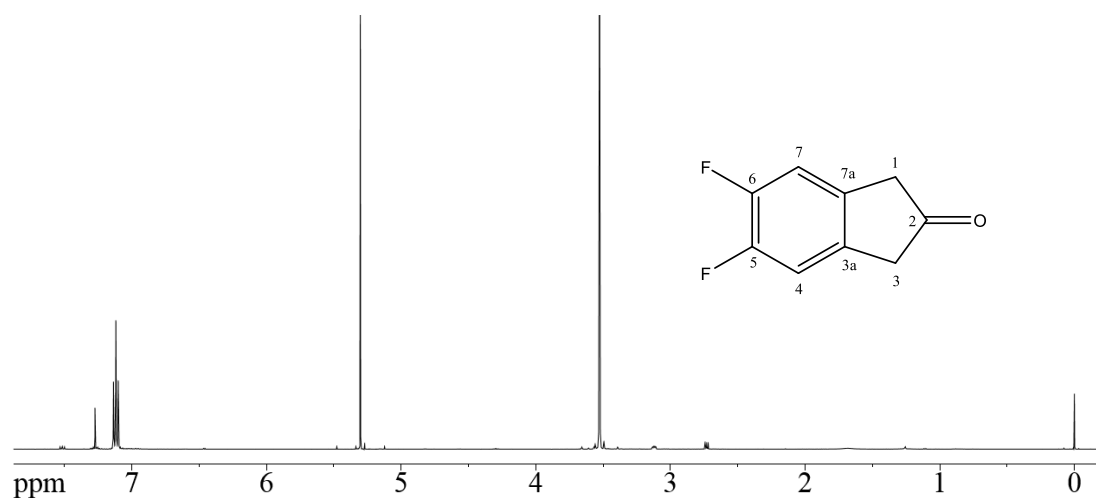


Figure 80. ^1H -NMR spectrum of 5,6-difluoro-2-indanone (**11c**) (500 MHz, CDCl_3).

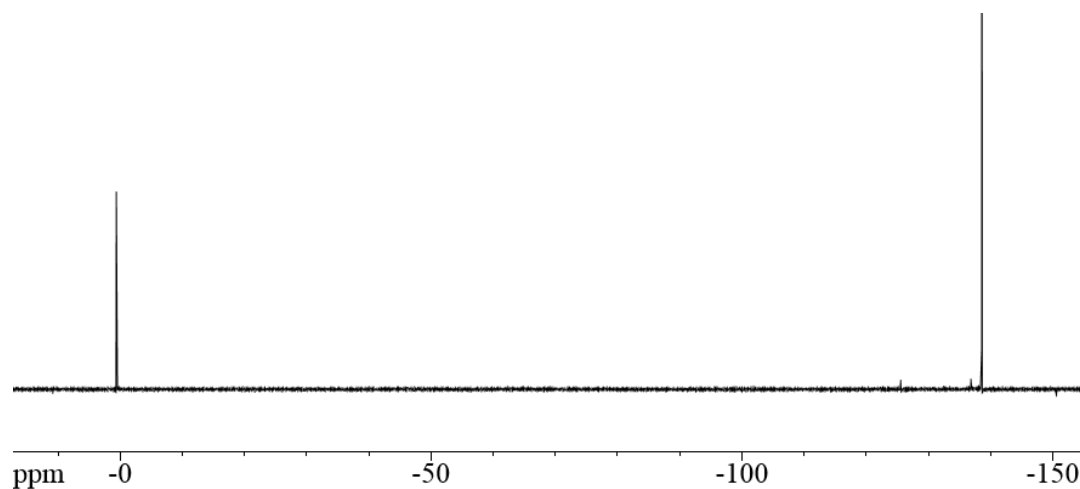


Figure 81. ^{19}F -NMR spectrum of 5,6-difluoro-2-indanone (**11c**) (300 MHz, CDCl_3).

Yield: 40%

^1H -NMR (500 MHz, CDCl_3): δ = 7.11 (t_{app} , 2H, 4-, 7-H), 3.52 ppm (s, 4H, 1-, 3-H) ppm

^{13}C -NMR (300 MHz, CDCl_3): δ = 43.8 (1-, 3-C), 114.0 (4-, 7-C), 133.8 (3a-, 7a-C),

150.1 (5-, 6-C), 213.3 (2-C) ppm

^{19}F -NMR (300 MHz, CDCl_3): δ = -139.2 (t_{app}) ppm

AT-IR: $\tilde{\nu}$ = 3464 (w), 3131 (w), 3078 (w), 3056 (w), 2954 (w), 2900 (w), 2850 (w), 1738

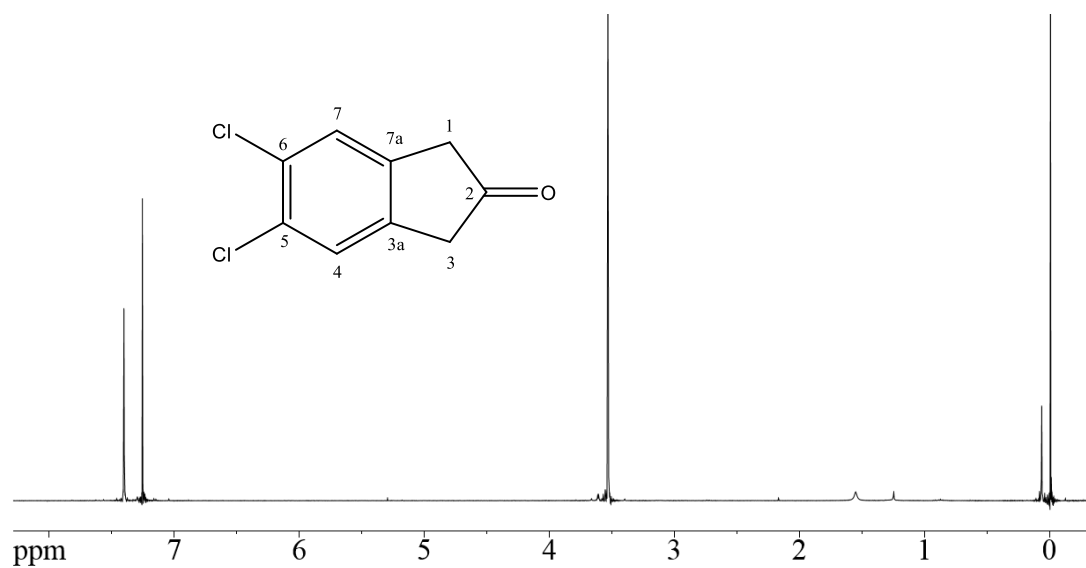
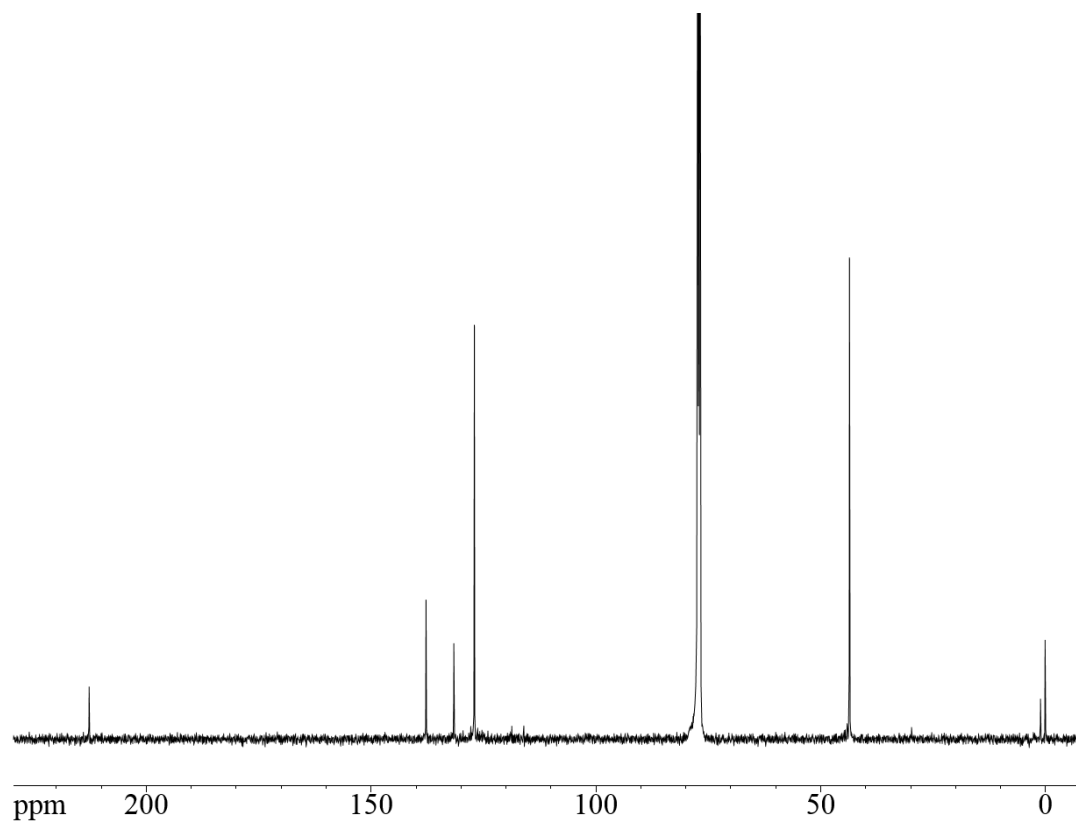
(s), 1625 (w), 1608, 1576 (w), 1555 (w), 1496 (s), 1456 (w), 1441, 1391 (s), 1333 (s),

1287, 1244, 1231, 1220 (s), 1197, 1144, 1097 (w), 1067, 964, 944 (w), 862 (s), 844, 801

(s), 752, 743, 686 (w) cm^{-1}

GC-MS (EI, 70 eV): m/z (%) = 168.0 (M^+ , 100), 140.0 (-CO, 100), 139.0 (29), 119.0

(14), 114.0 (30)

5,6-dichloro-2-indanone (11f):Figure 82. ¹H-NMR spectrum of 5,6-dichloro-2-indanone (**11f**) (500 MHz, CDCl₃).Figure 83. ¹³C-NMR spectrum of 5,6-dichloro-2-indanone (**11f**) (500 MHz, CDCl₃).

Yield: 10%

$^1\text{H-NMR}$ (500 MHz, CDCl_3): δ = 7.40 (s, 2H, 4-, 7-H), 3.53 (s, 4H, 1-, 3-H)

$^{13}\text{C-NMR}$ (500 MHz, CDCl_3): δ = 212.7 (C-2), 137.8 (C-4, -7), 131.6 (C-3a, -7a), 43.6 (C-1, -3) ppm

MS (EI, 70 eV): m/z (%) = 201.9 ($^{37}\text{Cl}_2$, 21), 199.9 ($^{37}\text{Cl}^{35}\text{Cl}$, 30), 173.9 ($^{37}\text{Cl}_2\text{-CO}$, 66), 171.9 ($^{35}\text{Cl}_2\text{-CO}$, 100), 136.9 (33), 102.0 (33), 101.0 (19), 75.0 (18), 68.0 (16), 51.0 (14)

AT-IR (KBr): $\tilde{\nu}$ = 3089 (w), 3073 (w), 3037 (w), 2931 (w), 2911 (w), 2853 (w), 1747 (C=O, s), 1598, 1557, 1466, 1435, 1392, 1375, 1295, 1270, 1250, 1210, 1181, 1116, 1058, 1008, 964, 927, 883, 865, 822, 865, 822, 782, 730, 686, 673 cm^{-1}

MP: 93-97 °C

4,5-dichloro-2-indanone (11f):

$^1\text{H-NMR}$ (300 MHz, CDCl_3): δ = 7.22-7.31 (m, 2H, 4-, 5-H), 3.55 (s, 2H, 3-H), 3.52 (s, 2H, 1-H) ppm

5,6-dichloro-2-indanone (11f):

To a solution of 105 mg (0.52 mmol) 1,2-epoxy-5,6-dichloro-indene in 2 mL benzene cooled to 10 °C, 200 mg ZnI_2 was added portionwise. The cold bath was removed and the light pink solution was stirred for 4 h. The solution was diluted with 5 ml chloroform and washed twice with 5ml water. After drying over MgSO_4 and concentration in vacuo, the crude material was subjected to column chromatography (7:1 hexanes:EtOAc, R_f = 0.2) to furnish 34 mg of the title compound (33% yield). (Note: Characterization is described above)

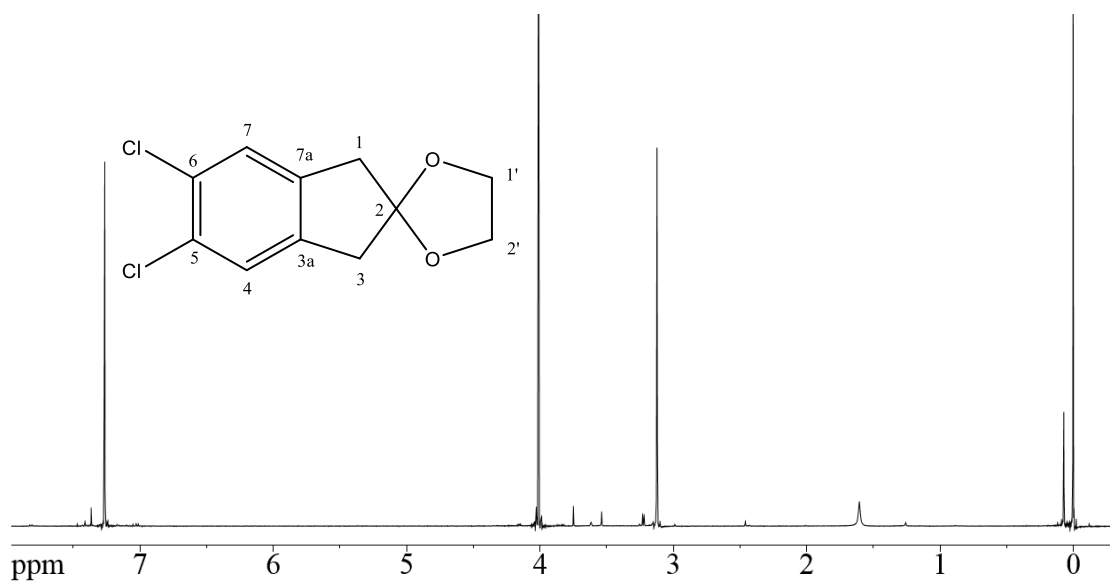
1',3'-dihydro-spiro[5,6-dichloro-1,3-dioxolane-2,2'-[2*H*]indene] (167**):**

Figure 84. ^1H -NMR spectrum of 1',3'-dihydro-spiro[5,6-dichloro-1,3-dioxolane-2,2'-[2*H*]indene] (**167**) (500 MHz, CDCl_3).

To a solution of 145 mg (0.73 mmol) 5,6-dichloro-2-indanone in 15 mL benzene, 90 μl (1.80 mmol) ethylene glycol and a catalytic amount of PTSA were refluxed in a 50 mL RBF fitted with a well-insulated Dean-Stark trap for 3 h. The resulting light yellow solution was washed once with 5 mL sat. aq. sodium bicarbonate, once with 5 mL water, dried over MgSO_4 and concentrated in vacuo to furnish 169 mg of the title compound as a colorless solid (96% yield).

^1H -NMR (500 MHz, CDCl_3): δ = 7.26 (s, 2H, 4-, 7-H), 4.00 (s, 4H, 1'-, 2'-H), 3.11 (s, 4H, 1-, 3-H) ppm

1,2-bis(bromomethyl)-4,5-dimethoxybenzene (80):

To a solution of 40.32 g (292 mmol) veratrol in 87 mL of glacial acetic acid, 17.55 g (1.02 mol) of paraformaldehyde was added to afford a murky white suspension. 125 ml 33% HBr in acetic acid (w/w) was added slowly to the suspension which produced a light yellow solution upon vigorous stirring. The product precipitated slowly over 20 h where yellow solid was evident after the first hour. Without isolation, the product was recrystallized by heating to 65 °C until all solid had dissolved to an orange solution and poured into ice water to precipitate the colorless to light yellow product. The product was subsequently collected in a fine frit and washed with 200 mL water. The off-white solid was dissolved in DCM and separated from the remaining water, dried over MgSO_4 and concentrated in vacuo to furnish 69.25 g (214 mmol) of the title compound as an off-white solid (73 % yield).

$^1\text{H-NMR}$ (300 MHz, CDCl_3): δ = 6.84 (s, 2H, 3-, 6-H), 4.63 (s, 4H, 1-, 6-H), 3.90 (s, 6H, $-\text{OCH}_3$) ppm

MP: 106–108 °C

1,2-bis(cyanomethyl)-4,5-dimethoxybenzene (81):

A solution of 61.80 g (190.8 mmol) 1,2-bis(bromomethyl)-4,5-dimethoxybenzene in 188 ml DMSO was added to a suspension of 21.40 g (426.7 mmol) NaCN in 188 ml DMSO and stirred at 90 °C for 3 h. The dark black suspension was subsequently diluted with 150 ml water and extracted with chloroform (4 x 100 ml). To remove a majority of the remaining DMSO, the combined organic phase was first washed with 100 mL 0.1 M aq. HCl. 50 ml chloroform were used to extract the acidic wash before being washed

once with 20 ml 0.1 M aq. HCl. The combined organic phase was washed twice with 100 ml brine, dried over MgSO₄ and concentrated in vacuo to afford 48.18 g (170.9 mmol) of the title compound as a brown oil (90% yield). When the reaction was scaled to 1 g, increased side products were present after workup.

¹H NMR (300 MHz, CDCl₃) δ = 6.90 (s, 2H, 3-, 6-H), 3.90 (s, 6H, OMe), 3.70 (s, 4H, CH₂) ppm

dimethyl-2,2'-(4,5-dimethoxy-1,2-phenylene)diacetate (82):

To a three-necked flask fitted with an intensive reflux condenser containing a solution of 20.30 g (94.0 mmol) crude 1,2-bis(cyanomethyl)-4,5-dimethoxybenzene in 145 mL MeOH, 39.6 mL (545.9 mmol) of SOCl₂ was added dropwise at room temperature via syringe over 1 h that effected a highly exothermic reaction. After the black solution was refluxed for 2 days, the reaction was cooled to room temperature, diluted with 150 ml EtOAc and washed with 100 ml water. 50 ml EtOAc were used to extract this aqueous layer and washed with 20 mL water before combining the organic phases. The resulting brown solution was dried over MgSO₄ and concentrated in vacuo to afford 19.58 g (69.4mmol) of the title compound as a brown oil (74 % yield).

¹H NMR (300 MHz, CDCl₃) δ = 6.76 (s, 2H, 3-, 6-H), 3.85 (s, 6H, OMe), 3.67 (s, 6H, CH₂*), 3.62 (s, 4H, CH₂*) ppm

1-carbmethoxy-5,6-dimethoxyindan-2-one (83):

To a stirring solution of NaOMe prepared from 3.85 g Na (16.7mmol) in 75 mL benzene, a solution of 23.90 g (8.48 mmol) diester **82** in 150 mL benzene was added

dropwise and heated to reflux for 1.5 h. The dark brown solution was subsequently poured into 100 mL water and extracted with ether (2 x 50 ml). The aqueous phase was acidified to pH 4 with half conc. HCl and the precipitate was collected in a fine fritted funnel. After extended drying under high vacuum, 8.36 g (3.34 mmol) of the title compound was obtained as a beige solid (39% yield). In select batches, the product contained less than 10% of its ene-ol tautomer as determined by ^1H NMR.

^1H NMR (300 MHz, CDCl_3): δ = 7.20 (s, 1H, 4-H), 6.92 (s, 1H, 6-H), 3.97 (s, 3H, OMe*), 3.93 (s, 3H, OMe*), 3.87 (s, 3H, OMe*), 3.53 (s, 2H, 1-H) ppm

MP: 132-135°C

5,6-dimethoxyindan-2-one (11h):

To a 40 mL solution of a 9:1 DMSO:water mixture (v:v), 3.92 g (15.7 mmol) of 1-carbmethoxy-5,6-dimethoxyindan-2-one (**83**) was added and heated to 120 °C for 2.5 h. The brown solution was subsequently poured into 50 ml water and extracted with chloroform (4 x 50 ml). To remove a majority of the remaining DMSO, the organic layer was first washed with 50 ml 0.1 M aq. HCl. 25 ml CHCl_3 was used to extract the acid wash once and washed once with 25 ml 0.1 M aq. HCl. The combined organic phase was washed twice with 50 ml brine, dried over MgSO_4 and concentrated in vacuo to afford 2.72 g (14.1 mol) of the title compound as a red crystalline solid (90 % yield).

^1H NMR (300 MHz, CDCl_3) δ 6.82 (s, 2H, 4-, 6-H), 3.88 (s, 6H, OMe), 3.51 (s, 4H, 1-, 3-H) ppm

MP: 117°C

5,6-dibromo-2-indanol (84):

To a solution of 2.0 g (15.2 mmol) 2-indanone in 15 ml MeOH, 630 mg (16.7 mmol) NaBH₄ was added portionwise and stirred 2 h. The light yellow solution was subsequently poured into 40 ml 1 M aq. HCl and extracted 4x20 ml DCM. The organic phases were combined, dried over MgSO₄ and concentrated in vacuo to afford 1.80 g of the title compound as a pale yellow waxy solid (88% yield).

¹H NMR (300 MHz, CDCl₃): δ = 7.31-7.18 (m, 4H, 4-, 5-, 6-, 7-H), 4.67 (s, 1H, 2-H), 3.05 (ddd, 4H, 1-, 3-H) ppm

indan-2-ol acetate (85):

To 1.80 g (13.4 mmol) indan-2-ol, 4.46 ml (66.3 mmol) acetyl chloride was added dropwise at 0°C. After stirring overnight, 50 ml sat. aq. Na₂CO₃ was added and the light yellow solution was extracted 4x50ml DCM. The organic phases were combined, dried over MgSO₄ and concentrated in vacuo to afford 2.34 g of the title compound as a pale yellow waxy solid (99% yield).

¹H NMR (300 MHz, CDCl₃): δ = 7.21 (m, 4H, 4-, 5-, 6-, 7-H), 5.52 (sept, 1H, 2-H), 3.17 (ddd, 4H, 1-, 3-H), 2.02 (s, 3H, -CH₃) ppm

5.2.2 Isoindenone Generation and Dimerization**General Silylation of 2-Indanone Derivatives**

To a solution of 5.6 mmol of the corresponding 2-indanone in 15 ml benzene, 990 mg (6.6 mmol) TBDMSCl was added followed by the dropwise addition of 1.00 g (6.6 mmol) DBU. Reaction progress was monitored by ¹H NMR and after typically 1 h, the

brown suspension was diluted with ether, washed twice with cold water, dried over MgSO_4 and concentrated in vacuo to afford the crude product as a brown oil in quantitative yield.

2-(*tert*-butyldimethylsiloxy)-5,6-difluoro-indene (89c**):**

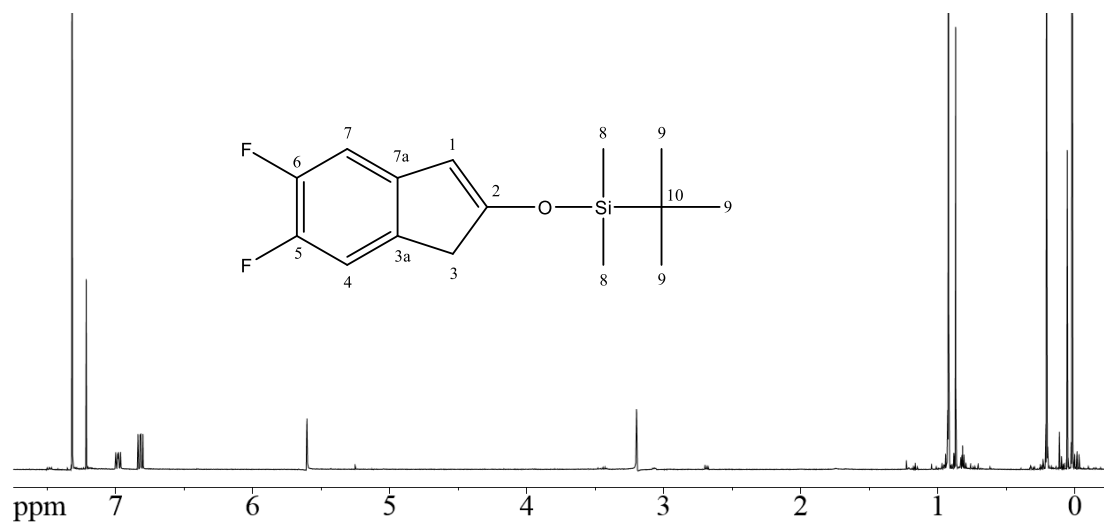


Figure 85. ^1H -NMR spectrum of 2-(*tert*-butyldimethylsiloxy)-5,6-difluoro-indene (**89c**) (500 MHz, CDCl_3).

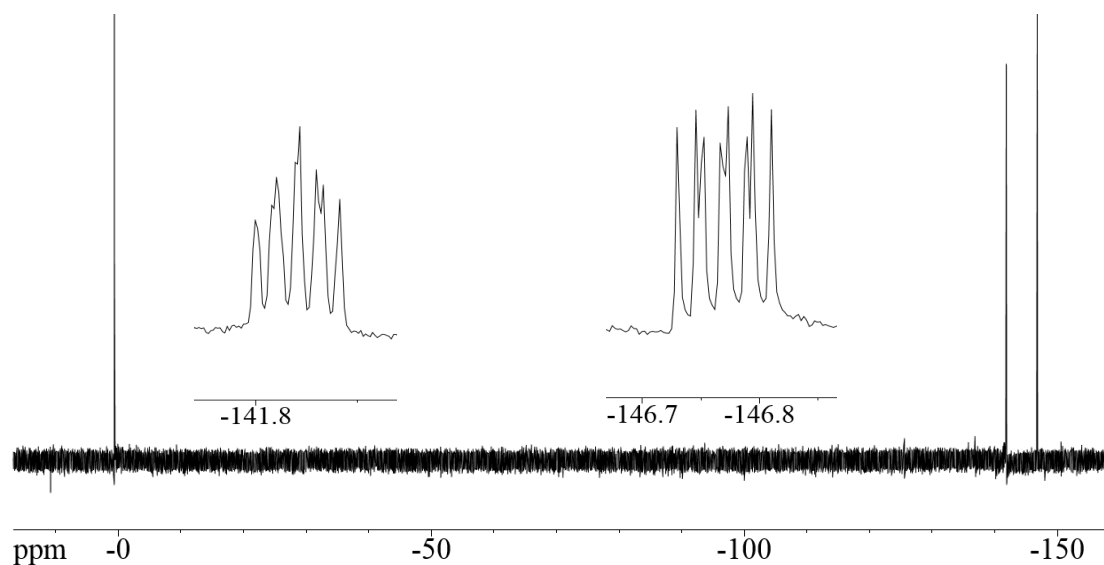


Figure 86. ^{19}F -NMR spectrum of 2-(*tert*-butyldimethylsiloxy)-5,6-difluoro-indene (**89c**) (500 MHz, CDCl_3).

Yield: 96%

$^1\text{H-NMR}$ (500 MHz, CDCl_3): δ = 7.03 (dd, 1H, H-7), 6.87 (dd, 1H, H-4), 5.65 (s, 1H, H-1), 3.24 (s, 2H, H-3), 0.97 (s, 9H, *t*-Bu), 0.25 (s, 6H, H-8) ppm

$^{19}\text{F-NMR}$ (500 MHz, CDCl_3): δ = -142.5 (m), -147.4 (m) ppm

MS (EI, 70 eV): m/z (%) = 283.1 (^{29}Si , 21), 282.1 (M^+ , 100), 226.1 (*t*-Bu, 21), 225.1 (38), 151.0 (70), 129.0 (18), 101 (24), 75 (17), 73.1 (82)

2-(*tert*-butyldimethylsiloxy)-5,6-dichloro-indene (89f):

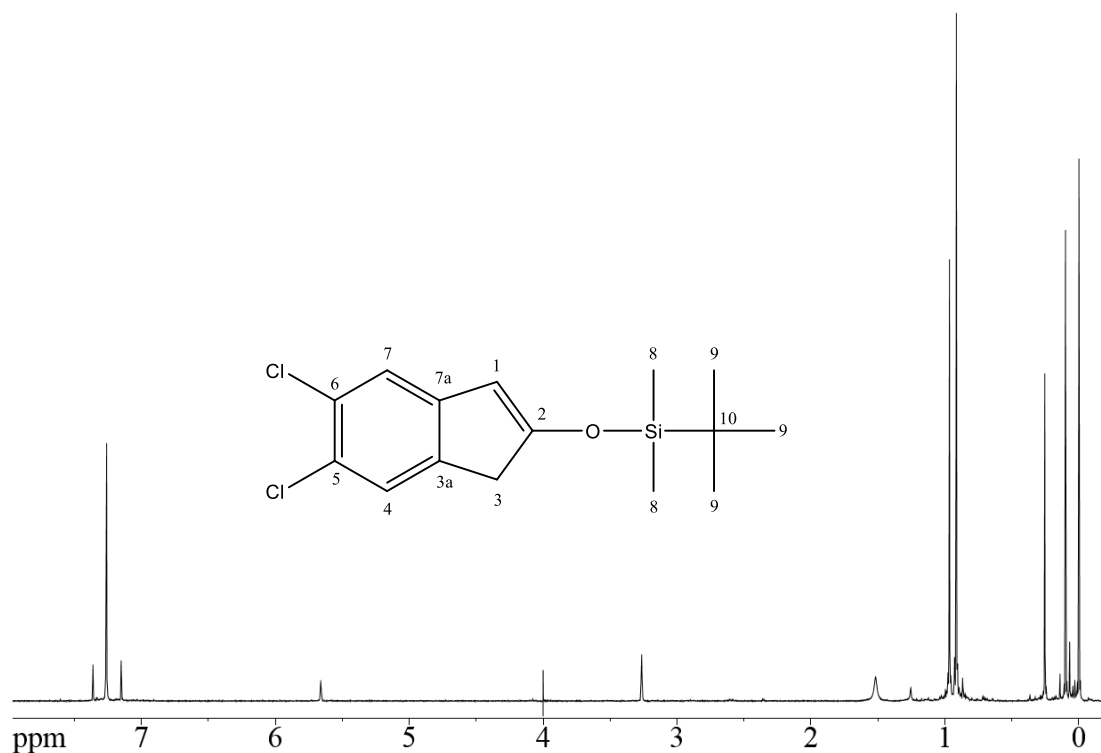


Figure 87. $^1\text{H-NMR}$ spectrum of 2-(*tert*-butyldimethylsiloxy)-5,6-dichloro-indene (**89f**) (500 MHz, CDCl_3).

$^1\text{H-NMR}$ (500 MHz, CDCl_3): δ = 7.35 (s, 1H, 7-H), 7.14 (s, 1H, 4-H), 5.64 (s, 1H, 1-H), 3.42 (s, 2H, 3-H) ppm

MS (EI, 70 eV): m/z (%) = 318.1 (9), 317.1 (9), 316.1 (49), 315.1 (16), 314.1 (73), 261.0 (7), 260.0 (13), 259.0 (31), 258.0 (20), 257.0 (*-t*Bu, 44), 187.0 (7), 186.0 (7), 185.0 (43), 184.0 (11), 183.0 (*-OTMS*, 66), 136.0 (6), 115.0 (5), 113.0 (5), 93.0 (5), 75.0 (20), 74.0 (9), 73.0 ($M^{++} - OTMS - ^{37}Cl$, 100), 59.0 (5)

2-(*tert*-butyldimethylsiloxy)-5,6-dimethoxy-indene (89h):

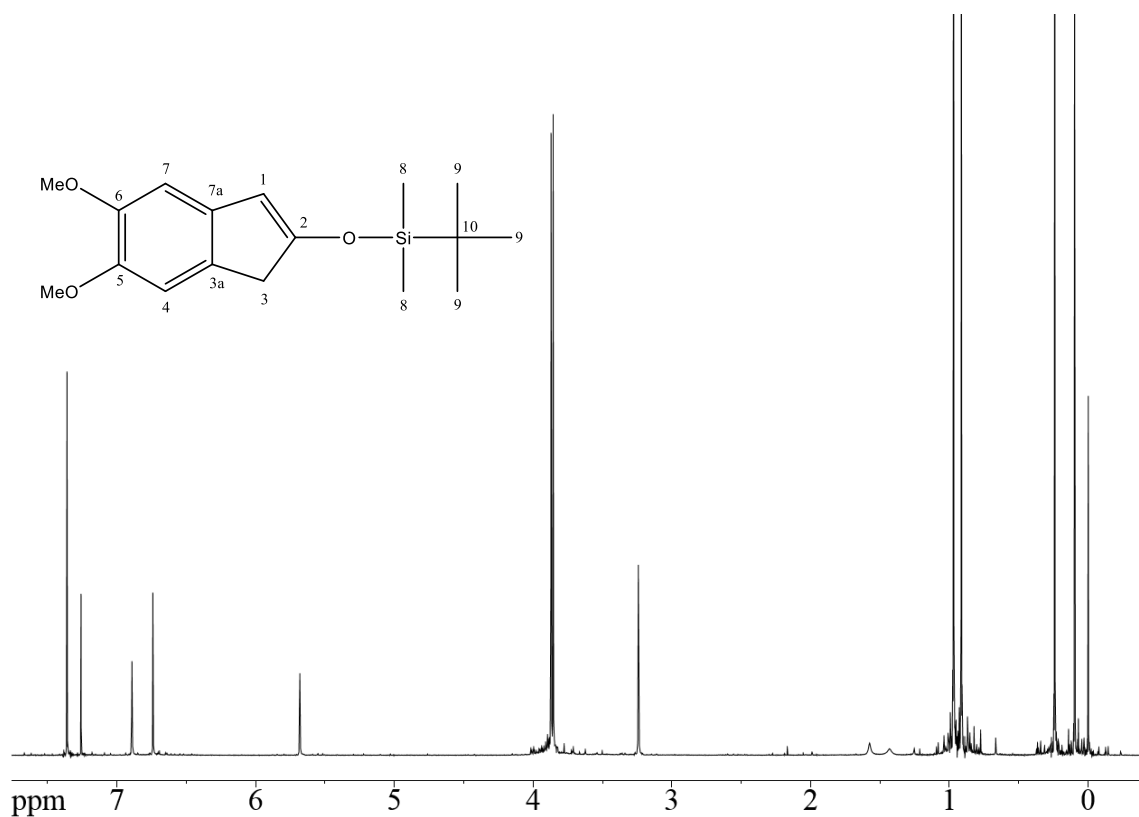


Figure 88. ¹H-NMR spectrum of 2-(*tert*-butyldimethylsiloxy)-5,6-dimethoxy-indene (**89h**) (500 MHz, CDCl₃).

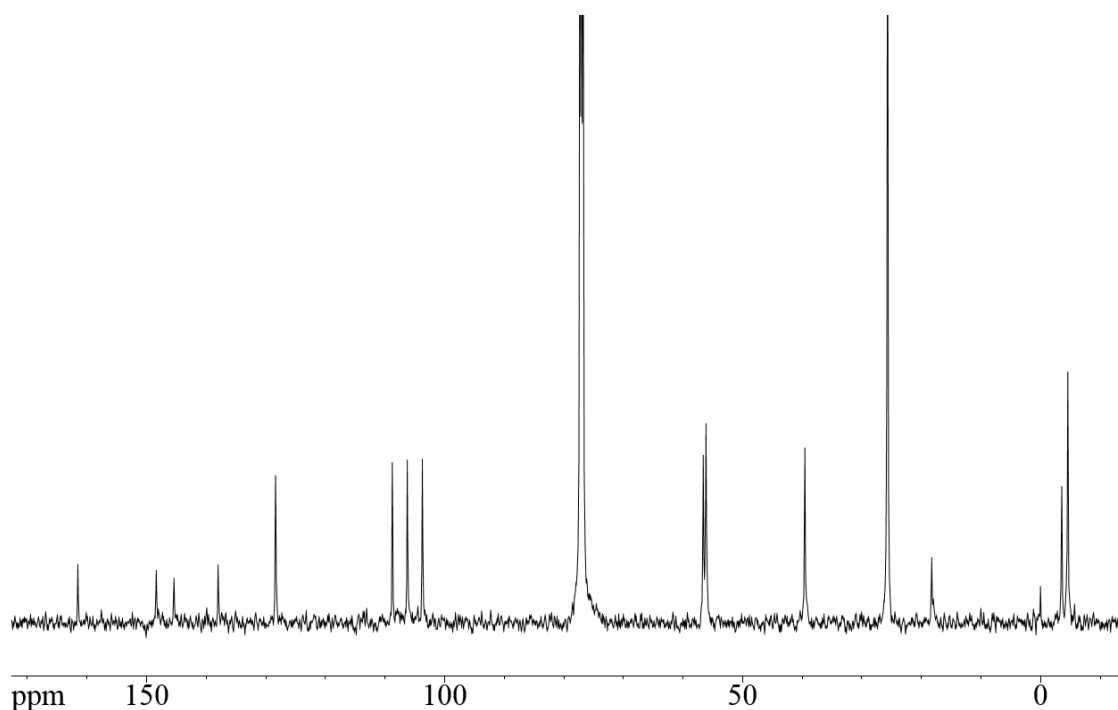


Figure 89. ^{13}C -NMR spectrum of 2-(*tert*-butyldimethylsiloxy)-5,6-dimethoxy-indene (**89h**) (500 MHz, CDCl_3).

Note: 5,6-dimethoxy-2-indanone was poorly soluble in benzene and 1.4 eq. of both TBDMSCl and DBU were required to drive the reaction to completion.

^1H NMR (500 MHz, CDCl_3): δ = 6.89 (s, 1H, 7-H), 6.74 (s, 1H, 4-H), 5.68 (s, 1H, 1-H), 3.87 (s, 3H, -OMe), 3.85 (s, 3H, -OMe), 3.24 (s, 2H, 3-H), 0.96 (s, 9H, -*t*Bu), 0.91 (s, 6H, 8-H) ppm

General Bromination of Silyl Enol Ether Derivatives

To a brown solution of 5.6 mmol of the corresponding silyl enol ether in 15 ml CCl_4 , 1.12 g NBS (6.3 mmol) and a catalytic amount of AIBN were added and heated to 80°C . Once reflux was obtained, the reaction was removed from the oil bath and checked by ^1H NMR to ensure completion. The suspension was subsequently filtered through a

fine frit and washed with 10ml CCl₄. The yellow to brown solution was concentrated in vacuo to afford the crude product as a brown oil in quantitative yield which was subjected to the subsequent reaction immediately.

3-bromo-2-(*tert*-butyldimethylsiloxy)-5,6-difluoro-indene (90c):

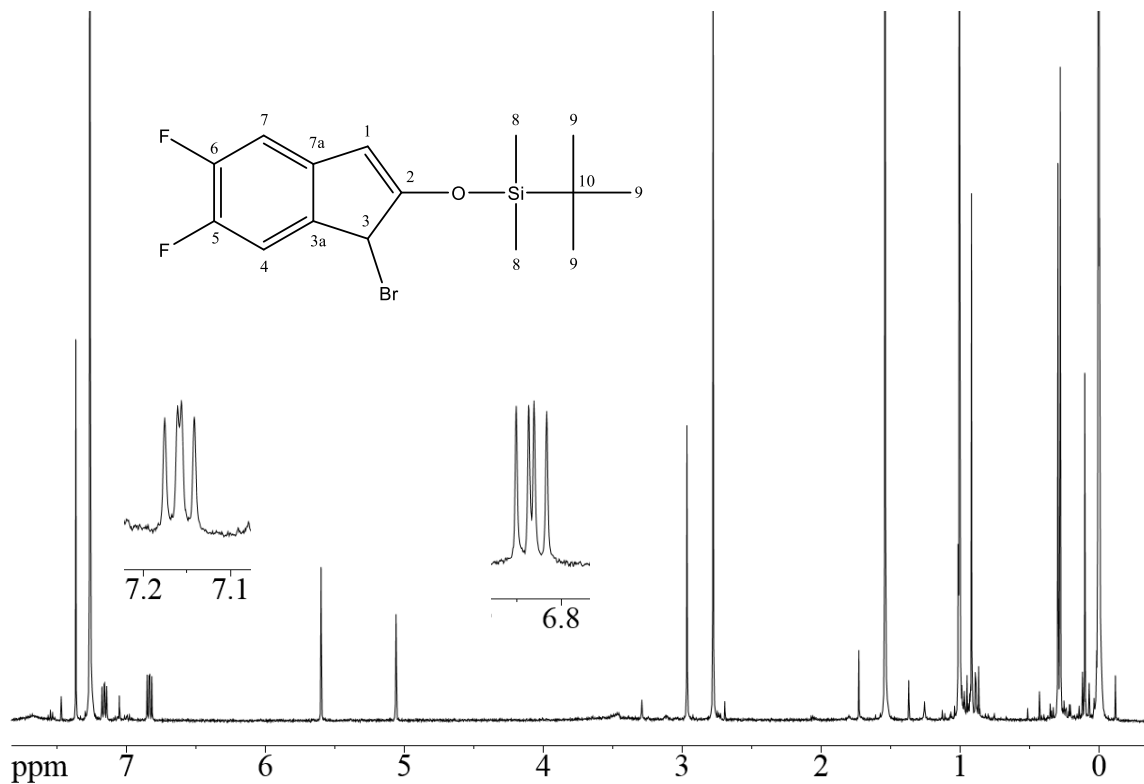


Figure 90. ¹H-NMR spectrum of 3-bromo-2-(*tert*-butyldimethylsiloxy)-5,6-difluoro-indene (**90c**) (500 MHz, CDCl₃).

¹H-NMR (500 MHz, CDCl₃): δ = 7.15 (dd, 1H, 7-H), 6.83 (dd, 1H, 4-H), 5.59 (s, 1H, 1-H), 5.05 (s, 1H, 3-H), 1.00 (s, 9H, *t*-bu), 0.28 (s, 6H, 8-H) ppm

¹⁹F-NMR (500 MHz, CDCl₃): δ = -138.2 (m), -144.5 (m) ppm

MS (EI, 70 eV): *m/z* (%) = 362.0 (35), 360.0 (34), 306.0 (30), 305.0 (84), 304.0 (30), 225.0 (26), 196.0 (16) 181.0 (42), 167.0 (15) 166.0 (67), 165.0 (44) 164.0 (19), 151.0

(41), 145.0 (23), 140.9 (22), 138.9 (54), 138.0 (37), 136.9 (33), 132.0 (17), 129.0 (16), 101.0 (18) 73.1 (100), 57.1 (71)

3-bromo-2-(*tert*-butyldimethylsiloxy)-5,6-dichloro-indene (90f**):**

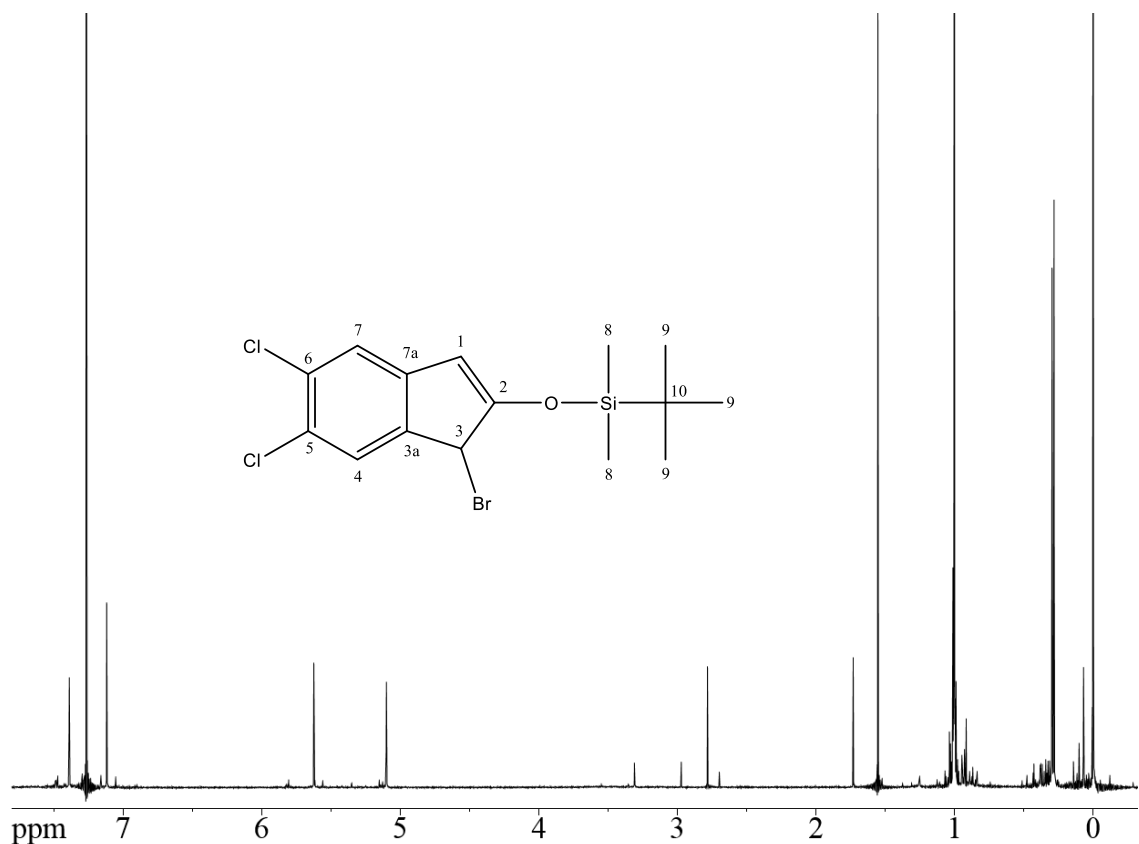


Figure 91. ^1H -NMR spectrum of 3-bromo-2-(*tert*-butyldimethylsiloxy)-5,6-dichloro-indene (**90f**) (300 MHz, CDCl_3).

Modifications: Refluxing for 30 min was required to ensure reaction completion

^1H -NMR (300 MHz, CDCl_3): δ = 7.38 (s, 1H, 7-H), 7.10 (s, 1H, 4-H), 5.62 (s, 1H, 1-H), 5.09 (s, 1H, 3-H), 0.99 (s, 9H, 9-H), 0.28 (s, 6H, 8-H) ppm

MS (EI, 70 eV): m/z (%) = 396.0 (7), 394.0 (14), 391.9 (8), 338.9 (22), 337.9(9), 336.9 (-*t*Bu, 32), 334.9 (22), 316.1 (21), 314.1 (-Br, 30), 281.1 (13), 259.0 (23), 258.0 (9), 257.0 (-*t*Bu-Br, 32), 212.9 (13), 207.0 (20), 199.9 (14), 197.9 (22), 184.9 (34), 183.0 (-OTMS-

Br, 49), 169.9 (10), 140.9 (13), 138.9 (24), 136.9 (13), 128.0 (9), 115.0 (13), 75.0 (17), 73.0 ($M^{++} - OTMS - ^{37}Cl - Br$ 100), 59.1 (13), 57.1 (44)

3-bromo-2-(*tert*-butyldimethylsiloxy)-5,6-dimethoxy-indene (90h):

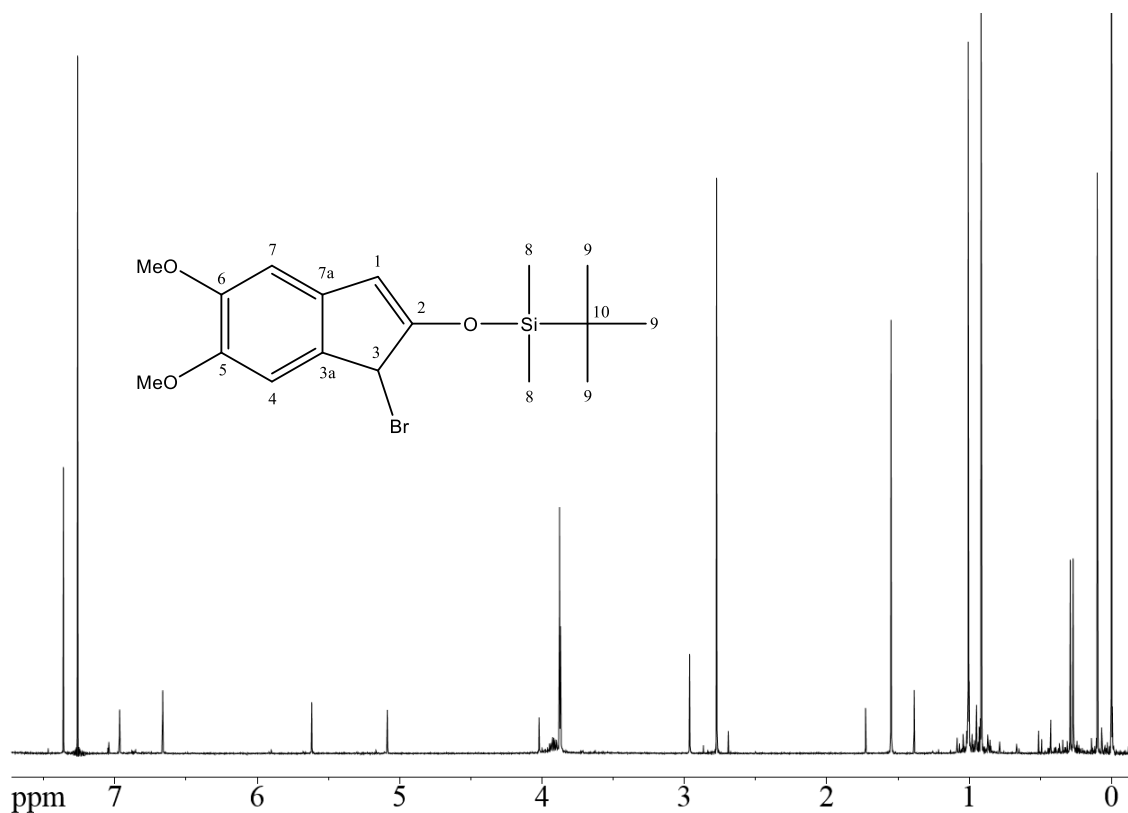


Figure 92. 1H -NMR spectrum of 3-bromo-2-(*tert*-butyldimethylsiloxy)-5,6-dimethoxy-indene (**90h**) (500 MHz, $CDCl_3$).

1H NMR (500 MHz, $CDCl_3$): δ = 6.95 (s, 1H, 4-H), 6.66 (s, 1H, 7-H), 5.61 (s, 1H, 3-H), 5.08 (s, 1H, 1-H), 3.87 (s, 3H, -OMe), 3.86 (s, 3H, -OMe), 1.00 (s, 9H, *t*-Bu), 0.91 (s, 6H, 8-H) ppm

Isoindenone Generation and Dimerization *via* Fluoride Induced Bromo-Silyl Enol Ether Cleavage

A solution of 5.6 mmol of the respective crude bromo-silyl enol ether in 20 ml dry degassed ACN was added over 1 h to a vigorously stirred suspension of CsF (2.0 g, 13 mmol) in 250 ml ACN of the same quality at 80 °C. Following complete addition of the substrate, the reaction mixture was stirred at reflux for an additional 2 h. After removal of the solvent in vacuo, the crude product was suspended in 200 ml water and extracted with DCM (3×100 ml). The combined organic phase was dried over MgSO₄ to furnish a quantitative mass balance of the crude dimer. The dark-brown crude product was purified by precipitating the product from a minimal amount of acetone with three times the volume of pentane thrice to furnish the product as a beige solid.

Note: The suspension of CsF in ACN should be set up and heating to reflux prior to the bromination step as hydrolysis of the corresponding bromo-silyl-eneol ether was demonstrated in solution. Incomplete removal of CCl₄ from bromo-silyl eneol ether had no effect on the reaction.

***anti*-3,4;7,8-bis[3,4-difluorobenzo]-tricyclo[4.2.1.1^{2,5}]deca-9,10-dione (**2c**):**

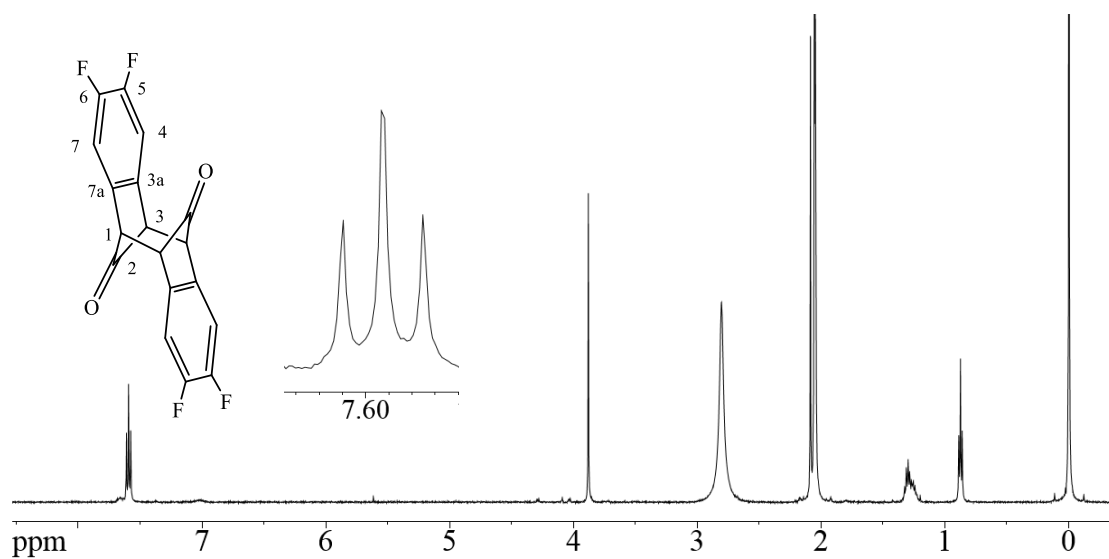


Figure 93. ¹H-NMR spectrum of *anti*-3,4;7,8-bis[3,4-difluorobenzo]-tricyclo[4.2.1.1^{2,5}]deca-9,10-dione (**2c**) (500 MHz, Acetone-D₆).

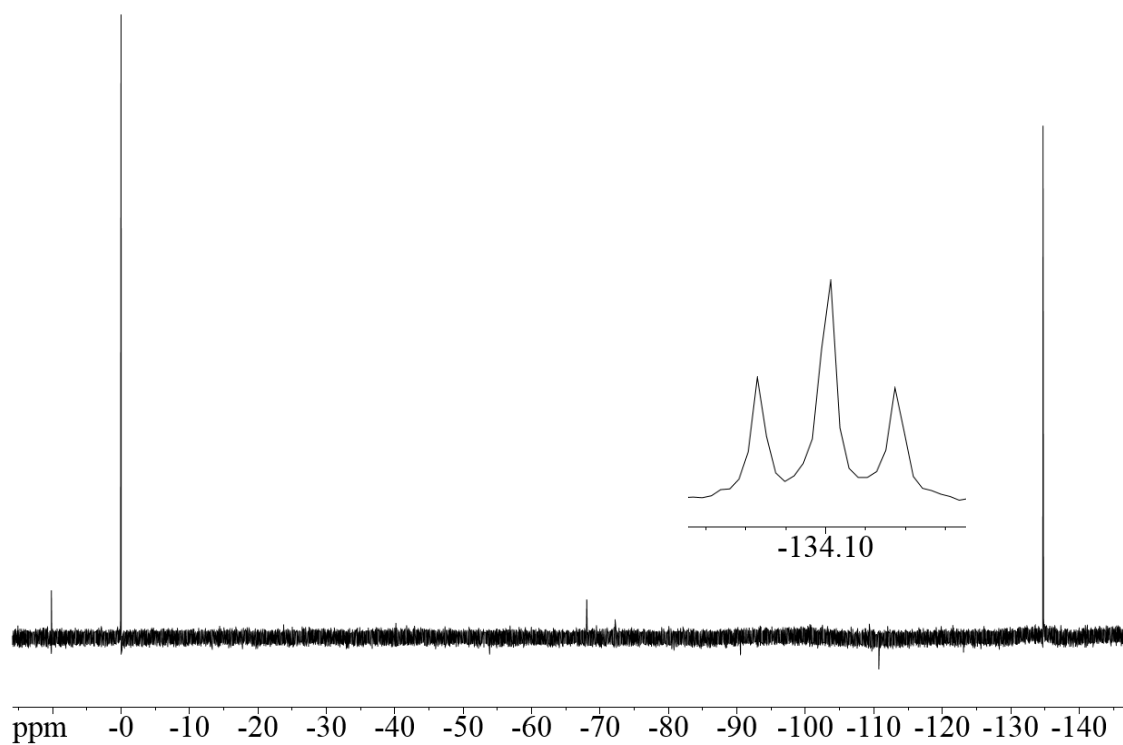


Figure 94. ¹⁹F-NMR spectrum of *anti*-3,4;7,8-bis[3,4-difluorobenzo]-tricyclo[4.2.1.1^{2,5}]deca-9,10-dione (**2c**) (500 MHz, CDCl₃).

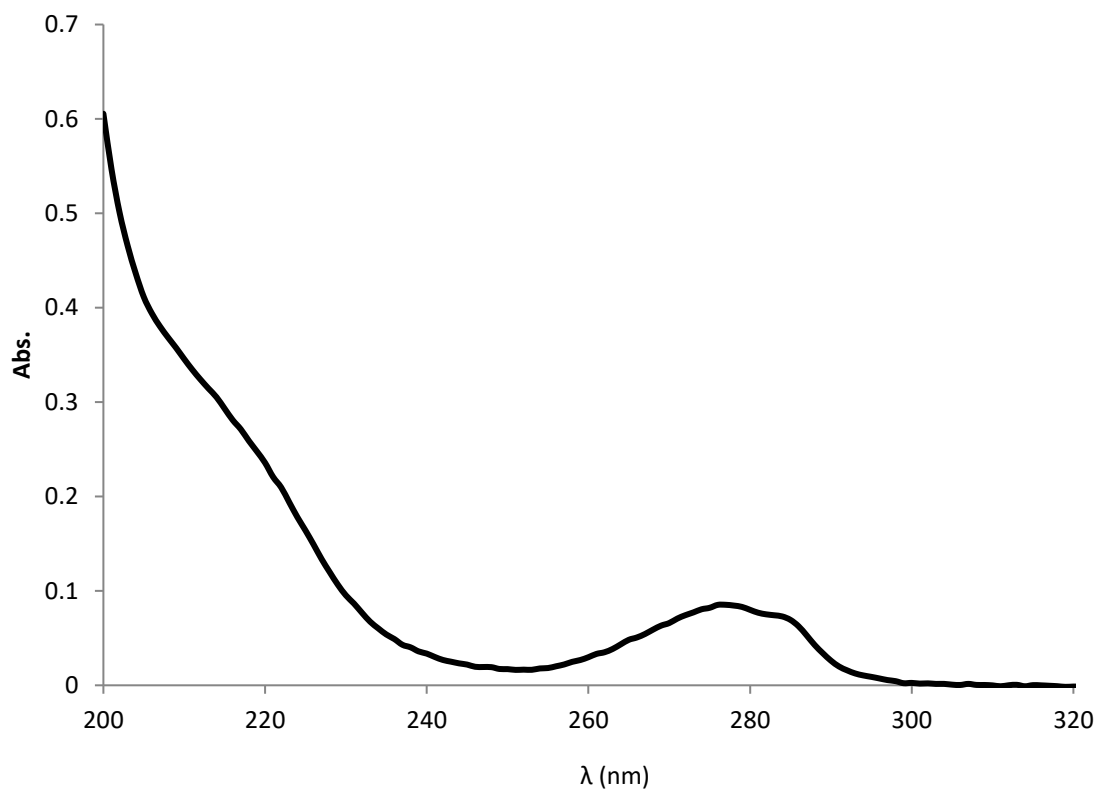


Figure 95. UV-VIS spectrum of *anti*-3,4;7,8-bis[3,4-difluorobenzo]-tricyclo[4.2.1.1^{2,5}]deca-9,10-dione (**2c**) recorded in ACN.

¹H-NMR (500 MHz, Acetone-D₆): δ = 7.60 (pt, 4H, 4-, 7-H), 3.88 (s, 4H, 1-, 3-H) ppm

¹H-NMR (500 MHz, CDCl₃): 7.29 (t_{app}, 4H, 4-, 7-H), 3.71 (s, 4H, 1-, 3-H) ppm

¹⁹F-NMR (500 MHz, Acetone-D₆): δ = -134.7 (t_{app}) ppm

FT-IR (KBr): $\tilde{\nu}$ = 3121 (w), 3064 (w), 1764 (s), 1730, 1605, 1573 (w), 1479 (s), 1440, 1340, 1265, 1247, 1215 (w), 1192, 1157, 1129, 1084, 1044 (s), 954, 883 (s), 835 (s), 791, 738, 664 cm⁻¹

MS (EI, 70 eV): m/z (%) = 332.0 (M⁺, 22), 304.0 (36), 303.1 (31), 276.1 (100), 275.1 (83), 274.0 (51), 257.1 (34), 256.0 (42), 138.0 (24), 128.0 (18)

MP: 255°C decomposition

UV/Vis (MeCN): λ_{max} (ϵ) = 223 (6439), 277 (2833), 284 (2423) nm ($\text{M}^{-1} \text{cm}^{-1}$).

***anti*-3,4;7,8-bis[3,4-dimethoxybenzo]-tricyclo[4.2.1.1^{2,5}]deca-9,10-dione (**2h**):**

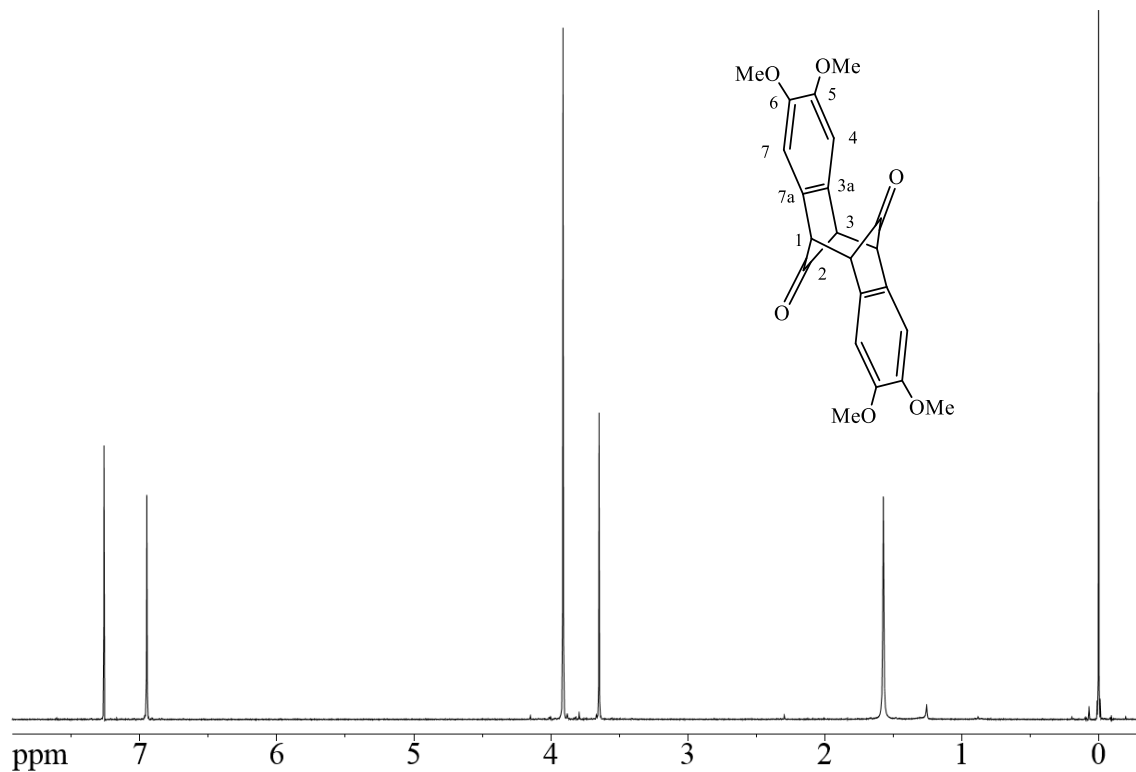


Figure 96. ¹H-NMR spectrum of *anti*-3,4;7,8-bis[3,4-dimethoxybenzo]-tricyclo[4.2.1.1^{2,5}]deca-9,10-dione (**2h**) (300 MHz, CDCl₃).

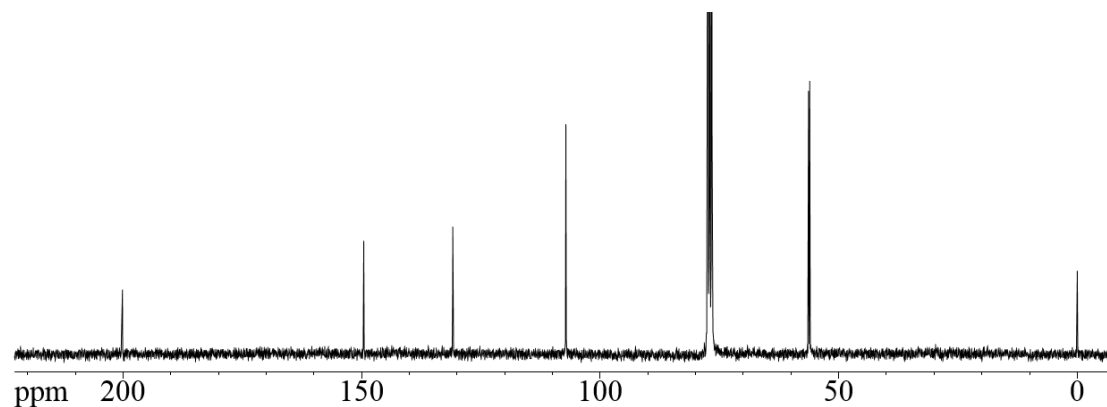


Figure 97. ¹³C-NMR spectrum of *anti*-3,4;7,8-bis[3,4-dimethoxybenzo]-tricyclo[4.2.1.1^{2,5}]deca-9,10-dione (**2h**) (300 MHz, CDCl₃).

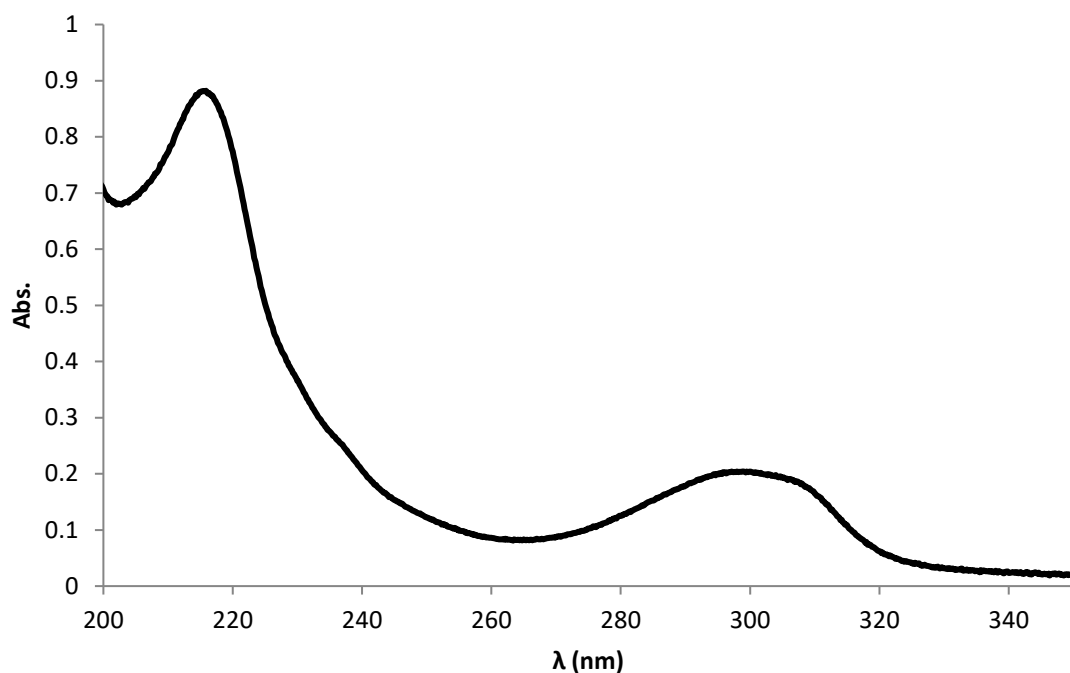


Figure 98. UV-VIS spectrum of *anti*-3,4;7,8-bis[3,4-dimethoxybenzo]-tricyclo[4.2.1.1^{2,5}]deca-9,10-dione (**2h**) recorded in ACN.

¹H NMR (300 MHz, CDCl₃): δ = 6.95 (s, 4H, 4-, 7-H), 3.91 (s, 12H, OMe-H), 3.65 (s, 4H, 1-, 3-H) ppm

¹³C NMR (300 MHz, CDCl₃): δ = 200.5 (2C, 2-C), 149.9 (4C, 5-, 6-C), 131.3 (4C, 3a-, 7a-C), 107.6 (4C, 4-, 7-C), 56.74 (4C, OMe-C), 56.48 (4C, 1-, 3-C) ppm

IR: $\tilde{\nu}$ = 3081 (Ar-H, w), 2962 (w), 2924, 2838, 1752 (C=O, s), 1726, 1603, 1580, 1493, 1457, 1420, 1305 (s), 1262, 1233 (s), 1189 (s), 1169 (s), 1075 (s), 1045, 989, 952, 865, 839, 789, 733, 667 cm⁻¹

DI-MS (EI, 70 eV): m/z (%) = 380.35 (25), 352.13 (66), 335.40 (12), 235.29 (78), 233.21 (63), 224.23 (80), 223.22 (100), 209.47 (42), 205.37 (12), 155.96 (25), 147.31 (75), 141.19 (86), 95.22 (45), 84.06 (34), 76.09 (67), 73.24 (56), 65.26 (49)

MP: 305°C decomposition

UV/Vis (MeCN): λ_{max} (ϵ) = 215 (52951), 237 (14895), 298 (12382) nm ($\text{M}^{-1} \text{cm}^{-1}$).

Carbonyl Reductions of Isoindenone Dimer Derivatives via LAH

A solution of 190 μmol of the respective dione in 10 ml dry THF was added slowly to a suspension of LAH (47 mg, 1.1 mmol) in 5 ml dry THF and stirred at room temperature for 3 h. The grey suspension was subsequently poured into ice water and acidified to pH 4 using 2 M aq. H_2SO_4 and extracted with DCM (3×15 ml). The combined organic phase was dried over MgSO_4 and concentrated in vacuo to furnish the crude product as a beige to brown solid. Purification was accomplished by precipitating the product from a minimal amount of acetone with three times the volume of pentane thrice to furnish the product as a beige solid.

***anti*-3,4;7,8-bis[3,4-difluorobenzo]-tricyclo[4.2.1.1^{2,5}]deca-9,10-diol (97c):**

Yield: 95%

^1H -NMR (300 MHz, CD_2Cl_2): δ = 7.14 (t, 4H, 4-, 7-H), 3.88 (m, 2H, 2-H), 3.18 (t, 4H, 1-, 3-H) ppm

^{19}F -NMR (500 MHz, CDCl_3): δ = -140.4 (t_{app}) ppm

FT-IR (KBr): $\tilde{\nu}$ = 3392 (broad, -OH), 3068 (-ArH, w), 2933 (w), 2895 (w), 1707, 1609, 1492, 1441, 1318, 1261, 1208, 1163, 1076, 1038, 879, 815, 767, 701, 672 cm^{-1}

DI-MS (EI, 70 eV): m/z (%) = 336.16 (1), 318.10 (-HOH, 4), 289.10 (7), 269.12 (10), 168.19 (70), 167.19 (90), 151.20 (100), 139.18 (73), 127.18 (51), 119.19 (71), 101.16 (44), 99.15 (34), 81.16 (17), 75.16 (43), 63.19 (49), 51.13 (53)

MP: decomposition at 238°C

***anti*-3,4;7,8-bis[3,4-dimethoxybenzo]-tricyclo[4.2.1.1^{2,5}]deca-9,10-diol (**97h**):**

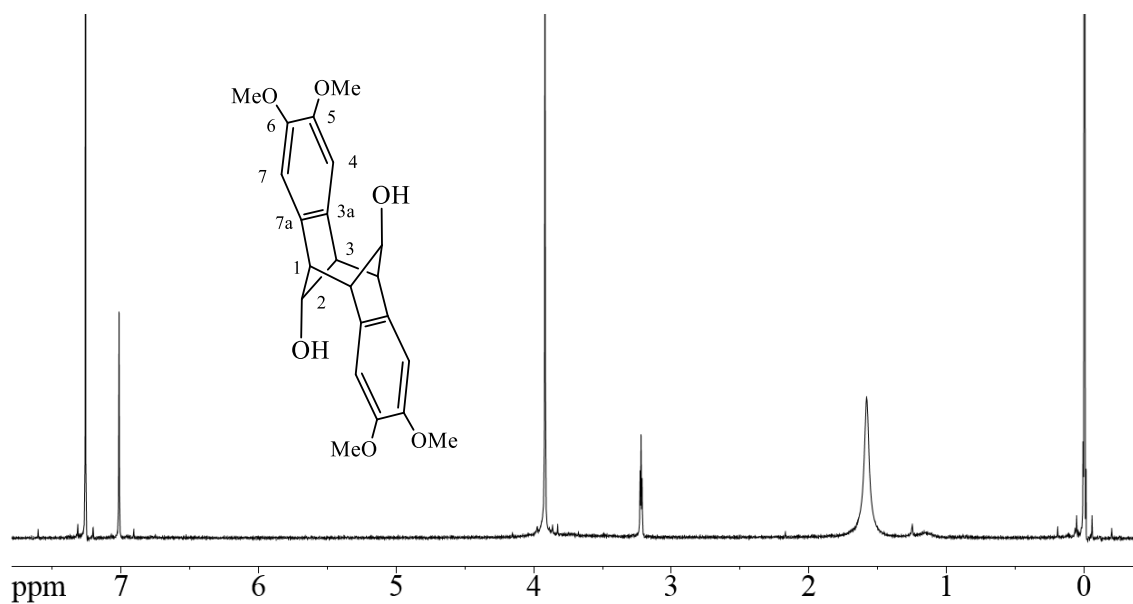


Figure 99. ¹H-NMR spectrum of *anti*-3,4;7,8-bis[3,4-dimethoxybenzo]-tricyclo[4.2.1.1^{2,5}]deca-9,10-diol (**97h**) (300 MHz, CDCl₃).

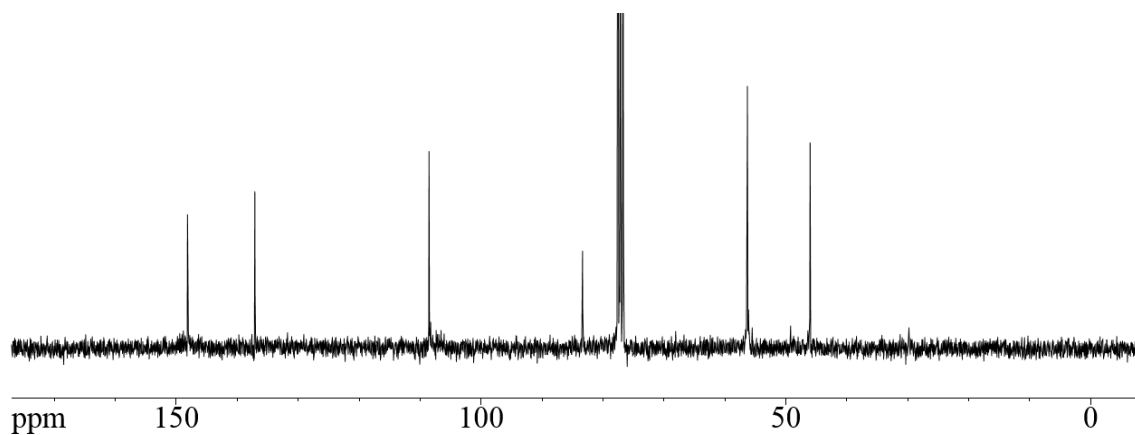


Figure 100. ¹³C-NMR spectrum of *anti*-3,4;7,8-bis[3,4-dimethoxybenzo]-tricyclo[4.2.1.1^{2,5}]deca-9,10-diol (**97h**) (300 MHz, CDCl₃).

Note: This reaction was easily scaled to 1g.

Yield : 99%

^1H NMR (300 MHz, CDCl_3): δ = 7.02 (s, 4H, 4-, 7-H), 3.92 (s, 16H, 2-, OMe-H), 3.22 (t, 4H, 1-, 3-H) ppm

^{13}C NMR (300 MHz, CDCl_3): δ = 148.2 (4C, 5-, 6-C), 137.1 (4C, 3a-, 7a-C), 108.6 (4C, 4-, 7-C), 83.3 (2C, 2-C), 56.3 (4C, OMe), 46.0 (4C, 1-, 3-C) ppm

IR: $\tilde{\nu}$ = 3572 (w), 3392 (-OH, broad), 2936 (w), 2836(w), 1704, 1603, 1576 (s), 1498, 1463, 1255, 1203, 1119, 1069, 1019, 848, 808, 737 cm^{-1}

DI-MS (EI, 70 eV): m/z (%) = 384.21 (M^+ , 61), 366.18 ($-\text{H}_2\text{O}$, 80), 348.12 ($-(\text{H}_2\text{O})_2$, 23), 337.21 (71), 349.23 (12), 306.14 (39), 209.02 (94), 190.14 (14), 194.04 (98), 181.02 (100), 177.11 (82), 164.04 (61), 163.13 (60), 149.11 (71), 121.16 (51), 91.15 (18), 73.13 (12)

MP: Decomp. at 230°C

Dichlorination of Isoindenol Dimer Derivatives via Thionyl Chloride

Thionyl chloride (0.58 mmol) was added dropwise to a solution of 0.26 mmol of the corresponding diol in 50 ml DCM and stirred at room temperature for 2 h. After solvent and excess thionyl chloride were removed directly on a high vacuum pump with two liquid nitrogen-cooled traps, the crude product was obtained as a dark-brown solid.

***anti*-3,4;7,8-bis[3,4-difluorobenzo]-tricyclo[4.2.1.1^{2,5}]deca-9,10-dichloro (**41c**):**

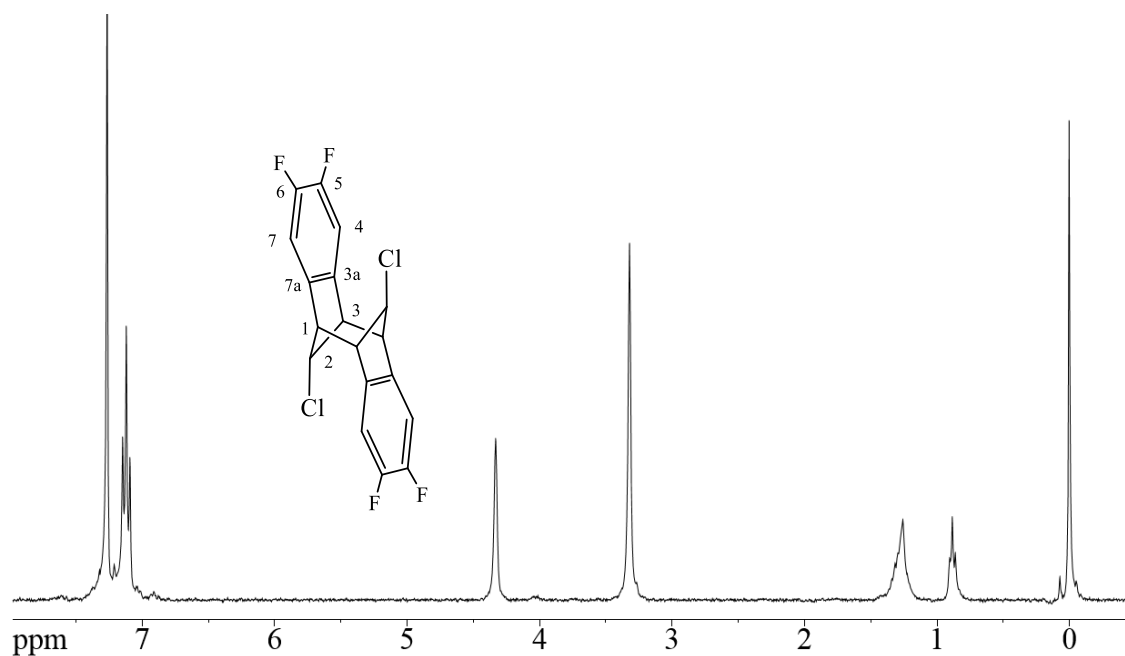


Figure 101. ¹H-NMR spectrum of *anti*-3,4;7,8-bis[3,4-difluorobenzo]-tricyclo[4.2.1.1^{2,5}]deca-9,10-dichloro (**41c**) (300 MHz, CDCl₃).

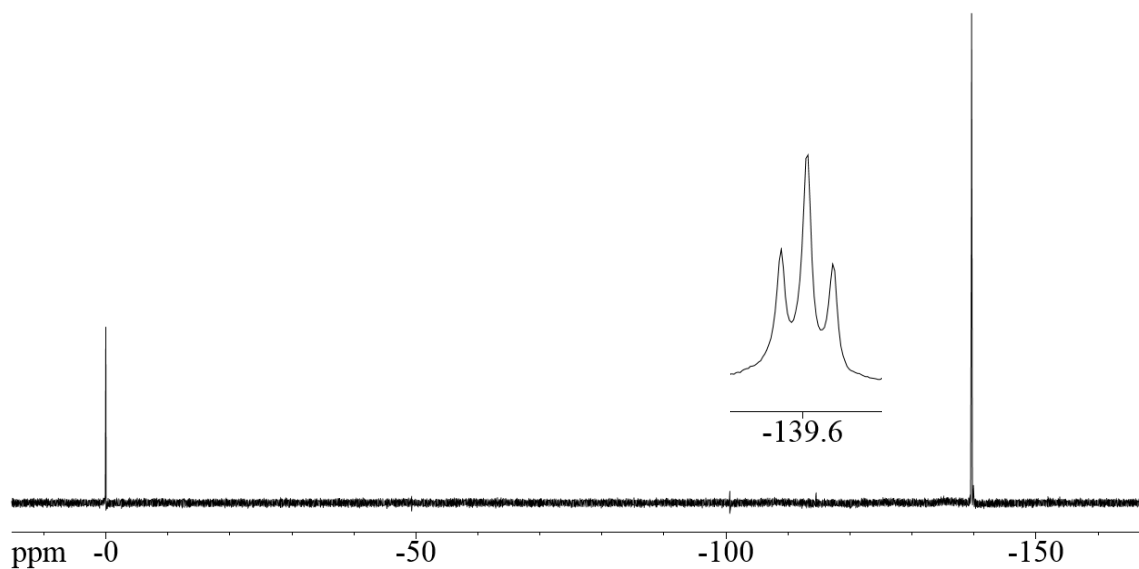


Figure 102. ¹⁹F-NMR spectrum of *anti*-3,4;7,8-bis[3,4-difluorobenzo]-tricyclo[4.2.1.1^{2,5}]deca-9,10-dichloro (**41c**) (300 MHz, CDCl₃).

Yield : 99%

$^1\text{H-NMR}$ (300 MHz, CD_2Cl_2): δ = 7.12 (t, 4H, 4-, 7-H), 4.33 (m, 2H, 2-H), 3.32 (t, 4H, 1-, 3-H) ppm

$^{13}\text{C-NMR}$ (300 MHz, CDCl_3): δ = 150.1 (4C, 5-, 6-C), 140.4 (4C, 4-, 7-C), 113.9 (4C, 1-, 3-C), 63.0 (2C, 2-C), 45.0 (4C, 1-, 3C) ppm

$^{19}\text{F-NMR}$ (300 MHz, CDCl_3): δ = -139.6 (t_{app}) ppm

AT-IR (KBr): $\tilde{\nu}$ = 3047 (Ar-H, w), 2972 (w), 2925 (w), 1718 (w), 1612, 1499 (w), 1474, 1437, 1384, 1347, 1330, 1316, 1263, 1231, 1195, 1124, 1073, 1040, 960, 896, 879, 832, 795, 740, 697, 671 cm^{-1}

DI-MS (EI, 70 eV): m/z (%) = 374.24 (1), 372.21 (2), 356.25 (2), 354.23 (3), 301.15 (11), 283.16 (14), 269.26 (11), 225.16 (11), 223.16 (63), 221.11 (86), 205.17 (29), 203.17 (47), 185.16 (51), 167.19 (52), 151.09 ($-\text{Cl}_2^{\cdot\cdot++}$, 100), 133.22 (86), 131.23 (17), 115.24 (17), 86.26 (12), 57.26 (16)

MP: 152-157°C

***anti*-3,4;7,8-bis[3,4-dimethoxybenzo]-tricyclo[4.2.1.1^{2,5}]deca-9,10-dichloro (**41h**):**

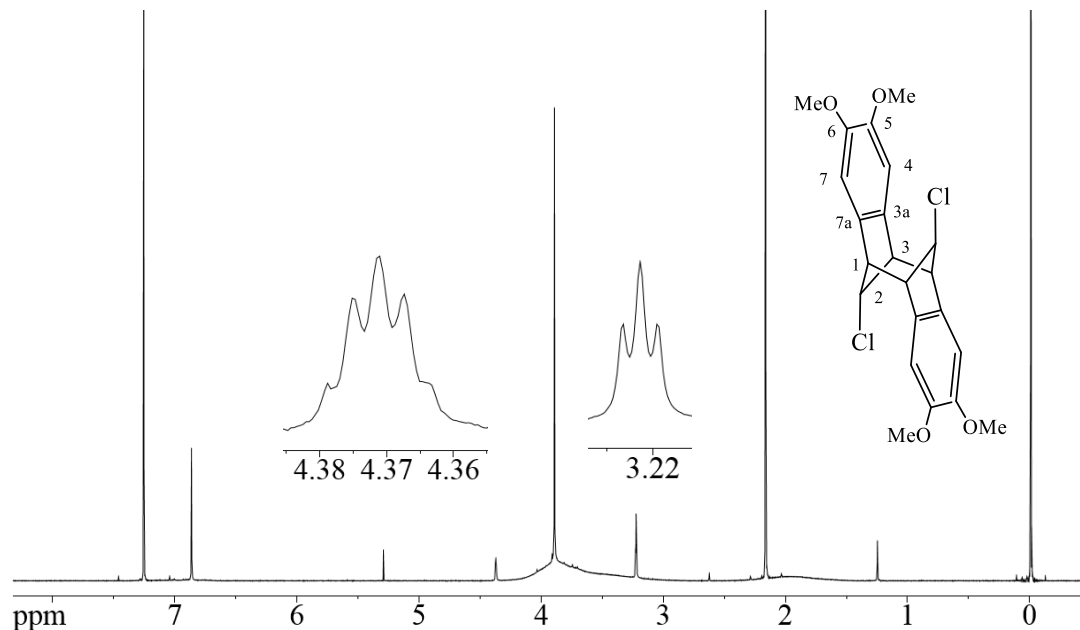


Figure 103. ¹H-NMR spectrum of *anti*-3,4;7,8-bis[3,4-dimethoxybenzo]-tricyclo[4.2.1.1^{2,5}]deca-9,10-dichloro (**41h**) (300 MHz, CDCl₃).

Yield : 99%

¹H NMR (300 MHz, CDCl₃): δ = 6.87 (s, 4H, 4,7-H), 4.37 (p, 2H, 2-H), 3.90 (s, 12H, -OMe), 3.23 (t, 4H, 1, 3-H) ppm

DI-MS (EI, 70 eV): m/z (%) = 424.25 (8) 422.12 (³⁷Cl₂, 45), 420.17 (³⁷Cl, 58), 385.21 (-Cl⁺, 29), 349.19 (-71, 40), 318.22 (33), 305.19 (42), 247 (54), 245.07 (74), 210.11 (59), 175.10 (-Cl₂⁺⁺⁺, 100), 176 (49), 131.16 (37), 102.01 (30), 64.12 (35)

MP: Decomp 265°C

***anti*-3,4;7,8-bis[3,4-dimethoxybenzo]-tricyclo[4.2.1.1^{2,5}]decane (**57h**):**

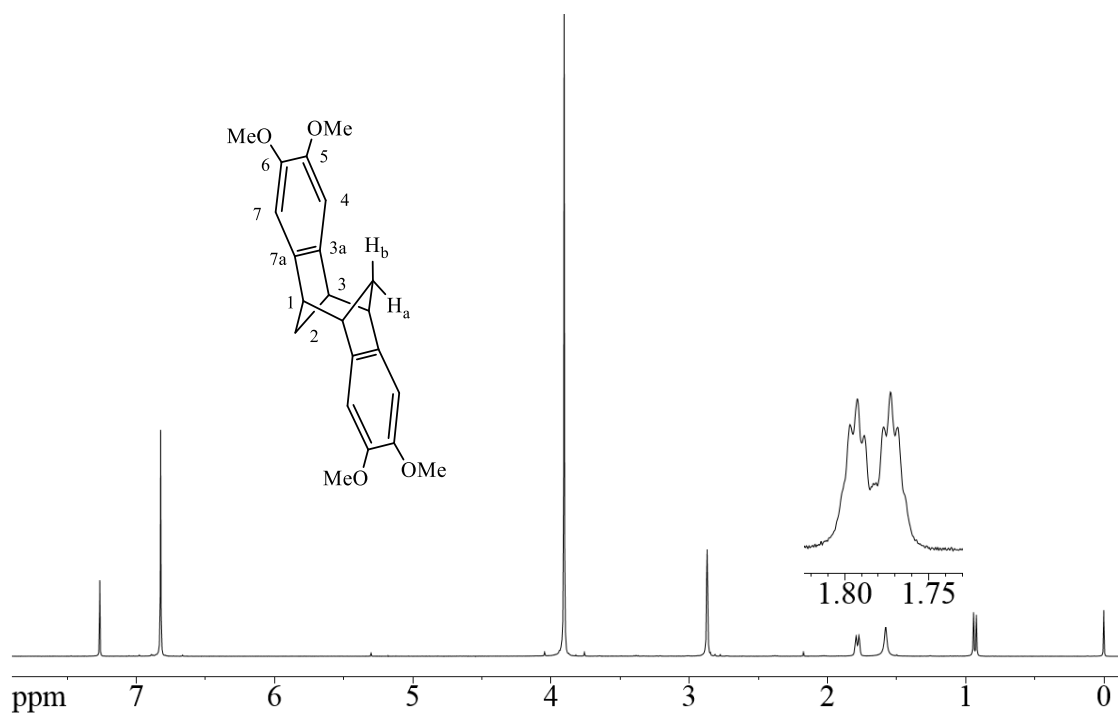


Figure 104. ¹H-NMR spectrum of *anti*-3,4;7,8-bis[3,4-dimethoxybenzo]-tricyclo[4.2.1.1^{2,5}]decane (**57h**) (300 MHz, CDCl₃).

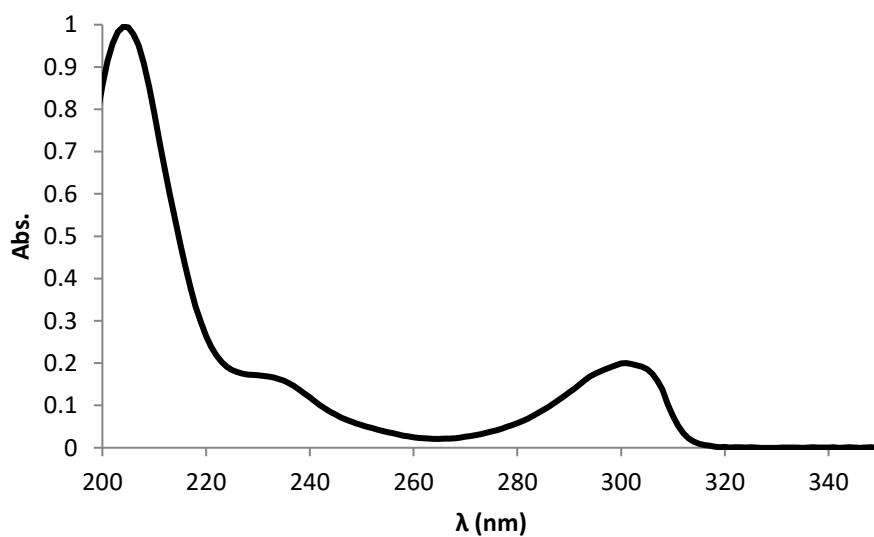


Figure 105. UV-VIS spectrum of *anti*-3,4;7,8-bis[3,4-dimethoxybenzo]-tricyclo[4.2.1.1^{2,5}]decane (**57h**) recorded in ACN.

To 22 mL absolute ethanol and 300 mL ammonia in a three-neck flask cooled to $-78\text{ }^{\circ}\text{C}$, a suspension of 1.56 g (3.70 mmol) dichloro **41h** in 28 mL dry THF was added and vigorously stirred. Fresh lithium pellets were added portion wise ($\sim 40\text{ mg}$) where subsequent additions occurred only after the prominent blue color indicating the presence of free electrons dissipated. After a total of 2.38 g (343 mmol) lithium were added, the dry ice/acetone bath was removed and ammonia was allowed to evaporate overnight. The mixture was subsequently suspended in 250 mL water and extracted with DCM (4x100 mL) and once with 100 mL EtOAc. Brine could be used to aid with the phase separation. The organic phase was dried over MgSO_4 and concentrated in vacuo to afford 540 mg of the crude product as a dark brown tacky solid containing no starting material. Column chromatography was utilized (2:1 pentane:EtOAc, $R_f = 0.30$) to afford 50 mg (4% yield) of the title compound as an analytically pure colorless solid. Significant streaking was observed on the column and resubjection of the MeOH column wash could afford up to an additional 5% of the product. The concentrated MeOH wash was triturated with warm ether to afford 230 mg of the title compound (18% yield) as a beige solid. An additional 80 mg (6% yield) could be obtained from the mother liquor in lower purity as a brown solid.

^1H NMR (300 MHz, CDCl_3): $\delta = 6.81$ (s, 4H, 4-, 7-H), 3.90 (s, 12H, -OMe), 2.86 (t, 4H, 1-, 3-H), 1.77 (dt, 2H, 2-H^b) ($^2J_{\text{C-H}} = 2.10\text{ Hz}$, $^3J_{\text{C-H}} = 5.16\text{ Hz}$), 0.92 (d, 2H, 2-H^a) ($^3J_{\text{C-H}} = 10.5\text{ Hz}$) ppm

^{13}C NMR (500 MHz, CDCl_3): $\delta = 147.6$ (4C, 5-, 6-C), 150.0 (4C, 3a-, 7a-C), 107.2 (4C, 4-, 7-C), 56.6 (4C, OMe-C), 44.7 (4C, 1-, 3-C), 43.5 (2C, 2-C) ppm

AT-IR (KBr): $\tilde{\nu}$ = 3063 (Ar-H, w), 2992 (w), 2972, 2930, 2878, 2836 (w), 2629 (w), 1756 (w), 1741 (w), 1702 (w), 1604, 1586, 1487, 1463 (s), 1414, 1316, 1292 (s), 1247, 1213 (s), 1184, 1161, 1137 (s), 1103 (s), 1066 (s), 1038, 1012, 965, 926, 879, 863, 846, 811, 734, 679 cm^{-1}

MP: 241-245°C

MS (EI, 70 eV): m/z (%) = 352.1 (M^+ , 8), 177.1 (isoindene + H, 100), 161.1 (15), 146.1 (15), 115.1 (8)

UV/Vis (MeCN): λ_{max} (ϵ) = 204 (94558), 236 (14481), 301 (19000) nm ($\text{M}^{-1} \text{cm}^{-1}$).

5.2.4 Toward Azaacenes

1,2-diamino-4-bromo-benzene (133):

To a fine yellow suspension of 4.00g (18.4mmol) 4-bromo-2-nitroaniline in 150 ml absolute ethanol, 27.2 g (120.6mmol) tin(II)chloride dihydrate was added and stirred 16 h at room temperature. The solvent was subsequently removed in vacuo to afford a bright orange oil that was suspended in 350 ml 2M aq. NaOH. The tan suspension was extracted 4x100 ml DCM to afford 3.30 g (17.5 mmol) of the title compound as a tan solid in 95% yield.

$^1\text{H-NMR}$ (300 MHz, CDCl_3): δ = 6.81 (m, 2H, 3-, 5-H), 6.65 (d, 1H, 6-H) ppm

6-bromo-2,3-dimethylquinoxaline (112):

In a 5 ml microwave tube, 0.3 ml (3.45 mmol) of freshly distilled butane-2,3-dione was added dropwise to 561 mg (3.00 mmol) 1,2-diamino-4-bromo-benzene. After heat evolution had subsided, the sealed vessel was stirred in a microwave reactor at 150 °C for

45 seconds. The product was recrystallized from 7:3 hexane:EtOAc to afford 690 mg of the title compound as a tan solid (97% yield).

¹H-NMR (300 MHz, CDCl₃): δ = 8.12 (s, 1H, 5-H), 7.82 (d, 1H, 8-H), 7.71 (dd, 1H, 7-H), 2.68 (s, 3H, 3-CH₃), 2.71 (s, 3H, 4-CH₃) ppm

Cinnamic Ethyl Esters via Heck Coupling

A light brown suspension containing 8.23mmol of the respective aryl bromide, 1.33 ml (12.5 mmol) ethyl acrylate, 188 mg (0.837mmol) palladium acetate, 510 mg (1.675 mmol) tri(*o*-tolyl)phosphine, 2.3 ml triethylamine and 40 ml ACN was purged with nitrogen for 15 min and stirred at reflux for at least 12 h. The solvent was removed in vacuo and the product was suspended in 100 ml of a 1:1 water:DCM mixture. After extracting the aqueous phase 4x50 ml DCM and drying over sodium sulfate, the solvent was removed in vacuo to afford the crude product mixed with tri(*o*-tolyl)phosphine oxide.

2,3-dimethyl-6-quinoxalinepropenoic ethyl ester (166):

Note: Tri(*o*-tolyl)phosphine oxide was removed by triturating the crude material with cold 2:1 hexane:EtOAc 3x5 ml

Yield: 65%, light brown solid

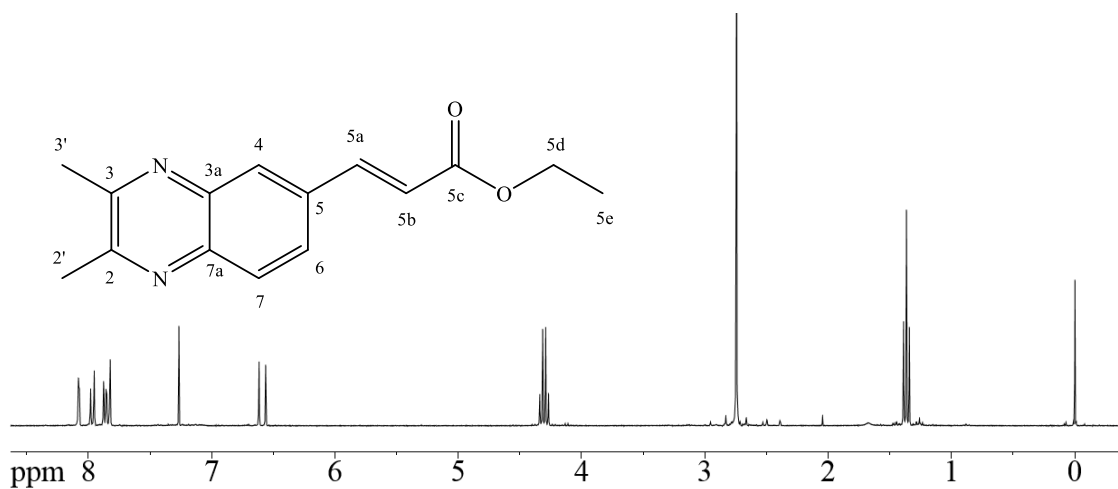


Figure 106. ^1H -NMR spectrum of 2,3-dimethyl-6-quinoxalinepropenoic ethyl ester (**166**) (300 MHz, CDCl_3).

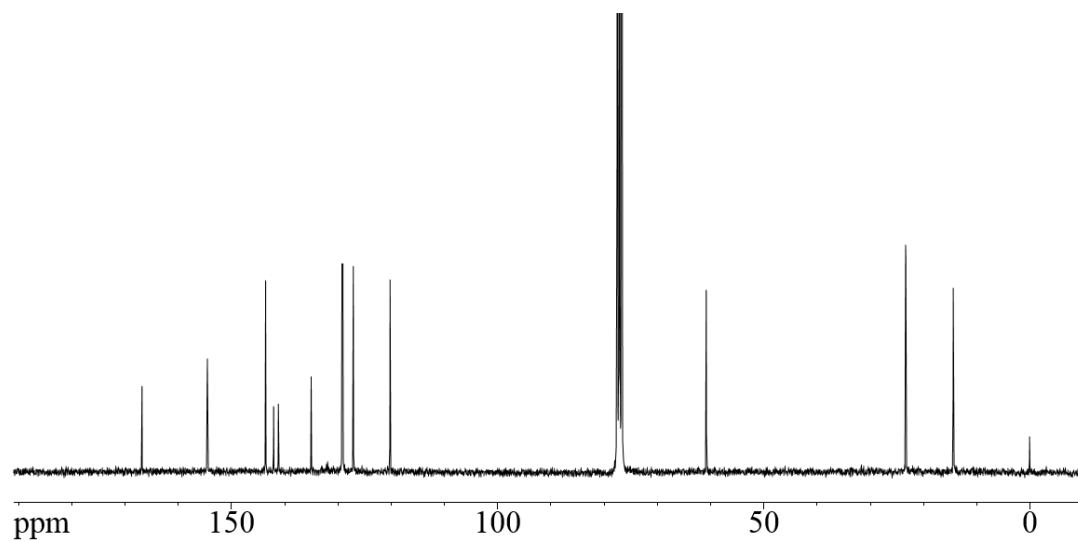


Figure 107. ^{13}C -NMR spectrum of 2,3-dimethyl-6-quinoxalinepropenoic ethyl ester (**166**) (300 MHz, CDCl_3).

^1H -NMR (300 MHz, CDCl_3): δ = 8.09 (d, 1H, 4-H), 7.97 (d, 1H, 7-H), 7.85 (dd, 1H, 6-H), 7.82 (s, 1H, 5a-H), 6.59 (d, 1H, 5b-H), 4.31 (q, 2H, 5d-H), 3.74 (s, 6H, 2', 3'-H), 1.37 (t, 3H, 5c-H) ppm

^{13}C -NMR (300 MHz, CDCl_3): δ = 166.8 (C-5c), 154.5 (C-5), 143.6 (C-4), 142.1 (C-5a*), 141.2 (C-5a*), 135.0 (C-2), 129.2 (C-7*), 129.1 (C-6*), 127.1 (C-4*), 120.2 (C-5b), 60.8 (C-2', -3'), 23.3 (C-5d), 14.4 (C-5e) ppm

MS (EI, 70 eV): m/z (%) = 256.1 (64), 227.1 (-Et, 14), 211.1 (-OEt, 100), 184.1 (40), 129.0 (9), 101.0 (19), 85.0 (12), 75.0 (15)

IR (KBr): $\tilde{\nu}$ = 3054 (w), 3005 (w), 2979 (w), 2938 (w), 1716 (-C=O, s), 1678, 1633, 1567, 1495, 1465, 1447, 1404, 1392, 1372, 1338, 1323, 1304, 1281, 1251, 1216, 1172 (s), 1163 (s), 1148 (s), 1125, 1093, 1030, 982, 966, 947, 916, 865, 845, 831, 786, 729, 716, 690, 675, 657 cm^{-1}

MP: 86-89°C

3-(4-amino-3-nitrophenyl)-2-propenoic ethyl ester (167):

Notes: Purification was accomplished by adsorbing the crude material onto silica gel and rinsing with a 2:1 mixture of hexane:EtOAc on a column until the filtrate became colorless, indicating no starting material (R_f = 0.38) remained. Washing the silica gel with MeOH provided the title compound along with 5 mol% tri(*o*-tolyl)phosphine oxide.

Yield: 35%

^1H -NMR (300 MHz, CDCl_3): δ = 8.27 (d, 1H, 2-H), 7.57 (dd, 1H, 5-H), 7.53 (s, 1H, 1a-H), 6.82 (d, 1H, 6-H), 6.34 (broad, 2H, -NH₂), 6.29 (d, 1H, 1b-H), 4.18 (q, 2H, 1d-H), 1.25 (t, 3H, 1e-H) ppm

MP: 158-162 °C

3-(3,4-diaminophenyl)-2-propanoic ethyl ester (168):

For procedure see "Propionic Acid Derivatives via Nickel Boride Mediated Reduction"

(p. 105)

MS (EI, 70 eV): m/z (%) = 208.1 (36), 163.0 (-OCH₃, 9), 134.1 (-HCO₂CH₂CH₃, 12), 133.1 (9), 122.1 (10), 121.0 (-CH₂CO₂CH₂CH₃, 100), 94.0 (9), 79.8 (9)

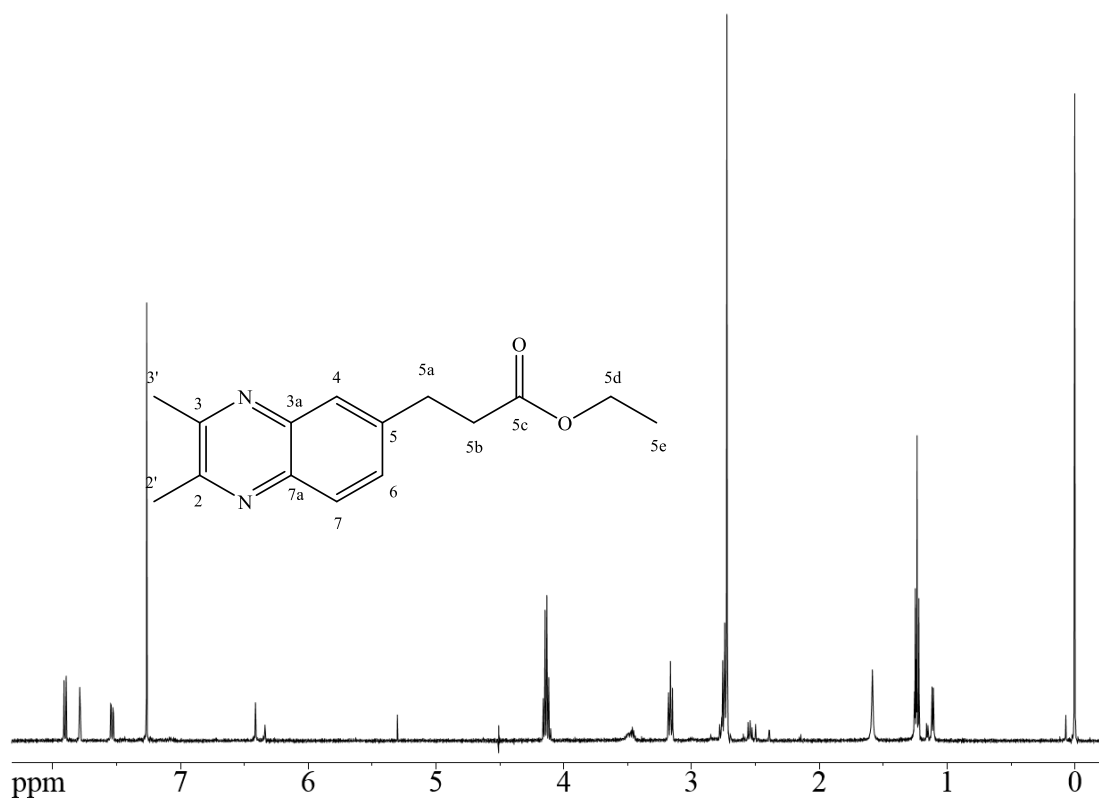
2,3-dimethyl-6-quinoxalinepropanoic ethyl ester (169):

Figure 108. ¹H-NMR spectrum of 2,3-dimethyl-6-quinoxalinepropanoic ethyl ester (**169**) (300 MHz, CDCl₃).

For procedure see "Propionic Acid Derivatives via Nickel Boride Mediated Reduction"

(p. 105)

$^1\text{H-NMR}$ (300 MHz, CDCl_3): δ = 7.89 (d, 1H, 6-H), 7.77 (d, 1H, 7-H), 7.52 (dd, 1H, 4-H), 4.22 (q, 2H, 5d-H), 3.14 (t, 2H, 5a-H), 2.74 (t, 2H, 5b-H), 2.71 (s, 6H, 2', 3'-H), 1.22 (t, 3H, 5c-H) ppm

MS (EI, 70 eV): m/z (%) = 258.1 (37), 213.1 ($-\text{OCH}_3$, 9), 187.1 (28), 185.1 ($-\text{CO}_2\text{Et}$, 50), 184.1 (100%), 171.1 (48), 143.1 (7), 102.0 (18), 89.0 (7), 77.0 (9)

2,3-dimethyl-6-quinoxalinepropanoic methyl ester (170):

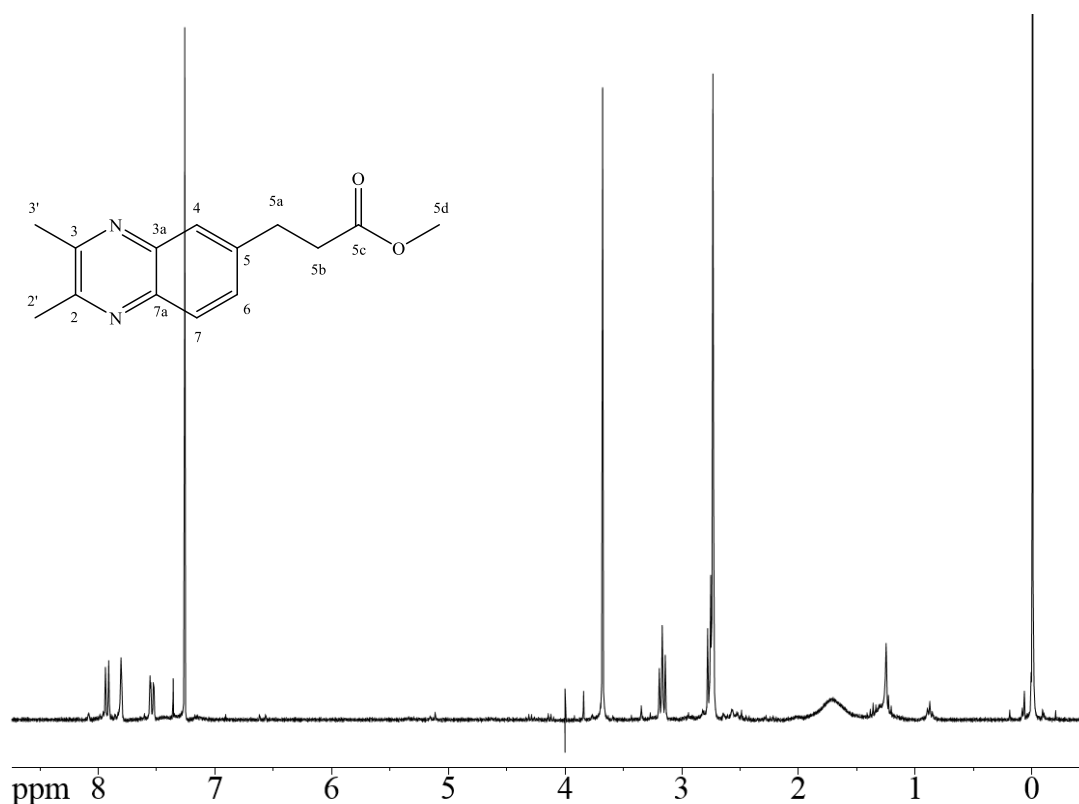


Figure 109. $^1\text{H-NMR}$ spectrum of 2,3-dimethyl-6-quinoxalinepropanoic methyl ester (**170**) (300 MHz, CDCl_3).

Note: Obtained from a column of the ethyl ester derivative (**169**) within a MeOH wash

$^1\text{H-NMR}$ (300 MHz, CDCl_3): δ = 7.92 (d, 1H, 4-H), 7.81 (d, 1H, 5-H), 7.53 (dd, 1H, 6-H), 3.69 (s, 3H, 5d-H), 3.17 (t, 2H, 5a-H), 2.74 (t, 2H, 5b-H), 2.73 (s, 6H, 2', 3'-H) ppm

2,3-dimethyl-6-quinoxalinepropanoic acid (135**):**

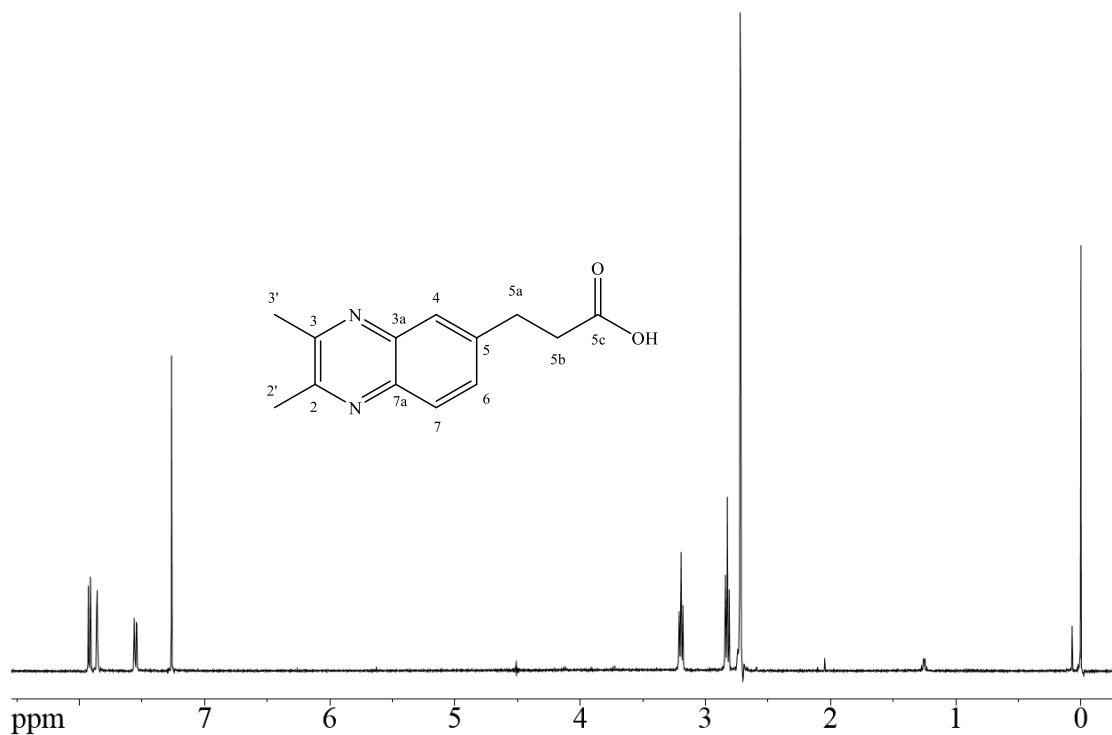


Figure 110. ^1H -NMR spectrum of 2,3-dimethyl-6-quinoxalinepropanoic acid (**135**) (500 MHz, CDCl_3).

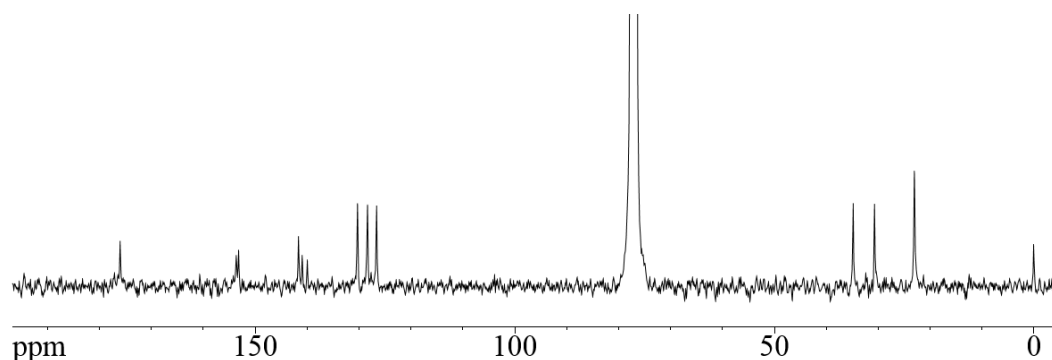


Figure 111. ^{13}C -NMR spectrum of 2,3-dimethyl-6-quinoxalinepropanoic acid (**135**) (300 MHz, CDCl_3).

To a solution of 500 mg (1.94 mmol) ester in 18 ml 95% EtOH, 310 mg (7.76 mmol) of powdered NaOH was added and heated to 65 °C for 1.5 h. This brown solution was subsequently poured into 50 ml water and acidified to pH 3 using 1 M HCl. This

phase was subsequently extracted with EtOAc 4x40 ml to afford the title compound quantitatively.

$^1\text{H-NMR}$ (500 MHz, CDCl_3): δ = 7.92 (d, 1H, 4-H), 7.86 (d, 1H, 7-H), 7.55 (dd, 1H, 6-H), 3.19 (t, 2H, 5a-H), 2.82 (t, 2H, 5b-H), 2.72 (s, 6H, 2'-, 3'-H) ppm

$^{13}\text{C-NMR}$ (300 MHz, CDCl_3): δ = 176.0 (C-5c), 153.2 (C-2*), 152.9 (C-3*) 141.7 (C-5), 140.9 (C-3a*), 139.9 (C-7a*), 130.3 (C-6**), 128.3 (C-7**), 126.6 (C-4**), 34.8 (C-5a), 30.7 (C-5c), 23.1 (C-2', -3') ppm

MP: 141-144 °C

3-(4-amino-3-nitrophenyl)-2-propanoic ethyl ester (171):

To a solution of 110 mg (0.47 mmol) 3-(4-amino-3-nitrophenyl)-2-propenoic ethyl ester in 5 ml absolute EtOH, 0.13 ml (9.5 mmol) hydrazine monohydrate was added dropwise and refluxed for 48 h to afford a crude mass balance of 72 mg containing the product in a ratio of 7:3 to the starting material (45% yield).

$^1\text{H-NMR}$ (300 MHz, CDCl_3): δ = 7.97 (d, 1H, 2-H), 7.21 (dd, 1H, 5-H), 6.75 (d, 1H, 6-H), 4.15 (q, 2H, 1d-H), 2.89 (t, 2H, 1a-H), 2.59 (t, 2H, 1b-H), 1.25 (t, 3H, 1e-H) ppm

MS (EI, 70 eV): m/z (%) = 238.1 (18), 221.1 (19), 220.1 (18), 179.0 (13), 178.0 (12), 167.0 (29), 164.0 (26), 151.0 ($-\text{CH}_2\text{CO}_2\text{CH}_2\text{CH}_3$, 100), 147.0 (16), 146.0 (16), 119.1 (20), 118.0 (24), 105.0 (42), 104.0 (33), 91.0 (18), 77.0 (13), 65.0 (11)

1,2-dimethyl-4,5-dinitrobenzene (146):

To a solution of 1.0 g (6.02 mmol) 1,2-dimethyl-4-nitroaniline in 50 ml glacial acetic acid, 6.01 g (60.2 mmol) sodium perborate was added and stirred for 16 h at 50°C. The yellow solution was subsequently cooled to RT, poured into 100 ml water and extracted 4x50 ml DCM. The combined organic phases were washed twice with 50 ml sat. aq. sodium bicarbonate, dried over MgSO₄ and concentrated in vacuo to afford 1.01 g of the title compound (86% yield).

¹H-NMR (500 MHz, CDCl₃): δ = 7.67 (s, 2H, 3-, 6-H), 2.41 (s, 6H, -CH₃) ppm

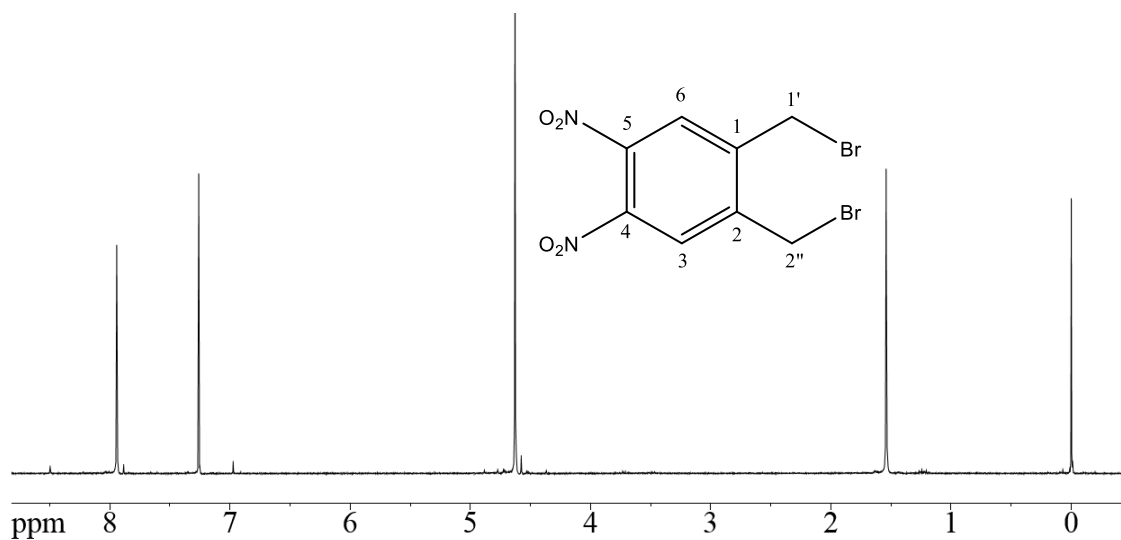
1,2-bis(bromomethyl)-4-nitrobenzene (147):

Figure 112. ¹H-NMR spectrum of 1,2-bis(bromomethyl)-4-nitrobenzene (**147**) (300 MHz, CDCl₃).

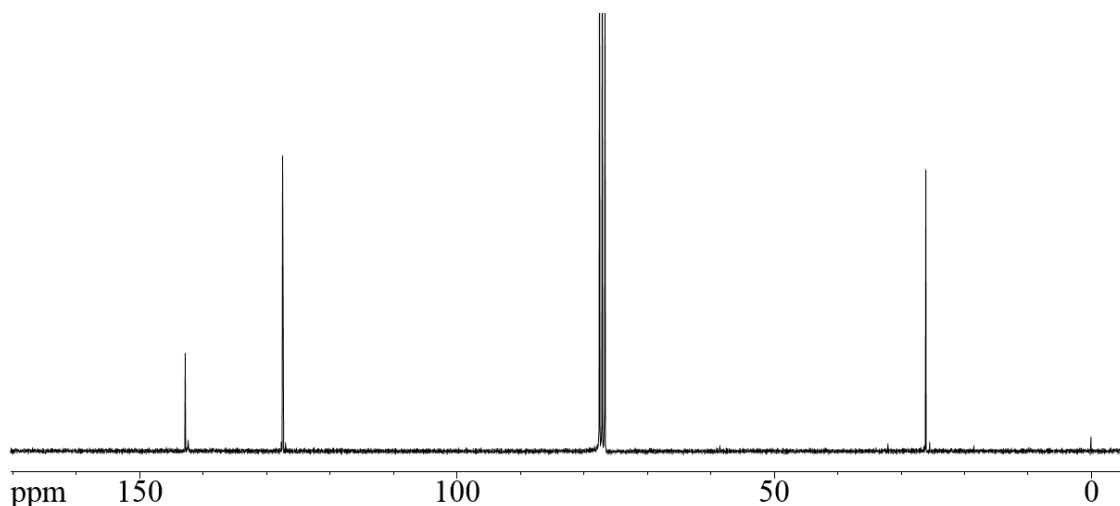


Figure 113. ¹³C-NMR spectrum of 1,2-bis(bromomethyl)-4-nitrobenzene (**147**) (300 MHz, CDCl₃).

To a vigorously stirred suspension of 1.45 g (7.42 mmol) 1,2-dimethyl-4,5-dinitrobenzene in 15 ml dichloroethane, 6.60 g (37.0 mmol) NBS and a catalytic amount of AIBN were added. Conversion was monitored by ¹H NMR and after typically 4 days, the reaction was filtered through a fine frit after 90% of the starting material was consumed to afford 1.70 g of the crude product. Two recrystallizations from a 6:1 mixture of pentane:EtOAc were required to afford 0.78 g of the title compound (30% yield). Column chromatography could also be employed (6:1 pentane:EtOAc, R_f = 0.3) to furnish the product in up to 75% yield. Tribromo **141** was isolated through chromatography as a side product in small quantities (R_f = 0.4)

¹H-NMR (300 MHz, CDCl₃): δ = 7.93 (s, 2H, 3-, 6-H), 4.62 (s, 4H, 1'-, 2'-H) ppm

¹³C-NMR (300 MHz, CDCl₃): δ = 142.8 (2C, 4-, 5-C), 142.4 (2C, 1-, 2-C), 127.5 (2C, 6-, 3-C), 26.1 (2C, 1'-, 2'-C) ppm

MS (EI, 70 eV): m/z (%) = 355.8 ($^{81}\text{Br}_2$, 2), 353.8 ($^{79}\text{Br}^{81}\text{Br}$, 3.5), 351.9 ($^{79}\text{Br}_2$, 1), 274.9 (^{81}Br , 98), 272.9 (^{79}Br , 100%), 194.0 (6), 136.0 (13), 102.0 (21), 90.0 (25), 89.0 (24), 76.0 (18), 63.0 (14), 51.0 (15)

FT-IR: 3117 (w), 2064 (w), 3031 (w), 2985 (w), 2883 (w), 2758 (w), 2427 (w), 2390 (w), 2163 (w), 1813 (w), 1801 (w), 1606 (w), 1532 (s), 1462, 1443, 1398, 1358 (s), 1346 (s), 1271, 1241, 1214, 1181, 1156, 1103, 1049, 911, 898, 850, 811 (s), 779, 757, 743, 706, 671 cm^{-1}

MP: 116-119 °C

1-(dibromomethyl)-2-(bromomethyl)-4,5-dinitrobenzene (151**):**

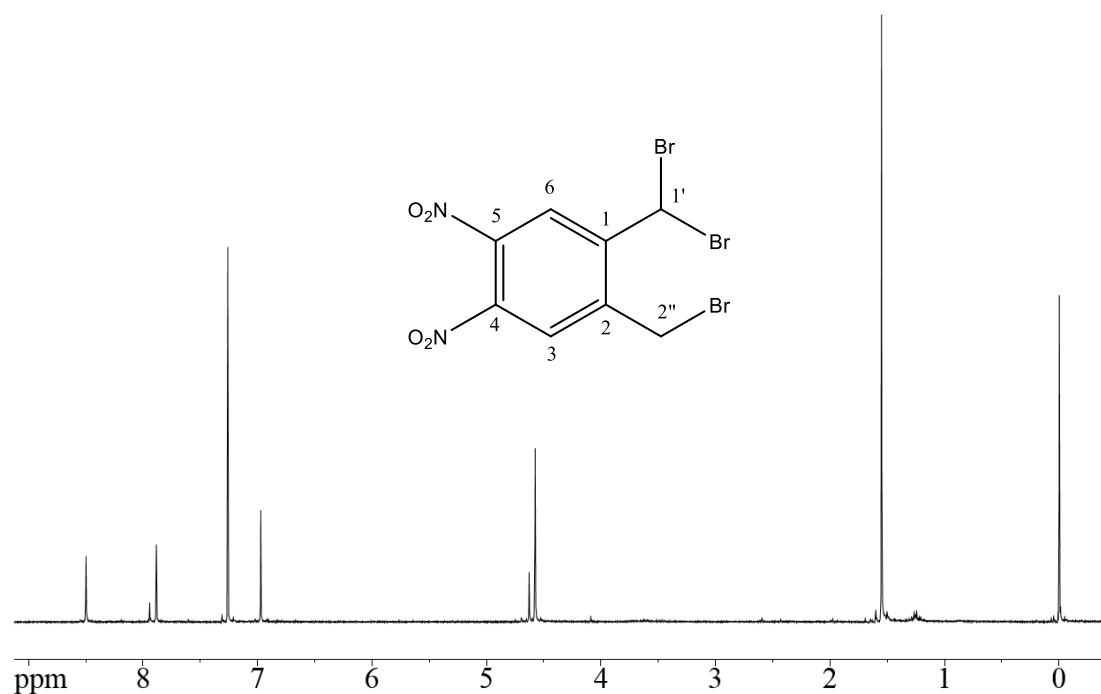


Figure 114. ^1H -NMR spectrum of 1-(dibromomethyl)-2-(bromomethyl)-4,5-dinitrobenzene (**151**) (500 MHz, CDCl_3).

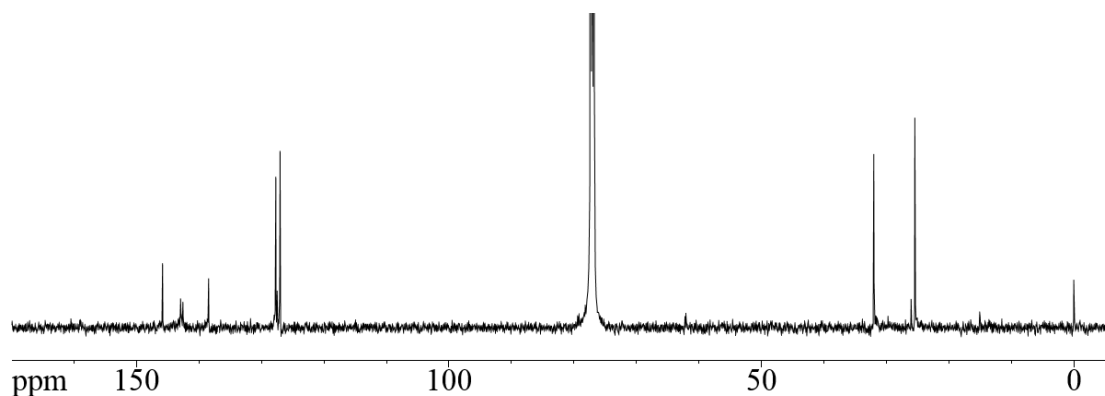


Figure 115. ^{13}C -NMR spectrum of 1-(dibromomethyl)-2-(bromomethyl)-4,5-dinitrobenzene (**151**) (500 MHz, CDCl_3).

^1H -NMR (500 MHz, CDCl_3): δ = 8.49 (s, 1H, 6-H), 7.88 (s, 1H, 3-H), 6.97 (s, 1H, 1'-H), 4.56 (s, 4H, 2'-H) ppm

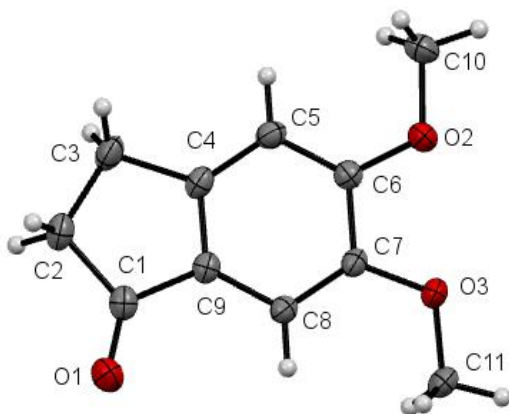
^{13}C -NMR (500 MHz, CDCl_3): δ = 145.7 (1C, 4-C), 142.8 (1C, 1-, 2-C*), 142.5 (1C, 1-, 2-C*), 127.6 (1C, 6-C), 126.9 (1C, 3-C) ppm

2,3-bis(bromomethyl)-quinoxaline (156):

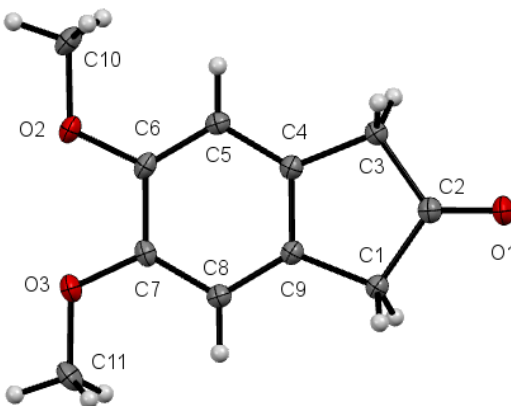
After grinding 1.0 g (7.1 mmol) *o*-phenylene diamine, 2.26 g (9.3 mmol) and 10 g silica together in a mortar and pestle for 15 min, the product was removed by washing twice with 20 ml DCM. After filtration, the solvent was removed in vacuo to afford 1.56 g (5.0 mmol) of the analytically pure title compound as a highly lachrymatory solid (54% yield).

^1H -NMR (500 MHz, CDCl_3): δ = 8.08 (ddd, 2H, 5-, 8-H), 7.79 (ddd, 2H, 6-, 7-H), 4.92 (s, 4H, 2'-, 3'-H) ppm

5.3 X-ray Crystallographic Reports

5,6-dimethoxy-1-indanone (69h):Figure 116. Crystal structure of 5,6-dimethoxy-1-indanone (**69h**).

Empirical formula	C ₁₁ H ₁₂ O ₃	
Formula weight	192.21	
Temperature, K	163	
Wavelength, Å	0.71073	
Crystal system	monoclinic	
Space group	P2 ₁ /c	
Unit cell dimensions	<i>a</i> = 8.1484(11) Å	$\alpha = 90^\circ$
	<i>b</i> = 5.9664(8) Å	$\beta = 96.685(1)^\circ$
	<i>c</i> = 6.8088(12) Å	$\gamma = 90^\circ$
unit cell volume, Å ³	957.1(2)	
<i>Z</i>	4	
Density (calculated), g cm ⁻³	1.334	
Absorption coefficient, mm ⁻¹	0.097	
<i>F</i> (000)	408.0	
Limiting indices (<i>h</i> , <i>k</i> , <i>l</i> _{max})	10, 7, 25	
Bond precision, Å	0.0014	

5,6-dimethoxy-2-indanone (11h):Figure 117. Crystal structure of 5,6-dimethoxy-2-indanone (**11h**).

Empirical formula	$\text{C}_{11}\text{H}_{12}\text{O}_3$	
Formula weight	192.21	
Temperature, K	100	
Wavelength, Å	1.54184	
Crystal system	orthorhombic	
Space group	<i>Pnma</i>	
Unit cell dimensions	$a = 10.1338(2)$ Å	$\alpha = 90^\circ$
	$b = 6.74384(13)$ Å	$\beta = 90^\circ$
	$c = 13.5012(3)$ Å	$\gamma = 90^\circ$
unit cell volume, Å ³	922.682	
Z	4	
Density (calculated), g cm ⁻³	1.384	
Absorption coefficient, mm ⁻¹	0.827	
F(000)	408.0	
Limiting indices (h, k, l _{max})	12, 8, 16	
Bond precision, Å	0.0022	

***anti*-3,4;7,8-bis[3,4-difluorobenzo]-tricyclo[4.2.1.1^{2,5}]deca-9,10-dione (**2c**):**

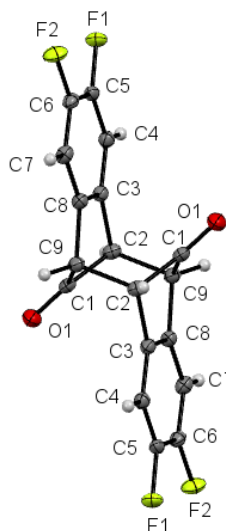


Figure 118. Crystal structure of *anti*-3,4;7,8-bis[3,4-difluorobenzo]-tricyclo[4.2.1.1^{2,5}]deca-9,10-dione (**2c**).

Empirical formula	C ₁₈ H ₈ F ₄ O ₂	
Formula weight	332.24	
Temperature, K	153	
Wavelength, Å	0.71073	
Crystal system	monoclinic	
Space group	P2 ₁ /c	
Unit cell dimensions	<i>a</i> = 8.4215(15) Å	$\alpha = 90^\circ$
	<i>b</i> = 2.098(2) Å	$\beta = 110.135(2)^\circ$
	<i>c</i> = 6.8088(12) Å	$\gamma = 90^\circ$
unit cell volume, Å ³	651.307	
<i>Z</i>	2	
Density (calculated), g cm ⁻³	1.694	
Absorption coefficient, mm ⁻¹	0.148	
F(000)	336.0	
Limiting indices (<i>h</i> , <i>k</i> , <i>l</i> _{max})	10, 15, 8	
Bond precision, Å	0.0018	

***anti*-3,4;7,8-bis[3,4-dimethoxybenzo]-tricyclo[4.2.1.1^{2,5}]decane (**57h**):**

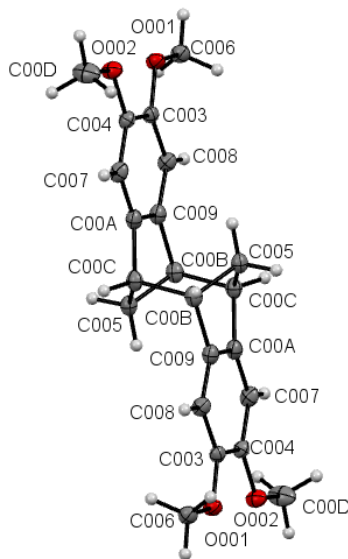


Figure 119. Crystal structure of *anti*-3,4;7,8-bis[3,4-dimethoxybenzo]-tricyclo[4.2.1.1^{2,5}]decane (**57h**).

Empirical formula	C ₂₂ H ₂₄ O ₄	
Formula weight	352.41	
Temperature, K	100	
Wavelength, Å	1.54184	
Crystal system	monoclinic	
Space group	P2 ₁ /c	
Unit cell dimensions	<i>a</i> = 9.3449(1) Å	$\alpha = 90^\circ$
	<i>b</i> = 10.1554(1) Å	$\beta = 93.996(1)^\circ$
	<i>c</i> = 9.4705(1) Å	$\gamma = 90^\circ$
Unit cell volume, Å ³	896.577(16)	
<i>Z</i>	2	
Density (calculated), g cm ⁻³	1.305	
Absorption coefficient, mm ⁻¹	0.716	
<i>F</i> (000)	376.0	
Limiting indices (<i>h</i> , <i>k</i> , <i>l</i> _{max})	11, 12, 12	
Final <i>R</i> indices [<i>I</i> > 2σ(<i>I</i>)]	<i>R</i> 1 = 0.0560, <i>wR</i> 2 = 0.1487	
Bond precision, Å	0.0020	

REFERENCES

1. W. Jones, D. and C. L. M. Ryder, T., "Generation and inter- and intra-molecular trapping of isoindenones (inden-2-ones)." *Chemical Communications* **1997**, 13, 1169-1170.
2. Bradshaw, D.P., Jones, D.W., and Nongrum, F.M., "Stability of alkoxy-substituted inden-2-ones and 6,7-dimethoxy-1,4-diphenyl-2,3-naphthoquinone." *Perkin Transactions I* **1991**, 1, 19-23.
3. Fuchs, B., Pasternak, M., and Scharf, G., "The dimer of 2,3-dimethyl-3,4-(*o,o'*-biphenylene) cyclopentadienone: thermal and photochemical transformations." *Chemical Communications* **1976**, 2, 53-54.
4. Jones, D.W., Pomfret, A., and Wife, R.L., "Stabilised 2, 3-naphthoquinodimethanes via transient 1, 3-diphenylbenz [*f*] inden-2-one." *Chemical Communications* **1980**, 10, 463-464.
5. Jones, D.W., "o-Quinonoid compounds. Part 12. Diels–Alder additions to 1,3-dimethylcyclopenta[*I*]phenanthren-2-one." *Perkin Transactions I* **1977**, 9, 980-987.
6. Fuchs, B., Pasternak, M., and Scharf, G., "The dimer of 2,3-dimethyl-3,4-(*o,o'*-biphenylene) cyclopentadienone: thermal and photochemical transformations." *Tetrahedron* **1976**, 37(14), 2501-2507.
7. Warrenner, R.N., Houghton, M.A., Schultz, A.C., Keene, F.R., Kelso, L.S., Dash, R., and Butler, D.N., "Preparation of 7,8-diazaphencyclone and its use in the construction of rigid, space-separated 1,10-phenanthroline donor–acceptor systems: new ligands for metal complexation." *Chemical Communications* **1996**, 10, 1151-1152.
8. Holland, J.M. and Jones, D.W., "Derivatives of isoindenone." *Chemical Communications* **1969**, 11, 587-588.
9. Holland, J.M. and Jones, D.W., "o-Quinonoid compounds. Part IV. 1, 3-Diphenylinden-2-one." *Journal of the Chemical Society C: Organic* **1971**, 17, 608-612.
10. Poater, J., Solà, M., Alkorta, I., and Elguero, J., "Aromaticity and Magnetic Properties of 1-and 2-Indenones and Their Aza Derivatives." *European Journal of Organic Chemistry* **2014**, 2014(24), 5370-5377.

11. Blatt, K. and Hoffmann, R.W., "Reactivity of 1,3-Dihalogenoisoidenones." *Angewandte Chemie International Edition* **1969**, 8(8), 606-606.
12. Holland, J.M. Ph.D. Thesis, University of Leeds, 1969.
13. Etzkorn, M., Smeltz-Zapata, S.D., Meyers, T.B., Yu, X., and Gerken, M., "From the *anti*-tricyclo[4.2.1.1^{2,5}]deca-3,7-diene framework to 4,5,6,7-tetrachloro-isoidenone derivatives." *Tetrahedron Letters* **2010**, 51(47), 6075-6077.
14. Laube, T., "X-ray Crystal Structures of a Benzonorbornenyl Cation and of a Protonated Benzonorbornenol." *Journal of the American Chemical Society* **2004**, 126(35), 10904-10912.
15. Surya Prakash, G.K., Rasul, G., Yudin, A., and Olah, G.A., "*Ab initio*/IGLO study of sandwiched bishomoaromatic *anti*-tricyclo [4.2. 1.1^{2,5}] deca-3, 7-diene-9, 10-diyl dication and the trishomoaromatic trishomocyclopropenium ion." *Gazzetta Chimica Italiana* **1996**, 126, 1-6.
16. Scholz, F., Himmel, D., Heinemann, F.W., Schleyer, P.v.R., Meyer, K., and Krossing, I., "Crystal structure determination of the nonclassical 2-norbornyl cation." *Science* **2013**, 341(6141), 62-64.
17. Prakash, G.K.S., Farnia, M., Keyanian, S., Olah, G.A., Kuhn, H.J., and Schaffner, K., "*anti*-Tricyclo [4.2.1.1^{2,5}] deca-3, 7-diene-9, 10-diyl dication: a sandwiched bishomoaromatic system." *Journal of the American Chemical Society* **1987**, 109(3), 911-912.
18. Salomon, A., Cahen, D., Lindsay, S., Tomfohr, J., Engelkes, V.B., and Frisbie, C.D., "Comparison of Electronic Transport Measurements on Organic Molecules." *Advanced Materials* **2003**, 15(22), 1881-1890.
19. Lin, Y., Li, Y., and Zhan, X., "Small molecule semiconductors for high-efficiency organic photovoltaics." *Chemical Society Reviews* **2012**, 41(11), 4245-4272.
20. Tang, C.W. and VanSlyke, S.A., "Organic electroluminescent diodes." *Applied Physics Letters* **1987**, 51(12), 913-915.
21. Pauliukaite, R., Ghica, M.E., Barsan, M.M., and Brett, C.M.A., "Phenazines and Polyphenazines in Electrochemical Sensors and Biosensors." *Analytical Letters* **2010**, 43(10-11), 1588-1608.
22. Bunz, U.H.F., "The Larger Linear N-Heteroacenes." *Accounts of Chemical Research* **2015**, 48(6), 1676-1686.

23. Bunz, U.H.F., "N-Heteroacenes." *Chemistry – A European Journal* **2009**, 15(28), 6780-6789.
24. Anthony, J.E., "Functionalized Acenes and Heteroacenes for Organic Electronics." *Chemical Reviews* **2006**, 106(12), 5028-5048.
25. Miao, Q., "Ten Years of N-Heteropentacenes as Semiconductors for Organic Thin-Film Transistors." *Advanced Materials* **2014**, 26(31), 5541-5549.
26. Li, J. and Zhang, Q., "Linearly Fused Azaacenes: Novel Approaches and New Applications Beyond Field-Effect Transistors (FETs)." *ACS Applied Materials & Interfaces* **2015**, 7(51), 28049-28062.
27. Jiang, W., Li, Y., and Wang, Z., "Heteroarenes as high performance organic semiconductors." *Chemical Society Reviews* **2013**, 42(14), 6113-6127.
28. Stolar, M. and Baumgartner, T., "Phosphorus-Containing Materials for Organic Electronics." *Chemistry–An Asian Journal* **2014**, 9(5), 1212-1225.
29. Bock, C., Pham, D.V., Kunze, U., Käfer, D., Witte, G., and Wöll, C., "Improved morphology and charge carrier injection in pentacene field-effect transistors with thiol-treated electrodes." *Journal of Applied Physics* **2006**, 100(11), 114517.
30. Bunz, U.H.F., Engelhart, J.U., Lindner, B.D., and Schaffroth, M., "Large N-Heteroacenes: New Tricks for Very Old Dogs?" *Angewandte Chemie International Edition* **2013**, 52(14), 3810-3821.
31. Winkler, M. and Houk, K.N., "Nitrogen-Rich Oligoacenes: Candidates for n-Channel Organic Semiconductors." *Journal of the American Chemical Society* **2007**, 129(6), 1805-1815.
32. Chen, X.-K., Guo, J.-F., Zou, L.-Y., Ren, A.-M., and Fan, J.-X., "A promising approach to obtain excellent n-type organic field-effect transistors: introducing pyrazine ring." *The Journal of Physical Chemistry C* **2011**, 115(43), 21416-21428.
33. Anthony, J.E., Induced π -Stacking in Acenes, In *Functional Organic Materials*, Wiley-VCH, 2007; p 511-545.
34. Castro, K.P., Clikeman, T.T., DeWeerd, N.J., Bukovsky, E.V., Rippy, K.C., Kuvychko, I.V., Hou, G.-L., Chen, Y.-S., Wang, X.-B., Strauss, S.H., and Boltalina, O.V., "Incremental Tuning Up of Fluorous Phenazine Acceptors." *Chemistry – A European Journal* **2016**, 22(12), 3930-3936.

35. Maly, K.E., "Acenes vs N-Heteroacenes: The Effect of N-Substitution on the Structural Features of Crystals of Polycyclic Aromatic Hydrocarbons." *Crystal Growth & Design* **2011**, 11(12), 5628-5633.
36. Zade, S.S., Zamoshchik, N., Reddy, A.R., Fridman-Marueli, G., Sheberla, D., and Bendikov, M., "Products and Mechanism of Acene Dimerization. A Computational Study." *Journal of the American Chemical Society* **2011**, 133(28), 10803-10816.
37. Hinsberg, O., "Ueber chinoxaline." *European Journal of Inorganic Chemistry* **1884**, 17(1), 318-323.
38. Bunz, U.H.F. and Engelhart, J.U., "The Palladium Way to N-Heteroacenes." *Chemistry – A European Journal* **2016**, 22(14), 4680-4689.
39. Kohl, B., Rominger, F., and Mastalerz, M., "A Pyrene-Fused N-Heteroacene with Eleven Rectilinearly Annulated Aromatic Rings." *Angewandte Chemie International Edition* **2015**, 54(20), 6051-6056.
40. Surry, D.S. and Buchwald, S.L., "Biaryl Phosphane Ligands in Palladium-Catalyzed Amination." *Angewandte Chemie International Edition* **2008**, 47(34), 6338-6361.
41. Hartwig, J.F., "Approaches to catalyst discovery. New carbon–heteroatom and carbon–carbon bond formation." *Pure and Applied Chemistry* **1999**, 71(8), 1417-1423.
42. Kosugi, M., Kameyama, M., and Migita, T., "Palladium-catalyzed aromatic amination of aryl bromides with *N,N*-di-ethylamino-tributyltin." *Chemistry Letters* **1983**, 12(6), 927-928.
43. Sunesson, Y., Limé, E., Nilsson Lill, S.O., Meadows, R.E., and Norrby, P.-O., "Role of the Base in Buchwald–Hartwig Amination." *The Journal of Organic Chemistry* **2014**, 79(24), 11961-11969.
44. Engelhart, J.U., Lindner, B.D., Tverskoy, O., Rominger, F., and Bunz, U.H.F., "Pd-Catalyzed Coupling of Non-Activated Dibromoarenes to 2,3-Diaminoarenes: Formation of *N,N'*-Dihydropyrazines." *Chemistry – A European Journal* **2013**, 19(45), 15089-15092.
45. Tverskoy, O., Rominger, F., Peters, A., Himmel, H.-J., and Bunz, U.H.F., "An Efficient Synthesis of Tetraazapentacenes." *Angewandte Chemie International Edition* **2011**, 50(15), 3557-3560.

46. Laha, J.K., Tummalapalli, K.S.S., and Gupta, A., "Palladium-Catalyzed Domino Double *N*-Arylations (Inter- and Intramolecular) of 1,2-Diamino(hetero)arenes with o,o'-Dihalo(hetero)arenes for the Synthesis of Phenazines and Pyridoquinoxalines." *European Journal of Organic Chemistry* **2013**, 36, 8330-8335.
47. Cope, A.C., Field, L., MacDowell, D., and Wright, M.E., "The Rearrangement of Allyl Groups in Three-carbon Systems. VI. Benzene and Phenanthrene Derivatives." *Journal of the American Chemical Society* **1956**, 78(11), 2547-2551.
48. Chang, B.-H., Kim, H., and Lee, H., "Photolysis and Catalysis of alpha-Diazoindanone Derivatives." *Journal of the Korean Chemical Society* **1992**, 36(5).
49. Bonfantini, E., Métral, J.L., and Vogel, P., "Ironcarbonyl Complexes of 5, 6-Dimethylidene-7-oxabicyclo [2.2. 1] hept-2-ene Derivatives. Synthesis of Substituted Tricarbonyl (ortho-quinodimethane) iron Complexes and 2-Indanones." *Helvetica Chimica Acta* **1987**, 70(7), 1791-1797.
50. Braterman, P.S., Walker, B.S., and Robertson, T.H., "Halide ion-induced disproportionation of cobalt carbonyls; formation of [Co (CO) 4]–and subsequent cyclic ketone synthesis." *Journal of the Chemical Society, Chemical Communications* **1977**, 18, 651-652.
51. Miwa, T., Kato, M., and Tamano, T., "Reactions of dehydrobenzene II. 7, 8-Benzobicyclo-[4.2.1] nona-2,4,7-trien-9-one; a 1, 6-cycloaddition product of dehydrobenzene." *Tetrahedron Letters* **1969**, 10(22), 1761-1764.
52. Ishikawa, F., Yamaguchi, H., Saegusa, J., Inamura, K., Mimura, T., Nishi, T., Sakuma, K., and Ashida, S., "Cyclic guanidines. XVI. Synthesis and biological activities of tetracyclic imidazo[2,1-b]quinazolinone derivatives." *Chemical and Pharmaceutical Bulletin* **1985**, 33(8), 3336-3348.
53. Yokokoji, O., Shimizu, K., and Inoue, S., "5,6-Difluoro-1H-indene derivatives: novel core structure of liquid crystals with high Δn and $\Delta\epsilon$." *Liquid Crystals* **2009**, 36(1), 1-6.
54. Runtz-Schmitt, V., Schnider, P., Dolente, C., and Fasching, B., Spiro-oxazolones. WO2015091411, **2015**.
55. Knoevenagel, E., "Condensation von Malonsäure mit aromatischen Aldehyden durch Ammoniak und Amine." *Berichte der Deutschen Chemischen Gesellschaft* **1898**, 31(3), 2596-2619.
56. Horan, J.E. and Schiessler, R.W., "2-Indanone." *Organic Syntheses* **2003**, 41, 53.

57. McCormick, K.D., Dong, L., Boyce, C.W., De, L.R.M., Fevrier, S., Wu, J., Zheng, J., Yu, Y., Chao, J., and Won, W.S., Biaryl spiroaminooxazoline analogues as α_2c adrenergic receptor modulators. WO2010042473 **2010**.
58. Ma, E.-S., "Synthesis of 5,6-difluoro-2-aminoindan.HCl." *Yakhak Hoeji* **1999**, 43(6), 751-755.
59. Guzi, T.J., Paruch, K., Mallams, A.K., Rivera, J.D., Doll, R.J., Girijavallabhan, V.M., Pachter, J.A., Liu, Y.-T., and Saksena, A.K., 17 β -hydroxysteroid dehydrogenase type 3 inhibitors for the treatment of androgen dependent diseases. WO2012035078, **2006**.
60. Lewis, J.W., Taylor, J.B., and Jacklin, M., "2-Amino-5,6-dihydroxyindan-2-carboxylic acid. A potential hypotensive agent." *Journal of Medicinal Chemistry* **1970**, 13(6), 1226-1227.
61. Liu, F., You, Q.-D., Li, M.-Y., Shen, W.-B., and Xia, L., "Convenient and rapid preparation of indene dimers from indenenes or indanols." *Organic Preparations and Procedures International* **2006**, 38(5), 490-494.
62. Hutchison, G.I., Marshall, P.A., Prager, R.H., Tippet, J.M., and Ward, A.D., "Central nervous system active compounds. IV. Synthesis of 3-aminobenzylphthalides." *Australian Journal of Chemistry* **1980**, 33(12), 2699-2715.
63. Tayama, E., Takedachi, K., Iwamoto, H., and Hasegawa, E., "1,2-Dimethoxy-4,5-dimethylene : A new protecting group for acyclic amino acid derivatives prepared by Stevens rearrangement." *Tetrahedron letters* **2012**, 53(11), 1373-1375.
64. Kapat, A., Kumar, P.S., and Baskaran, S., "Synthesis of crispine A analogues via an intramolecular Schmidt reaction." *Beilstein Journal of Organic Chemistry* **2007**, 3, 49-49.
65. Honzicek, J., Mukhopadhyay, A., Bonifacio, C., and Romão, C.C., "Molybdenum complexes containing substituted cyclopenta[1]phenanthrenyl ligand." *Journal of Organometallic Chemistry* **2010**, 695(5), 680-686.
66. Hashimoto, S. and Anada, M., Polymer-supported metal complex catalyst for stereoselective addition reactions. WO2008013009, **2008**
67. Yadav, J.S., Reddy, G.S.K.K., Sabitha, G., Krishna, A.D., Prasad, A.R., Hafeez, U.R.R., Vishwaswar Rao, K., and Bhaskar Rao, A., "Daucus carota and baker's yeast mediated bio-reduction of prochiral ketones." *Tetrahedron: Asymmetry* **2007**, 18(6), 717-723.

68. Suzuki, T., Okuyama, H., Takano, A., Suzuki, S., Shimizu, I., and Kobayashi, S., "Synthesis of Dibarrelane, a Dibicyclo[2.2.2]octane Hydrocarbon." *The Journal of Organic Chemistry* **2014**, 79(6), 2803-2808.
69. Yamamura, M.T., Hirata, Y., "Modified Clemmensen Reduction: Chloestane." *Organic Syntheses* **1973**, 53, 86.
70. Caglioti, L., "Reduction of Ketones by Use of the Tosylhydrazone Derivatives: Androstan-17 β -ol." *Organic Syntheses* **1972**, 52, 122.
71. Kuehne, M.E. and Lambert, B.F., "1,4-Dihydrobenzoic Acid." *Organic Syntheses* **2003**, 43, 22-23.
72. Jessup, D.W., Paschal, J.W., and Rabideau, P.W., "Metal-ammonia reduction of fluorinated aromatic compounds." *The Journal of Organic Chemistry* **1977**, 42(15), 2620-2621.
73. Tsukanov, S.V. and Comins, D.L., "Total Synthesis of Alkaloid 205B." *The Journal of Organic Chemistry* **2014**, 79(19), 9074-9085.
74. Curti, C., Brindani, N., Battistini, L., Sartori, A., Pelosi, G., Mena, P., Brighenti, F., Zanardi, F., and Del Rio, D., "Catalytic, Enantioselective Vinylogous Mukaiyama Aldol Reaction of Furan-Based Dienoxy Silanes: A Chemodivergent Approach to γ -Valerolactone Flavan-3-ol Metabolites and δ -Lactone Analogues." *Advanced Synthesis & Catalysis* **2015**, 357(18), 4082-4092.
75. Chatgililoglu, C. and Ferreri, C., "Progress of the Barton-McComble Methodology: From tin hydrides to Silanes." *Research on Chemical Intermediates* **1993**, 19(8), 755-775.
76. Xin, Z., Lu, Y., Xing, X., Long, J., Li, J., and Xue, X., "Synthesis of (-)-agathic acid and (-)-copalic acid from andrographolide via a regioselective Barton-McCombie reaction." *Tetrahedron* **2016**, 72(4), 555-562.
77. Etzkorn, M. Ph.D. Thesis, Albert Ludwigs Universitaet Freiburg.
78. Gilman, H. and Kirby, R.H., "DL-Methylethylacetic Acid." *Organic Syntheses* **1925**, 5, 75.
79. Matsumura, S. and Tokura, N., "Reduction of aralkyl halides with diborane in nitromethane." *Tetrahedron Letters* **1969**, 10(5), 363-365.
80. Srivastava, S. and le Noble, W.J., "Set mechanism in the lithium aluminum deuteride reduction of chloroadamantanes, and its induction by remote substituents." *Tetrahedron Letters* **1984**, 25(43), 4871-4874.

81. Krishnamurthy, S. and Brown, H.C., "Selective reductions. 31. Lithium triethylborohydride as an exceptionally powerful nucleophile. A new and remarkably rapid methodology for the hydrogenolysis of alkyl halides under mild conditions." *The Journal of Organic Chemistry* **1983**, 48(18), 3085-3091.
82. Noriega, R. and Salleo, A., Charge Transport Theories in Organic Semiconductors, in *Organic Electronics II*, Wiley-VCH, 2012; p 67-104.
83. Musa, A., Saeed, M.A., Shaari, A., Sahnoun, R., and Lawal, M., "Effects of delocalised π -electrons around the linear acenes ring ($n = 1$ to 7): an electronic properties through DFT and quantum chemical descriptors." *Molecular Physics* **2015**, 113(11), 1347-1358.
84. Cao, J., Lu, H.-Y., and Chen, C.-F., "Synthesis, structures, and properties of peripheral *o*-dimethoxy-substituted pentiptycene quinones and their *o*-quinone derivatives." *Tetrahedron* **2009**, 65(39), 8104-8112.
85. Zhao, J.-M., Lu, H.-Y., Cao, J., Jiang, Y., and Chen, C.-F., "Highly selective synthesis of triptycene *o*-quinone derivatives and their optical and electrochemical properties." *Tetrahedron Letters* **2009**, 50(2), 219-222.
86. Deslongchamps, P., Bélanger, A., Berney, D.J., Borschberg, H.-J., Brousseau, R., Doutheau, A., Durand, R., Katayama, H., Lapalme, R., and Leturc, D.M., "The total synthesis of (+)-ryanodol. Part I. General strategy and search for a convenient diene for the construction of a key tricyclic intermediate." *Canadian Journal of Chemistry* **1990**, 68(1), 115-126.
87. Shopsowitz, K.E., Edwards, D., Gallant, A.J., and MacLachlan, M.J., "Highly substituted Schiff base macrocycles via hexasubstituted benzene: a convenient double Duff formylation of catechol derivatives." *Tetrahedron* **2009**, 65(39), 8113-8119.
88. Zhang, Y., Tortorella, M.D., Wang, Y., Liu, J., Tu, Z., Liu, X., Bai, Y., Wen, D., Lu, X., and Lu, Y., "Synthesis of deuterated benzopyran derivatives as selective COX-2 inhibitors with improved pharmacokinetic properties." *ACS Medicinal Chemistry Letters* **2014**, 5(10), 1162-1166.
89. Huang, W.-B., Guo, Y., Jiang, J.-A., Pan, X.-D., Liao, D.-H., and Ji, Y.-F., "An Efficient Strategy for Protecting Dihydroxyl Groups of Catechols." *Synlett* **2013**, 24(06), 741-746.
90. Sugihara, Y., Noda, K., and Nakayama, J., "Synthesis and Structure of Sterically Congested, New Alkenes, *syn*- and *anti*-9,9'-Bibenzonorbornenylidenes." *Bulletin of the Chemical Society of Japan* **2000**, 73(10), 2351-2356.

91. Morales-Castellanos, J.J., Ramírez-Hernández, K., Gómez-Flores, N.S., Rodas-Suárez, O.R., and Peralta-Cruz, J., "Microwave-assisted solvent-free synthesis and in vitro antibacterial screening of quinoxalines and pyrido [2,3b] pyrazines." *Molecules* **2012**, 17(5), 5164-5176.
92. Bürli, R.W., Luckhurst, C.A., Aziz, O., Matthews, K.L., Yates, D., Lyons, K.A., Beconi, M., McAllister, G., Breccia, P., and Stott, A.J., "Design, synthesis, and biological evaluation of potent and selective class IIa histone deacetylase (HDAC) inhibitors as a potential therapy for Huntington's disease." *Journal of Medicinal Chemistry* **2013**, 56(24), 9934-9954.
93. Sharma, G., Raisinghani, P., Abraham, I., Pardasani, R.T., and Mukherjee, T., "Synthesis of quinoxaline quinones and regioselectivity in their Diels-Alder cycloadditions.", *Indian Journal of Chemistry* **2009**, 48, 1590-1596.
94. Buckley III, T. and Rapoport, H., "Dependence of aryl ether acylation upon Lewis acid stoichiometry." *Journal of the American Chemical Society* **1980**, 102(9), 3056-3062.
95. Khalaf, A., Abdel-Wahab, A., El-Khawaga, A., and El-Zohry, M., "Modern Friedel Crafts chemistry. XIII. Intra- and intermolecular cyclization of some carbonyl derivatives under Friedel-Crafts conditions." *Bulletin de la Société Chimique de France* **1984**, 7, 285-291.
96. Amano, Y., Noguchi, M., Nakagomi, M., Muratake, H., Fukasawa, H., and Shudo, K., "Design, synthesis and evaluation of retinoids with novel bulky structures." *Bioorganic & Medicinal Chemistry* **2013**, 21(14), 4342-4350.
97. Dhakshinamoorthy, A., Navalon, S., Sempere, D., Alvaro, M., and Garcia, H., "Reduction of alkenes catalyzed by copper nanoparticles supported on diamond nanoparticles." *Chemical Communications* **2013**, 49(23), 2359-2361.
98. Strawn, L.M., Martell, R.E., Simpson, R.U., Leach, K.L., and Counsell, R.E., "Iodoaryl analogs of dioctanoylglycerol and 1-oleoyl-2-acetylglycerol as probes for protein kinase C." *Journal of Medicinal Chemistry* **1989**, 32(9), 2104-2110.
99. Hoeg, D.F. and Lusk, D.I., " α -Halo carbanion intermediates." *Journal of Organometallic Chemistry* **1966**, 5(1), 1-12.
100. Kalir, A. and Mualem, R., "One-step synthesis of 2- and 4-nitrobenzyl cyanides." *Synthesis* **1987**, 1987(5), 514-515.
101. Tiffany B, M. M.S. Thesis, UNC Charlotte, **2012**.